AGING, PROTEIN SYNTHESIS, AND MISTRANSLATION IN HUMAN CELLS

AGING, PROTEIN SYNTHESIS, AND MISTRANSLATION IN CULTURED HUMAN CELLS

By

Calvin B. Harley, B.Sc.

A Thesis

Submitted to the School of Graduate Studies

in Partial Fulfilment of the Requirements

for the Degree

Doctor of Philosophy

McMaster University

December, 1979

Doctor of Philosophy (1979)
(Biochemistry)

McMaster University
Hamilton, Ontario, Canada
L8S 4J9

TITLE: Aging, Protein Synthesis, and Mistranslation in Cultured Human Cells

AUTHOR: Calvin Bruce Harley, B.Sc. (University of Waterloo)

SUPERVISOR: Dr. Samuel Goldstein

NUMBER OF PAGES: xxi, 258

ABSTRACT

The synthesis and degradation of proteins were studied during aging of cultured human fibroblasts. Equations were derived to yield expressions for the rates of protein degradation, export, and synthesis during exponential growth and steady state from the approach to equilibrium method of radioactively labeling protein. Old cells (cells from normal donors at late passage, cells from old donors, or cells from subjects with the accelerated aging phenotypes of Hutchinson-Gilford (progeria) and Werner syndromes) have a reduced growth rate (0.3-1.3%/hour) when cultured at low density compared to young cells (early-passage cells from normal donors) (2.0-2.5%/hour). Prior to the terminal passage in old cultures, this reduction in growth rate is related primarily to an increased rate of protein degradation (0.96-1.3%/hour in old cells compared to less than 0.55%/hour in young cells). Early-passage cells achieve rapid growth in low density cultures by increasing the protein synthetic rate and decreasing the degradation rate. In high density cultures where the net growth rate was close to zero, the rates of degradation and synthesis were similar in young and old cells prior to their terminal passage (1.9-2.5%/hour). In all cases the rate of protein export was small (less than 0.5%/hour) compared to the rate of protein synthesis.

Proteins synthesized by young and old cells were analyzed by two-dimensional gel electrophoresis and were found to be essentially identical in molecular weight and isoelectric points. Induction of synthesis of aberrant proteins by histidine starvation in the presence of histidinol did not reveal differences between early- and late-passage cells from young or old normal donors or from subjects with progeria or Werner Syndrome. Futhermore, there was no correlation between *in vitro* lifespan and the synthesis of aberrant protein.

It is concluded that the increased degradation of proteins and the slow net growth of old cells and the reduced lifespan of cells from old normal donors and subjects with progeria or Werner Syndrome are not due to abnormal protein synthesis. This is contrary to the predictions of the error catastrophe theory of aging.

The aberrant proteins synthesized during amino acid starvation are believed to result from amino acid substitution. Several observations reported here are consistent with this hypothesis: (i) No turnover of either native or substituted actins synthesized during histidine starvation of cultured human cells was detected; (ii) Changes in the isoelectric points of native and substituted actins are predicted by analyses based on the presumed changes in their amino acid composition; (iii) Estimates of the protein synthetic error rates during normal protein synthesis can be

derived from a computer model of mRNA translation based on the proposed mechanism of mistranslation; these estimates are consistent under a variety of starvation conditions and are close to other estimates obtained independently for the error frequency in mammalian cells.

In both young and old cultured human fibroblasts the error frequency at the histidine codon was calculated to be $1.1 \pm 0.1 \times 10^{-4}$ (mean+S.E.). Three lines of SV40-transformed human fibroblasts had error frequencies 2-5 fold greater than their untransformed counterparts. Studies with a variety of other human and non-human cell types did not support the conclusion that transformation in general increased the rate of mistranslation. The observation of increased error frequencies in SV40-transformed human cells may be restricted to this viral transformation.

The computer simulations of mRNA translation have provided a means of extrapolating error frequencies determined during amino acid starvation to the error frequency during normal protein synthesis. This model is of great interest for its potential use as a method of rapidly quantifying protein synthetic error frequencies in cultured cells.

I dedicate this thesis to my family: my parents, my brothers and sisters, my children and my wife; but especially to my wife, who was a tremendous help in the homestretch.

ACKNOWLEDGEMENTS

It is with gratitude that I acknowledge the advice and support of my supervisor, Dr. S. Goldstein, throughout the course of this work.

Special thanks for many helpful discussions are also due to the members of my supervisory committee: Dr. K.B. Freeman, Dr. H.P. Ghosh, and Dr. F.L. Graham; and to my collaborators in Toronto: Dr. J.W. Pollard and Dr. C.P. Stanners.

I also wish to thank my colleagues in Dr. Goldstein's laboratory for contributing in many ways to a good research environment: S.R. Ballantyne, J.J. Elliot, E.J. Moerman, Dr. R.J. Shmookler Reis and R.I. Wojtyk.

TABLE OF CONTENTS

List of Figures

List of Tables

ABBREVIATIONS

A	adenosine[a];aminoacyl-tRNA acceptor site
AA-AMP	aminoacyl adenylic acid
α-actin	major actin species of muscle cells
β-actin	major actin species of non-muscle cells
γ-actin	minor actin species of non-muscle cells
AMP,ADP,ATP	adenosine 5'-mono-, di-, and triphosphate
C	cytidine[a];carbon
^{14}C	radioactive isotope of carbon
2-D	two-dimensional
DNA	deoxyribonucleic acid
Enz.	enzyme (aminoacyl-tRNA synthetase)
Enz.AA~AMP	aminoacyl-AMP-enzyme complex in a high energy state
EF, EF-Tu	elongation factor
eIF	eukaryotic initiation factor
FCS	fetal calf serum
G	guanosine[a]
G6PD	glucose-6-phosphate dehydrogenase
GMP,GDP,GTP	guanosine-5'-mono-,di-, and triphosphate
H	hydrogen; histidine
^{3}H	radioactive isotope of hydrogen
H1-H5	hypothetical proteins (see section 3.2.3)
his-OH	histidinol
I	inosine[a]

IEF	isoelectric focusing
K_m	Michaelis-Menten constant (see Lehninger, 1976)
m	methyl
MEM	minimal essential medium
mRNA	messenger RNA
MS2-RNA	a bacteriophage RNA
MWw	weight-average molecular weight
N	nitrogen; normal (i.e. gram equivalents per liter of solution); a non-specified nucleotide; asparagine
O	oxygen
Old cells	cells from normal donors at late passage, cells from old donors, or cells from subjects with progeria or Werner syndrome
NaOH	sodium hydroxide
P	ribosomal site which binds peptidyl-tRNA
PBS	phosphate buffered saline
6PGD	6-phosphogluconate dehydrogenase
pH	negative log of the hydrogen ion concentration
pI	pH at which the net charge of a protein is zero
ΔpI	difference in pI between two proteins
ppGpp	guanosine 5'-diphosphate-3'-diphosphate
PP_i	pyrophosphate
pppGpp	guanosine 5'-triphosphate-3'-diphosphate
Q	a derivative of guanosine
R_f	distance travelled by sample relative to that of the fastest moving component of the system
RF	release factor

RNA	ribonucleic acid
^{35}S	radioactive isotope of sulfur
S	Svedberg unit (1×10^{-13} seconds)
30S, 50S, 40S, 60S	small and large prokaryotic and small and large eukaryotic ribosomal subunits, respectively
70S, 80S	prokaryotic and eukaryotic ribosomal couples, respectively
40Sn	small eukaryotic ribosomal subunit complexed with eIF-3 (p. 21)
SDS	sodium dodecylsulfate
S_i	protein containing i amino acid substitutions (errors)
stp	stop codon
SV40	a simian virus
Sx	aminoacyl-tRNA synthetase specific for amino acid X
t	time
TCA	trichloroacetic acid
t	doubling time
tRNA	transfer RNA
X-tRNA	tRNA acylated to amino acid X
tRNA-Y	tRNA specific for amino acid X
X-tRNA-Y	tRNA-Y acylated to amino acid X
tRNAi	eukaryotic initiator tRNA
tRNAf	prokaryotic initiator tRNA
Ts, Tu	prokaryotic elongation factors
U	uridine
v/w	volume per weight
w/w	weight per weight
Young cells	cells from young normal donors at early passage

[a] a sequence of nucleoside abbreviations, for example CAU, represents a portion of a polynucleotide (i.e. phosphates join the nucleosides in 5'-3' linkages, the left-most nucleotide is closest to the 5'-end of the sequence).

amino acids

ala	alanine
arg	arginine
asp	aspartic acid
asn	asparagine
cys	cysteine
glu	glutamic acid
gln	glutamine
gly	glycine
his	histidine
ile	isoleucine
leu	leucine
lys	lysine
met	methionine
phe	phenylalanine
pro	proline
ser	serine
thr	threonine
trp	tryptophan
tyr	tyrosine
val	valine
cit	citrulline
hyp	hydroxyproline
orn	ornithine
tau	taurine

Cells (see also Table 3-1)

A. Human

WI38, WI38-SV40 (SV40-transformed WI38), MRC5, MRC5-SV40 (SV40-trnasformed MRC5): human lung

A1, A2, GM37, GM37-SV40 (SV40-transformed GM37), J004, J069, J088, RE, TM: human skin, normal donors

P5, P18: human skin, progeria donors

WS2, WS3, WS4: human skin, Werner syndrome donors

293: human kidney, adenovirus transformed

HeLa: human cervical carcinoma cells

B. Non-human

Vero: African green monkey kidney cells

CHO: Chinese hamster ovary cells

asn-7: temperature-sensitive mutant of CHO involving asparaginyl-tRNA synthetase

CHF: Chinese hamster embryo (fibroblasts)

HA: Syrian hamster embryo

T: polyoma virus-transformed HA cells

Nil: hamster embryo

Nil-HSV: hamster sarcoma virus-transformed Nil cells

3T3: mouse cells

CEF: chick embryo fibroblasts

CEF-RSV: Rous sarcoma virus-transformed CEF

CEF-RSVts: CEF transformed with a temperature-sensitive mutant of RSV

E. coli: Escherichia coli (a bacterium)

rel- E. coli: mutant E. coli lacking the stringent response (section 1.5.3)

rel+ E. coli: E. coli which display the stringent response (section 1.5.3)

Mathematical Symbols

The lists of symbols found on pages 154, 155, and 242 define the abbreviations and variables used in the computer simulations of protein synthesis. Other mathematical symbols are used less frequently and are defined in the relevant sections. The following standard functions are used:

e^x exponential function $(2.71828...)^x$

$\ln(x)$ natural log function (inverse function of e)

$\sum_{i=a}^{i=b}(x_i)$ summation function $(x_a + x_{a+1} + x_{a+2} + ... + x_b)$

$\binom{n}{x}$ combination function $(n!/\{x!(n-x)!\})$ where $n! = 1 \times 2 \times 3 \times \ldots \times (n)$; $0! = 1$.

1 INTRODUCTION

1.1 Purpose

Aging is a fundamental aspect of our life, and man's curiosity about this process dates to antiquity. Finding a "fountain of youth" is perhaps still the incentive of modern gerontologists, although another less ambitious goal is simply to define the mechanisms of aging with the hope of mitigating age related diseases. However, even though advances have been made, and new techniques and ideas have been developed which are of general interest in biology, the basic cause of aging still eludes us.

The introduction below describes the model of aging used in these studies and reviews the relevant areas of research. Because the scope of material is broad, certain areas receive only brief treatment. The theoretical and applied studies of mistranslation during amino acid starvation are meant to be the focus of the thesis and will accordingly receive the most emphasis.

1.2 The Cellular Model of Aging

It has been argued that longevity in various animal and plant species is not an essential characteristic of basic biochemical processes, but rather reflects the ability of the species to cope with predation, competition, fire, disease,

and to bridge lengthy periods unfavourable to reproduction (Todd, 1978). The strong correlation between longevity and the possession of these characteristics suggests that evolution grants the appropriate lifespan to each species according to these qualifying components of its phenotype.

The gerontologist is concerned with the mechanisms of aging within a species (usually man), upon which evolution is capable of acting to alter longevity. The most basic approach to the study of aging is at the level of the molecule. Although radioisotopes can be thought of as "aging atoms" and the mutagenic effect of radioactive decay may play a role in aging, it appears that aging can proceed independent of radiation damage (Hirsch, G.P., 1978; Morrow and Garner, 1979). The study of "atomic aging" in this sense can yield no direct information on the fundamental process of biological aging. However, it has not been possible to exclude all types of deleterious changes in macromolecules which accumulate with time from a causal relationship to aging of the individual. Although damage to macromolecules may not prove to be the cause of biological aging (see section 1.2.2), the mechanism of aging must ultimately be reducible to the molecular level.

Aging in multicellular organisms is a complex process, and it may be extremely difficult or even impossible to detect its fundamental molecular basis without simultaneously studying the interactions between the many cellular and organ

systems involved in the cooperative maintenance of life. For this reason, the *in vitro* model of cellular senescence (Hayflick and Moorhead, 1961; Hayflick, 1965) was welcomed by many gerontologists as an intermediate level of study. The cellular model of aging proposes that at least some critical somatic cells have a finite lifespan and the death of the organism results directly from the progressive loss of function in these essential cell populations. The basic premise of the *in vitro* model of cellular senescence is that the mechanisms conferring mortality to cultured cells are the same as those which lead to the loss of function in senescing populations of cells *in vivo* . It is *not* important that the cultured cell *in vitro* be of the same type as the critical cell *in vivo* .

Historically, Swim and Parker (1957) first observed that there was a limited ability to propagate cells from a variety of human tissues *in vitro* . Their studies were extended by Hayflick and Moorhead (1961) who showed that the limited lifespan *in vitro* of human fibroblasts was not due to depletion of an essential nutrient or accumulation of toxic substances in the medium, but apparently reflected a limited potential of the cell to divide. Hayflick (1965) formulated these observations into the *in vitro* model of cellular senescence.

Hayflick's model in practice, therefore, is the study of changes in cellular function during the culture lifespan of

normal cells, from early passage through late passage. However, cells from old donors and subjects with genetically determined disorders of accelerated aging (such as progeria (Hutchinson-Gilford) or Werner Syndromes tend to have reduced lifespans *in vitro* (figure 1-1) (see Goldstein, 1978). Thus typical analysis of a cellular property for age-related changes in the *in vitro* model of senescence will include comparisons of cells from young and old normal donors and from subjects with features of accelerated aging in addition to comparisons at early and late passage.

In the past fifteen years, a great deal of evidence has accumulated supporting the *in vitro* model of cellular senescence (for reviews see Daniel, 1977; Hayflick, 1977; Goldstein, 1978; Schneider, 1978). The premise of this model which has been most frequently questioned is not that cellular senescence is causative to organismic death (although this has not been definitely shown), but rather that the limited capacity of cultured cells to replicate represents true cellular senescence. This proliferative limit does not appear to be an artifact of culture conditions (Hayflick, 1965; Dell'Orco et al., 1973; Goldstein and Singal, 1974; Harley and Goldstein, 1978; Harley and Goldstein, 1980), but it has alternatively been suggested that it may be a form of "terminal differentiation". However, this concept is still compatible with the *in vitro* model of cellular senescence as discussed below (section 1.2.2.2).

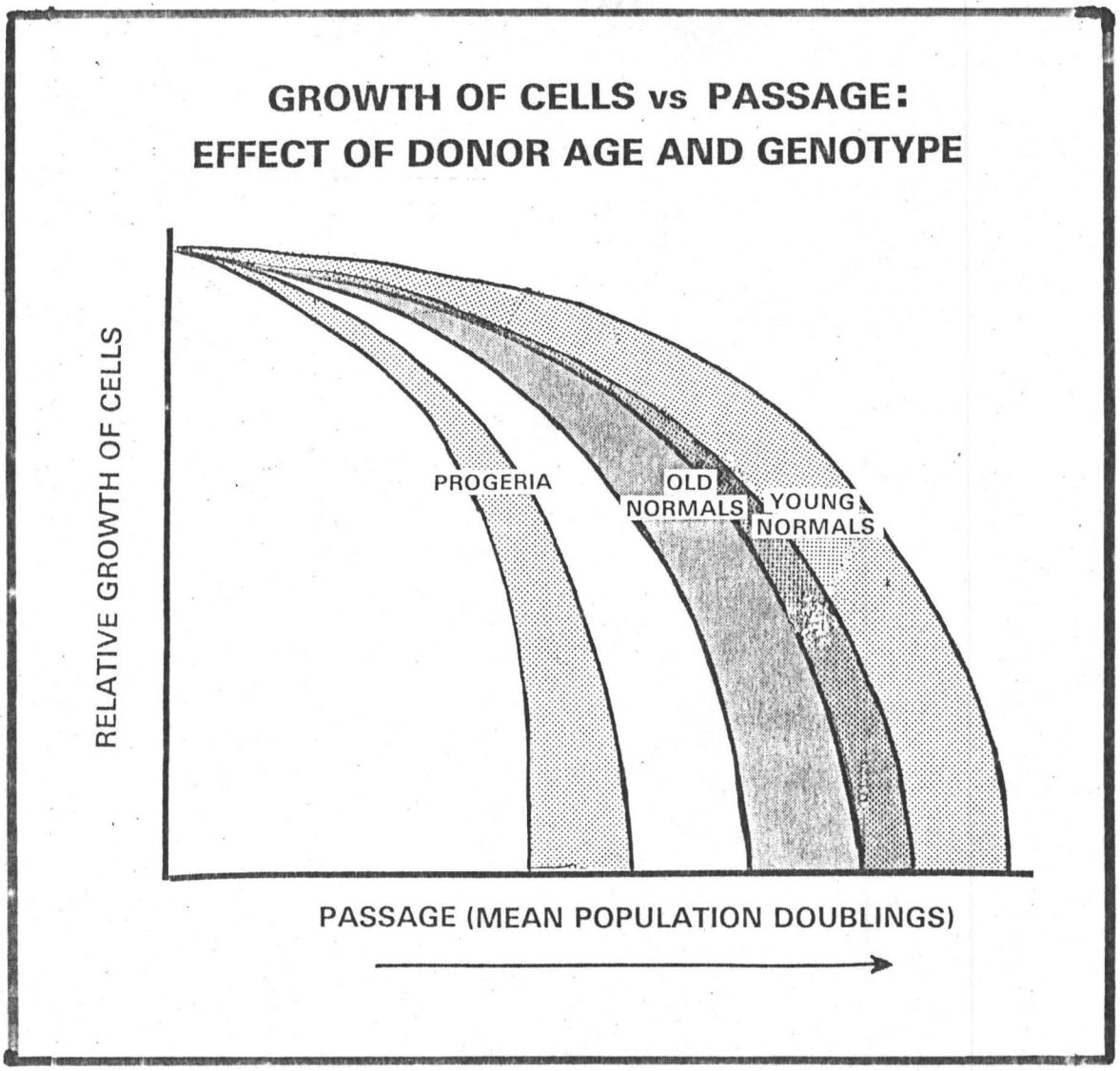

Figure 1-1

The *in vitro* model of cellular senescence. The growth of human cells in culture is a function of both passage (mean population doublings) and the donor age and genotype. This schematic depicts the observed decline in the relative growth potential of cells as a function of passage and the reduced lifespan of cells from old normal and progeric donors. These observations provide support for the *in vitro* model of cellular senescence, which postulates that the loss of growth capacity in a critical cell mass *in vivo* is responsible for organismic death, and the limited lifespan of fibroblasts *in vitro* is analogous to *in vivo* senescence.

An ironclad defense against criticisms of this model cannot be constructed (see Morrow and Garner, 1979). Which model is "best" for aging research will not be known until some breakthrough indicates special promise in some area of study. Unfortunately most of the advance to date has been simply to define the problem (Comfort, 1978). Although many theories have been proposed, most have done little to advance our knowledge, partly because they do not suggest practical experiments on the basis of which the theory can be refuted (Popper, 1965). An exception to this statement is Orgel's error catastrophe theory (Orgel, 1963) which is very testable (see section 1.2.2.2(b)). This theory has been examined indirectly in cultured cell- and whole-animal models of aging perhaps more than any other theory, and there is much indirect evidence both for and against it. Experiments which directly test the error catastrophe theory of aging in cultured cells are discussed in section 3.1.

The short discussion of theories below indicates other activity in aging research and illustrates the variety of approaches at the molecular level. It is not meant to be a comprehensive review of theories of aging. Treatises which deal with aging at a specific cellular or tissue level, such as immunological and hormonal theories of aging are not discussed since the primary consideration here is basic molecular mechanisms; which cell or organ system these mechanisms might affect most and how they influence the phenotypic expression of aging are reviewed elsewhere (for

example, see Finch, 1977; Makinodan, 1977).

1.2.1 Aging and Transformation in Cultured Cells

The mortal cell strains of Hayflick (1965) retained an essentially normal (diploid) karyotype throughout their lifespan. Two other important characteristics of these cells were their requirement for solid surfaces on which to grow, and their inability to form tumors in animals. Hayflick distinguished these cells from immortal cell lines (transformed cells) which were unstable in karyotype, grew in relaxed culture conditions (for example in suspension or on agar), and many of which could cause tumors in appropriate recipients.

For aging research, the most interesting feature of transformed cells is their immortality. But in addition to these abnormal cells, germ cells and unicellular organisms are also apparently capable of unlimited proliferation and aging theories must be able to account for their immortality. Although many plants or their cells may be immortal, this discussion is restricted to animal cells, since these are most relevant to our understanding of human aging. Research on plant differentiation and "aging" of certain plant tissues however, may provide clues to the mechanisms of animal cell senescence (Woolhouse, 1974). Not all cells taken from normal somatic tissues are mortal in vitro . In fact, cells from many non-human animal sources undergo a "crisis" in which most cells apparently senesce but a few immortal ones survive

to establish a permanent line (see Littlefield, 1976; Hayflick, 1978). Such spontaneous transformation has never been observed in normal cells from humans. Although studies have not been as extensive with other sources of tissue, cells from several non-human species also appear to undergo a senescent decline *in vitro* without spontaneous transformation: chick embryo fibroblasts (Lima and Macieira-Coelho, 1972), heart tissue from the kangaroo rat (Simons, 1970), bovine lung (Lithner and Ponten, 1966) and skin fibroblasts from Galapagos tortoise (Goldstein, 1974).

But immortality and the transformed phenotype can be achieved in all cells tested so far with either viral or chemical agents (see Littlefield, 1976). Thus aging and transformation of cultured cells are intimately linked, and studies of these two phenomena may be simply different approaches to the same fundamental question: what dictates the fate of a cell?

1.2.2 Theories of Aging and Transformation

Since lifespans within the animal kingdom vary over several orders of magnitude, it is clear that there is a genetic influence on the aging rate (for reviews, see Sacher, 1978; Todd, 1978). However, it is not clear whether there is an intrinsic biological clock which determines lifespan or whether it is the interplay between extrinsic factors (the environment) and the physical-chemical makeup of an otherwise immortal cell (figure 1-2). If we could place the cell or

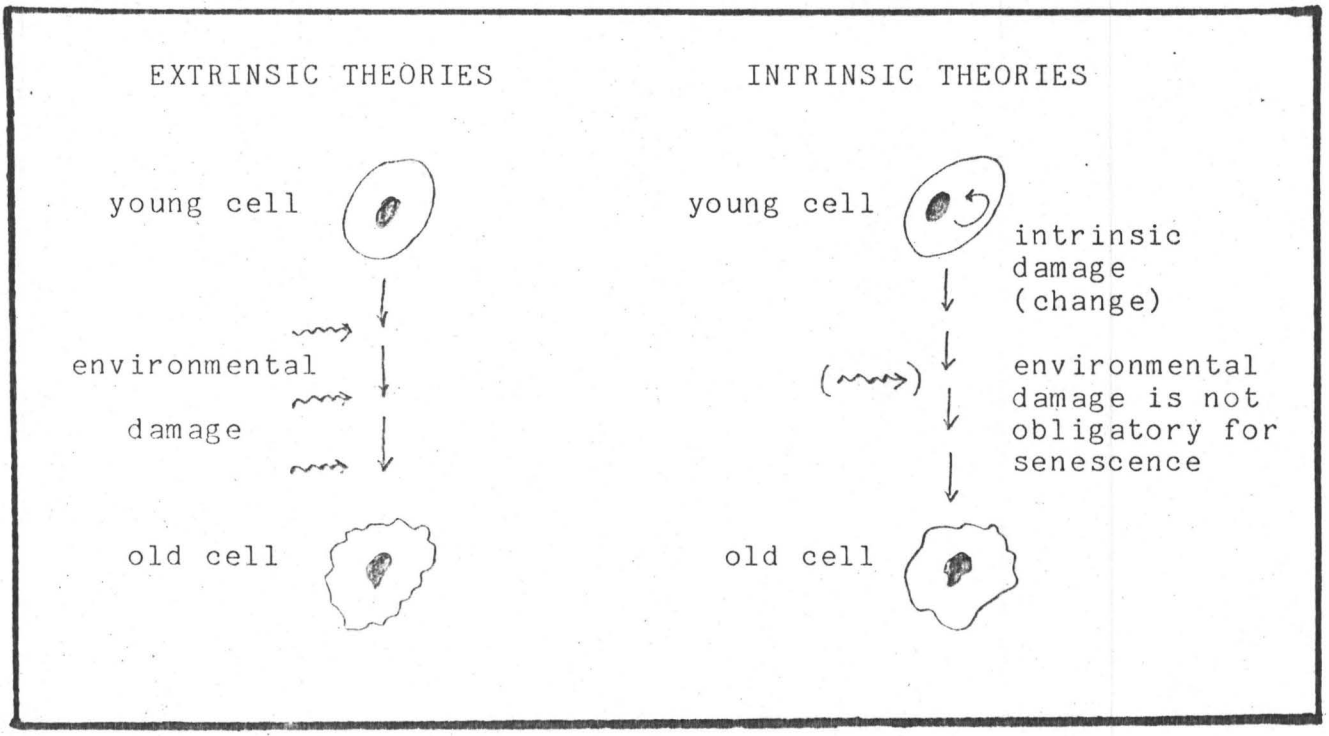

Figure 1-2

Theories of Aging. Extrinsic theories postulate that environmental damage to either genetic or nongenetic material is sufficient and necessary for senescence. Intrinsic theories do not involve environmental damage in the mechanism of aging; a genetic clock or intrinsic errors in the cellular apparatus result in time dependent loss of function.

organism could be put in an environment in which it did not senesce, then the aging mechanism would be of the extrinsic type.

1.2.2.1 Extrinsic Mechanisms of Aging

(a) Mutational Theory

Since all environments contain mutagenic agents, including cosmic rays, trace levels of radioactive atoms and certain natural chemical compounds, it is possible that the inevitable senescence of metazoan organisms is a result of accumulated damage to somatic cells by these agents. Support for this theory comes from studies which showed that ionizing radiation accelerated certain aspects of the aging process in experimental animals (Prasad, 1974). Furthermore, the ability to activate or inactivate mutagenic compounds in the environment may influence the lifespan of the organism. Schwartz and Moore (1977) found an inverse correlation between the binding to DNA of 7,12-dimethylbenz(a)anthracene, a known mutagen, and species lifespan. The correlation was highly significant with cells from six species ranging from rat (lifespan 3.5 years) to man (lifespan 110 years). However, these studies may be coincidental. The similar effects of radiation damage and natural aging do not necessarily imply similar causes, and it remains to be seen whether the findings of Schwartz and Moore (1977) extend to other species and mutagens.

Attempts to achieve the perfect environment for cells or organisms have not resulted in a substantial increase in the lifespan (Upton, 1977). However, it is possible that lifespan is regulated by a background mutagenic level which cannot be altered (eg. cosmic radiation), or by mutagenic agents arising from within the cell itself (in which case the mutational theory of aging becomes an intrinsic theory (section 1.2.2.2)).

(b) Theories of Environmental Damage to Nongenetic Material

In this category are theories which propose that age related changes to extracellular or intracellular macromolecules (other than DNA) are the direct cause of cellular or organismic death (Kohn, 1971; Zs.-Nagy, 1978). For example, cross linking of collagen from free radical or oxidative attack or the natural action of lysyl-oxidase on susceptible lysine residues causes in time the connective tissue of old individuals to become inflexible (for review, see Balazs, 1977). This could hamper tissue and organ function and possibly provide a barrier to the diffusion of nutrients. Although this might explain many aspects of the aging phenotype (Kohn, 1971), such theories cannot readily account for the senescence of cultured cells after a critical number of divisions (Harley and Goldstein, 1978).

1.2.2.2 Intrinsic Theories

Intrinsic theories of aging assume that cells senesce as a result of their inherent genotype, regardless of deleterious effects from the environment. Such theories are subdivided according to whether the progressive, time dependent change (the "clock") occurs within the DNA itself, or within some nongenetic component. Theories belonging to the former class are often termed "programmed death" or "terminal differentiation" theories. Theories belonging to the latter class have often been mistaken for extrinsic theories but might be more appropriately classified as "intrinsic-error" theories: the progressive loss of function is associated with a phenotypic "defect", but its source is genetic.

(a) Terminal Differentiation

The loss of proliferative capacity in cultured cells has been termed terminal differentiation (Hayflick, 1973; Martin, 1974; Holliday et al., 1977; Engelhardt et al., 1979; Bell et al., 1979; Kontermann and Bayreuther, 1979) No gross changes in aging cells could be shown to account for their sudden loss of replicative capacity, and once nonmitotic, these cells remained viable for extended periods of time. These observations are consistent with the playing out of a genetic program which simply limits replicative lifespan.

But if in fact the finite lifespan of cultured cells is

an example of classical differentiation, this does not weaken its use as a model of aging. If function depends on the presence of healthy cells, then senescence (the diminution or loss of certain functions with age) could be the result of an increasing fraction of terminally differentiated cells.

There have been several proposals of mechanisms for programmed senescence (for review, see Holliday, 1975). Only two theories of terminal differentiation which have recently attracted attention are discussed below.

(i) Commitment Theory

Kirkwood and Holliday (1975a) and Holliday et al. (1977) have proposed a commitment theory to explain the finite lifespan in culture of human diploid fibroblasts. In brief, they assert that all cells initially belong to a class of uncommitted or immortal cells. At each division a fraction of these cells enters the committed or mortal class which after an additional number of divisions ceases to divide. As the culture expands, the uncommitted population accounts for a diminishing fraction of the total. Since this fraction is about 10^{-6} after 43 generations (about passage 20) (Holliday et al., 1977), there is a good chance of losing the uncommitted population by generation 43 if the number of cells retained at each subcultivation is not greatly in excess of 10^{6}. The authors conclude that the finite replicative lifespan of human fibroblasts is an artifact created by carrying a relatively small number of cells in

culture. However, on the basis of changes in the fraction of nondividing cells with passage, it has been argued that the commitment theory of cellular aging is untenable as proposed, and that even if the theory were correct in principle, the finite lifespan of human fibroblasts would still reflect the age-dependent decline of cellular function *in vivo* (Harley and Goldstein, 1980).

(ii) Marginotomy

Olovnikov (1971) conjectured that since DNA polymerase cannot replicate the ends of linear duplex DNA (see Watson, 1972), somatic cells may experience a progressive loss of marginal DNA at each generation, a process he termed "marginotomy". Once "buffer" telogenes are exhausted, lethal deletions are made, or possibly further replication is halted by the lack of some essential component provided by the telogenes (for example, initiation sites).

Olovnikov suggested that highly repetitious DNA found in all eukaryotic organisms (Britten and Kohne, 1968) may play the role of telogenes. Evidence consistent with this theory was found by Shmookler Reis and Goldstein (1979), who showed that human fibroblasts apparently lose a fraction of certain populations of repetitious DNA during their *in vitro* lifespan. However, loss of repetitious DNA *in vitro* may be accounted for by other mechanisms including unequal recombination, if recombinants with a reduced repetitious DNA content have a selective advantage (Harley et al., 1979b).

Mechanisms to overcome marginotomy allowing indefinite growth potential in germ cells, unicellular organisms, transformed cells, viruses and other small replicating systems are discussed in detail by Olovnikov in a subsequent paper (1973).

(b) Intrinsic-error Theories

A basic premise of all theories of cellular aging is that each zygote commences life with a "clean" or "clean-as-can-be" set of macromolecules and cellular constituents. In intrinsic-error theories of aging, the progressive loss of cellular function is part of the intrinsic nature of the cellular apparatus, as dictated by the genotype. This loss of function is independent of deleterious effects from the environment (cf. section 1.2.2.1).

(i) Waste-Product Theory

The waste-product theory of aging (Strehler, 1962; Hirsch, H., 1978) assumes that certain products of normal metabolism are injurious to cell function when they reach a critical concentration. Since the medium of senescent cells was shown to contain no toxic substances (Hayflick and Moorhead, 1961; Hayflick, 1965), the waste product is necessarily intracellular. A well studied candidate for this substance is lipofuscin (Schneider and Nandy, 1977), but no direct evidence is available to show its noxious effect on

cells.

(ii) Error Catastrophe Theory

Orgel (1963) argued that since it is impossible for any real system to operate with perfect fidelity, errors in self-replicating systems could become autocatalytic, ultimately leading to loss of function. This theory is appealing for its relevance to aging and its testability. Hence it has become famous as "Orgel's Error Catastrophe Theory of Aging" even though Orgel made it clear that he was not proposing a mechanism of aging per se (Orgel, 1963).

Orgel restricted his discussion of error catastrophe to the protein synthetic apparatus, but it could also be applied to DNA or RNA replicating systems. In brief, Orgel first proposed that the initial error content p would be increased at each generation by an amount linearly proportional to the number of errors present at the previous generation:

$$dp/dt = kp$$

The solution to this equation is

$$p = p_o e^{kt}$$

which shows that the error content increases exponentially for all positive values of k (i.e. all allowable values of positive feedback).

Orgel (1970) later corrected this original treatment by extending the form of dp/dt to include all forms of linear dependence on p:

$$dp/dt = R + (k-1)p$$

In a discrete system where p_n denotes the error level at generation n and the error content of the first generation is the residual R, the solution to this equation is

$$p_n = R(1 + k + k^2 + \ldots + k^{n-1})$$

Values of k greater than 1 lead to increasing error levels as before, but now values of k less than 1 lead to a steady state error frequency of R/(1-k). Orgel warned that arguments concerning the value of k are subtle and k may not be greater than 1 under all circumstances. In essence, this modification allows for the possibility that the synthetic efficiency of error-containing proteins may not be as great as that of normal proteins. A mathematical analysis of the cellular parameters affecting k has been given by Hoffmann (1974), modified by Kirkwood and Holliday (1975b), and the evidence keenly debated by Burrans and Kurtz (1977), Gallant and Palmer (1978), and Kurtz (1979).

Escape from the error catastrophe was discussed by Orgel, but not in terms of cellular transformation. Normal cells may achieve very long or indefinite lifespans by rapid degradation of aberrant protein or by genetic selection of proteins which give either particularly low error frequencies or are inactivated by any amino acid substitution. However, Orgel beleived that such molecular mechanisms were inadequate. He proposed instead selection at the cellular level. Holliday (1975), on the other hand, proposed that transformation might affect parameters leading to

stabilization of error rates, thus preventing the putative catastrophe and establishing immortality at an error frequency above that of young cells. In any event, if error-containing proteins are the cause of cell death, terminal cells should have a greater abundance of aberrant protein and/or higher error frequencies than either young cells or transformed cells. Direct experimental testing of this prediction has not been done because of difficulties in obtaining quantitative estimates of the error frequency during normal protein synthesis. Although direct measurements of error frequencies in proteins of animal cells by analysis of sequence and composition were made in 1963 (Loftfield, 1963) and refined in 1972 (Loftfield and Vanderjadt, 1972), this technique has not been applied to the study of aging. A great deal of indirect evidence supporting the catastrophe theory has maintained interest in the hypothesis to this date. Lewis and Holliday (1970) found evidence in certain aminoacyl-tRNA synthetase mutants of Neurospora that senescence was associated with an increased synthesis of defective protein. Holliday and Tarrant (1972) showed that cultured cells accumulate heat-labile enzymes during the final stages of their lifespan. In fact, numerous examples of age-related changes in activity or heat lability of enzymes has been found both in vitro and in vivo (see Hayflick, 1977). Insects and mammals fed nontoxic doses of amino acid analogs accumulate aberrant protein and experience shortened lifespans (Harrison and Holliday, 1967; Holliday and Stevens,

1978). And proteins from terminal-passage cells *in vitro* appear to be degraded at elevated rates (Bradley et al., 1975).

However, for each item supporting the error catastrophe theory, there is at least one parallel, contrary example. Thus, many proteins do not lose activity with age (see Hayflick, 1977) and for those that do, alternative explanations are readily available (Duncan et al, 1977; Gershon, 1979; Rothstein, 1979); amino acid analogs do not always shorten *in vitro* or *in vivo* lifespan (Ryan et al., 1974; Shmookler Reis, 1976); late-passage cells fully support viral replication (Holland et al., 1973) and these viruses are not heat labile (Csullog, 1976); induction of high level errors in *E. coli* does not lead to error catastrophe (Gallant and Palmer, 1979a); several tissues from old mice do not incorporate increased amounts of amino acid analogs (Hirsch et al, 1978); cell-free preparations of the protein synthetic apparatus from old liver (Kurtz, 1975) or late-passage human cells (Wojtyk and Goldstein, submitted) do not show elevated error frequencies in translating synthetic mRNA. And not all studies have shown increased degradation of cellular proteins in old cells (see for example, Prasanna and Lane, 1979).

However, none of these studies directly tests whether amino acid substitution is naturally elevated in late-passage cells or in cells from old donors. In section 3.1 the first measurements of this kind are described. The results do not support the error catastrophe theory of aging.

1.3 Protein Turnover: Synthesis and Degradation

1.3.1 Mechanisms of Protein Synthesis

Like all polymer reactions involving linear condensation of monomers, synthesis of proteins can be considered in three steps: initiation, elongation, and termination. However, unlike most polymer reactions, protein synthesis is a highly ordered process involving complex interactions between precursors, template, and the synthetic apparatus. During the synthesis of a typical protein, there are about 300 to 400 elongation processes between each initiation and termination. Consequently, except for special cases, considerations of fidelity require a more detailed analysis of elongation. The short review below outlines the present knowledge of protein synthesis in eukaryotic cells, with additional information on elongation borrowed from the prokaryotic systems. For more thorough reviews and references for most of what is simply stated in this section, see Safer and Anderson, 1978; Kozak, 1978; and Sprinzl and Cramer, 1979.

1.3.1.1 Initiation

Initiation is the assembly of ribosomes, mRNA and initiator met-tRNAi by various factors into a competent 80S initiation complex (figure 1-3a). Newly released 40S ribosomal subunits bind eIF-3 to form native 40S ribosomal subunits 40Sn, which in turn binds met-tRNAi through the

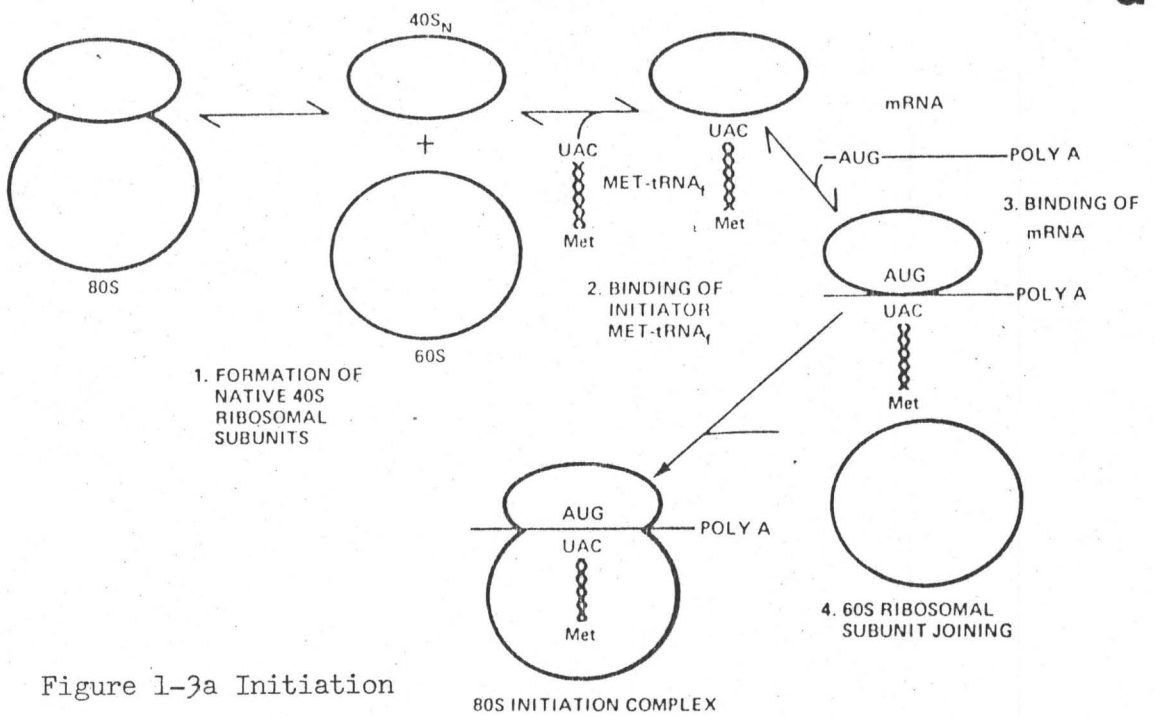

Figure 1-3a Initiation

The four basic steps in the pathway of 80S initiation complex formation

Formation of native 40S ribosomal subunits. The first step of 80S initiation complex formation is the binding of eIF-3 to the 40S ribosomal subunits which are released upon termination of polypeptide synthesis. No other initiation factors or energy source are required. Binding of eIF-3 to form 40S$_N$ prevents the spontaneous reassociation of 40S and 60S ribosomal subunits that would occur under in vivo ionic conditions. In vitro, formation of inactive 80S ribosomal couples is promoted by decreased K^+/Mg^{++}. Other major components associated with 40S$_N$ are Met-tRNA$_f$ hydrolase and eIF-2A.

Met-tRNA$_f$ binding to 40S$_N$. The second step of 80S initiation complex formation is the binding of Met-tRNA$_f$ to 40S$_N$. This is accomplished through the formation of a ternary complex composed of Met-tRNA$_f$, eIF-2, and GTP. eIF-1 and eIF-4C appear to stabilize the [40S:eIF-3:eIF-2:Met-tRNA$_f$:GTP] preinitiation complex. Physiological regulation of this early step of protein synthesis may be mediated through the greater affinity of eIF-2 for GDP than GTP. This results in the formation of an inactive eIF-2:GDP binary complex when the energy charge of the cell is low. Binding of the ternary complex occurs independent of the initiation codon AUG. In contrast, mRNA binding is absolutely dependent on Met-tRNA$_f$ binding to 40S$_N$.

Binding of mRNA to the 40S preinitiation complex. The third step of initiation complex formation is mRNA binding to the [40S:eIF-3:eIF-2:Met-tRNA$_f$:GTP] complex. Three initiation factors are required for translation of mRNA: eIF-3, eIF-4A and eIF-4B. It is not known at the present time whether the eIF-3 already bound to 40S$_N$ can serve this function. Actively translated messenger RNA is associated with characteristic proteins which appear to be tightly and specifically bound to the mRNA. The relationship of these proteins to initiation factors is unknown, but no convincing evidence has been obtained for the general existence of message-specificity factors (see text). Binding of these ribonucleoprotein particles (mRNP) requires ATP hydrolysis.

60S ribosomal subunit joining. Joining of the 60S ribosomal subunit to the 40S$_N$-mRNA complex is associated with release of bound eIF-2 and eIF-3. eIF-5-dependent GTPase activity appears to mediate factor release prior to 80S initiation complex formation. A stable association of eIF-5 with the Met-tRNA$_f$:40S$_N$:mRNA complex has not been observed. Indirect evidence for an eIF-2 recycling mechanism before reformation of the ternary complex by released eIF-2 has been obtained (see Section V.F.3).

Figure 1-3

Steps in protein synthesis. Figures1-3a (initiation) and 1-3b (elongation) are taken directly from Safer and Anderson (1978).

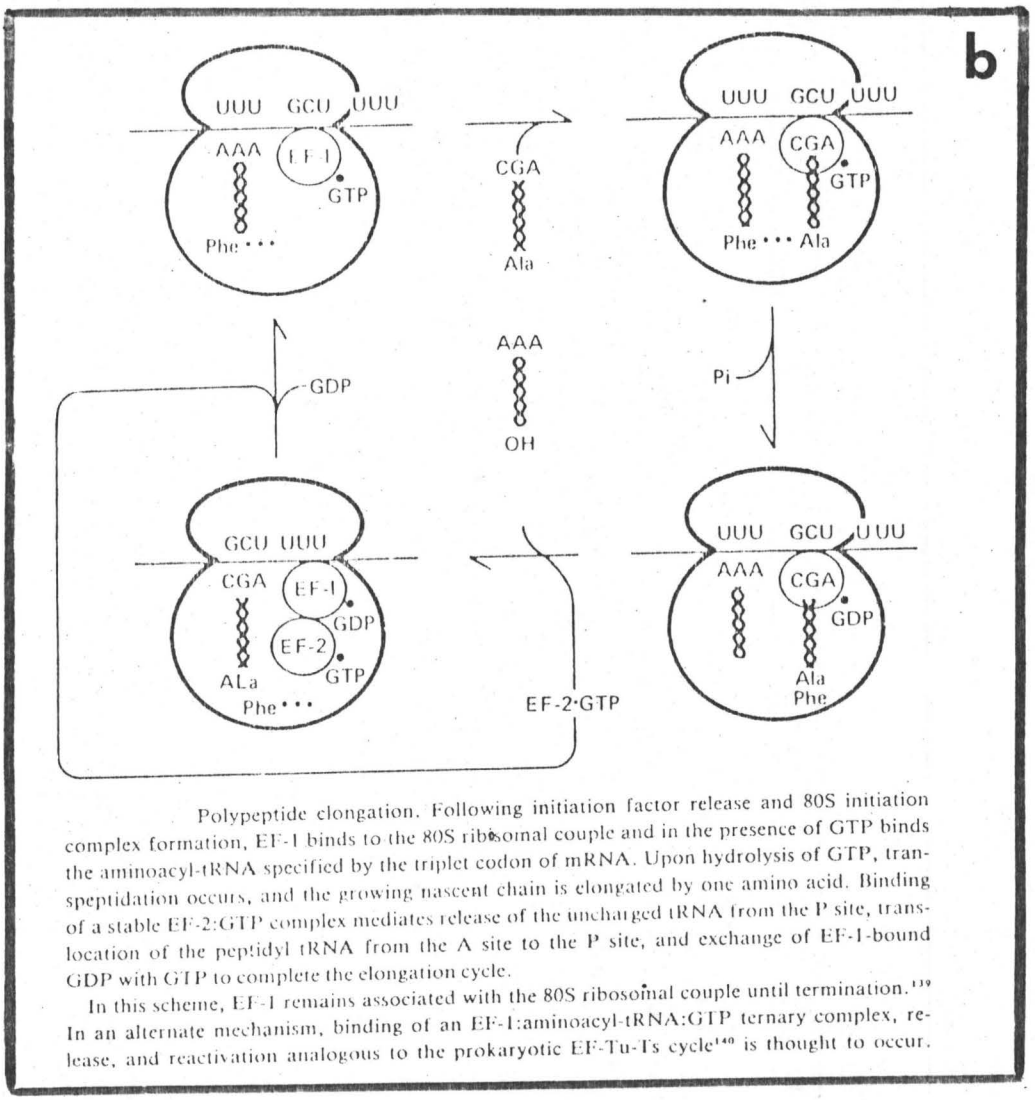

Polypeptide elongation. Following initiation factor release and 80S initiation complex formation, EF-1 binds to the 80S ribosomal couple and in the presence of GTP binds the aminoacyl-tRNA specified by the triplet codon of mRNA. Upon hydrolysis of GTP, transpeptidation occurs, and the growing nascent chain is elongated by one amino acid. Binding of a stable EF-2:GTP complex mediates release of the uncharged tRNA from the P site, translocation of the peptidyl tRNA from the A site to the P site, and exchange of EF-1-bound GDP with GTP to complete the elongation cycle.

In this scheme, EF-1 remains associated with the 80S ribosomal couple until termination.[139] In an alternate mechanism, binding of an EF-1:aminoacyl-tRNA:GTP ternary complex, release, and reactivation analogous to the prokaryotic EF-Tu-Ts cycle[140] is thought to occur.

Figure 1-3b Elongation

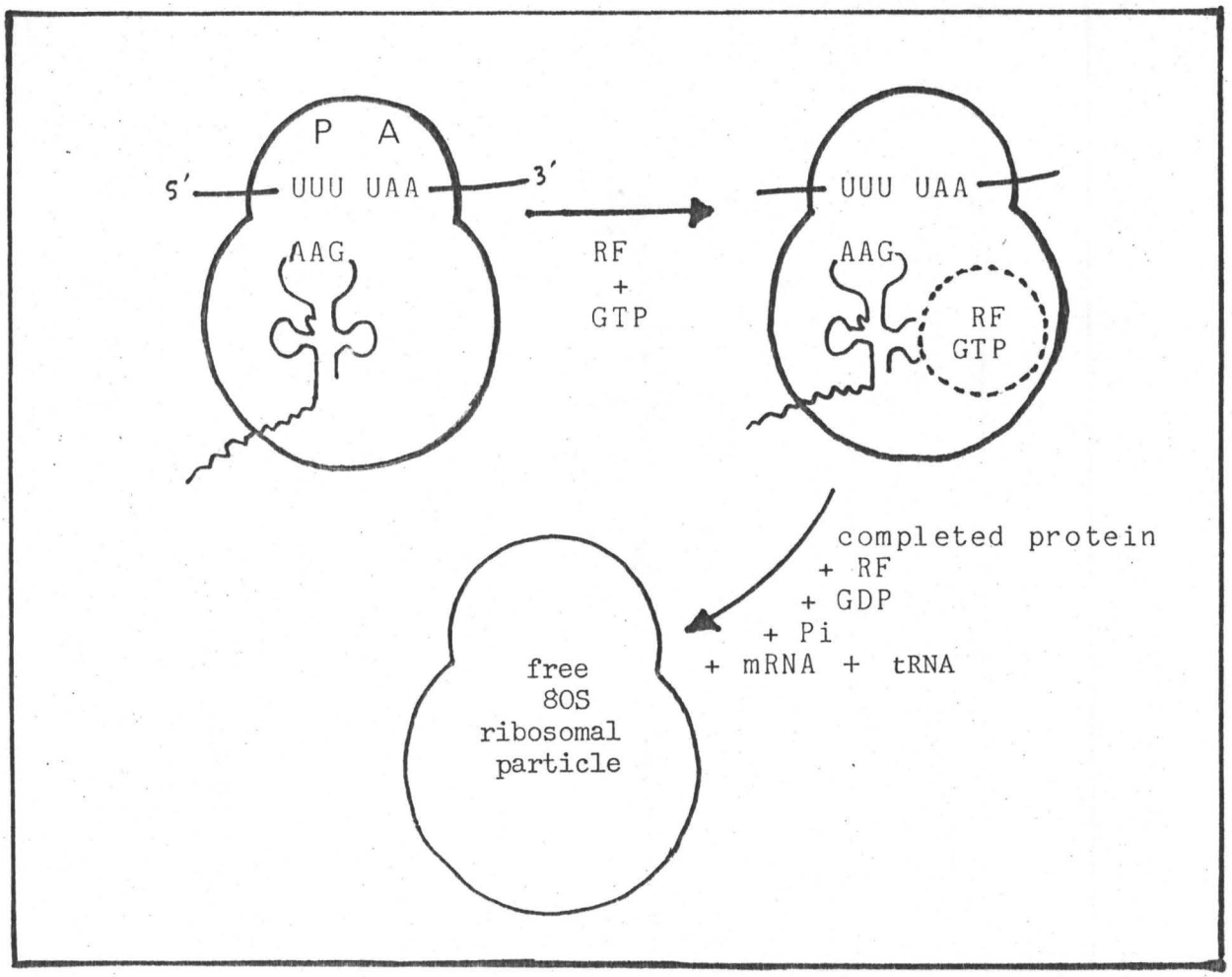

Figure 1-3c Termination

Alignment of a termination codon in the A site allows binding of release factor (RF) and GTP. This stimulates hydrolysis of the peptidyl-tRNA ester bond, presumably by peptidyltransferase, and comcomitant hydrolysis of GTP. Release of the completed protein and other components liberates the ribosome couple, which after dissociation, can reinitiate on mRNA (Figure 1-3a).

ternary complex eIF-2.GTP.met-tRNAi. The preinitiation complex GTP.met-tRNAi.40Sn (still containing eIF-2 and eIF-3) then binds the initiator sequence of an mRNA in an energy-dependent series of steps. Factors eIF-4A, eIF-4B and ATP are required in this process. The final step in the formation of the 80S initiation complex is the binding of a 60S ribosomal subunit to the GTP.met-tRNAi.40Sn.mRNA preinitiation complex. This step requires eIF-5 and at some time prior to or just after the 60S binding, the other initiation factors are released.

The sequence of bases on the 5' side of the message's initiation codon and the 5'-m7G(5')pppN "cap" are important for binding of eukaryotic mRNA to the preinitiation complex. A cap binding protein and other specific factors associated with the 40S ribosomal subunit may be involved in recognition and binding of the proper initiation sequence. It has been suggested that the ATP hydrolyzed in this step may be required for translocation of the bound complex to align the met-tRNAi anticodon with the start codon.

1.3.1.2 Elongation

Elongation is the sequential addition of amino acids to the nascent polypeptide chain (Figure 1-3b). Elongation factor EF-1 binds non-initiator aminoacyl-tRNA in the presence of GTP to the A site of 80S ribosomal-(mRNA) couples, and upon hydrolysis of GTP an amide bond is formed between the -carboxyl group of met-tRNAi or peptidyl-tRNA in

the P-site and the free -amino group of the aminoacyl-tRNA in the A-site. Deacylated tRNA is released from the P site before a second factor EF-2, also requiring GTP hydrolysis, mediates translocation of the new peptidyl-tRNA and associated mRNA codon from the A site to the P site.

In E.coli , EF-Tu is roughly analogous to eukaryotic EF-1. It has been shown that the presence of an aminoacyl residue on the tRNA is an absolute requirement for formation of the ternary EF-Tu.GTP.aa-tRNA complex; uncharged tRNA, fMet-tRNAf, and N-acetylaminoacyl-tRNA are not substrates. Although EF-Tu recognizes both 2'- and 3'-aminoacyl derivatives of charged tRNA, the binding constant for the 2' isomer is somewhat smaller. It is thought that since 2'-isomers are required in the elongation process, once the ternary complex is formed, EF-Tu catalyzes conversion of all 3'-isomers to 2'-isomers (Sprinzl and Cramer, 1979).

Extensive work with "nonisomerizable"-tRNA and tRNA fragments in studies of binding of ternary complexes to competent ribosomes and subsequent peptidyl transfer has provided evidence for the following scheme:

(i) EF-Tu.GTP accepts either 2'- or 3'-aminoacyl-tRNA species, but after binding, EF-Tu.GTP.2'-aminoacyl-tRNA is formed exclusively and this complex binds to the ribosome A site. In the 2' position, the α-amino group of the amino acid .oiety is held away from the active ribosomal peptidyltransferase center by EF-Tu. No amide bond can be

formed in this configuration of the aminoacyl-tRNA.

(ii) If the tRNA-mRNA interaction occurring at the other end of the molecule is cognate, hydrolysis of EF-Tu-bound GTP takes place. If the interaction is noncognate, the entire EF-Tu.GTP-aminoacyl-tRNA complex falls off the ribosome (most of the time, see section 1.4.2.2).

(iii) After GTP hydrolysis, EF-Tu.GDP release occurs and the aminoacyl residue moves to the 3' position by transacylation. In the 3' position, ribosomal proteins hold the -amino group of the aminoacyl-tRNA in the reactive ribosomal peptidyltransferase center and formation of a new peptide bond is allowed. Accompanying GTP hydrolysis the new 3'-peptidyl-tRNA in the A-site is translocated, with its codon, to the P site which is vacated by the deacylated tRNA.

According to this model, the function of EF-Tu on the ribosome in holding the aminoacyl-tRNA in the 2' position is to provide sufficient time for codon-anticodon recognition before irreversible peptide bond formation occurs. EF-Tu thus plays a critical role in the fidelity of translocation.

In the P site, the function of the 2'-hydroxyl is not clear, although it is required for peptidyl transfer. It may be involved in activation of the peptidyl-ester bond, interaction with the ribosome, or in accepting the peptidyl chain as an intermediate step in transfer to the A site aminoacyl-tRNA.

1.3.1.3 Termination

Release of completed peptides from peptidyl-tRNA on the P site of the ribosome at the last sense codon is achieved after recognition of the terminator codon (UAA, UAG or UGA) in the A site by release factor RF (Figure 1-3c). The first step in the recognition process is binding of RF and GTP to the termination codon-A site region. RF and peptidyl transferase then interact, with concomitant hydrolysis of GTP, to hydrolyze the ester bond of the peptidyl-tRNA. RF is then dissociated from the ribosome. The ribosomal couple transiently dissociates into free subunits upon subsequent release from the mRNA. Nonenzymatic reassociation of the subunits to non-functional 80S couples is favored, but the stoichiometric binding of eIF-3 to 40S units prevents nonspecific binding of the 60S subunit and initiates the sequence of events leading to formation of another initiation complex.

1.3.2 Models of Protein Synthesis

Various models of protein synthesis have been devised to answer specific questions. Vassart et al. (1971) developed a computer program to simulate translational control of protein synthesis at the level of initiation, elongation or termination. They analyzed in particular the effects of initiation frequency and overall elongation rate on polysome profiles and the rate of protein synthesis. Within the limitations of their assumptions, they concluded that

enhanced initiation results in a shift of polysome profiles towards heavier polysomes and an increased synthetic rate, with only a slight increase in transit time. Reduced initiation has the opposite effects. Increased rates of elongation cause a shift of polysomes to lighter aggregates, a transient increase in protein synthetic rate (unless elongation is limiting) and a possible queue at the 3' end of the message. Reduced elongation rates will cause the ribosome number on mRNA to increase, synthetic rate to decrease, transit time to increase, and a homogeneous distribution of ribosomes on mRNA. These effects are all fairly intuitive.

Lodish (1974) used the model of MacDonald and Gibbs () to derive analytical expressions for the synthesis of protein as a function of factors which affect initiation. His theoretical results were in accord with known changes in the relative rates of α- and β-globin synthesis in the presence of initiation inhibitors where preferential inhibition of mRNAs with low rate constants for initiation were observed.

Neither Vassart nor Lodish however allowed the rate of elongation to vary along the message. Evidence suggesting slight variations in the elongation rate of ribosomes, possibly resulting from mRNA secondary structure, has been provided by analysis of length distributions of nascent polypeptides (Naughton and Dintzis, 1962; Nishimura, 1972; Prozel and Morris, 1974;). However, other data have failed to

resolve any such variations (Winslow and Ingram, 1966; Hunt et al., 1968; Hunt et al., 1969; Luppis et al., 1972). It would appear that during normal protein synthesis, the rate of ribosome movement along the mRNA is relatively uniform. Nevertheless, Heijne et al. (1978) analyzed simulations of protein synthesis to determine which characteristics best distinguish between models that propose a constant rather than a variable elongation rate.

Ames and Hartman (1963) proposed that mRNA translation could be regulated by availability of certain tRNAs: elongation would be slowed at codons for which the corresponding aminoacyl-tRNAs were limiting. Smith (1975) provided evidence that the availability of all tRNAs except the leucine tRNA species in reticulocytes follows their usage in globin mRNA translation. He suggested that leucyl-tRNA might be limiting and provides a rate limiting step for control of globin translation. Evidence for such control is not available and Litt (1976) has questioned Smith's data pointing out that measurements of absolute tRNA concentrations are difficult. However the effects of tRNA restriction on inhibition of protein synthesis are well documented in cell-free systems. Holmes et al., (1978) showed that in extracts of E.coli , restriction of leucine tRNA apparently blocked ribosomal movement at leucine codons in MS2-RNA.

Starvation of cells for a single amino acid may have a

similar effect on protein synthesis *in vivo* as restriction of tRNA *in vitro* since the amount of the corresponding aminoacyl-tRNA is reduced in both instances. However it is important to distinguish between the effects due to absence of charged tRNA in preventing ribosome movement at the relevant codon and effects of uncharged tRNA on other translational parameters. For example, uncharged tRNA may play a role in regulation of protein synthesis at the level of initiation (Allen et al., 1969; Vaughan and Hansen, 1973; Stanners et al., 1978; Lofgren and Thompson, 1979). The effects of amino acid starvation on initiation and elongation rates in intact cells and its implications for mistranslation are discussed in greater detail in sections 1.5 and 3.2.

1.3.3 Protein Degradation

Extensive reviews of the literature on protein degradation are given by Goldberg and Dice (1974), Goldberg and St. John (1976), Fox (1976), and Ballard (1977). Assertions made in this section without specific references can be found in these reviews. There have been many differences found between various cell types in the regulation and mechanisms of protein degradation, and a comprehensive review of the literature is not possible here. Within the aging field there are also conflicting results. This section will only provide a superficial introduction to studies of proteolysis in cultured cells.

Degradation can occur by the action of neutral proteases in the cytoplasm or by acid optimum proteases in lysozymes. Overall rates of protein degradation are influenced by the nutritional status of the cell, such as amino acid concentration, freshness of serum, and presence of certain hormones. Some cells exhibit dependence of degradation rates on stages of growth (ie. quiescent vs exponential growth) while others do not (see Baxter and Stanners, 1978). Viral transformation of some cells but not others affects degradation and its regulation (see Ballard, 1977; and Bradley 1977). Finally, the physical properties of individual proteins influence their susceptibility to proteolytic attack. There is a correlation between size and isoelectric point of proteins and their degradative rate (see Dice et al, 1979) and many studies have shown that error-containing proteins are degraded at enhanced rates (see Ballard, 1977).

Bradley et al. (1975) first showed that terminal-passage WI38 fibroblasts accumulate proteins which are more susceptible to proteolytic attack; late-passage cultures which still had at least one population doubling remaining before death did not show this effect. Later, they indicated that short-lived proteins were turned over at a greater rate in late-passage cultures (Bradley et al., 1976). Furthermore, late-passage WI38 cells did not degrade canavanine-containing proteins as efficiently as early-passage cells.

Dean and Riley (1978) found that late-passage MRC5 fibroblasts degraded normal and canavanine-containing proteins as efficiently as early- passage MRC5 fibroblasts. Their results were consistent with the observations of Shakespeare and Buchanan on early- and late-passage MRC5 (1976). In cultures of chick embryo fibroblasts, Kaftory et al. (1978), found that slow growing late-passage cells had reduced synthetic and degradative rates compared to early-passage cells, but were not impaired in their ability to degrade abnormal puromycin peptides. Interestingly, in one study of aging in an intact organism (a nematode) the rate of total protein degradation declined progressively during aging (Prasanna and Lane, 1979).

Part of the reason for the discrepancies in results from different laboratories may reside in the different experimental protocols used. Reutilization of amino acid from protein degradation prior to equilibration with the external pool in either pulse-chase or approach to equilibrium methods of measuring degradation causes an overestimation of the protein half-lives. To minimize reutilization excess unlabeled amino acid is routinely used during the chase of labeled proteins. However, since degradation is sensitive to amino acid concentration, this may affect the turnover of protein. For short pulse-chase experiments, the acid-soluble pool of radioactive material in the cell is as large or larger than the acid-insoluble pool. It is impossible to

know exactly how much of that pool represents amino acid from the medium or amino acid from protein degradation. Extensive rinsing with cold or warm medium could adversely affect protein degradation. The method of labeling protein to equilibrium to obtain overall turnover rates overcomes some of these difficulties (Bradley et al., 1976). In chapter 2, I report studies on protein turnover in young and old cells using this method.

1.4 Mistranslation

Errors in information flow from generation to generation can occur during the replicative or synthetic phase of the major macromolecules (DNA, RNA, protein) or during their post-synthetic lifetime. Mistranslation relates only to errors in synthesizing protein from an mRNA template. We assume that the mRNA contains a "proper" coding sequence: it need not be the correct transcript of the DNA, but it must contain a sequence of 3n nucleotides (n, a whole number) between an initiation and termination sequence. Errors in translating this mRNA into the unique polypeptide which it specifies are of two major types: synthetase errors and ribosomal errors.

1.4.1 Synthetase Errors

1.4.1.1 Nature of Synthetase Errors

Aminoacyl-tRNA synthetases (amino acid:tRNA ligases) could conceivably make four types of errors (figure 1-4).

Error Type	Amino Acid	Synthetase	tRNA	Product
(none)	X	Sx	tRNA-X	X-tRNA-X
1	X	Sz	tRNA-X	X-tRNA-X
2	Y	Sx	tRNA-X	Y-tRNA-X
3	X	Sx	tRNA-Y	X-tRNA-Y
4	Y	Sx	tRNA-Z	Y-tRNA-Z

Figure 1-4

Types of Aminoacyl-tRNA Synthetase Errors

Errors of type 1 and 4 require a double recognition error and may be extremely infrequent; they are included for completeness only. No direct evidence exists for misacylation *in vivo* (but see 1.4.1.3 below). However both amino acid- and tRNA-recognition errors have been observed *in vitro*. For example, leucyl-tRNA synthetase will acylate valine to tRNA-leu and phenylalanyl-tRNA synthetase will acylate phenylalanine to tRNA-val. While examples of amino acid-recognition errors are numerous in both homologous and heterologous systems (intra- and inter-species, respectively), instances of tRNA-recognition errors are mainly confined to heterologous systems (Loftfield, 1972).

Loftfield could cite only one case of a synthetase ligating its cognate amino acid to a noncognate but homologous tRNA: formation of valyl-tRNAile (Arca et al., 1967). One other example which has appeared in the literature is the formation of ile-tRNA-phe E.coli by isoleucyl-tRNA synthetase E.coli (Yarus, 1972). Since it appears that the overall tRNA shape is involved in recognition (see Loftfield, 1972), one could argue that the synthetase has more specificity for its cognate tRNA than its cognate amino acid. However, another explanation for the low frequency of tRNA-recognition errors is available. A comparison of the K_m's for amino acids and tRNAs indicates that the synthetases will be complexed to their cognate tRNA most of the time (Jacobson, 1968). Therefore, under physiological conditions synthetases may not have the opportunity to acylate noncognate tRNAs: not only do they have a lower affinity for the noncognate tRNA, they must also compete with the correct synthetase. It is for this reason that measures of synthetase fidelity in isolated systems may not be indicative of misacylation in vivo . Parallel charging of tRNAs by their respective synthetases will lower the frequency of misacylation well below that observed in assays in vitro . Furthermore, the binding to the synthetase of the cognate tRNA has been shown to increase the fidelity of the subsequent binding of the amino acid (Loftfield and Eigner, 1965).

Nevertheless, noncognate amino acids are plentiful and if amino acid shares charge and shape properties with the cognate amino acid, it may bind to the synthetase-cognate-tRNA complex and lead to misacylation (for review, see Loftfield, 1972). Therefore the contribution of synthetase errors to mistranslation of mRNA will chiefly be a function of the ability of the synthetase to distinguish one amino acid from another in charging its cognate tRNA. It is noteworthy that Savageau and Freter (1979b) analyzed the energy cost and efficiency of proofreading aminoacylation and found that net error rates due to faulty tRNA recognition are much less frequent than the net error rate due to certain cases of faulty amino acid recognition. These arguments will become crucial to a consideration of misacylation during amino acid starvation (sections 1.5.3 and 3.1, 3.2).

The amino acid moiety of the aminoacyl-tRNA plays no role in codon-anticodon recognition (Chapeville et al., 1962). Indeed, this lack of an effect first observed by chemically reducing cys-tRNA-cys to ala-tRNA-cys has been extended to tRNA chimeras as unlikely as phe-tRNA-val produced in heterologous systems (Jacobson, 1966). However, there is probably a nonspecific recognition of the ligated amino acid on the 3'-end of the tRNA by the ribosome since uncharged tRNA apparently does not bind, or binds very poorly, to ribosomes (Gordon, 1967; Skoultchi et al., 1968, Sprinzl and Cramer, 1979; but also see section 1.5.1).

1.4.1.2 Mechanism of Aminoacylation and Proofreading

Some controversy exists about the overall mechanism by which a synthetase ligates the amino acid to its cognate tRNA. For some synthetases it is clear that three discrete steps are possible *in vitro* :

$$AA + ATP + Enz \rightleftharpoons Enz.(AA\sim AMP) + PP_i \quad (1)$$

$$Enz.(AA\sim AMP) + tRNA \rightleftharpoons Enz.(AA\text{-}tRNA) + AMP \quad (2)$$

$$Enz.(AA\text{-}tRNA) \rightleftharpoons Enz + AA\text{-}tRNA \quad (3)$$

However, not all synthetases were found to react via an enz.(AA~AMP) intermediate (Mitra and Smith, 1969). Furthermore, kinetic data on the reversible synthesis of ATP from Enz + AA-tRNA +AMP + PP_i have indicated a dependence on pyrophosphate (Jakubowski et al., 1978). Since the first reaction is more rapid than the second in both directions these data are not consistent with the reaction taking place in discrete steps as outlined. Rather, the data suggest a concerted reaction where all four elements Enz, ATP, AA, tRNA are present simultaneously in a quaternary complex during normal aminoacylation (Loftfield, 1972, Jakubowski et al, 1978). Other recent work indicates that two cations are also involved in this complex, for a total of six elements, which therefore should be called senary (Lovgren et al., 1978).

Even though the aminoacylation of tRNAs *in vivo* may proceed through the senary complex, it is clear that an Enz.AA~AMP complex can form *in vitro* with many synthetases,

and the dissection of the pathway into steps has helped to identify the relative importance of different events in the fidelity of tRNA charging. Thus, it was found that isoleucyl-tRNA synthetase and valyl-tRNA synthetase had low fidelity in this step, readily accepting noncognate amino acids. For these synthetases the high specificity of charging was shown to reside in the process of transferring the amino acid to the tRNA (Norris and Berg, 1964). It was later suggested that an editing step occurred involving specific hydrolysis of misacylated tRNA (Yarus, 1972). Different schemes for the mechanism of proofreading have been proposed. "Kinetic proofreading" (Hopfield, 1974) involves differences in the kinetics of substrate binding and hydrolysis of ATP to drive a reaction in which noncognate amino acids are freed from the tRNA at a greater rate than cognate amino acids. Cramer (see Sprinzl and Cramer, 1979) has argued that no evidence exists for kinetic proofreading. In his scheme, the editing function of synthetases is mediated by a hydrolytic action of the nonaccepting hydroxyl at the -N-C-C-A end of the tRNA: a process called "chemical proofreading". Evidence for the function of the nonaccepting hydroxyl is available from studies involving 2'- and 3'-deoxy-derivatives of tRNAs (von der Haar, 1976; Fersht and Kaethner, 1976; Sprinzl and Cramer, 1979).

Earlier, there was some question about the physiological significance of synthetase proofreading (see Bonnet, 1974). However, Fersht and Dingwall (1979a) explain the failure to

find a rapid and specific deacylation of noncognate aminoacyl-tRNA in some systems (i.e. Bonnet, 1974) by the fact that in these studies, misacylated tRNAs were charged with substrates larger than the cognate amino acid were used. Such errors would normally be excluded by steric hindrance and thus, once they occur artificially in vitro , could be expected to resist hydrolytic editing. Presumably, proofreading evolved to limit errors of charging with substrates smaller than or isosteric with the correct amino acid.

In any case, the extensive studies by Fersht and coworkers (for references see Fersht and Dingwall, 1979b) indicate that different synthetases use different mechanisms for achieving high fidelity. For example, in contrast to the low specificity of the leucyl- and valyl-tRNA synthetases for their cognate amino acid, tyrosinyl-tRNA synthetase has an affinity for tyrosine roughly 10^8 times greater than for phenylalanine (the most likely competitor). This discrimination ratio is presumably effected by the specificity of the tyrosyl-tRNA synthetase for the para-hydroxyl group of tyrosine. Similarly, cysteinyl-tRNA synthetase binds cysteine preferentially compared to smaller analogs such as serine and alanine, giving an error rate based on this molecular specificity of less than 10^{-8}. Unless other synthetases mischarge tRNA-tyr or tRNA-cys, the need for a subsequent proofreading mechanism for these tRNAs is obviated. Tyrosyl-tRNA synthetase is one of the few

synthetases that will aminoacylate either the 2'- or 3'-hydroxyl of its tRNA. This observation is consistent with the proposal that the tyrosyl- tRNA synthetase does not have an editing function since the non-accepting hydroxyl of the tRNA is thought to be required for hydrolytic editing (Fersht and Dingwall, 1979a; Sprinzl and Cramer, 1979).

Amino acid analogs such as ∝-aminoisobutyric acid are incorporated into proteins in vivo at detectable levels when supplied as substrate (Hirsch et al., 1978). However, measurements of this type of error give information about natural amino acid substitutions only in proportion to what is known about the relative ability of the synthetase to discrimate between analogs and the natural amino acid during editing.

Although most changes in the base composition of tRNAs have provoked almost no change in the specificity of aminoacylation, some modifications of tRNA can increase the error frequency of charging (see Davies, 1969; Chambers, 1971; Sprinzl and Cramer, 1979). There have been reports of age-related alterations in tRNA methylation and isoacceptor patterns which might account for the reduced ability of synthetases to aminoacylate tRNAs from old drosophila in vitro (see Hosbach and Kubli, 1978a, 1978b), but whether these changes play a role in increasing misacylation has not been determined. In studies on the phenylalanyl tRNA synthetase, Goldstein and Varmuza (1978) reported no

significant differences in the K_m and V_{max} for phenylalanine or ATP in progeria cells or late-passage cells compared to controls.

1.4.1.3 Evidence for Misacylation *in vivo*

Previously Loftfield (1972) had shown that valine was incorporated into normally non-valine containing peptides of rabbit α-globin *in vivo* at a rate of 2×10^{-4} to 6×10^{-3}. This error was assumed to occur by replacement of isoleucine by valine (figure 1-5). Not only is the isoleucine codon similar to that of the valine codon, but the misacylation of tRNA-ile with the smaller substrate valine by the isoleucine synthetase is readily observed *in vitro* (see Loftfield, 1972). Furthermore, Savageau and Freter (1979b) have recently shown that proofreading of val-tRNA-ile occurs at a "high-cost, low accuracy" rate compared to other types of misacylation.

Figure 1-5

Structure of Valine, Isoleucine and Threonine and their Codons

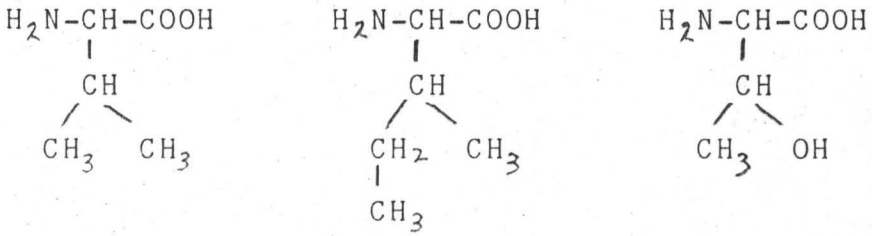

VALINE	ISOLEUCINE	THREONINE
GUU	AUU	ACU
GUC	AUC	ACC
GUA	AUA	ACA
GUG	AUG	ACG

It is therefore surprising that Loftfield and coworkers (Coons et al., 1979) have recently indicated by amino acid sequencing that the error is apparently replacement of a threonine residue with valine. Since the valine and threonine codons are not similar (figure 1-5), such an error probably occurs by infidelity of the threonyl-tRNA synthetase in synthesizing val-tRNA-thr. A tRNA-recognition error by valyl-tRNA synthetase may not be as likely (section 1.4.1.1).

Other explanations for the substitution include a very low level expression of a globin gene which contains the observed replacement (valine-threonine), or a mutant cell expressing an altered α-globin gene. However, these

possibilities are unlikely since a double mutation in the threonine codon is required to generate a valine codon (figure 1-5). Although threonine has the polar hydroxyl group on its β-carbon in place of valine's second methyl group, valine and threonine are roughly isosteric and it is not unreasonable to suggest that the threonyl-tRNA synthetase could misacylate its tRNA with valine. The converse reaction, misactivation of threonine by valyl-tRNA synthetase to form thr-tRNA-val has been observed in vitro (Fersht and Kaethner, 1976). On the other hand, to invoke codon-anticodon mispairing of any sort to explain aberrant valine incorporation, either a second position error must occur; or in the first position, one of U,C or A has to be misread for G; all of these are unlikely ribosomal errors (see Woese, 1978, and section 1.4.2). For incorporation at threonine sites, errors at both first and second positions are required. No form of codon misreading at the third position, the most likely site of ribosomal error, could generate misincorporation of valine. Therefore, valine substitution in protein synthesis may occur most frequently via synthetase errors as suggested by Coons et al., (1979).

It should also be mentioned that one cannot rule out the possibility in these studies that other peptide species may have contaminated the presumed purified peptides from isolated globin, even though several chromatographic steps were employed. Indeed, some preparations had a relatively high apparent substitution frequency (Coons et al., 1979)

which probably reflects difficulty in obtaining essentially 100% purity of the relevant peptide.

1.4.2 Ribosomal Errors

Specificity of codon-anticodon base pairing in the absence of ribosomes depends solely on the differential energy of binding between cognate and noncognate tRNAs at the codon. This energy difference has been estimated at 1-2 kcal and could account for a factor of about 10^{-2} in the error frequency of protein synthesis (Thompson and Stone, 1977). Wobble in the third position of the triplet interaction reduces the specificity of binding even further (Crick, 1966). Since Loftfield (1963) estimated that at least a difference of 5 kcal between correct and incorrect interactions is required to account for a discrimination ratio of better than 3000:1, it seems unlikely that codon-anticodon interactions alone can account for the fidelity of this step of translation. Nonenzymatic binding of tRNAs at the A site was sufficient to decipher the genetic code (Nirenberg and Leder, 1964), but to obtain error rates on the order of 10^{-4}-10^{-5}, ribosomes must utilize specific factors and energy from ATP or GTP hydrolysis (Hopfield, 1974; Jelenc and Kurland, 1979).

1.4.2.1 Nature of Ribosomal Errors

Most of the early work in dissecting codon-anticodon errors came from analysis of synthetic mRNA translation in

vitro using prokaryotic factors and ribosomes and suboptimal translation conditions (for reviews see Woese, 1967; Davies, 1969; Gorini, 1974). It is important to recognize the limitations of these studies. Optimal translation in these systems is well below the synthetic rate in vivo . Undoubtedly this results in part from a low frequency of initiation on mRNAs which lack proper initiation sequences and from disrupting and diluting the components of the synthetic apparatus. But these very factors might influence the nature of errors. Thus, under "optimal" conditions for translation of poly(U) in vitro , incorporation of leucine is 1%, which is at least one or two orders of magnitude above error frequencies determined in vivo . It is noteworthy that Jelenc and Kurland (1979) recently showed that adjusting the concentration of nucleoside triphosphates had a drastic effect on the rate of mistranslation in vitro . They were able to achieve error frequencies on the order of 1/10000 in poly(U) directed synthesis of poly(phe). These data are consistent with the role of ATP hydrolysis in kinetic proofreading (Hopfield, 1974).

An examination of the genetic code (Figure 1-6) shows that third position errors can only be detected in a limited number of cases; nearly five times as many substitutions are possible through first position misreading (Table 1-1). Thus it is difficult to compare the frequency of each type of error. Original estimates may have been biased for first position errors simply because these were easiest to detect.

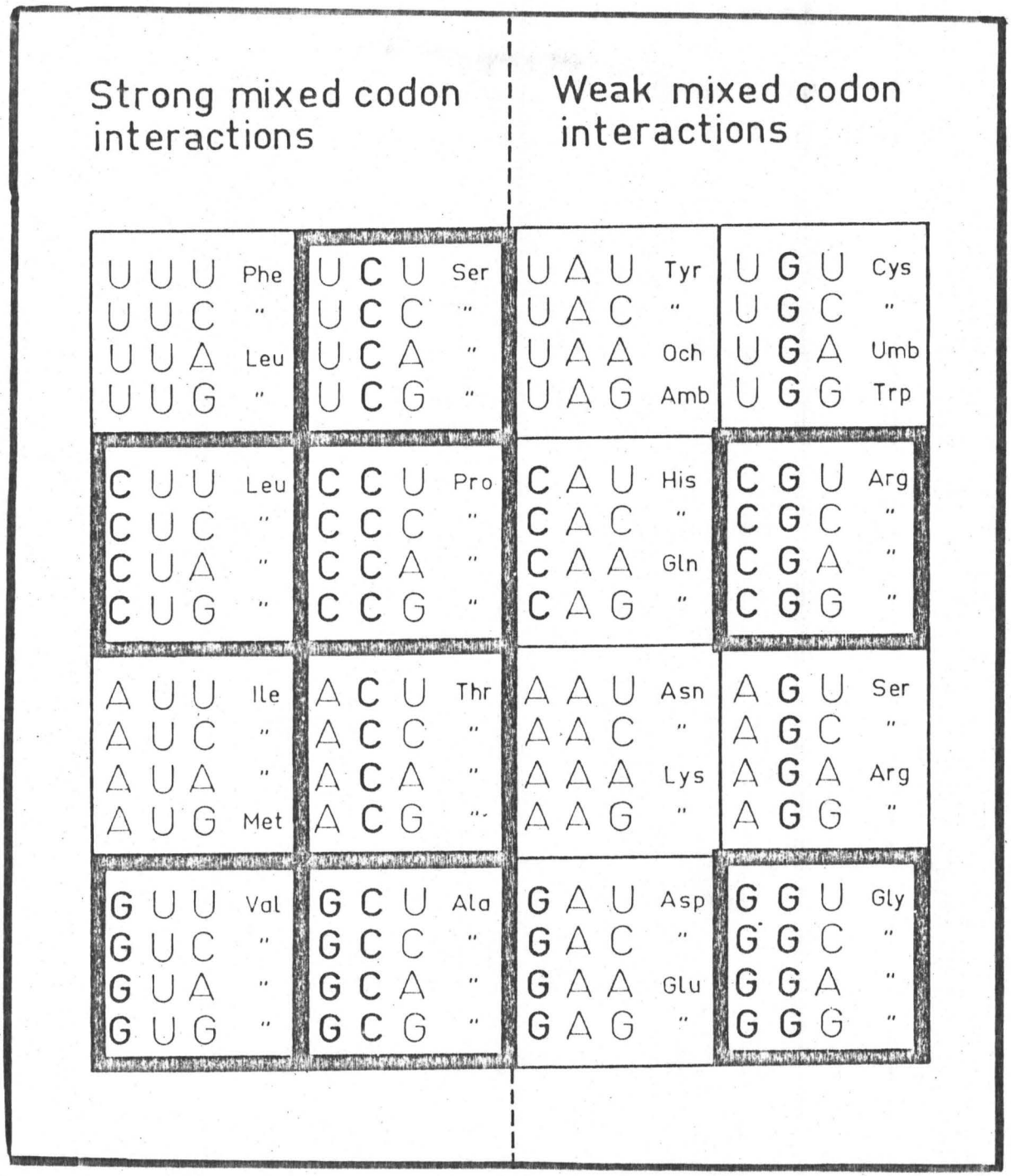

Figure1-6

The genetic code. This figure is taken from Lagerkvist (1978, figure 1). The blocked-in codon sets are families, i.e. groups of four codons differing only in the wobble base and all coding for the same amino acid. The definitions of strong and weak mixed interactions are defined in section 1.4.2.1.

TABLE 1-1

Amino Acid Substitutions Caused by First and Third Position Misreading of the Genetic Code

Cognate A.A.	Substituted A.A.		Charge Changes Due to Misreading	
	First Position Error	Third Position Error	First Position	Third Position
phe	leu,ile,val	leu	0	0
leu	phe,ile,met,val	-	0	0
ile	phe,leu,val	met	0	0
met	leu,val	ile	0	0
val	phe,leu,ile,met	-	0	0
ser	ser,arg,gly	arg		
	pro,thr,ala		1	1
pro	ser,thr,ala	-	0	0
thr	ser,pro,ala	-	0	0
ala	ser,pro,thr	-	0	0
tyr	his,asn,asp	(stp)	2	0
his	tyr,asn,asp	gln	3	1
gln	(stp),lys,gln	his	2	1
asn	tyr,his,asp	lys	2	1
lys	(stp),gln,glu	asn	2	1
asp	tyr,his,asn	glu	3	0
glu	(stp),gln,lys	asp	2	0
cys	arg,ser,gly	(stp),trp	0	0
trp	arg,gly	(stp),cys	1	0
arg	cys,trp,ser			
	(stp),gly	ser	4	0
gly	(stp),cys,arg,ser	-	1	0
Total Number	61	13	23	5

In fact, analysis of mRNA translation dependent on exogenous tRNA indicates that for codon "families" (i.e. sets of four codons differing only in the third position and all coding for the same amino acid), "errors" in the third position may be natural. Thus, some species of valyl-tRNA fully support MS2-RNA translation even though this requires all four forms of the valine codon to be recognized by a single tRNA-val anticodon (Mitra, 1978). This phenomenon has been termed "two out of three" translation (Lagerkvist, 1978).

Lagerkvist (1978) proposed that the strength of base pairing in the first two positions of the codon-anticodon interaction dictates the probability of two out of three translation. He argued that two out of three translation will be prevalent in codon families where the effect is inconsequential, but must be avoided in non-family codon sets where the effect is amino acid substitution (Figure 1-6). Therefore, to be consistent with the distribution of families in the code, the strength of codon-anticodon interactions must follow these rules:

(i) strongest interactions involve two GC bonds in the nonwobble positions.

(ii) mixed interactions involve one GC bond (and hence one AU bond) in these positions. Strong mixed interactions occur when either the anticodon contains both purines or the G is in the middle position of the anticodon.

(iii) weak interactions involve no GC bonds in the nonwobble positions or one GC bond where the purines are either not both in the anticodon or the G is not in the middle position of the anticodon.

These rules are consistent with the fact that GC pairs are stronger than AU pairs (having three rather than two hydrogen bonds). But Lagerkvist did not propose a structural argument for the constraints on the position of the two purines in the nonwobble position of the anticodon for strong interactions. However, Romaniuk (1979) has shown that stacking interactions between bases on one strand are facilitated by the symmetric placement of purines in short oligonucleotide duplexes. Such interactions may be more important in stabilizing the exposed bases of the tRNA anticodon loop than in stabilizing the bases of the mRNA codon and hence account in part for Lagerkvist's rules.

Because of the nature of redundancy in the genetic code, errors in the third position do not have as great an effect on information flow as first or second position errors. Thus, one can argue that restraints on third position base-pairing are more relaxed and result in a higher probability of error. A similar argument can be used to rationalize the wobble extensions of standard Watson-Crick base-pairing (Crick, 1966).

A review of mistranslation at the level of the ribosome suggests the following general hierarchy of errors (see Woese, 1967):

(a) Third position errors are more frequent than first position errors, and second position errors seldom, if ever occur during normal protein synthesis.

(b) A pyrimidine is more likely to be mistaken for another pyrimidine than is a purine for another purine.

(c) A pyrimidine is more likely to be mistaken for a purine (resulting in a pyrimidine-pyrimidine base pair), than is a purine likely to be mistaken for a pyrimidine (which necessitates a purine-purine base pair).

Refinements to these general rules exist, for example U is more likely to be mistaken for C than the reverse. However the basic rules outlined above allow an educated guess about the most likely errors in misreading a codon and provide some insight into the molecular basis of ribosomal fidelity.

1.4.2.2 Proofreading of the Codon-Anticodon Interaction

Stable association of the ternary complex aminoacyl-tRNA.GTP.EF-Tu with the A site of the bacterial ribosome involves specific anticodon-codon interactions (section 1.3.3.2). If the interaction is cognate, GTP is hydrolysed, EF-Tu dissociates, and the aminoacyl-tRNA assumes a configuration that allows peptidyl transfer from the P site. In most cases, if the codon-anticodon interaction is noncognate, the ternary complex dissociates without GTP hydrolysis. But what if the interaction is "almost cognate" so that discrimination at the substrate level fails? Thompson and Stone (1977) have shown that with poly(U)-coded ribosomes precharged with N-acetylphenylalanyl-tRNA-phe in the P site, leucine- and

isoleucine- containing ternary complexes stimulate GTP hydrolysis. The noncognate aminoacyl-tRNAs do not remain bound to the ribosome, nor do they lead to formation of appreciable levels of AcPhe-leu or AcPhe-ile dipeptides. Thompson and Stone (1977) conclude that a small fraction of the leu- and ile-ternary complexes escapes rejection by the reverse of the binding reaction but is rejected in a subsequent GTP-dependent proofreading reaction. The anticodons of tRNA-leu and tRNA-ile differ from tRNA-phe anticodons in the 5' wobble position (leu) or 3' position (leu and ile). Aminoacyl-tRNAs which differed in other positions did not stimulate GTP hydrolysis in these experiments. Thus, substrate discrimination based on initial binding can reject most noncognate tRNAs.

Hopfield's (1974) proposal of kinetic proofreading is consistent with these data: the ternary complex passes through a high energy intermediate with the rate constant for noncognate aminoacyl-tRNA dissociation from the ribosome greater than that for cognate aminoacyl-tRNA. If GTP hydrolysis is coupled to the selection mechanism of codon-anticodon interactions, the energy difference in the pathway for standard and nonstandard pairing can theoretically be doubled, which could account for the fidelity of protein synthesis. However, the existence of the high energy intermediate has not been shown and other methods of proofreading are not ruled out by these observations (Thompson and Stone, 1977).

1.4.2.3 Involvement of P-Site Recognition in Mistranslation

Recent experiments indicate that noncognate peptidyl-tRNA binding in the P-site inhibits binding of the cognate tRNA in the A-site (Luhrmann et al., 1979; Wurmbach and Nierhaus, 1979). Luhrmann's studies involved EF-Tu mediated binding of phe-tRNA-phe to the hexanucleotides AUGUUU, GUAUUU and UAUUUU in the presence of GTP, 70S ribosomes and various deacylated tRNA. Only the cognate deacylated tRNAs, i.e. tRNAf-met, tRNA-val and tRNA-tyr, respectively, bound at the P site of the ribosome-hexanucleotide complex, stimulated binding of phe-tRNA-phe. If this phenomenon applies in vivo , it poses an important question: To what degree does noncognate peptidyl-tRNA, i.e. the product of codon-anticodon mispairing at the A-site of the previous elongation step, influence (a) elongation and (b) mistranslation at the new A-site? This matter is discussed in section 3.2.4.

1.4.2.4 Are Eukaryotic Ribosomes More Faithful than Prokaryotic Ribosomes?

All available data from in vitro assays of ribosomal fidelity indicate that animal ribosomes are more faithful and are less susceptible to error-inducing agents than prokaryotic ribosomes (for reviews see Weinstein et al, 1966; Burrans and Kurtz, 1977; and Kurtz, 1979). Burrans and Kurtz (1977) have used these data to caution against the extrapolation from certain cases of infidelity in E.coli to

involvement of errors in animal senescence. They concluded that animal ribosomes should not be expected to engage in an error catastrophe.

Although the mass of *in vitro* data compells us to believe that the greater complexity of the eukaryotic ribosome allows for increased fidelity, the extrapolation from *in vitro* to *in vivo* must also be viewed with caution. There has been only one direct measurement of error frequency in prokaryotic cells (Edelmann and Gallant, 1977a) and this frequency was as low or lower than measurements of mistranslation in eukaryotic cells (Loftfield, 1963; Loftfield and Vanderjadt, 1972, Harley et al., 1980; sections 3.1 and 3.2). Edelmann and Gallant used cysteine incorporation into bacterial flagellin as a measure of mistranslation, but for several reasons, this error may not be representative of the fidelity of the bacterial ribosome (section 3.2.4). Nevertheless, until more experimental data are available on *in vivo* mistranslation in both prokaryotes and eukaryotes, it remains undetermined whose ribosomes have the greater fidelity. It should be mentioned that measurements of cell viability and error rates during induction of ribosomal ambiguity with streptomycin in *E.coli* indicated that these prokaryotic cells do not engage in error catastrophe (Gallant and Palmer, 1979). This observation is the first evidence for the alternative to the error catastrophe: a plateau at an elevated error frequency (Orgel, 1970; section 1.2.2.2.(b)).

1.4.3 Do Observed Errors Reflect Infidelity of the Synthetase or the Ribosome?

Unfortunately, in natural systems the relative contribution of ribosomal and synthetase errors is still unknown. It may be that both are equally involved in mistranslation overall, but with different situations displaying a greater frequency of one type of error over the other. In fact, if during evolution of the protein synthetic apparatus, specificity compromised speed (Kurland, 1977) and infidelity was selected against, it is difficult to imagine how one type of error would become less likely than the another. Once the fidelity of aminoacylation reactions surpassed ribosomal fidelity, for example, there would be greater selective pressure on improving the specificity of the ribosome-tRNA-mRNA interaction than on further decreasing synthetase errors. A stable error frequency would be achieved when fidelity in both systems was about equal and any further improvement was of such small consequence as to be offset by the metabolic costs incurred.

1.5 Amino Acid Starvation

1.5.1 General Cellular Effects

The effects of starvation for a single essential amino acid on cellular metabolism are exceedingly complex. Amino acids are substrates in numerous pathways of carbohydrate, lipid, protein, and nucleic acid metabolism (Lehninger,

1976), and these will all be directly affected by substrate limitation. Further secondary responses from disturbances in these pathways are likely to involve all aspects of cellular metabolism until the cell ultimately dies. However, amino acids are primarily utilized in growing cells for protein synthesis, and the effect of acute starvation for a single, essential amino acid should be most pronounced in this pathway.

Interestingly, in wild type bacteria the principle effect of amino acid starvation was observed to be a rapid inhibition of stable RNA synthesis: the "stringent response" (for review, see Cashel and Gallant, 1974). Mutants displaying relaxed phenotypes (rel-) were shown genetically to have an altered, recessive allele at one of several loci, the relA locus being the most common. A wide variety of unrelated cellular activities were in fact affected by amino acid starvation in rel+ (stringent) bacteria but not in rel- bacteria. The pleiotypic effector of these activities was found to be one or another of two novel nucleotides termed "magic spot" I and II: guanosine 5'-diphosphate-2'-(3'-)diphosphate (ppGpp) or the analogous pentaphosphate (pppGpp) (see Cashel and Gallant, 1974). Restricting the activity of various tRNA synthetases, even in the presence of all amino acids, also produced ppGpp and the pleiotypic stringent response, but inhibition of protein synthesis at the level of the ribosome did not. Thus, it was postulated that the synthesis of ppGpp was mediated by

uncharged tRNA.

Pedersen et al. (1973) and Haseltine and Block (1973) demonstrated that uncharged tRNA binds in a codon-specific manner at the ribosomal A site to induce synthesis of magic spot. A stringent factor, the product of the relA gene, enzymatically catalyzes synthesis of ppGpp or pppGpp from GDP or GTP and ATP (see Block and Haseltine, 1974). The mechanism by which uncharged tRNA and stringent factor interact and the possible relevance of guanosine tetra- or pentaphosphate synthesis to normal cellular metabolism is not clear.

In stringent bacteria, obviously, amino acid starvation cannot be understood simply on the basis of substrate limitation. However, in relaxed bacteria, which lack regulation by magic spot nucleotides, one might expect direct effects of amino acid starvation on protein synthesis. O'Farrell (1978) has found this to be the case (see below and section 3.2.4).

A phenomenon similar to the stringent response in bacteria has been sought in animal cells, but generally without success (see Pollard and Parker, 1977; Pollard et al, submitted). Stanners and Thompson (1974) did not find synthesis of ppGpp or pppGpp in CHO cells or in a temperature sensitive leucyl-tRNA synthetase mutant of CHO cells at either permissive or nonpermissive temperature. Pollard and

Parker (1977) found that animal ribosomes are unable to synthesize the tetra- or pentaphosphate *in vitro* except in the presence of bacterial stringent factor. Therefore the response of animal cells to amino acid starvation, like that of rel- bacteria, may occur chiefly through substrate limitation. This greatly simplifies analysis of the effects amino acid starvation has on translation and mistranslation of mRNA (O'Farrell, 1978, and sections 1.5.2, 1.5.3) and allows modeling of these processes to yield estimates of the error frequency during normal protein synthesis (sections 3.1 and 3.2).

1.5.2 Inhibition of Protein Synthesis

The immediate precursor for protein synthesis is aminoacyl-tRNA, and during normal growth all tRNAs are nearly 100% charged (see Yegian and Stent, 1969; Stanners and Thompson, 1974). Therefore, the arrest of protein synthesis upon amino acid starvation is most simply explained by a depletion of charged tRNA. In fact, direct measurements of aminoacyl-tRNA during starvation in both bacteria and mammalian cells show that the relevant tRNA species (the ones corresponding to the missing amino acid) are reduced to low levels, while other irrelevant tRNAs remain 80-100% charged (Yegian and Stent, 1969; Stanners and Thompson, 1974). If it is assumed that the inhibition of protein synthesis is due to limitation of the relevant aminoacyl-tRNA then the relative concentration of these charged tRNAs should be much lower

than the relative rate of protein synthesis: these tRNAs represent only about 1/20 of the total precursor pool (O'Farrell, 1978). Instead, it has been observed that the measured levels of charged relevant tRNAs are not reduced below the relative rate of protein synthesis and in some cases are significantly greater (Martin et al., 1963; Ezekiel, 1964; Yegian and Stent, 1969; Stanners et al., 1978; Lofgren and Thompson, 1979).

A simple model proposed by O'Farrell (1978) for the direct inhibition of protein synthesis during amino acid starvation will indicate the magnitude of the discrepancy between observed and expected levels of charged tRNA. Assuming that only the step time of the ribosome at the relevant codon is affected by exhaustion of the relevant aminoacyl-tRNA, then the relative increase in the transit time of the ribosome is approximated by (19S + S')/20S where S is the normal mean step time and S' is the step time at the relevant codon (O'Farrell, 1978). If this increase alone accounts for inhibition of protein synthesis and the increase in step time at the relevant codon is directly proportional to the reduction in the charged levels of the relevant tRNA, then a 10-fold reduction in the protein synthetic rate implies a 180-fold reduction in the level of charged, relevant tRNA. A small improvement in O'Farrell's model is made by taking into account the observed reduction in the number of functioning ribosomes and the actual frequency of the amino acid in cellular protein (Harley et al., 1979a).

However, a major oversight in these analyses is the indirect effect of ribosome queuing at the relevant codons on initiation frequency and step times at irrelevant codons. This effect has now been studied in detail through computer simulations of protein synthesis (section 3.2).

It is important to realize that these models make no assumption about the relationship between charged tRNA levels and step time. It is conceivable that a nonlinear relationship exists between these parameters such that a 10-fold reduction in the measured concentration of the relevant charged tRNA could, for example, be associated with a 100-fold increase in the step time at the relevant codon. Although no evidence exists for a cooperative action between relevant tRNAs and the rate of elongation at their codons, it is possible that methods for assaying the levels of charged tRNA do not reflect the actual concentrations at the site of protein synthesis. Another possibility is that the high levels of charged tRNA may be an artifact of the isolation procedure. For example, it was found that chilling of cells in phosphate buffered saline immediately inhibited protein synthesis yet allowed appreciable charging of tRNA with residual amino acid prior to the tRNA assay (Stanners et al., 1978). Although buffers have now been changed, it is still possible that a technical artifact leads to overestimation of the state of aminoacylation.

It is also possible that not all tRNAs are involved in

protein synthesis under all conditions; certain species may have special functions, perhaps in response to amino acid starvation, and do not become deacylated even though aminoacyl-tRNA is limiting. Yegian and Stent (1969) found that in stringent strains of E.coli starved for leucine, the residual acylated tRNA-leu was only partly composed of leu-tRNA-leu; the remaining tRNA-leu was protected by some other group which apparently was neither leucine nor any of the other 19 amino acids.

Figure 1-7 illustrates the standard technique to distinguish charged from uncharged tRNA. Total acceptor capacity is measured by reaction sequence A. Since vicinal diols are cleaved by periodate, protected acceptor capacity can be measured by reaction sequence B. Yegian et al. (1966) first found by amino acid analysis that the amount of leucine liberated by mild alkaline hydrolysis could not account for all of the protected species of tRNA in population I. Furthermore, it was found that mild alkaline hydrolysis did not "deprotect" all of the tRNA since periodate oxidation after alkali reduction did not totally obliterate the acceptor capacity for leucine (Yegian and Stent, 1969). The protector however was exchanged for leucine during the aminoacylation reaction. Since this exchange did not depend on AMP or pyrophosphate, Yegian and Stent concluded that it represented hydrolysis of the tRNA-protector bond catalyzed by an enzyme present in the preparation of aminoacyl-tRNA synthetase. The protector function was shown not to result

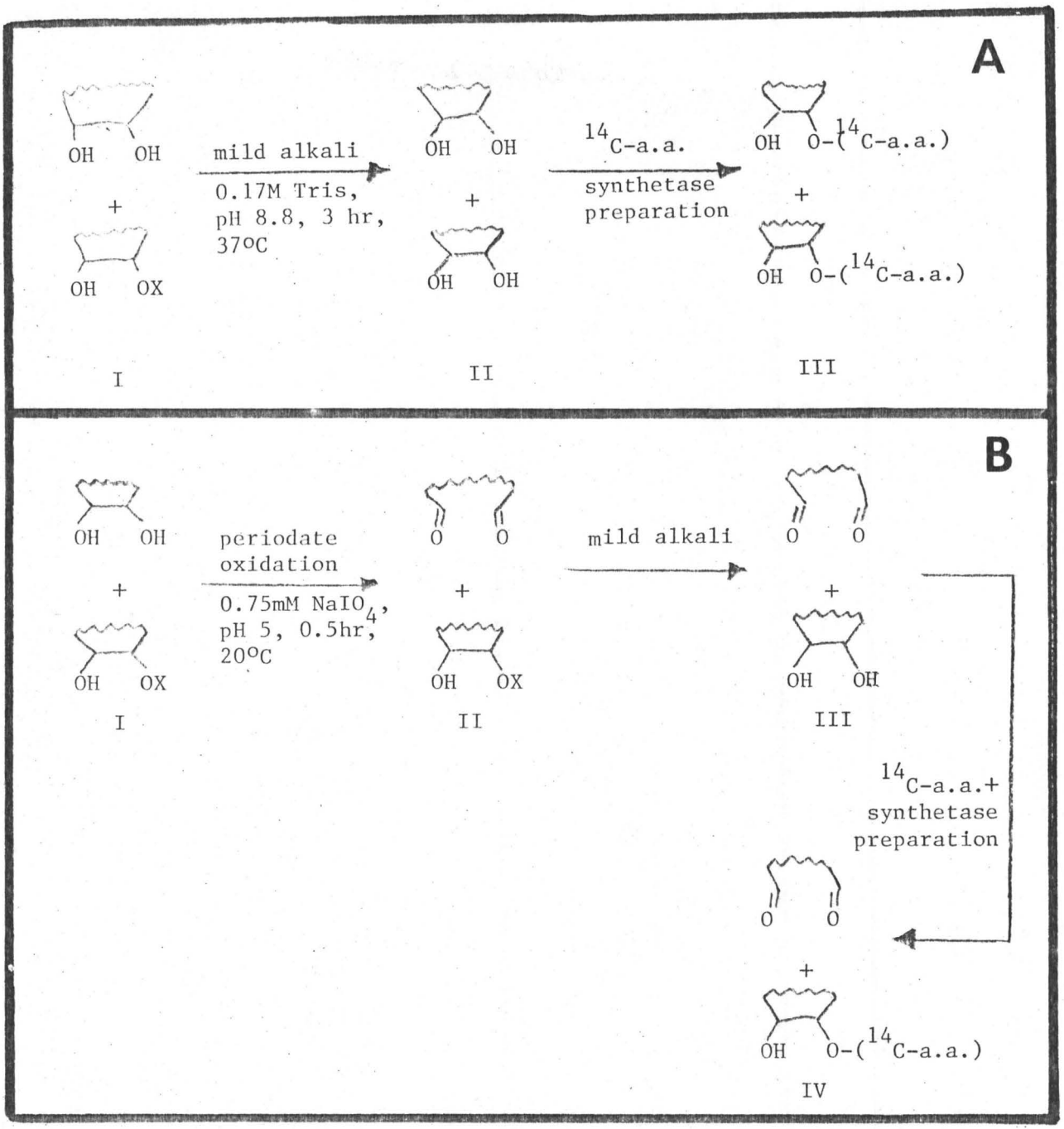

Figure 1-7

Techniques to discriminate charged from uncharged tRNA. Total acceptor capacity is determined by reaction scheme A, where mild alkali hydrolysis and acylation with ^{14}C-amino acid fully charges all acceptor species. Protected acceptor is determined by scheme B, where periodate oxidation first destroys all unprotected vicinal diols (potential acceptors).

from some peculiarity of the tRNA which rendered it stable to periodate oxidation (for example if the 3' end was deoxyadenosine); the acceptor capacity of tRNA which was deacylated then oxidized after charging *in vitro* with leucine according to scheme A was essentially zero.

The distribution of the protector among the isoaccepting species of tRNA-leu was not random. In resolving leu-tRNA-leu into two species, Yegian and Stent (1969) found that nonacylated tRNA, representing 80% of the total during leucine starvation was equally distributed over species I and II, but of 20% of the protected tRNAleu, 11% represented leu-tRNA-leu(II) while all of the remaining 9% was species I complexed to the unknown protector. Thus, the cognate aminoacylation of one (or more) of the isoaccepting species during amino acid starvation may in fact be essentially zero and the drastic reduction of ribosome movement at the codons corresponding to these species could account for the inhibition of protein synthesis (O'Farrell, 1978). In general, however, it is only necessary to postulate that all of the residual charged tRNAs are not directly engaged in protein synthesis (see section 3.2.5).

Starvation for other amino acids was also accompanied by high residual amounts of protected tRNA, but only during leucine starvation was an appreciable fraction of the protected tRNA stable to alkali hydrolysis (Yegian and Stent, 1969). Furthermore, the observation of an alkali stable

protector complexed to tRNA-leu was restricted to stringent strains of E.coli . Leucine starvation of two relaxed strains showed high residual protected capacity but only a small fraction of this capacity was alkali stable. However, it is not known whether the protected tRNAs in these other situations actually reflect cognate aminoacyl tRNA, and if they do, whether they participate in protein synthesis during amino acid starvation. Further experimental work is required to determine the significance of the residual levels of apparently charged or protected tRNAs during amino acid starvation.

1.5.3 Induction of Mistranslation

It has been known for some time that restriction of amino acids for protein synthesis could induce errors. In cell-free extracts, poly(U) directed incorporation of leucine increases when phenylalanine is limiting (Gorini, 1969). In tRNA-dependent cell-free lysates, the absence of a required tRNA slows synthesis and provokes misreading at the relevant codon (Holmes et al., 1978). There is now very strong evidence that amino acid starvation induces mistranslation in intact cells. O'Farrell first observed this phenomenon in E.coli using 2-D gel electrophoresis to detect charge changes in substituted proteins (Parker et al., 1978; O'Farrell, 1978). Parker et al. (1978) studied several cases of amino acid starvation in animal and bacterial cells and concluded that errors induced by amino acid starvation were

caused by codon-anticodon mispairing in the third position. Attempts to obtain sufficient quantity of pure, labeled, error-containing protein for sequencing of selected peptides are in progress (J.W.Chamberlain, personal communication) but so far the direct test of the proposed substitutions has not been made. In this section I will review the indirect evidence and arguments in support of the theory.

Figure 1-8 illustrates the application of 2-D gel electrophoresis to the resolution of error-containing proteins. If the substituted amino acid carries a charge different than the correct amino acid, the aberrant protein will have an altered pI. With several substitutable sites in the native protein, a family of "stutter" spots will appear in the isoelectric focusing dimension trailing the native species towards the acidic or basic end of the gel. The charge changes oberved upon extreme starvation for different amino acids in both animal and bacterial cells are shown in figure 1-9.

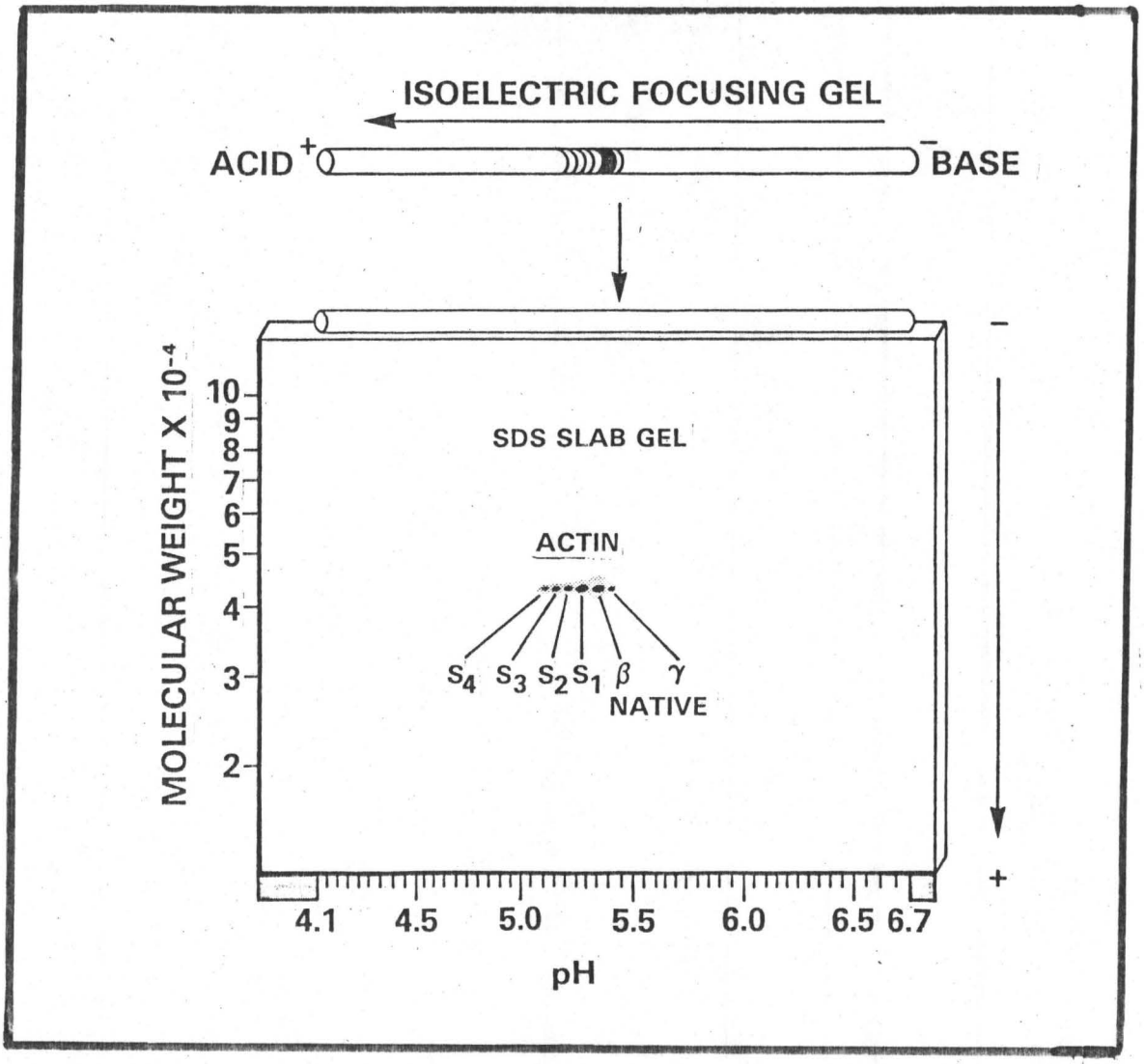

Figure 1-8

Two-dimensional gel electrophoresis for resolution of error-containing proteins. Proteins are resolved in the first dimension (isoelectric focussing rod gel) under denaturing conditions (urea, β-mercaptoethanol and nonionic detergent) according to their pI and in the second dimension (SDS slab gel) according to their molecular weight. This schematic shows the application of the technique to the resolution of native and substituted forms of actin.

Amino Acid Starvation	Charge Changes	Direction of Stutter
his	yes	acidic
asn	yes	basic
gln	no	
lys	no	
met	no	
leu	no	
val	no	
ala	no	

Figure 1-9

Existence and Direction of Stuttering During Amino Acid Starvation

Data from Parker et al. (1978) and Pollard et al., in preparation.

This pattern can be entirely accounted for by pyrimidine-pyrimidine mispairing in the third position (see Figure 1-6) and no other error such as misacylation or first- or second-position ribosome error can easily account for it. Post-translational modification of proteins is also an unlikely explanation for these observations since the stuttering is amino acid specific. Furthermore, pulse-chase analysis of actin stuttering (section 3.2) indicates that native actin is not the precursor of the altered species.

The proposal that codon-anticodon mispairing in the third position is the mechanism of stuttering is consistent with three observations reported in this thesis: first,

error frequencies calculated for normal protein synthesis on the basis of this model are consistent over a range of protein synthetic rates (section 3.2); second, these error frequencies agree with previous estimates of the error frequency in mammalian cells (section 3.2); and third, the observed changes in isoelectric points of stuttered species are predicted by the proposed changes in the amino acid composition (section 3.3). However, the best evidence that stuttering reflects ribosomal ambiguity comes from work with streptomycin resistant E.coli .

Streptomycin is known to bind in E.coli to a 30S ribosomal protein, S12 (see Gorini, 1974). This protein is involved in the specificity of tRNA-ribosome binding since binding of streptomycin increases ribosomal errors during mRNA translation both in vitro and in vivo . Mutant strains of E.coli resistant to streptomycin have an altered S12 protein which is apparently unaffected by the drug: the fidelity of protein synthesis is maintained except at very high concentrations of streptomycin. This dependence of error frequency on streptomycin concentration in the mutant cells is observed during amino acid starvation (Parker and Friesen, 1979). In the absence of streptomycin, under starvation conditions which induce stuttering in wild type cells, the resistant cells do not stutter. Only with very high concentrations of streptomycin is the amino acid-specific stuttering observed in these cells.

Together, these data constitute very strong evidence for errors at the level of codon-anticodon pairing during amino acid starvation. In fact, there perhaps is no evidence more direct than this. Even amino acid sequencing of error containing peptides is not conclusive: it cannot completely rule out misacylation, and there is always the possibility of contaminating species complicating the analysis.

Figures 1-10 through 1-12 illustrate the proposed model for mistranslation of actin mRNA during histidine starvation. During normal protein synthesis, histidine is added to the growing peptidyl-tRNA chain whenever the histidine codon is encountered (figure 1-10). To bring about acute starvation for histidine in animal cells, it does not suffice to simply remove histidine from the growth medium; degradation of cellular protein provides enough histidine to maintain steady state synthesis for several hours at 70-90% of the normal rate (see Parker et al., 1978; section 3.1). Furthermore, it is not desirable to remove histidine completely from the growth medium of human cells since this would require dialysis of the serum component and other low molecular weight factors essential for normal growth would also be lost. Therefore, histidine is removed from the defined (non-serum) component of the growth medium and the histidine analog, histidinol is added.

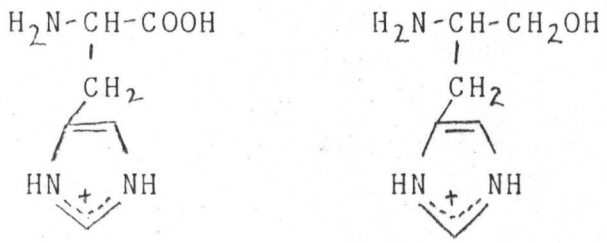

histidine histidinol

Histidinol binds to histidyl-tRNA synthetase and blocks acylation of tRNA-his (Hansen et al., 1972). Histidinol is not required if histidyl-tRNA synthetase can be made defective by other means. This is achieved at the nonpermissive temperature of temperature sensitive mutants of CHO cells involving histidyl-tRNA synthestase (see Parker et al., 1978). According to the proposed mechanism, these conditions of histidine starvation reduce the concentration of his-tRNA-his to levels low enough to induce detectable rates of errors which result from mispairing in the third position of the codon with a charged tRNA (gln-tRNA-gln) (figure 1-11). Thus, glutamine is added to peptidyl-tRNA at sites corresponding to histidine codons. If errors at histidine codons in a given mRNA are randomly distributed, all species corresponding to 0,1,2,3... substitutions will be observed simultaneously (section 3.4). In actin mRNA there are 9 histidine codons. some of the mistranslated species are illustrated in figure 1-12. Since glutamine is a neutral amino acid, while about 90-95% of the histidine residues are positively charged at the isoelectric point (pI) of actin, glutamine substitution lowers the pI of actin (section 3.3).

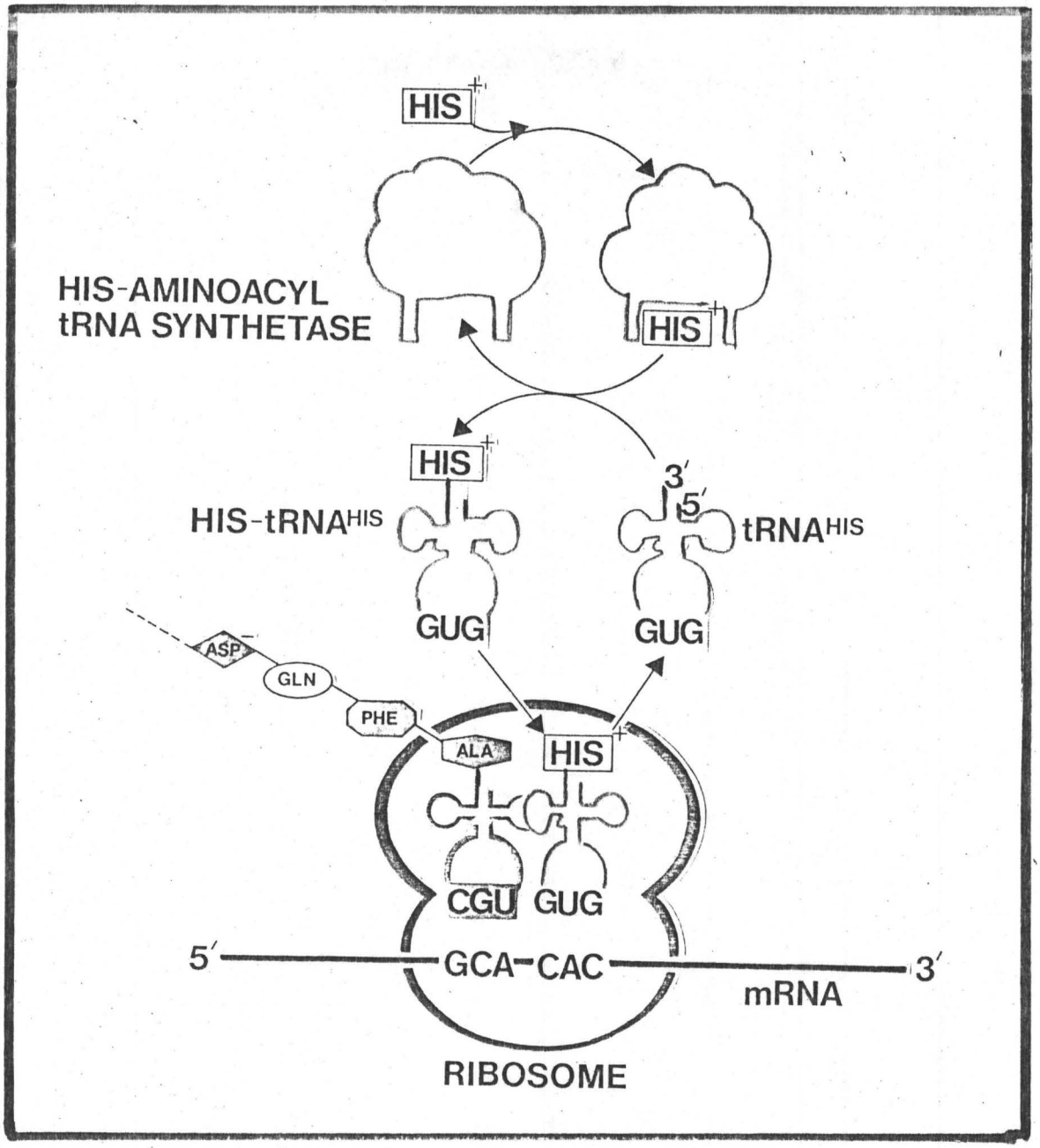

Figure 1-10

Addition of histidine to peptidyl-tRNA at sites corresponding to histidine codons. In the presence of histidine, histidyl-tRNA synthetase acylates tRNAhis. This allows incorporation of histidine into growing peptides at sites corresponding to histidine codons. The components of the protein synthetic apparatus are not shown to scale.

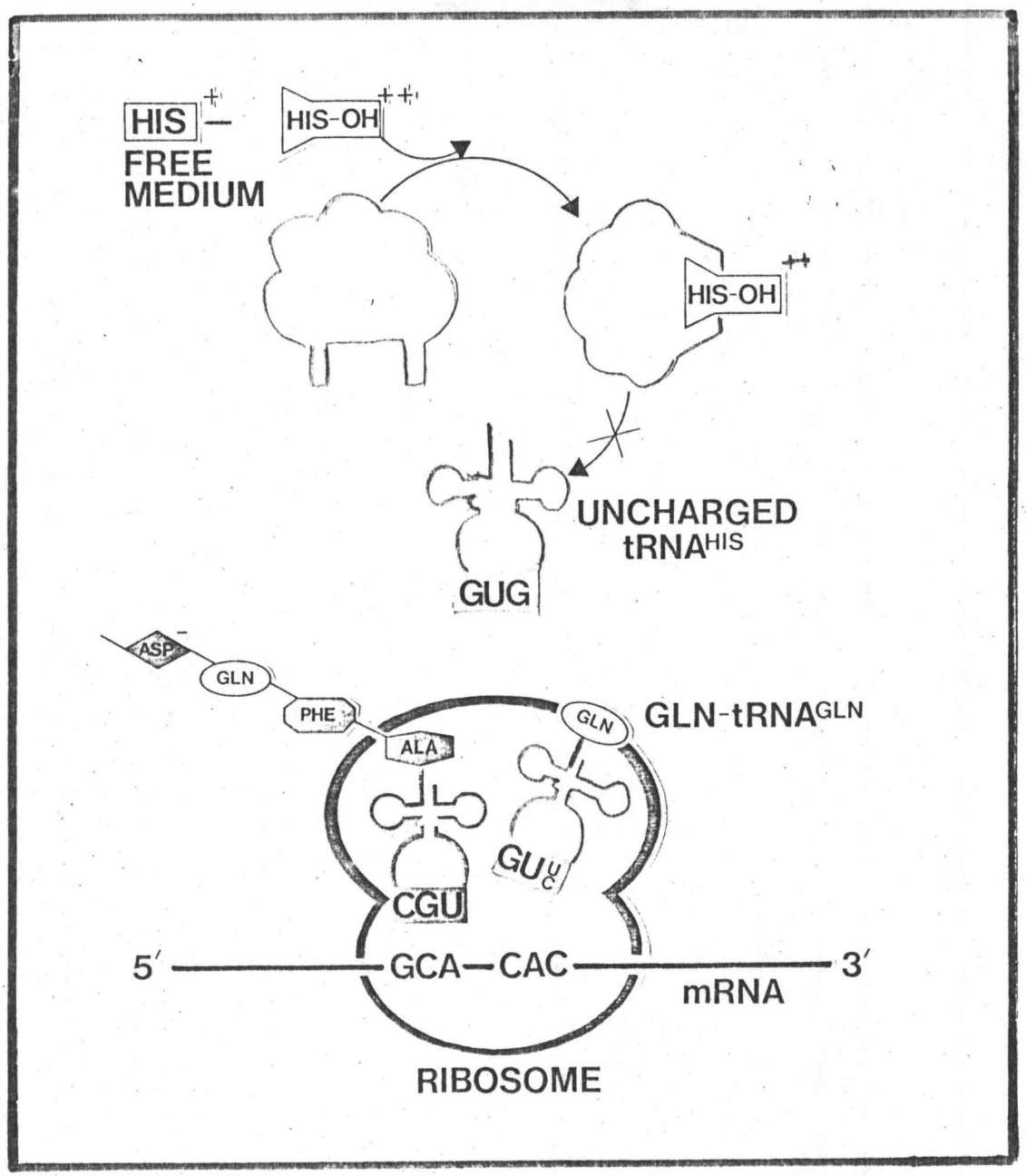

Figure 1-11

Addition of glutamine to peptidyl-tRNA at sites corresponding to histidine codons. In the absence of histidine and in the presence of the analog histidinol, histidyl-tRNA synthetase is blocked from charging tRNAhis. In the absence of his-tRNAhis, the ribosome pauses at the histdine codon sufficiently long to allow glutamine substitution, purportedly, by mispairing of the histidine codon and gln-tRNAgln at the wobble position.

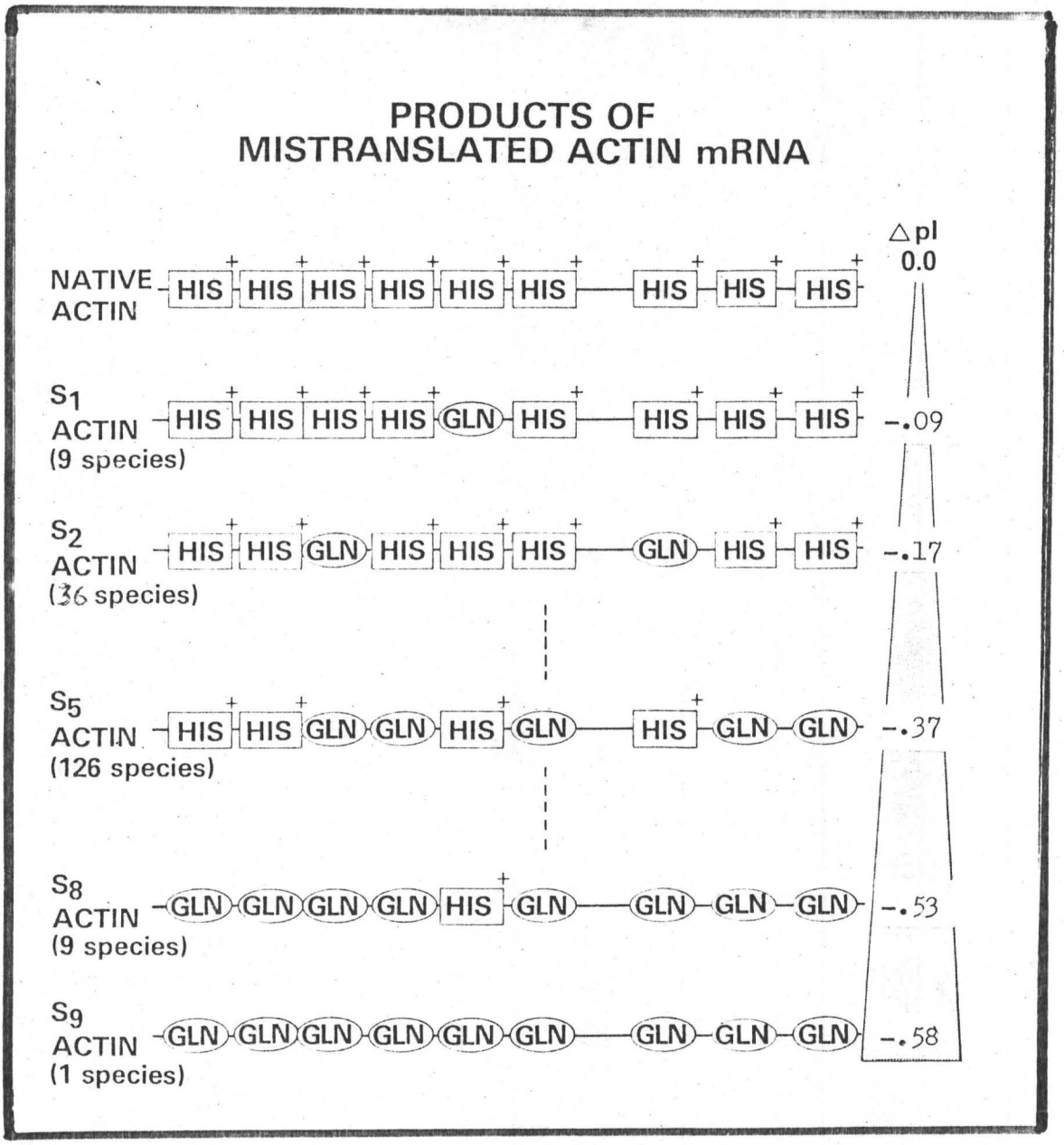

Figure 1-12

Products of mistranslated actin mRNA. This schematic shows native actin containing 9 histidine residues. Several examples of substituted actins are shown together with the calculated ΔpI of the substituted species relative to native actin. The calculations of isoelectric points are described in section 3.3. The number of species S_i containing i substitutions is $\binom{9}{i}$.

The negative change in pI of substituted actins is also illustrated in figure 1-12. This effect allows dectection of stuttered protein on 2-D gel electrophoresis.

Accurate quantitation of stuttering during amino acid starvation was not reported by either Parker et al. (1978) or O'Farrell (1978). Figure 1-13 illustrates three possible means to quantify the error frequency of actin synthesis during histidine starvation. Although it is most accurate to cut out and count portions of the gel corresponding to stuttered protein, it is not practical since very little radioactivity is incorporated. The methods used to quantify and compare error frequencies during histidine starvation in a variety of cells in tissue culture are described in section 3.1.

QUANTIFYING ERROR FREQUENCIES

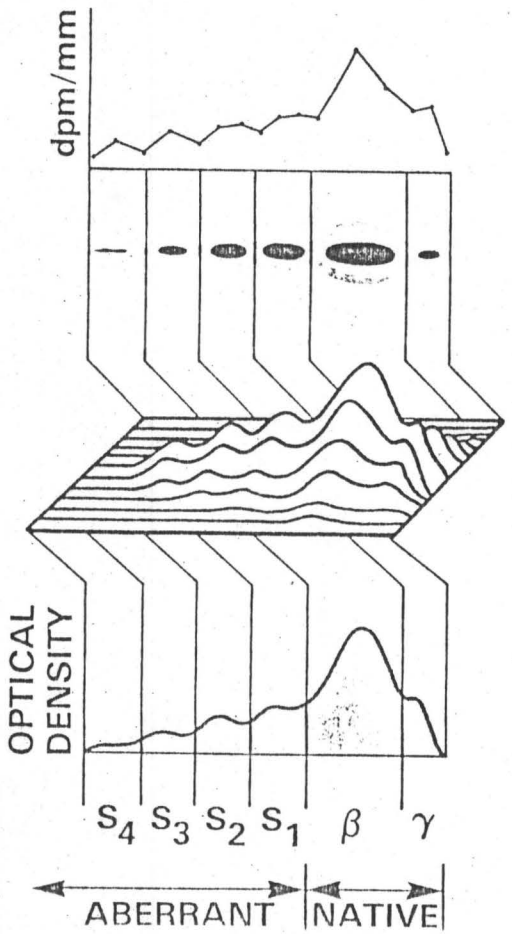

$$\text{FRACTION OF ABERRANT PROTEIN} = \frac{S_1+S_2+S_3+\ldots}{\gamma+\beta+S_1+S_2+S_3+\ldots}$$

$$\text{FRACTION OF SUBSTITUTED SITES} = \frac{S_1+2S_2+3S_3+4S_4+\ldots}{9(\gamma+\beta+S_1+S_2+S_3+S_4+\ldots)}$$

Figure 1-13

Quantifying error frequencies. Substituted actins labeled with ^{35}S-methionine are detected on autoradiograms of 2-D gels. Three methods of obtaining values for the amount of labeled protein in the native and stutter spots are shown: cutting out and counting portions of the gel (top); roster scanning of autoradiograms (i.e. slit height is small compared to the diameter of the spots), (middle); and scanning of autoradiograms where the slit height is at least as great as the diameter of the largest spot scanned (bottom). In each case the fraction of aberrant protein and the fraction of substituted sites are determined by the equations shown.

1.6 Summary of Introduction

The cellular model of aging and some theories for the senescent decline *in vitro* have been reviewed. Of particular interest is the error catastrophe theory which predicts alterations in protein synthesis with age. Two aspects of this theory which have not been dealt with previously are: (i) comparisons of the rates of protein turnover during exponential growth of young and old cells; and (ii) comparisons of direct substitution frequency of natural amino acids during protein synthesis in young and old cells. The first comparison is possible with the approach to equilibrium method of labeling proteins and by direct measurements of protein synthetic rates and net growth rates. The second comparison is not possible with present techniques, but a new method of inducing synthesis of aberrant proteins by amino acid starvation has provided a more direct assay than was previously available. The studies reported here have used these techniques for comparing early- and late-passage cells from young and old donors and from subjects with genetically determined syndromes of accelerated aging.

2 PROTEIN SYNTHESIS AND DEGRADATION IN CULTURED HUMAN CELLS

This chapter describes some observations on protein turnover in aging cells using two procedures: (1) the approach to equilibrium method of labeling proteins; and (2) measurements of protein synthetic and net growth rates. These methods have not been used extensively, and to my knowledge, no one has previously developed the labeling to equilibrium method for use with cells in exponential growth. In addition, measurements of protein export rates are not usually included in studies of protein turnover. I have derived equations to determine export rates in approach to equilibrium experiments during both exponential and steady-state growth.

These protocols for measurements of protein turnover in aging cells yield gross "averages" of synthetic, degradation, and export rates. A more thorough analysis would include studies of (a) individual protein turnover by two-dimensional gel electrophoresis; (b) turnover of short-lived and analog-containing proteins by pulse-chase methods; (c) turnover of specific and total cellular proteins in cell-free extracts; and (d) fractionation of the degradative apparatus. Several of these studies have been done in Dr. Goldstein's laboratory by my colleague, J.J.Elliot (PhD thesis, in preparation; Elliot and Goldstein, submitted). My results from labeling to equilibrium analysis are in general

agreement with his.

2.1 Theory: Approach to Equilibrium

Figure 2-1a shows the components of protein turnover and the differential equations describing their time rate of change. These equations are appropriate for a homogeneous population of proteins. The solutions to these equations are given in figure 2-1b. The expressions for the amounts of radioactive protein in the system when labeled amino acid is used as a tracer are obtained by placing a factor "k" in the equations for P_c and P_m, i.e. $P_c^* = kP_c$ and $P_m^* = kP_m$. The factor k will be a function of the specific activity of the precursor aminoacyl-tRNA (and hence the specific activity of the labeled amino acid) and the molar fraction of the tracer amino acid in the protein. I have assumed that (1) the intracellular and extracellular amino acid pools are in rapid equilibration; (2) the specific activity of the aminoacyl*-tRNA is the same as that of the corresponding amino acid. These assumptions are valid under the conditions routinely used for labeling cellular protein in tissue culture reported here (sections 2.2.2.2 and 3.1.3.2).

Figure 2-1b gives the expressions needed for deriving values of degradation, export, and growth rates from the approach to equilibrium method of labeling protein. The turnover parameter during steady state (d+e) is obtained from the negative slope of the line describing $\ln(1-P_c^*/P_{c\infty}^*)$ as a

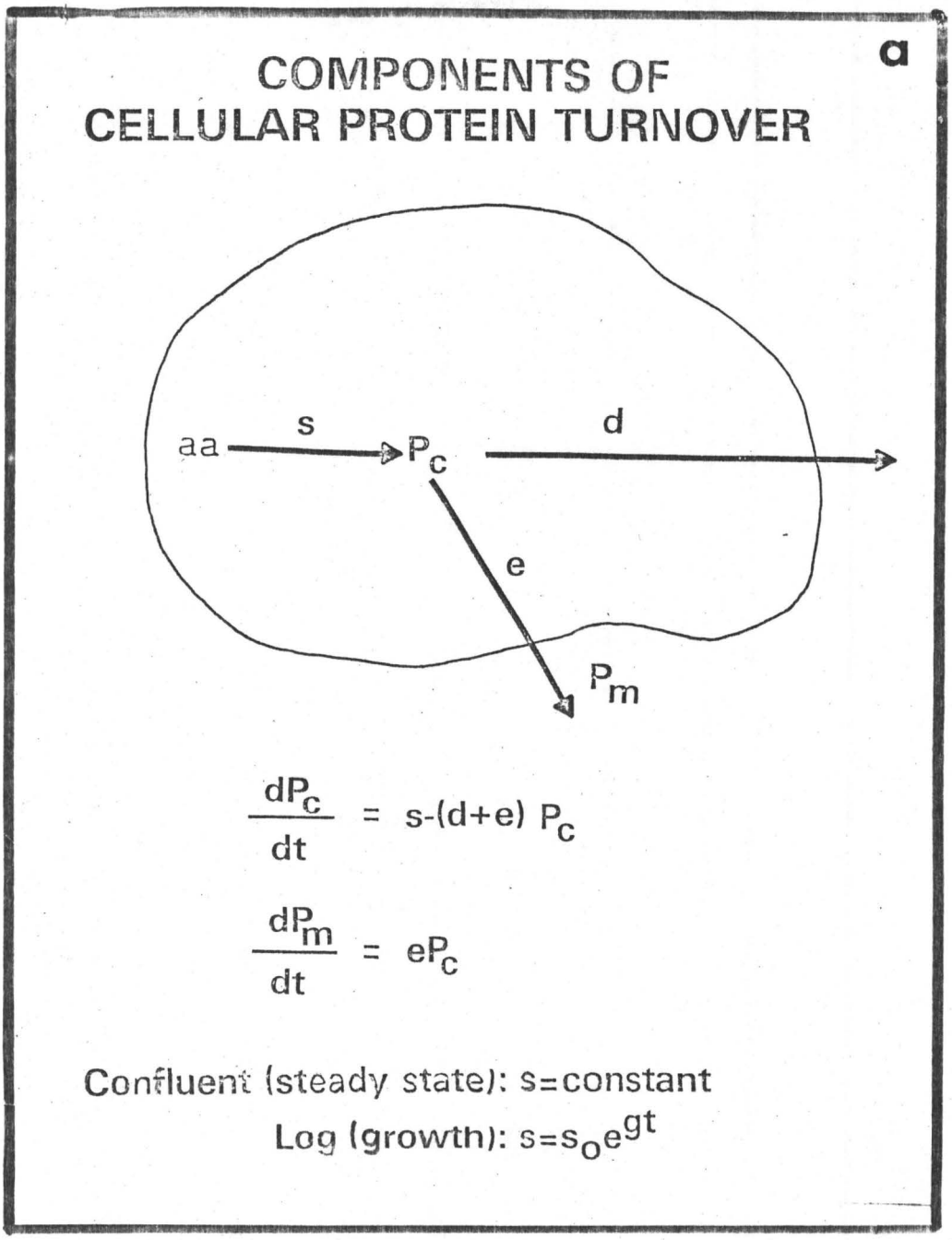

Figure 2-1

Cellular protein turnover: Differential equations and their solutions. The scheme (a) depicts synthesis of cellular protein P_c from amino acids with zero order rate constant (s) and the removal of P_c from the intracellular population by degradation and export (first order rate constants (d) and (e), respectively). There is no degradation of the extracellular pool of protein P_m. The differential equations are shown and their solutions for steady state and exponential growth are given in part (b) of this figure.

SOLUTIONS TO THE DIFFERENTIAL EQUATIONS **b**

A. Steady State

$$\frac{dP_c}{dt} = s - (d+e)P_c \qquad \frac{dP_m}{dt} = eP_c$$

$$P_c = \frac{s}{d+e}\left(1 - e^{-(d+e)t}\right) \qquad P_m = \frac{es}{d+e}\left(t + \frac{1}{d+e}e^{-(d+e)t}\right) - \frac{es}{(d+e)^2}$$

$$\ln\left(1 - \frac{P_c}{P_{c\infty}}\right) = -(d+e)t \qquad P_m(t \gg 0) \approx \frac{es}{d+e}t$$

B. Growth

$$\frac{dP_c}{dt} = s_o e^{gt} - (d+e)P_c \qquad \frac{dP_m}{dt} = eP_c$$

$$P_c = \frac{s_o}{d+e+g}\left(1 - e^{-(d+e+g)t}\right)e^{gt} \qquad P_m = \frac{es_o}{g(d+e+g)}\left[1 + \frac{g}{d+e}e^{-(d+e+g)t}\right]e^{gt} - \frac{es_o}{g(d+e)}$$

$$\bar{P}_c = \frac{s_o/P_{co}}{d+e+g}\left(1 - e^{-(d+e+g)t}\right) \qquad \bar{P}_m = \frac{es_o/P_{co}}{g(d+e+g)}\left[1 + \frac{g}{d+e}e^{-(d+e+g)t}\right] - \frac{es_o e^{-gt}}{P_{co}\,g(d+e)}$$

$$\ln\left(1 - \frac{\bar{P}_c}{\bar{P}_{c\infty}}\right) = -(d+e+g)t \qquad \bar{P}_m(t \gg 0) \approx \frac{es_o/P_{co}}{g(d+e+g)}$$

Figure 2-1, continued

function of time (t). Subscript ∞ indicates that the value is obtained at large values of t. The slope of P_m^* as a function of time at large t is kes/(d+e). Since $dP_c^*/dt = 0$ during steady state, $s=k(d+e)P_c^*$, and thus e can be obtained from dP_c^*/dt and P_m^*. The degradation rate d is obtained by subtracting e from d+e. The synthetic rate s is a zero order constant and thus has units of (mass/time). The sum d+e = s/P gives the total synthetic rate normalized to protein mass.

During growth, the first order degradation and export rates are assumed to remain unchanged as a function of time since they are intrinsic properties of the protein and are independent of mass. But the total synthetic rate s is dependent on protein mass. For exponential growth, I assume that s is directly proportional to total protein content so that $s = s_o e^{gt}$. The growth rate g is obtained from analysis of total protein accumulation. Solutions to the differential equations (figure 2-1b) provide expressions which allow experimental determination of the total turnover parameter (d+e+g) and the export rate e. The equations for P_c and P_m involve e^{gt}. Since unlabeled protein increases according to $P_{co} e^{gt}$, where P_{co} is the initial protein content, dividing P_c by $P_{co}e^{gt}$ removes the exponential time function and yields a more useful value, $\bar{P}_c$. $\bar{P}_c$ can be linearized as shown in figure 2-1b. Similarly, $\bar{P}_m = P_m/P_{co}e^{gt}$. Export rate $e = \bar{P}_m^*(t>>0) \times g/\bar{P}_c^*$. Degradation is obtained by subtracting measured values of g and e from the total turnover parameter d+e+g.

When P_c and P_m represent the sum of a heterogeneous population of proteins, these transformations of the data are not strictly valid. During steady state growth, for example,

$$P_c^* = \sum_{i=1}^{n} (k_i s_i / d_i + e_i)(1 - e^{-(d_i + e_i)t})$$

where k_i, s_i, e_i, and d_i are different for each protein class $i=1,2,3,\ldots n$. But where the majority of proteins have a similar turnover rate and amino acid composition, the approximation

$$P_c^* \doteq (n k_{i\text{"avg"}} s_{i\text{"avg"}} / d_{i\text{"avg"}})(1 - e^{-(d_i + e_{i\text{"avg"}})t})$$

can be made. Here, "avg" is not meant to represent a true average, for the approximation is invalid even for n=2. Experimentally, plots of $\ln(1 - P_c^*/P_{c\infty}^*)$ are linear for at least one "average" half-life (i.e. the points fall on a straight line from ordinate values 0 through -0.693). Thus, the transformation given above provides an objective means of comparing the turnover of proteins in different cell strains.

2.2 Increased Degradation During Growth of Cultured Human Fibroblasts with Age *in vitro*

2.2.1 Introduction

Orgel (1963) proposed that cellular senescence *in vitro* (Hayflick and Moorhead, 1961) may be caused by synthesis of aberrant protein (section 1.2.2.2.b). Since it is known that certain abnormal proteins are degraded faster in both prokaryotic and eukaryotic cells (see Ballard et al., 1977; Dean and Riley, 1978), many investigators have analyzed protein turnover in aging cells to test Orgel's theory. However, differences in the rates of degradation between young and old cells need not be the result of changes in the amounts of abnormal protein; instead they may indicate differences in the regulation of protein degradation.

Bradley et al. (1976) showed that WI38 cells degraded long-lived proteins at a constant rate until terminal passage when degradation increased. Short-lived proteins were apparently degraded faster throughout late passage, but late-passage cells were defective in the degradation of analog-containing proteins. In contrast, Dean and Riley (1978) found no passage-dependent reduction in the capacity of MRC5 cells to degrade either normal or analog-containing proteins. Results from other cells *in vitro* and *in vivo* show no consensus regarding the effects of aging on

protein turnover (see section 1.3.3 and Dean and Riley, 1978).

These discrepancies may result in part from the fact that protein synthesis and degradation are regulated processes which are sensitive to growth state, cell density, nutritional status (for example amino acid concentration), temperature, pH and other factors (see Goldberg, 1974; Ballard, 1977). In this section I report on studies of protein turnover in young and old cells using two protocols which were designed to minimize perturbations of cell metabolism. The results indicate that old cells have an increased rate of degradation during exponential growth.

2.2.2 Materials and Methods

2.2.2.1 Cell Culture

Human skin fibroblasts were obtained from anterior forearm biopsies as described by Goldstein and Littlefield (1969). A description of cell types used in this study is found in Table 3-1. The regular growth medium consisted of Eagle's minumal essential medium supplemented with 15% fetal calf serum (FCS, GIBCO, Lot A781020), nonessential amino acids, glucose, and pyruvate (Goldstein and Littlefield, 1969). Definitions of early- and late-passage cells are given in section 3.1.3.1. Highly reproducible inoculation of cells into petri dishes was achieved by harvesting an appropriate number of cells with 0.125% trypsin (Difco) and suspending

them in a large volume of growth medium using a magnetic stirrer. With continued stirring, 2.00 or 5.00 ml of cell suspension was rapidly and accurately dispensed into empty, replicate 35 or 60 mm dishes, respectively.

2.2.2.2 Amino Acid Analysis

Cells from two normal donors (A2 and TM) were grown to confluence in 100 mm petri dishes (Corning Plastics). Five dishes of each strain were rinsed twice with PBS and then precipitated in the dishes with 10 ml of 5% TCA. The precipitated material was washed three times with 5% TCA and once rapidly with H_2O then solubilized with 0.4% sodium deoxycholate in 0.1N NaOH (1.5ml/dish, 15 minutes with shaking). The solutions from all dishes were pooled. An equal volume of 50% TCA was added and the precipitate collected by centrifugation (3000g, 10 min.). Lipids were extracted with 95% ethanol by resuspending and respinning the precipitate. The precipitate was then suspended in 5% TCA and heated for 15 minutes at 90°C. The precipitate was collected, dried, and hydrolyzed with 10 volumes of 6N HCl (v/w) at 120° C for 24 hours. The hydrolysate was spun at 8000g for 5 minutes and the supernatant dried under vacuum. The solid was dissolved in 1000 volumes of H_2O and the composition determined by a Beckman automated amino acid analyzer (Table 2-1). The average amino acid residue weight was calculated as described in Table 2-1.

Table 2-1

Amino Acid Composition of Total Protein
from Human Fibroblasts

Cultured Human Fibroblasts			Dayhoff's Average‡
amino acid	molar frequency	residue weight x frequency§	molar frequency
ala	0.073	5.19	0.087
arg	0.054	8.43	0.045
asn*	0.042	4.79	0.043
asp*	0.053	6.10	0.057
cys‖	0.005	0.52	0.031
gln*	0.044	5.64	0.041
glu*	0.061	7.87	0.058
gly	0.080	4.57	0.088
his	0.023	3.2	0.021
ile	0.045	5.1	0.046
leu	0.086	9.8	0.072
lys	0.064	8.3	0.066
met	0.018	2.36	0.017
phe	0.034	5.0	0.035
pro	0.058	5.63	0.056
ser	0.056	4.87	0.072
thr	0.065	7.22	0.058
trp‖	0.036	6.69	0.012
tyr	0.028	4.57	0.035
val	0.075	7.43	0.066
SUM	1.000	113.3	1.000

§The residue weight is the molecular weight of the amino acid minus 18, i.e. the weight of the residue as it occurs in peptide linkage. The sum of all (residue weight x frequency) gives the mean molecular weight of residues in overall protein.

‡Dayhoff's Average is the average molar frequency of amino acids taken from a pool of 108 protein sequences , each from a different family of proteins (Dayhoff, 1972).

* Since acid hydrolysis deamidates asparagine and glutamine to aspartic acid and glutamic acid, the values given for these amino acids are derived from the measured values of asp and glu and the ratios asn/asp and gln/glu determined from Dayhoff's Average.

‖The concentration of cysteine and tryptophan cannot be determined accurately by the methods used here (Haurowitz, 1963). The amounts shown assume 10% loss of cysteine and 90% loss of tryptophan.

The amino acid composition of fetal calf serum (GIBCO lot A781020) was determined as described by de Wolfe et al. (1967).

2.2.2.3 Measurements of Protein Synthetic Rate

At indicated times, the regular growth medium from replicate cultures was rapidly replaced with identical medium containing additional phenylalanine (0.400 mM final concentration) and ^{3}H-phenylalanine (New England Nuclear, 20 Ci/mmol, 1.0 μCi/ml final concentration). The labeling medium was equilibrated in an incubator prior to addition to the cultures which were not rinsed. Dishes were removed from the incubator at 10-20 minute intervals and rinsed twice rapidly with ice cold PBS. Protein was precipitated in the dish with cold 5% TCA containing excess phenylalanine (1 mM) and rinsed twice with 5% TCA followed by a rapid and thorough rinse with H_2O. Precipitated material was solubilized with 0.4% sodium deoxycholate in 0.1N NaOH (10 minutes with shaking at 20°C). A portion of the solution was counted in a liquid scintilation counter (efficiency = 30%) and two other portions of differing volume were assayed for total protein by the method of Lowry et al. (1953). The contribution of labeled aminoacyl-tRNA to this material was insignificant compared to labeled protein as shown by control experiments in which the solubilized material was reprecipitated, washed, and resolubilized prior to counting. Other expreiments in which the original precipitates were heated to 90°C in 5% TCA

also gave identical measures of incorporation rates. All samples and standards were prepared in the same volume of 0.1N NaOH, 0.4% sodium deoxycholate prior to liquid scintilation counting or protein determination. Incorporation rates were corrected for counting efficiency and specific activity of ^{3}H-phenylalanine. A single lot of fetal calf serum was used for these experiments. The concentration of phenylalanine in this lot of serum was determined by amino acid analysis (Table 2-2) and used in the specific activity calculations. Synthetic rates were then expressed as nmoles phe incorporated/hour·dish, or after normalization to protein content per dish as nmoles phe incorporated/hour · mg protein. The validity of these methods is discussed in section 3.1.3.2.

2.2.2.4 Approach to Equilibrium Measurements of Protein Degradation.

Cells were inoculated at indicated densities into 35mm or 60mm petri dishes. Growth medium was replaced with labeling medium 1-3 days after inoculation of cells and dishes assayed at intervals thereafter for total protein content and phenylalanine incorporation as described above. In some experiments, the labeling medium from dishes was saved for assay of acid-precipitable counts to determine the export rate.

Table 2-2

Free Amino Acid Composition of Fetal Calf Serum*

amino acid	concentration (mM)
ala	1.13
arg	0.050
asp	0.131
gln	0.600
glu	0.942
gly	0.838
his	0.110
ile	0.162
leu	0.280
lys	0.248
met	0.055
phe	0.153
pro	0.254
ser	0.344
thr	0.199
trp	0.133
tyr	0.100
val	0.408
cit	0.077
hyp	0.151
orn	0.278
tau	0.133

*GIBCO Lot # A781020. Analysis was performed as described in section 2.2.2.2. Only the amino acids whose molar concentrations were determined are shown.

2.2.2.5 Measurements of Synthetic Minus Net Growth Rate

Net growth rates were determined from measurements of total cellular protein (Lowry et al., 1953). Growth rate parameter g was obtained from linear regression analysis of ln(protein content) versus time. Measurements of protein synthetic rate were determined as described above. To calculate mg total amino acid incorporated/mg cell protein, the measured synthetic rate was divided by the mole fraction of phenylalanine in protein labeled to equilibrium and multiplied by the mean molecular weight of amino acids in total protein (Table 2-1). The degradation rate of protein was calculated by subtracting the net growth rate at the time of the synthetic rate determination from the total protein synthetic rate.

2.2.3 Results

Figure 2-2 shows the growth curves for early and late passage cells from A2, a young normal donor, and P5, a progeric child (Table 3-1). The first order growth rate constant g is obtained from the slope of the growth curves on semi-(natural)log plots. The curves are linear during exponential growth, but begin to plateau when the growth rate declines due to density dependent inhibition of growth and/or depletion of serum factors. It is noteworthy that cells were visibly confluent before the growth rate declined appreciably, indicating that exponential growth of protein content continues beyond a monolayer of cells.

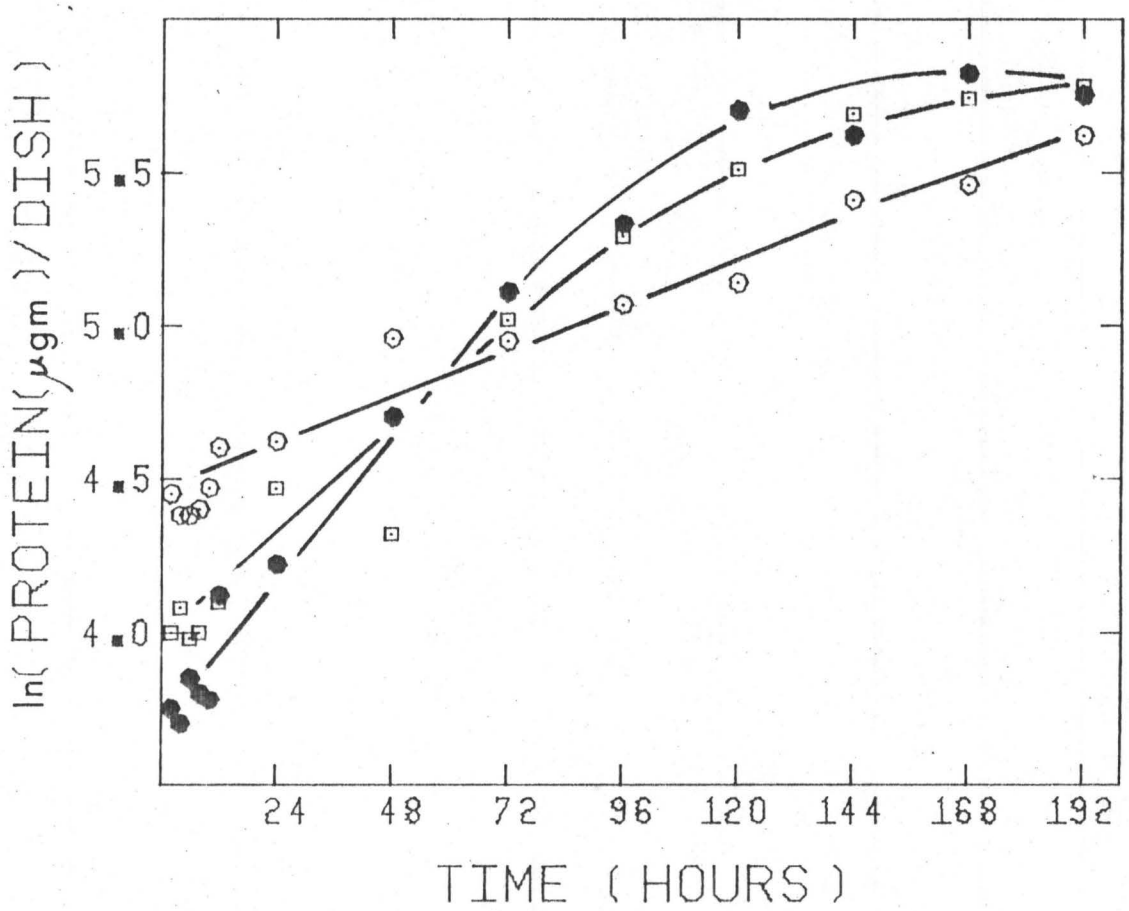

Figure 2-2

Analysis of total protein per dish to determine the net rate of protein accumulation during exponential growth. Cells from a young donor, A2, at early (●) and late passage (○) and cells from progeria P5 (□) at early passage were inoculated at low densities at time t=-24 hours. Label was added for incorporation rate determinations at t=0 and dishes were removed for assay at the indicated times. Linear regression analysis of ln(protein content/dish) over the linear portion of these curves (indicating exponential growth) provided the following data:

	g (±S.D.)(hr^{-1})	t_{DBL}(hr)
A2 early passage (●)	0.0216 (0.0024)	34
A2 late passage (○)	0.0065 (0.0004)	112
P5 early passage (□)	0.0130 (0.0022)	57

In other experiments, cell number was determined as well as protein content (figure 2-3). The rates of increase of protein and cell number were identical during exponential growth. Cell number plateaus slightly faster than protein content indicating that the protein content of confluent cells is greater than that of exponentially growing cells.

The approach to equilibrium of labeled protein normalized to total protein is shown in figure 2-4. The plateau level of incorporation was determined and the data transformed as described in section 2.1 (figure 2-5). The turnover parameter (d+e+g), obtained by linear regression analysis of the data in figure 2-5 was similar in early- and late-passage normal and progeria cells despite the fact that the contribution of net growth (g) to this parameter was significantly different for the three cell populations.

To calculate the export rate (e) of protein, which includes both exocytosis of proteins and sloughing of cells from the surface of the dish, samples of the labeling medium were assayed for acid-insoluble radioacitivity at intervals during the labeling period (figure 2-6). Export rate (e) was calculated from $\bar{P}^*_{m\infty}$, g, and $\bar{P}^*_{\ell\infty}$ as described in section 2.1.

Values from three experiments for the combined turnover parameter (d+e+g), the growth rate (g), and export rate (e), for two normal strains at early or late passage and two progeria strains at early passage are shown in Table 2-3. The degradation rate d is obtained from these data by

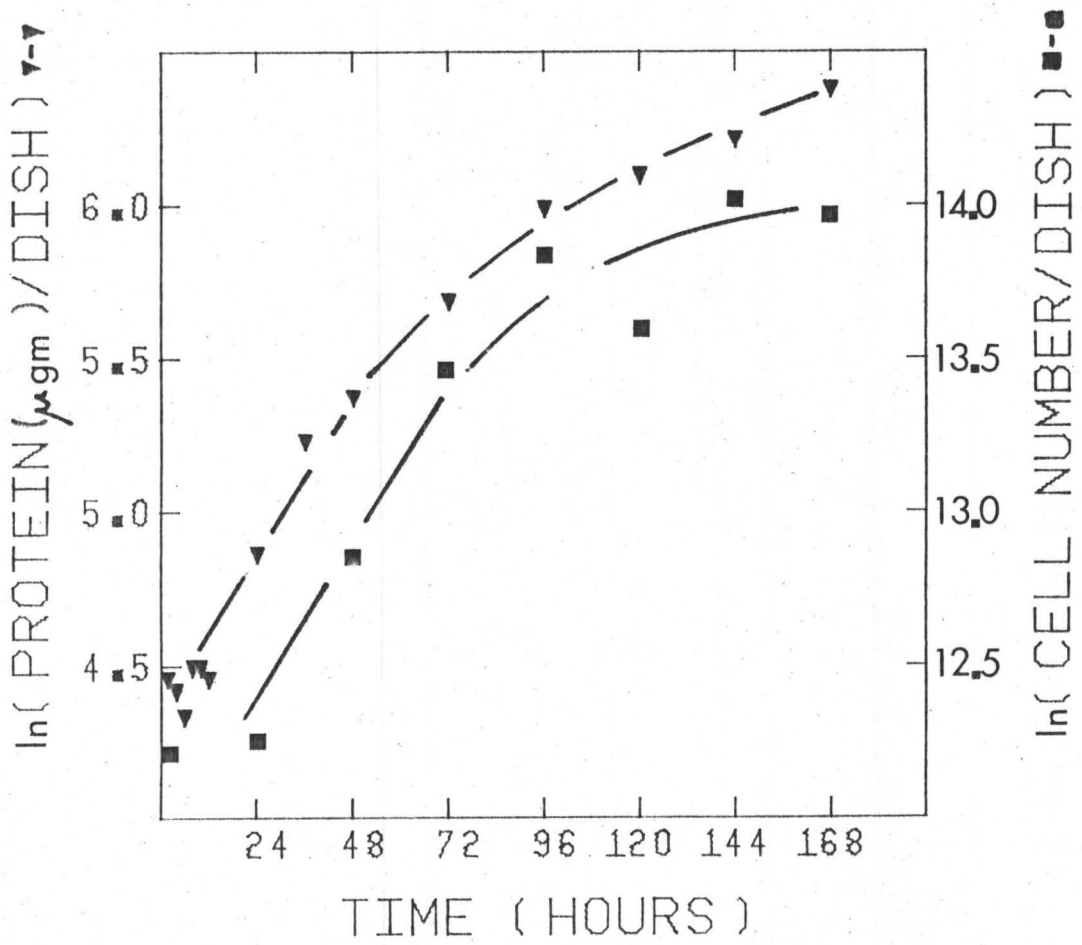

Figure 2-3

Comparisons of Protein Accumulation and Net Growth Rates. The natural log of net protein (▼) from early passage A2 cells was determined as described in figure 2-2. Replicate dishes in this experiment were harvested with trypsin (0.125%) and cell number per dish determined with a hemocytometer. The natural log of this number (■) is plotted as a function of time. The exponential growth rate of net protein, determined by linear regression analysis, was 0.023 ± 0.002, while the exponential growth rate of cell number was 0.024 ± 0.002.

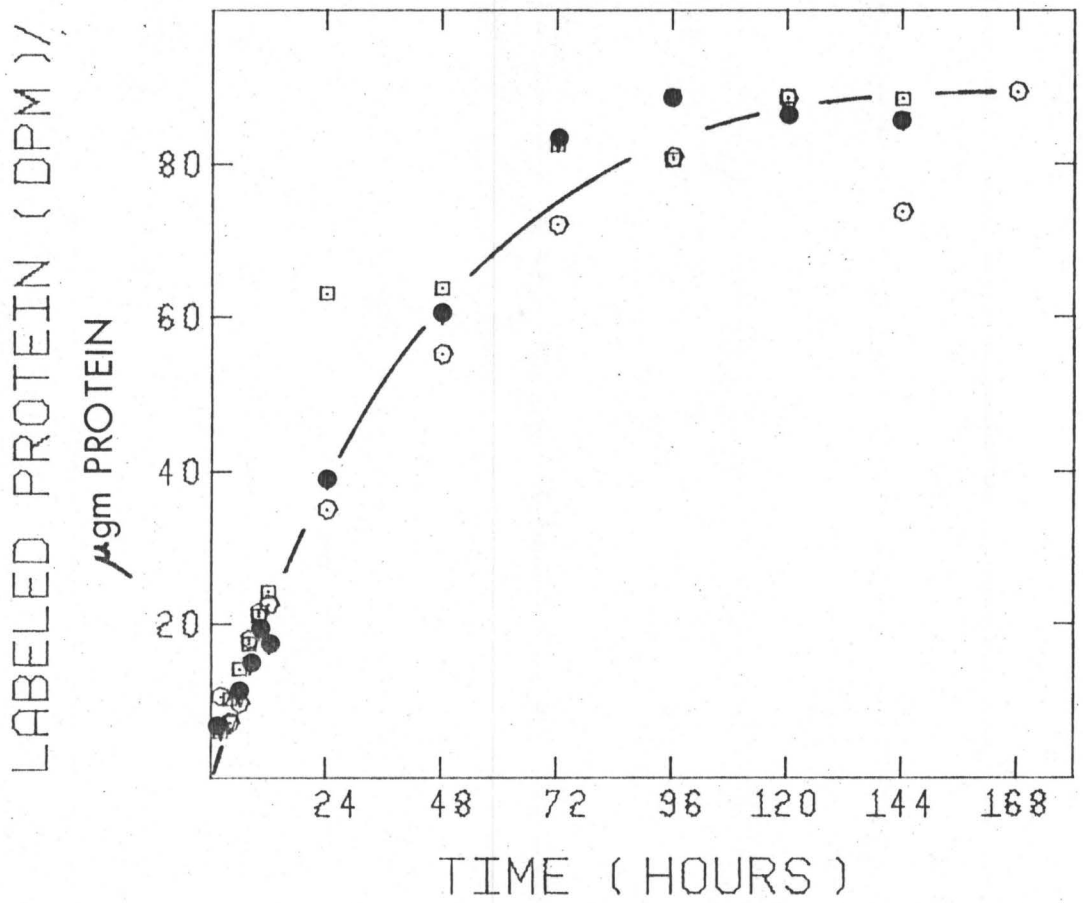

Figure 2-4

Approach to equilibrium of labeled protein during exponential growth. Early (●) and late passage A2 (O) and progeria P5 (□) cells were treated as described in figure 2-2. The amounts of labeled protein (dpm/dish) were divided by the total protein (μg/dish) and plotted as a function of time.

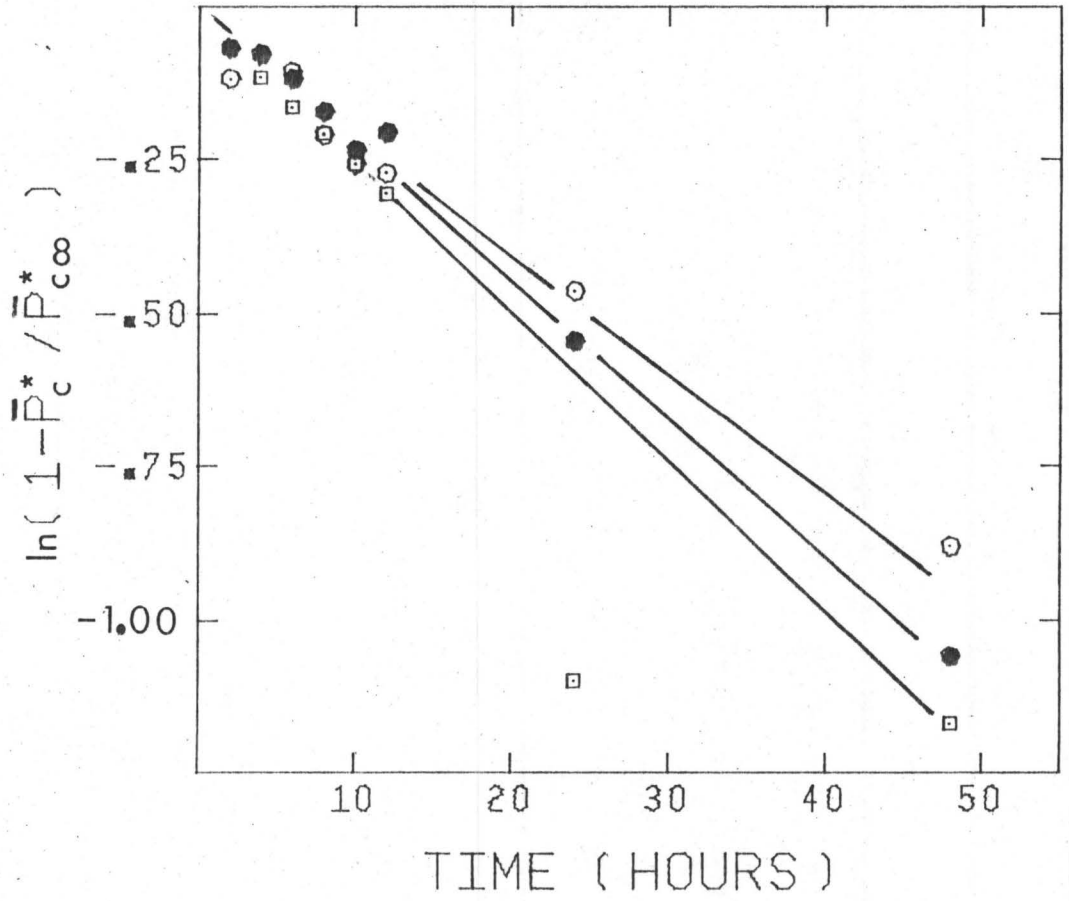

Figure 2-5

Determination of the turnover parameter (d+e+g) during exponential growth. The data from figure 2-4 were transformed as described in section 2.1.1 and plotted as a function of time for early- (●) and late- (○) passage normal A2 and progeric P5 (□) cells. For $t > 50$, $\bar{P}^*_c \approx \bar{P}^*_{c\infty}$ and the transformation of the data involves taking the natural log of a small number. Since this greatly amplifies experimental error, the linearization is only valid at small values of t (less than two half-lives). Linear regression of all points shown except (□) at t = 24 hours provided the following data:

	(g+d+e) h^{-1} (± S.D.)
A2 early passage (●)	0.0221 (0.001)
A2 late passage (○)	0.0197 (0.0004)
P5 early passage (□)	0.0243 (0.002)

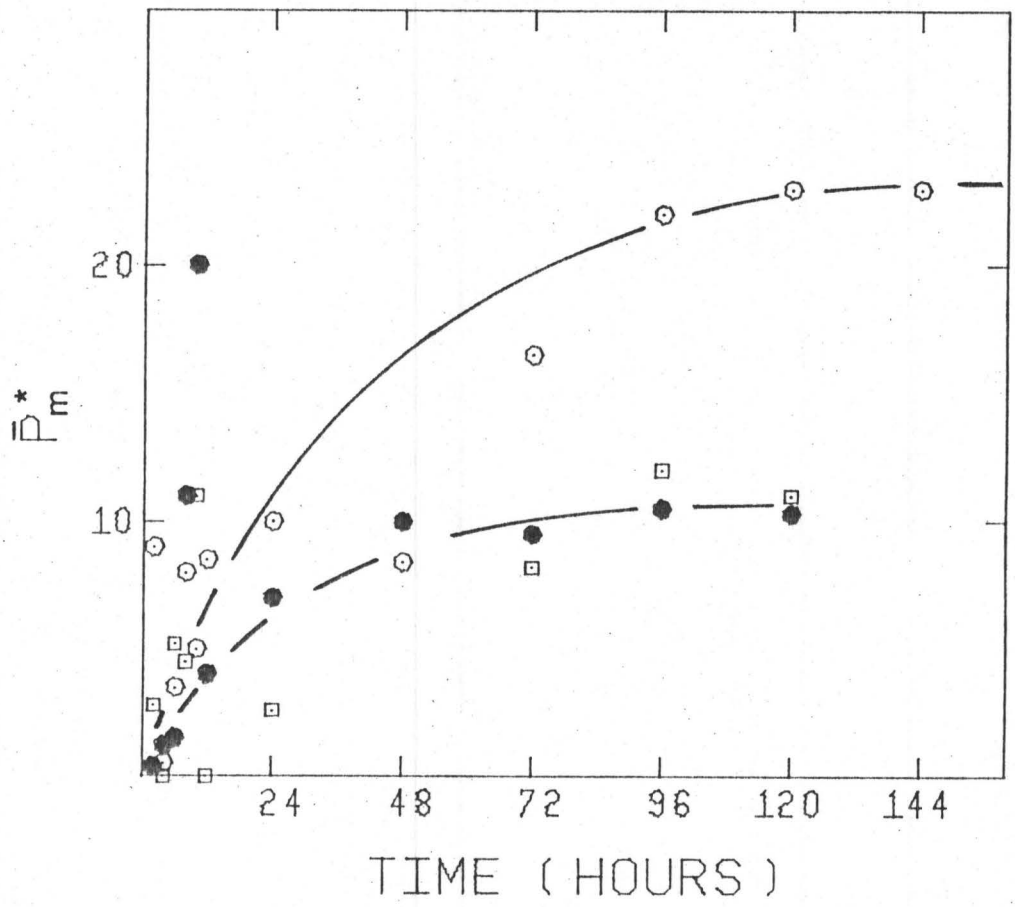

Figure 2-6

Export of protein into the medium. Early- (●) and late-passage normal A2 (O) and progeric P5 (□) cells were treated as described in figure 2-2. Labeled protein in the medium was determined by precipitating an aliquot of the medium with an equal volume of 20% TCA and washing the precipitate twice by centrifugation and resuspension. The precipitate was solubilized in 0.1 N NaOH in 0.4% sodium deoxycholate, dissolved in counting fluid, and counted in a liquid scintillation counter. The amounts of labeled protein in the medium (dpm/dish) were normalized to the amounts of total cellular protein (μg/dish) to obtain $\bar{P}_m^*$ and plotted as a function of time. The plateau value of $\bar{P}_m^*$ was multiplied by g and divided by $\bar{P}_{\xi\infty}^*$ to obtain e. In this experiment, the values of e were 0.0024 (early-passage normal), 0.0016 (late-passage normal) and 0.0017 (progeria P5).

Table 2-3

Protein Turnover During Exponential Growth

Experiment	Cell	Total Turnover (d+e+g)	Net Growth (g)	Export (e)	Degradation (d)
1	Normal A2 early passage	0.0221	0.0216	0.0024	0-0.0005
	Normal A2 late passage	0.0197	0.0065	0.0016	0.0116-0.0132
	Progeria P5 early passage	0.0243	0.0130	0.0017	0.0096-0.0113
2	Normal A2 early passage	0.0266	0.023	0.0002	0.0034-0.0036
	Normal A2 late passage	0.0279	0.0080	0.0005	0.0149-0.0154
	Progeria P5 early passage	0.0252	0.0133	0.0002	0.0099-0.0101
3	Normal A1 early passage	0.0222	0.0167	-	0.0044-0.0055
	Progeria P18	0.0228	0.0098	-	0.0119-0.0130

All values have units $(hours)^{-1}$. Data from figures 2-2 through 2-6 were analyzed as described in section 2.1.1 to obtain (d+e+g), (g) and (e). The degradation rate (d) is obtained by subtracting (g) and (e) from (d+e+g). The error in determining the rate of protein export is largely due to difficulties in completely rinsing labeled amino acid from serum proteins in the medium (see figure 2-6). Therefore the export rate represents a maximum value and the true degradation rate lies between d and d+e. The upper bound (d+e) is also shown.

For experiment 3, export rates were not determined. The lower bound on degradation in this experiment was obtained by subtracting the mean value of (e) obtained in experiments 1 and 2 from (d+e).

subtracting (g) and (e) from (d+e+g). In these experiments, the derived value for the degradation rate during exponential growth was smaller in early-passage normal cells than in late-passage normal or progeric cells. The total turnover rate of protein (d+e+g) represents the protein synthetic rate normalized to protein content. This parameter did not vary systematically between early- and late-passage normal and progeric cells. Thus the substantial reduction in net growth rate of late-passage and progeric cells is not due to a reduced rate of protein synthesis or an increased rate of protein export, but is accounted for by their relatively high rate of degradation.

When cells have been confluent for several days, the increase in cell number and net accumulation of protein are close to zero (figure 2-7). Analysis of approach to equilibrium data during confluence yields a combined rate parameter (d+e) (section 2.1) (figures 2-8 and 2-9). Acid-insoluble counts in the medium were used to estimate the export rate as described in section 2.1. The export rate was less than 10% of the total turnover rate (d+e) for early- and late-passage normal cells as well as progeria cells in two experiments in which the medium was analyzed (not shown). Since the rate of export is small, the degradation rates are approximated by the turnover parameter (d+e) obtained directly from linearizing the approach to equilibrium data. No age-related differences of total protein turnover during steady state growth have been detected (figure 2-9).

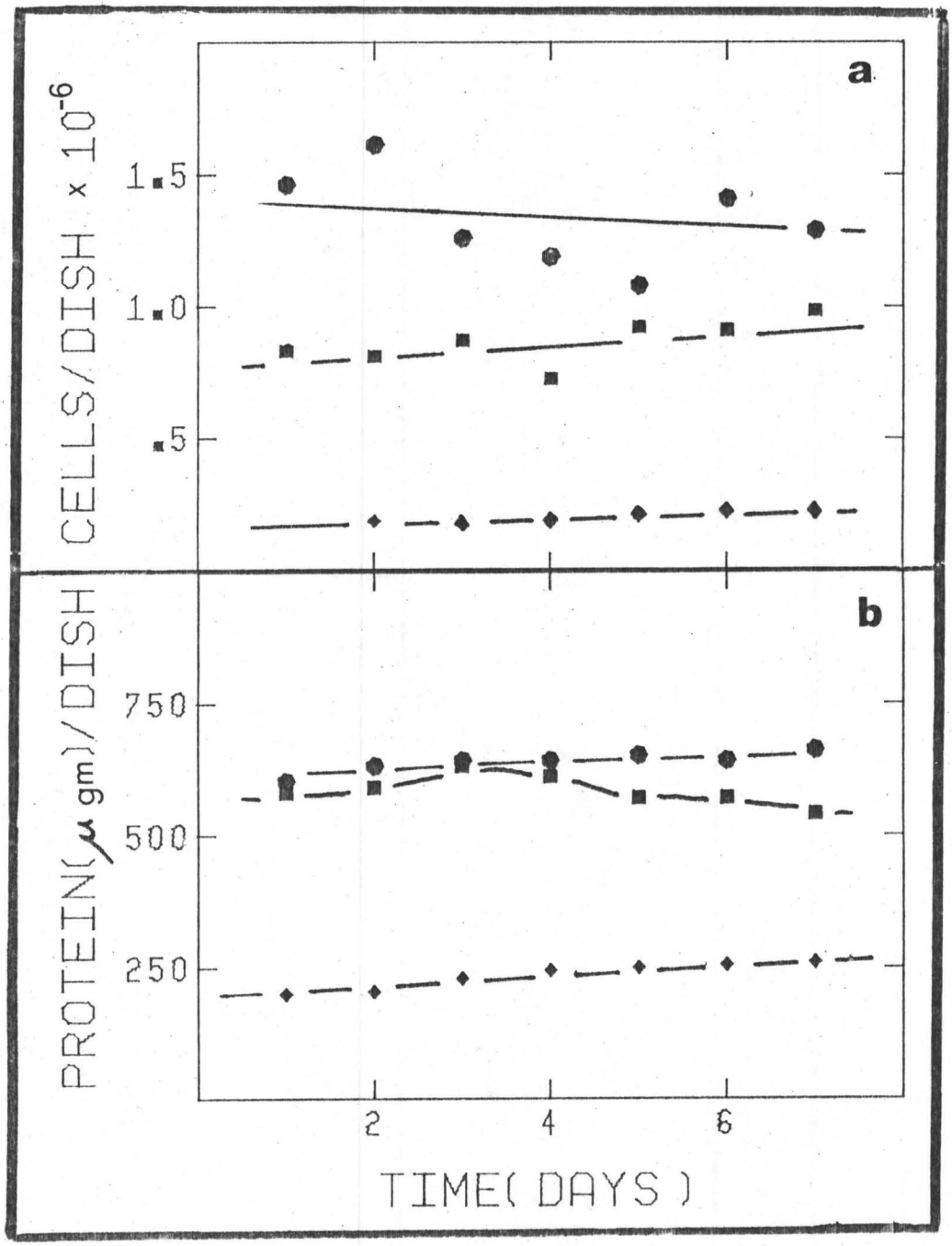

Figure 2-7

Cell number and protein content of confluent cultures.
Cells from a young donor, A2, at early (●) and late passage (◆), and cells from progeria P5 (■) at early passage were inoculated at high density at time t=-60 hours and refed at t=-24 hours. Label was added at time t=0 and dishes were removed for assay at indicated times. Cell number (a) and protein content per dish (b) were determined.

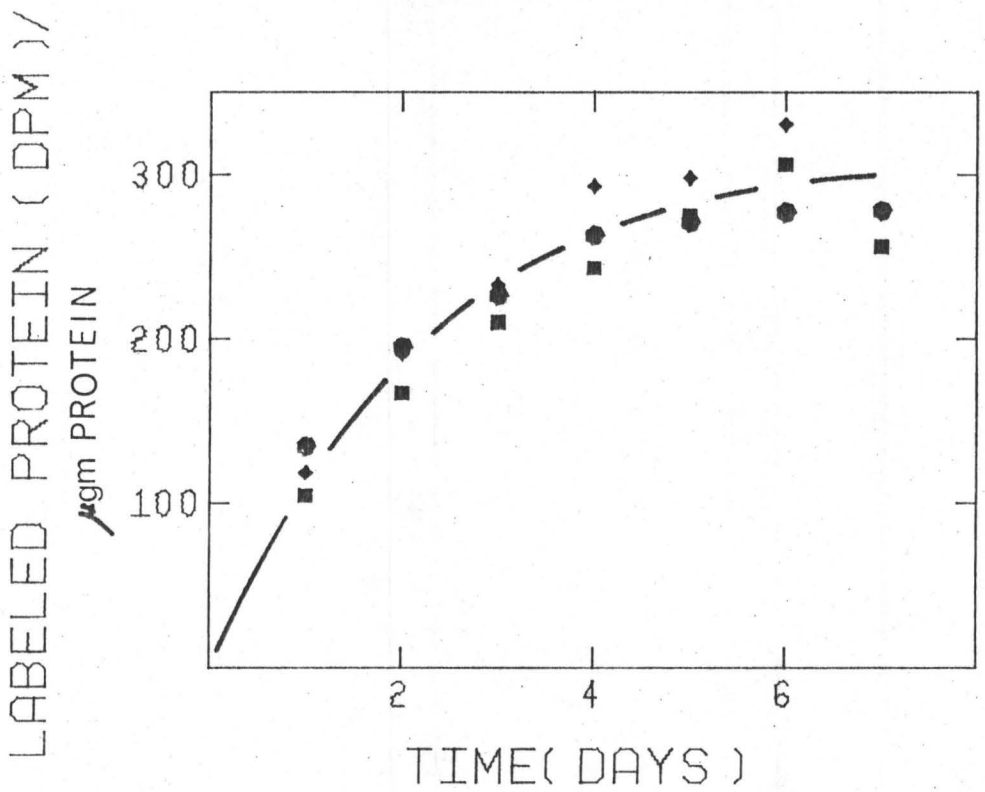

Figure 2-8

Approach to equilibrium of labeled proteins during confluence. Early (●) and late (◆) passage A2 and progeria P5 (■) cells were treated as described in figure 2.7. The amounts of labeled protein (dpm/dish) were divided by the total protein (µgm/dish) and plotted as a function of time.

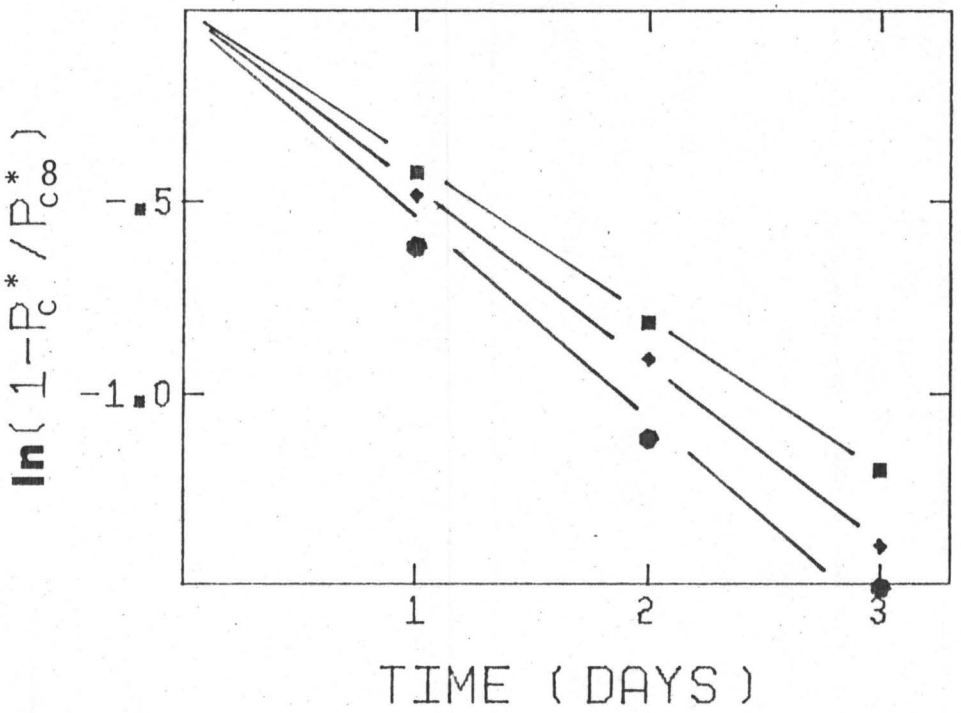

Figure 2-9

Determination of the turnover parameter (d+e) during confluence. The data from figure 2-8 were transformed as described in section 2.1.1 and and plotted as a function of time for early (●) and late (◆) passage A2 and progeric P5 (■) cells. Linear regression of the points shown provided the following data:

	(d+e) (h^{-1})
A2 early passage	0.022 ± 0.003
A2 late passage	0.019 ± 0.002
P5 early passage	0.018 ± 0.002

Similar results were found in two other experiments.

To determine if degradative rates obtained from approach to equilibrium analysis were consistent with direct measurements of protein synthetic and net growth rates, incorporation rates of phenylalanine were converted to total synthetic rates (mg amino acid incorporated/mg protein) by taking into account the mole fraction of phenylalanine in protein labeled to equilibrium. Figure 2-10 shows the determination of synthetic rates in early passage normal cells (donor A2) during exponential growth and during early and late stages of confluence. The legend to figure 2-10 also shows the synthetic rates in mg amino acid incorporated/mg total protein hour and the growth rate in mg net protein synthesized/mg protein hour. The difference between these values is the degradation rate. In this experiment it is again seen that for early passage cells, the degradation rate during exponential growth is small while the growth rate is large. The reduction in growth rate during confluence is first achieved by an increase in the degradation rate and later by a decrease in the synthetic rate. The decrease in the synthetic rate may be related to the freshness of the growth medium (see figure 2-11).

Other cell strains were analyzed by this method over a ten day period (figure 2-11). Cells from young donor A2 were studied at early, mid, and late passage; cells from old donor J088 were studied at early and late passage; cells from a subject with Werner syndrome, WS2, and two subjects with progeria, P5 and P18, were studied at early passage. Protein

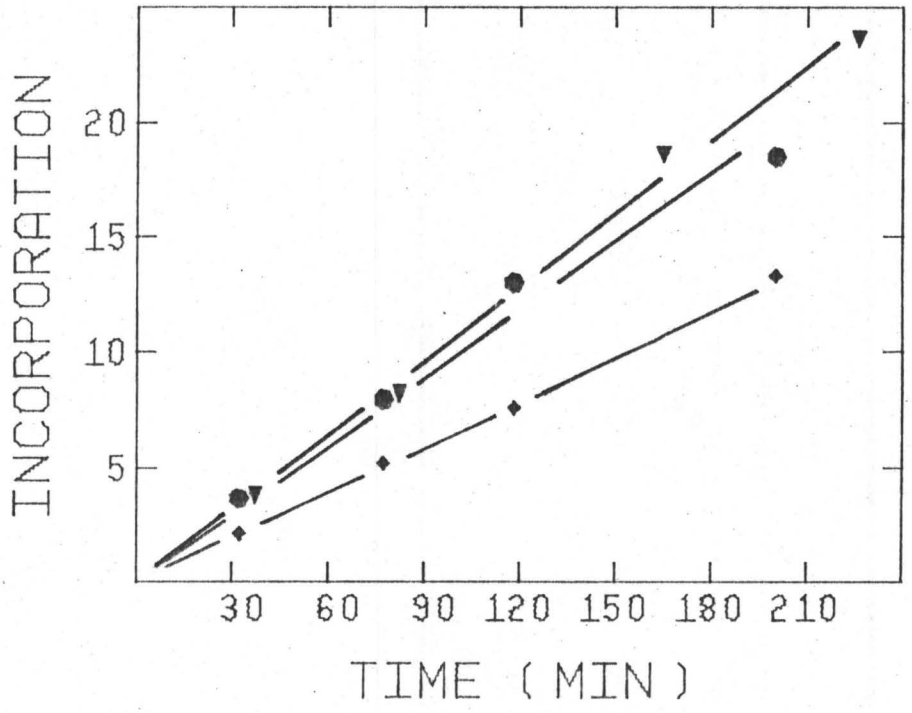

Figure 2-10

Determination of protein synthetic rates. Synthesis of protein in nmoles phenylalanine incorporated/mg total protein is shown as a function of time for early passage young donor A2 during exponential growth (●) and when cultures were 2 days confluent (▼) and four days confluent (◆). The slopes of these lines were determined and the incorporation rate of total mg amino acid/mg protein calculated from the specific activity of protein labeled to equilibrium. The net protein growth rates were determined by total protein assays as described in section 2.2.2. The following results were obtained:

	(a) synthetic rate mg a.a. incorp./ mg protein x hr	(b) growth rate mg net protein/ mg protein x hr	(c) degradation (a)-(b) (hr^{-1})
exponential growth	0.031	0.026	0.005
2-days confluent	0.032	0.0091	0.023
4-days post confluent	0.020	0.0044	0.016

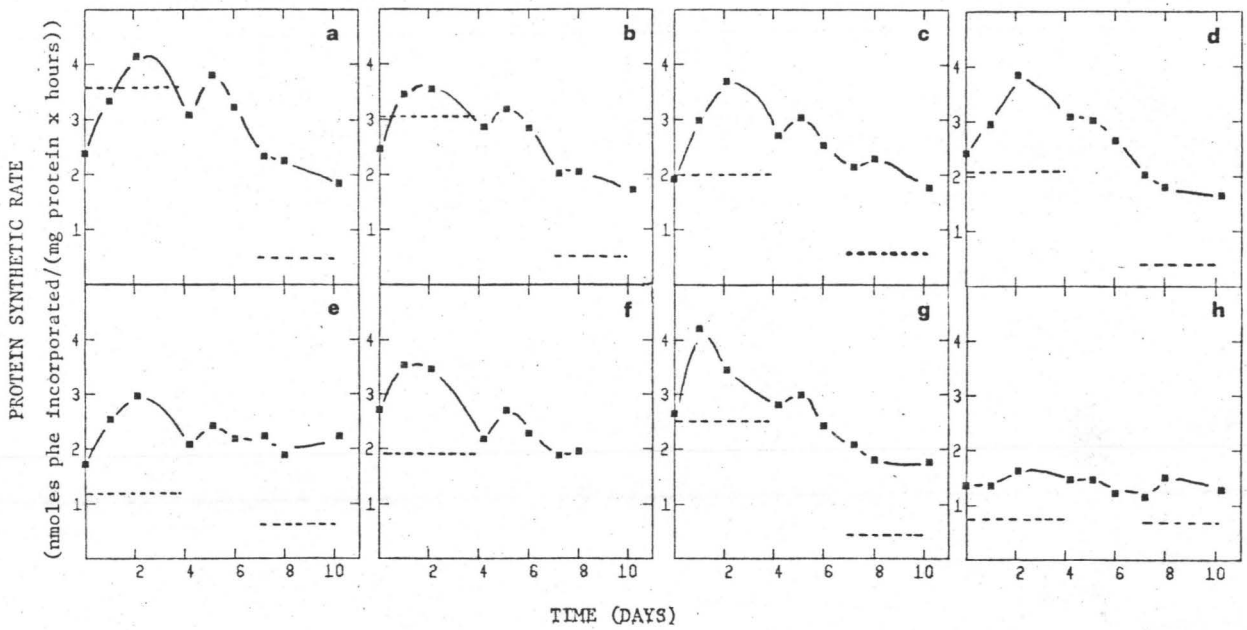

Figure 2-11

Protein synthetic rates and net growth rates. Protein synthetic rates (■—■) are shown as nmoles phenylalanine incorporated/mg protein x hour for cells from young donor A2 at early (a), mid (b) and late (c) passage; Werner Syndrome WS2 at early passage (d); progeria donors P5 (e) and P18 (f) at early passage; and old donor J088 at early (g) and late (h) passage. Cells were inoculated at low density 24 hours prior to time 0. At indicated times, growth medium on four dishes of each cell strain was replaced with labeling medium and cultures subsequently treated at 15 minute intervals to determine protein synthetic rate as described in section 2.2.2. Each point represents the slope of the incorporation data normalized to specific activity of labeled phenylalanine and the total protein content per dish at the time of the analysis. All dishes were refed on day 4.

Net growth rates (- - - -) from day 0 through day 4 and day 7 through day 10 were determined from analysis of total protein. From day 0 to day 4, all cells were in exponential growth. From day 7 to day 10, all strains were confluent except the old donor J088 at late passage and progeric strain P5. Dishes were not available for progeric strain P18 on day 10. Growth rates are expressed as rates of phenylalanine incorporation on the basis of the equilibrium content of phenylalanine in total protein.

synthetic rates could be determined accurately at daily intervals but net growth rates could only be averaged over three- or four-day periods during which plots of ln(protein.content) versus time were linear. It is apparent that in most cell strains, the protein synthetic rate varies throughout the growth period and is probably a complex function of cell density, freshness of medium, passage level *in vitro*, and genotype of donor. Most cell strains showed an increase in protein synthetic rate from day 0 to day 1, perhaps due to conditioning of medium and/or greater intercellular communication as the cell density increased. Between day 3 and day 4, most strains showed a decline in protein synthetic rate, perhaps due to depletion of serum factors. Refeeding of cells on day 4 caused another increase in protein synthetic rate which then gradually declined to day 10 as cell density increased and the medium aged.

Despite the unknown factors involved in regulation of growth in these experiments, a comparison of the growth and protein synthetic rates again shows the same trend as observed with approach to equilibrium analysis: early passage cells from young normal donors have a net exponential growth rate which is greater than that of "old" cells and which approximates the total protein synthetic rate, implying a degradation rate close to zero. Cells at late passage and cells from old donors or subjects with features of accelerated aging all have reduced exponential growth rates which are principally accounted for by an increased

degradation rate. The total synthetic rates of young and old cells are similar. An exception to this rule is the terminal-passage cells from old donor J088 which had a substantially reduced protein synthetic rate which accounted in part for their low net growth rate. But even in these cells, the net growth rate was only about half the protein synthetic rate.

Between days 7 and 10 the growth rates had declined substantially in all cell strains except late-passage J088 and progeria P5, both of which had not reached confluence. The decrease in growth was partially due to a decreased synthetic rate. The protein synthetic rates of all cells except terminal passage J088 were similar between days 7 and 10.

2.2.4 Discussion

Old cells (cells from normal donors at late passage or cells from old donors or sujects with features of accelerated aging (progeria or Werner Syndrome)) have reduced growth rates when cultured at low density compared to young cells (early-passage cells from young normal donors). Net accumulation of protein corresponds to the increase in cell number observed during exponential growth. The reduced rate of growth in old cells, prior to terminal passage, is accounted for by an increased rate of protein degradation. The rate of export of cellular protein was small compared to

the rate of protein synthesis for all cell strains studied.

It is not known whether the increased protein degradation of old cells is caused by an increased proportion of aberrant proteins which evokes an elevated rate of degradation, or an inability to regulate protein turnover in response to growth signals. In view of the fact that differences between young and old cells are growth-stage dependent, the latter possibility seems more likely. Furthermore, direct attempts to observe abnormal protein on two-dimensional gel electrophoresis and increased error rates during amino acid starvation failed to reveal differences between young and old cells (Harley et al., submitted; section 3.1). Since young cells during confluence have a degradation rate essentially identical to that of old cells, the increased degradation of low-density old cultures may result from an inability to inhibit protein degradation in response to growth signals. It is known that the number of lysosomes per cell increases during confluence and during aging in vitro (Robbins et al., 1970; Cristofalo, 1970). These degradative organelles may be responsible for the increased rates of degradation seen in confluent, young cultures and low-density old cultures.

Terminal passage cells have a reduced activity of both protein synthesis and degradation when normalized to total protein (figure 2-11). Since there are nonviable cells in terminal passage cultures (unpublished observations) part of

the reduced turnover of protein may be caused by dilution of active protein with protein from dead cells.

Regulation of net growth rates in early-passage cells from young donors is achieved by changes in both the rate of protein synthesis and the rate of protein degradation. Other workers have made similar observations in WI38 (Castor, 1977), Balb 3T3 cells (Hendil, 1977) and rate embryo fibroblasts (Warburton and Poole, 1977). However, there are also reports that protein degradation is invariant during the various stages of growth for chick embryo fibroblasts (Wever, 1972), WI38 (Bradley, 1977), Vero cells (Lee and Engelhardt, 1977), and hamster and rat embryo cells (Baxter and Stanners, 1978). The reason for these discrepancies is not clear. There may be species differences (Hendil, 1977), but in addition, different methods of measuring degradation and different methods of inducing growth and steady-state conditions may themselves produce different rates of protein degradation in the same cell strain (see also section 1.3.3). Direct measurements of net growth and synthetic rates provide means of validating the measurements of protein degradation (Baxter and Stanners, 1978). In view of the potential artifacts in assays of protein degradation, it is advisable that this method be used in conjunction with others. The measured rates of protein growth, export, and degradation in human cells using analysis of labeling to equilibrium are in agreement with my direct measurements. I conclude that the rapid growth of young cells results from an increased rate of

protein synthesis coupled with a decreased rate of protein degradation while the slow growth of old cells is caused by an inability to reduce protein degradation during conditions of exponential growth.

3 MISTRANSLATION DURING AMINO ACID STARVATION

Nearly all of the material presented in this section represents work I did in Dr. S. Goldstein's laboratory during our collaboration with Dr. C.P. Stanners, Dr. J.W.Pollard, and J.W. Chamberlain (Ontario Cancer Institute, Toronto). Some data, as indicated, were collected by Dr. Pollard and J.W. Chamberlain in Dr. Stanners' laboratory.

Two major findings resulted from this collaboration. First, error frequencies were shown not to increase during aging of human fibroblasts. And second, certain types of transformed cells were shown to be associated with an increased level of mistranslation. I conducted the aging studies in Dr. Goldstein's lab and they were confirmed in Dr. Stanners' laboratory. The first indication of a dramatic increase in the error frequency of transformed cells came from my observations with three strains of normal human cells and their SV40-transformed counterparts. This was also confirmed and extended to normal versus SV40-transformed 3T3 cells in Dr. Stanners' laboratory. Other types of transformation, studied in both of our laboratories, were not associated with marked increases in the error frequency.

The manuscripts submitted or in preparation as a result of our collaboration are:

1. Protein Synthetic Errors Do Not Increase During Aging of Cultured Human Fibroblasts. C.B.Harley, J.W.Pollard, J.W.Chamberlain, C.P.Stanners, and S.Goldstein (Proc. Natl. Acad. Sci. U.S.A., in press) (section 3.1)

2. SV40-Transformation is Associated with an Increased Protein Synthetic Error Frequency in Cultured Cells. J.W.Pollard, C.B.Harley, J.W.Chamberlain, S.Goldstein, and C.P.Stanners (in preparation)

3. A Model of mRNA Translation During Amino Acid Starvation Applied to the Calculation of Error Rates. C.B.Harley, J.W.Pollard, C.P.Stanners, and S.Goldstein (submitted) (section 3.2)

4. Calculation of Isoelectric Points Applied to Analysis fo Amino Acid Substitutions in Proteins. C.B.Harley and S.Goldstein (submitted) (section 3.3)

We decided to publish the aging and transformation results separately (the first two manuscripts above) but for this thesis I have pooled my relevant data into one section (3.1) entitled "SV40-Transformation but not Aging is Associated with Increased Mistranslation in Cultured Human Cells". Nevertheless, this section is very similar to the submitted manuscript (1, above) and I acknowledge, therefore, the help of my colleagues in writing this section of the thesis.

3.1 SV40 Transformation but not Aging is Associated with Increased Levels of Mistranslation in Cultured Human Cells

3.1.1 Abstract

To test the error catastrophe theory of aging we determined the error frequency of protein synthesis in cultured human fibroblasts from young and old donors at early and late passage. Error rates were calculated from analysis of native and substituted actins on two-dimensional gels of cellular proteins following induction of mistranslation by histidine starvation in the presence of histidinol. Early passage cells from fetal, young and old donors and cells from subjects with the Hutchinson-Gilford syndrome of accelerated aging (progeria) had similar error frequencies. Late-passage cells from fetal, young and old normal donors had similar or lower error frequencies than their corresponding early-passage cells. No correlation was observed between error frequency, donor age or maximum lifespan in vitro . To determine if immortal cells had a reduced error frequency, we also examined SV40-transformed WI38 fibroblasts. These cells had a significantly elevated rate of mistranslation ($2.8 \pm 0.2 \times 10^{-4}$) compared to either their untransformed counterparts (WI38) ($0.6 \pm 0.1 \times 10^{-4}$, mean + S.E.) or all diploid cells combined ($1.1 \pm 0.1 \times 10^{-4}$). Taken together the data fail to support the error catastrophe theory of aging.

3.1.2 Introduction

The error catastrophe theory of cellular aging (Orgel, 1963) postulates that errors in protein synthesis lead to a protein synthetic machinery with progressively lower fidelity and the eventual accumulation of a lethal proportion of aberrant proteins (section 1.2.2.2(b)). A corollary of this hypothesis is that the abrogation of senescence by transformation of fibroblasts into permanent lines should be associated with a lower rate of translational errors.

A major difficulty in testing these predictions has been the lack of a rapid and direct measure of error frequencies in intact eukaryotic cells. Parker et al. (1978) and O'Farrell (1978) have recently developed a method in which the synthesis of error-containing proteins can be induced in bacterial and animal cells by amino acid starvation (section 1.5.3). Due to specific amino acid substitution after starvation for a particular amino acid, proteins are synthesized with altered isoelectric points. These proteins appear on 2-D polyacrylamide gels (O'Farrell, 1975) as a series of satellite spots trailing the native protein spots in the isoelectric focusing dimension (Parker et al., 1978; O'Farrell, 1978), a phenomenon known as stuttering.

In this section, I describe the development of this system into a quantitative assay and its application to the measurement of error frequencies in a variety of cultured

human fibroblasts. The data are contrary to the error catastrophe theory of aging: error frequencies of late-passage cells and cells from old donors or subjects with progeria are not increased compared to early-passage cells from young donors while the error frequency of SV40-transformed permanent lines are significantly increased.

3.1.3 Materials and Methods

3.1.3.1 Cell Culture

The cells strains used in this study are listed in Table 3-1. "Early passage" denotes cultures with less than 50% of the lifespan completed (Hayflick, 1965) and with greater than 80% of cells capable of proliferation using the thymidine labeling index (Cristofalo, 1976). "Late passage" denotes cultures with greater than 90% of the lifespan completed or with a thymidine labeling index of 20% or less (Harley and Goldstein, 1978). Cells were grown on plastic surfaces at 37° C in an atmosphere of 95% air, 5% CO_2 using Eagle's minimal essential medium supplemented with 15% fetal calf serum (FCS, Gibco, U.S.A.), nonessential amino acids, glucose and pyruvate (Goldstein and Littlefield, 1969).

3.1.3.2 Amino Acid Starvation and Labeling Conditions

Cells were subcultured into 35 mm dishes (Corning Plastics, U.S.A.) at 3-5 x 10^4 cells/dish. After 2-4 days, cells were rinsed once with α-MEM (Stanners et al., 1972) minus histidine and methionine supplemented with 0.2 mM

Table 3-1

Description of Cell Types

Tissue of Origin	Cell Strain	Donor Age (years)	Reference
Human lung	WI38	fetus	Hayflick, 1965
	WI38-SV40	fetus	Girardi et al., 1970
	MRC5	fetus	Jacobs et al., 1978
	MRC5-SV40	fetus	a
Human Skin	A2	11	Harley and Goldstein, 1978
	GM37	18	b
	GM37-SV40	18	b
	RE	11	c
	JOO4	24	c
	JO88	76	Goldstein et al., 1979
	JO69	69	Goldstein et al., 1979
	P5 (progeria)	9	Goldstein and Moerman, 1975
	P18 (progeria)	5	Goldstein and Harley, 1979
	WS2 (Werner Syndrome)	37	Yatscoff et al, 1978
	WS3 (Werner Syndrome)	17	Yatscoff et al, 1978
	WS4 (Werner Syndrome)	41	c
Human Kidney adenovirus type-5 transformed	293[d]	fetus	Graham et al., 1977
Human cervical carcinoma	HeLa[e]		Gey et al., 1952
Chinese hamster ovary	CHO[f]		see Pollard and Stanners, 1979
Chinese hamster embryo	CHF[f]		Pollard and Stanners, 1979
Hamster embryo	Nil[f]		Zavada and MacPherson, 1970
	Nil-HSV (hamster sarcoma virus transformed Nil)[f]		Zavada and MacPherson, 1970

Table 3-1 continued

Chick embryo fibroblasts	CEF[g]	see Kawai and Hanafusa, 1971
	CEF-RSV (Rous sarcoma virus transformed CEF)[g]	Kawai and Hanafusa, 1971
	CEF-RSVts (ts-68 RSV transformed CEF)[g]	Kawai and Hanafusa, 1971

Footnotes to Table 3-1

[a] R.Holliday and L. Hauschka, unpublished results, from Dr. R. Holliday

[b] Human Genetic Mutant Cell Repository List of Genetic Mutants (1978), Dept. of Health, Education and Welfare, U.S.A.

[c] S.Goldstein, unpublished observations

[d] from Dr. F.L.Graham

[e] from Dr. H.P.Ghosh

[f] from Dr. C.P.Stanners

[g] from Dr. P.E.Branton

all other cells were obtained from Dr. S.Goldstein

phenylalanine and 5% undialyzed FCS and then incubated for 40 minutes in this medium containing either 0.1 mM histidine (unstarved conditions) or 2-20 mM histidinol (Calbiochem, U.S.A.) (starved conditions). These media were then replaced with identical media containing either 2-15 μCi/ml ^{3}H-phenylalanine (NEN, 20 Ci/mmole) for measurement of protein synthetic rates or 5-150 μCi/ml ^{35}S-methionine (NEN, > 500 Ci/mmole) for labeling of proteins for analysis by 2-D gel electrophoresis. To measure the rate of protein synthesis, ^{3}H-labeled cells were rinsed rapidly with ice-cold PBS and precipitated directly on the dish with 5% TCA at 10 minute intervals for a total labeling period of 40 minutes. Cells were rinsed thoroughly with 5% TCA, rapidly with H2O and finally solubilized with 0.4% sodium deoxycholate in 0.1 N NaOH. Samples were taken for measurement of radioactivity in a liquid scintillation counter or for measurement of protein by the method of Lowry et al. (1951). For 2-D gel analysis, S-labeled cells were rinsed rapidly at the end of the 40 minute pulse with ice-cold PBS and directly solubilized by addition of 400 ul lysis buffer A (O'Farrell, 1975) at room temperature. Ten minutes later the lysate was removed from the dish and frozen -70°C until used.

The comparison of protein synthetic error rates in different cell types is critically dependent on accurately measuring the rate of protein synthesis and the validation of these methods has been discussed in detail (Baxter and Stanners, 1978; Stanners et al., 1979). In brief, a very

small quantity of radioactively labeled amino acid was added to medium containing a large amount of unlabeled precursor, and after a short lag period, linear incorporation of the isotope into protein was observed. Incorporation rates measured under varying concentrations of non-radioactive precursors (0.2-4.0 mM) were proportional to the specific activity of the labeled amino acid in the medium (figure 3-1). This shows that the intracellular pool of aminoacyl-tRNA rapidly reaches a constant specific activity equal to that of the amino acid in the medium (McKee et al., 1978; Stanners et al., 1979). For 2-D gel analysis, labeling with ^{35}S-methionine was carried out in medium lacking methionine to increase the radioactivity incorporated. Control experiments showed that omission of methionine had no effect on the protein synthetic rate either under normal or starvation conditions (Table 3-2).

The measurement of total protein synthesis and the analysis of error-containing proteins are also dependent on the rate of protein turnover during the 40 minute labeling period. However, protein degradation of either native or substituted actins was not seen during a two-hour chase after the standard pulse (see section 3.2.2.2).

3.1.3.3 Two-dimensional Polyacrylamide Gel Electrophoresis

Two-dimensional separation of proteins was carried out as described by O'Farrell (1975) with minor modifications. The ^{35}S-labeled cell lysates were centrifuged at 8000g for 3

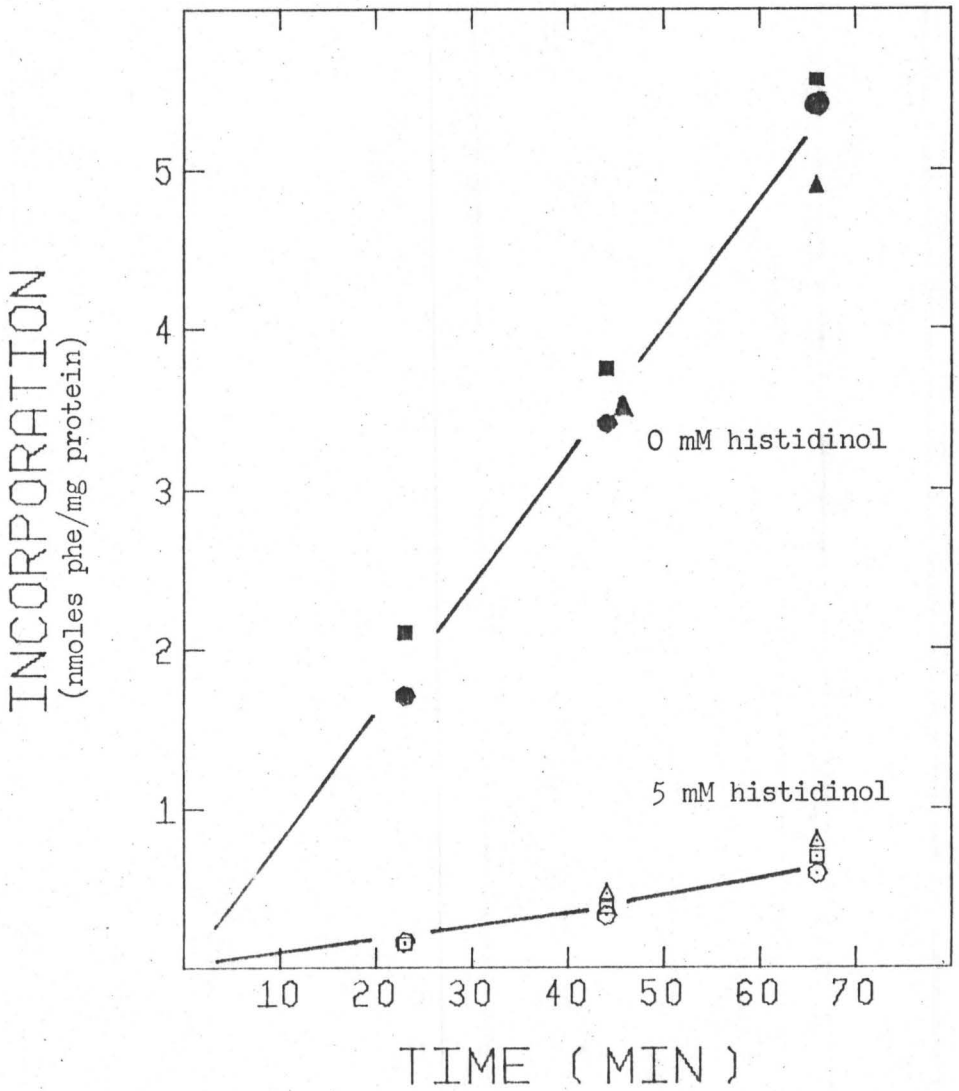

Figure 3-1

Protein synthetic rates at various concentrations of phenylalanine in the medium. Cultures of WI38-SV40 cells were treated as described in section 3.1.3.2 for unstarved and starved conditions (5mM histidinol) as shown, except the medium concentration of phenylalanine was 0.2mM (●,○), 1.1mM (▲,△)or 4.8mM (■,□). The incorporation of total radioactive plus nonradioactive phenylalanine in nmoles/mg protein was determined for each case assuming that the specific activity of ^{3}H-phe-tRNAphe was identical to the specific activity of ^{3}H-phe in the medium. There was 0.405 mg protein/dish in this experiment. Similar results were obtained with WI38, early- and late-passage A2, and progeria P5 cells.

Experiment	Cell	Omission	Addition	Synthetic Rate (Arbitrary Units)
1	A2	his,met	-	1240 ± 40
		his,met	NaCl 40mM	1190 ± 70
2	A2	his,met	-	8.4 ± 0.3
		his,met	phe 0.9mM	7.9 ± 0.4
		his,met	phe 4.6mM	7.8 ± 0.3
		his,met	his-OH 5mM	0.7 ± 0.1
		his,met	his-OH 5mM + phe 0.9mM	0.7 ± 0.1
		his,met	his-OH 5mM + phe 4.6mM	0.8 ± 0.1
3	WI38	his,met	-	4.8 ± 0.2
		his,met	phe 0.8mM	4.9 ± 0.2
		his,met	phe 2.0mM	4.8 ± 0.2
		his,met	his-OH 5mM	1.1 ± 0.1
		his,met	his-OH 5mM + phe 0.8mM	1.2 ± 0.1
		his,met	his-OH 5mM + phe 2.0mM	1.2 ± 0.2
4	WI38	-	-	23 ± 1
		met	-	24 ± 1
		his	-	20 ± 1
		his,met	-	19 ± 1
5	WI38	his,met	his-OH 5mM	765
		his	his-OH 5mM	769
6	A2 E.P.	his,met	-	100 ± 11
		his,met	his-OH 2mM	16 ± 1
		his,met	his-OH 5mM	10 ± 3
		his,met	his-OH 10mM	5.7 ± 0.5
	A2 L.P.	his,met	-	100 ± 10
		his,met	his-OH 2mM	17 ± 1
		his,met	his-OH 5mM	10 ± 1
		his,met	his-OH 10mM	5.6 ± 0.5
7	A2 E.P.	-	-	1.5 ± 0.1
		-	his 0.1mM	1.5 ± 0.1
	A2 L.P.	-	-	1.3 ± 0.1
		-	his 0.1mM	1.3 ± 0.1
8	WI38	-	-	9.5 ± 1
		his	his-OH 5mM	0.8 ± 0.2
		his	his-OH 5mM + his 0.1mM	8.9 ± 1

Table 3-2

Protein Synthetic Rates During
Amino Acid Starvation

Cells were treated as described in section 3.1.3.2 with the omissions or additions as indicated. Synthetic rates are in arbitrary units.

minutes to pellet nuclei and membrane fragments, and portions of the supernatants containing 30-80 μg protein were directly layered on pre-run isoelectric focusing rod gels (1.6% 4-6 ampholine, 0.4% 3.5-10 ampholine (LKB)) and electrophoresed for 20 hours at 400 volts. These gels were equilibrated for 30 minutes in SDS sample buffer O (O'Farrell, 1975) and sealed to 9% SDS slab gels with agarose (O'Farrell, 1975). The second dimension electrophoresis was for 800 volt-hours after which the gels were fixed in ethanol/acetic acid/water (1:0.4:2). Gels were dried with or without staining (Coomassie Brilliant Blue) or impregnation with 2,5-diphenyloxazole (Bonner and Laskey, 1974) and exposed to X-ray film (Kodak XR-1). Since the response of X-ray film is not linear to exposure at low intensities of light, gels used for quantitative analysis were neither stained nor impregnated with 2,5-diphenyloxazole.

3.1.3.4 Quantifying Autoradiograms

Actin was chosen as a reference protein for three reasons: it is the major protein synthesized in human fibroblasts; it has a known number of substitutable histidine residues; and its stutter spots can be readily resolved and quantified. The actin regions of autoradiograms were scanned with a Joyce-Loebl microdensitometer using a slit height that encompassed the largest spot scanned. The available condensers on this microdensitometer did not allow a slit height of greater than 4mm. To obtain a slit height of 6mm,

which was required for some autoradiograms, a new condenser was built. A 70mm focal length, 1 inch diameter, single convex lens was used. To accommodate the increased focal length of the condenser, a plexiglass stage 1.5 cm in height was built to sit on the existing sample stage.

Selected points on the scan were given coordinates and areas integrated numerically with a computer programmed to correct for non-linearity of the X-ray film (saturation) (section 6.2 and figure 3-7). The fraction of the total area under the scan was determined for native actin (and) and each stutter spot S_i (i represents the number of substitutions). These fractions were used to calculate the fraction of substituted sites or error frequency P':

$$P' = \sum_{i=1}^{9} iS_i/9(\gamma + \beta + \sum_{i=1}^{9} S_i) = \sum_{i=1}^{9} iS_i/9$$

Since there are 9 histidine residues in both β- and γ-actin (Collins and Elzinga, 1975; Vandekerckhov and Weber, 1978) the possible range of i is 1 to 9. However, the more highly substituted actins were seen only with extreme starvation, and in most cases i did not exceen 4 or 5. The valleys between peaks of scans showing clear stutter spots were identified to assign integration boundaries between native and substituted actins. The observed differences in pI between stutter spots (0.065-0.085 pH units) agreed well with the theoretical value of $\approx$0.07 based on the amino acid composition of actin (section 3.3), and this value was used to assign integration boundaries when the spots were not well

resolved (see Figure 3-7). The difference in the isoelectric point of β- and γ-actin is 0.02 pH units (Garrells and Gibson, 1976). This difference is exactly the difference calculated on the basis of the amino acid composition of these actins (section 3.3). Such calculations show that substituted species of β- and γ-actin are also separated by 0.02 pH units. This difference in isoelectric points is expected to result in some loss of resolution between stutter spots but it is assumed that areas calculated for each β-actin stutter spot include the corresponding -actin stutter spot (see also section 3.4).

Since the densitometer averages transmittance rather than absorbance, optical densities obtained by scanning autoradiographic spots containing a non-uniform distribution of grain densities are not strictly proportional to the absolute number of grains present. However, as suggested by O'Farrell (1975), the relative areas under the scans were found to be in close agreement with the relative intensities determined by the more accurate but time consuming method of quantitative roster scanning (figure 3-8 and Table 3-4).

3.1.4 Results

Figure 3-2 shows autoradiograms of newly synthesized proteins resolved by 2-D gel electrophoresis from early- and late-passage human skin fibroblasts. The error catastrophe theory predicts that late-passage cells will have increased levels of mistranslation which should be visualized as an

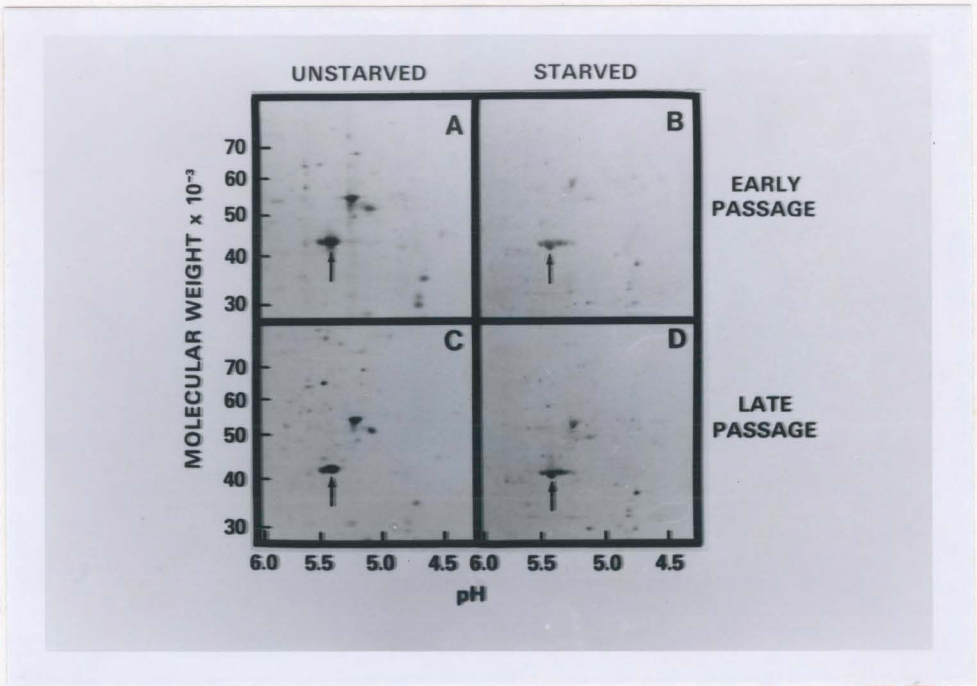

Figure 3-2

Autoradiograms of proteins from early- and late-passage cells during unstarved and starved conditions. Early-passage (a,b) and late-passage (c,d) human fibroblasts (A2) were grown in medium lacking methionine (a,c) or in medium lacking histidine and methionine and containing histidinol at 20mM (b) or 10mM (d). The arrow indicates the position of β-actin. The pH gradient was determined from the isoelectric focusing gel and molecular weights estimated from proteins of known molecular weights co-electrophoresed in the second dimension.

altered pattern of proteins, particularly in the isoelectric focusing dimension. Figure 3-2A and C show that under normal (unstarved) conditions, most proteins form a single discrete spot. This suggests that extensive heterogeneity is not present in either the charge or molecular weight of proteins from late-passage cells. When extracts of labeled proteins from early- and late-passage cells were co-electrophoresed, virtually all the proteins were identical in molecular weight and isoelectric point.

To induce detectable levels of mistranslation, cells were starved for histidine. Due to the relatively high rate of protein degradation in animal cells (Stanners and Baxter, 1978; section 2.2) acute depletion of the intracellular amino acid pool cannot be achieved by removal of histidine from the medium alone. However, histidine starvation can be effected by treating cultures with histidinol in histidine- free medium. Histidinol competes with histidine for the active site on the histidyl-tRNA synthetase but does not become ligated to histidyl-tRNA (Hansen et al., 1972). Proteins synthesized under these conditions exhibited a trail of stutter spots leading from the native form towards the acidic end of the 2-D gel (figure 3-2B and D). This has been interpreted to be the consequence of substituting glutamine (a neutral amino acid) for histidine (a basic amino acid) resulting in new proteins with similar molecular weights but reduced isoelectric points (Parker et al., 1978). The extent of mistranslation at equivalent degrees of inhibition of

protein synthesis was similar in the early- and late-passage fibroblasts (figure 3-2B and D).

In order to induce stutter spots that could be readily quantified, protein synthetic rates were required that were 2-10% of unstarved rates. All cultures of human fibroblasts required similar concentrations of histidinol (5-20 mM) to reduce the synthetic rates to these levels. It is unlikely that histidinol itself produces an artifactual response in the cell since in the presence of normal medium concentrations of histidine, histidinol had no effect on either the protein synthetic rate or the pattern of spots seen on 2-D gel autoradiograms (figure 3-3). Furthermore, in studies with a temperature-sensitive mutant of CHO cells affecting histidyl-tRNA synthetase, cells starved for histidine at the non-permissive temperature in the absence of histidinol synthesized native and error- containing proteins similar to those of wild-type cells following histidine starvation with histidinol (Pollard et al., unpublished observations). The patterns of proteins synthesized under unstarved conditions were essentially identical in all cell strains (figures 3-4 and 3-5, left side). With histidine starvation, all of these cell strains exhibited similar levels of mistranslation at equivalent degrees of inhibition of protein synthesis (figure 3-5, right side).

A corollary to the error catastrophe theory is that transformation, which rescues cells from senescence, should

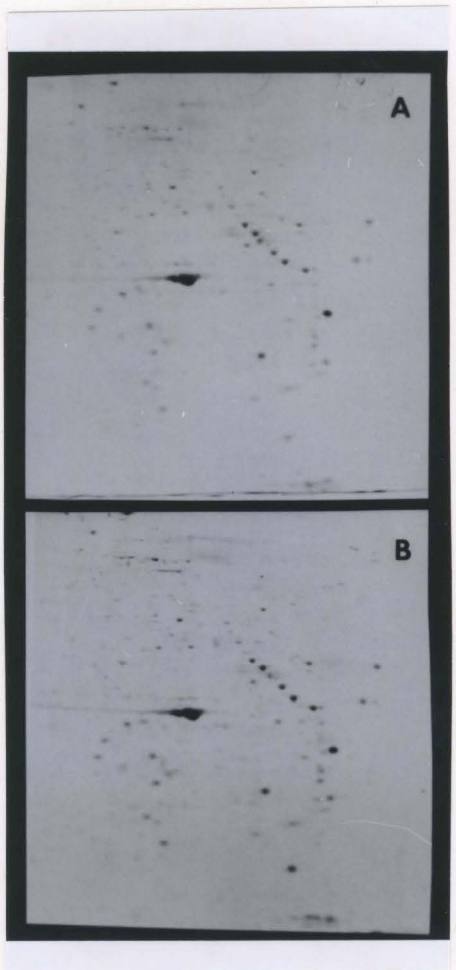

Figure 3-3

Autoradiograms of proteins synthesized in the presence of histidinol plus histidine. Cultures of WI38 cells were treated as described in section 3.1.3.2 for unstarved (a) or starved conditions (b) except in (b), histidine (0.1mM) was added in addition to 5mM histidinol. The protein synthetic rate of cultures given histidine plus histidinol was similar to control synthetic rates (Table 3-2). The synthetic rate of replicate cultures given 5mM histidinol alone in this experiment was 8.2%.

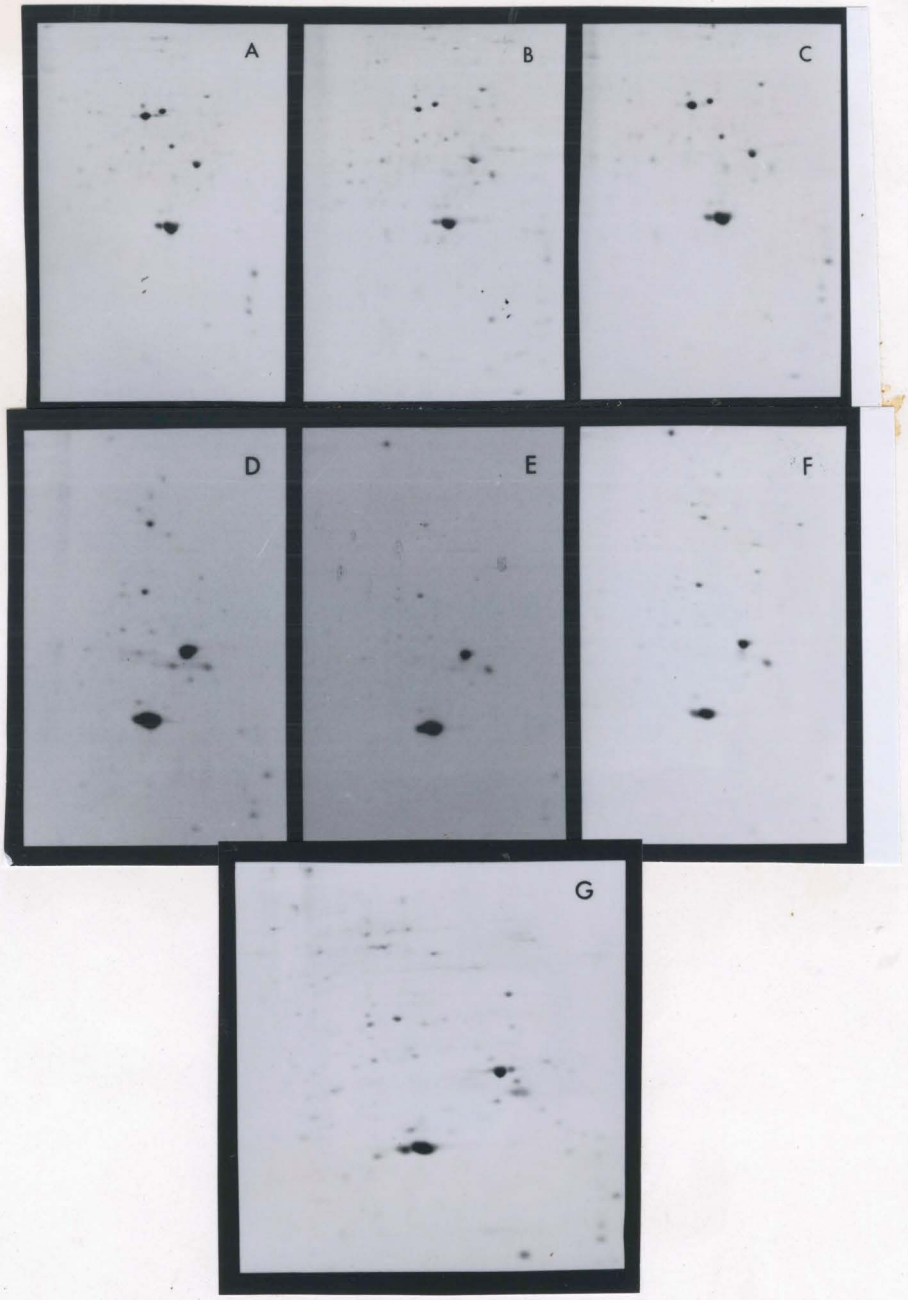

Figure 3-4

Autoradiograms of proteins synthesized during unstarved conditions in several strains of human fibroblasts. Cultures were labeled with ^{35}S-methionine in methionine-free medium for 1 hour and prepared for 2-D gel electrophoresis as described in section 3.1.3.2. Shown are the central regions of autoradiograms of proteins from the following donors: normal child RE (A); normal young adult J004 (B); progeria P5 (C); young adult GM37 (D); progeria P5 (E); progeria P18 (F); and old normal donor J069 (G). These autoradiograms come from gels run in three separate experiments over the course of two years. Since the technique changed slightly during this time (for example longer first dimension gels were adopted), the autoradiograms are not directly comparable. Autoradiograms A,B,C come from the same experiment, as do D,E,F.

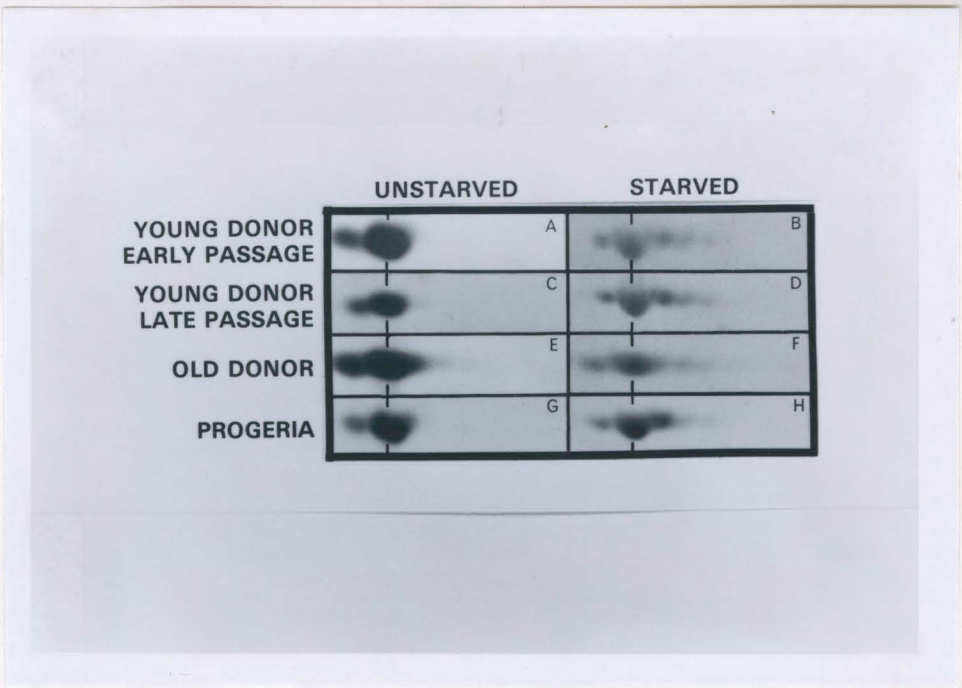

Figure 3-5

Autoradiograms of the actin region showing protein synthesized in several strains of human fibroblasts during unstarved and starved conditions. Cells were labeled in complete medium lacking methionine (left panels) or in medium lacking histidine and methionine and containing histidinol at 20 mM (b) or 10 mM (d,f,h). Cell strains include early- (a,b) and late- (c,d) passage A2 fibroblasts, old donor J069 (e,f) and the premature aging syndrome progeria P5 (g,h). The lines are drawn through β-actin.

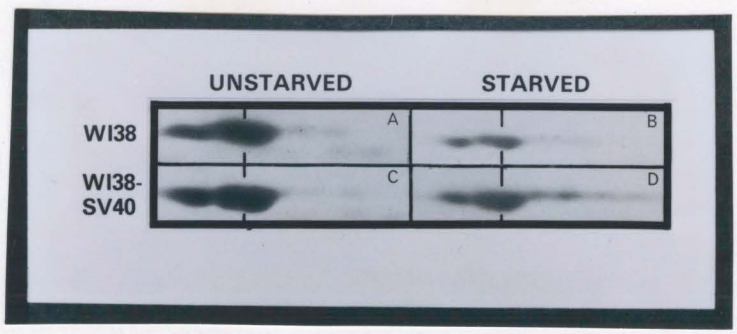

Figure 3-6

Autoradiograms of the actin region showing protein synthesized in WI38 and WI38-SV40 cells during unstarved and starved conditions. Cells were labeled in medium lacking methionine (a,c) or in medium lacking methionine and histidine and containing histidinol at 10mM (b) or 5mM (d). The lines are drawn through β-actin.

reduce the error rate in protein synthesis, at least below the rate observed in late-passage cells. Therefore, we compared the degree of mistranslation upon histidine starvation of SV40-transformed human fibroblasts versus the parental diploid strain. Figure 3-6 shows the actin region of autoradiograms from WI38 and its SV40-transformed counterpart. Contrary to expectation, transformation was associated with a greatly increased error rate in protein synthesis. Similar results were obtained with SV40-transformants of two other human cell strains: another fetal lung fibroblast, MRC5, and an adult skin fibroblast, GM37.

To quantify mistranslation, actin regions of the autoradiogram were scanned (figure 3-7). The error frequency (fraction of substituted histidine sites) was calculated by weighting the fractional areas on scanning densitometry which corresponded to aberrant proteins by the number of substituted histidine sites (see section 3.1.3.4). The fraction of substituted sites calculated from the scans in figure 3-7 was greatly increased in WI38-SV40 compared to WI38 (Table 3-3 and 3-4). The fraction of aberrant proteins, i.e. the fractional area of the combined stutter spots, was also elevated in the transformed cell line. These differences were quantitatively similar to those found with the more accurate method of roster scanning (figure 3-8 and Table 3-4).

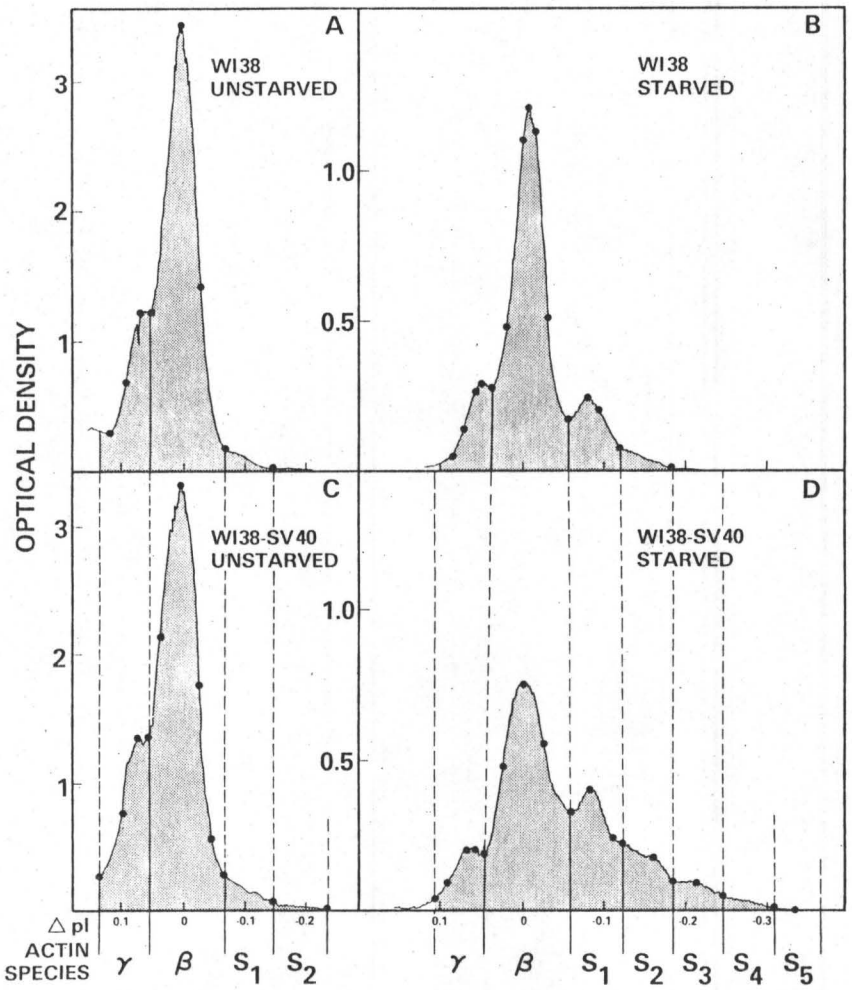

Figure 3-7

Quantifying error frequencies. Densitometric traces from the actin region of autoradiograms of proteins synthesized by WI38 (a,b) and WI38-SV40 (c,d) are shown for unstarved (a,c) and starved conditions (10mM histidinol) (b,c). The units from the densitometer scan have been scaled to show optical density (y-axis) and pH relative to β-actin (x-axis). Coordinates were assigned to points on the scans (●) and the fractions of the total area corresponding to native actin (β,γ) and substituted actins S1, S2, S3,... were calculated (Table 3-3).

Table 3-3

Quantitation of Error Frequencies

Cell Strain		Relative rate of protein synthesis	Fraction of the total area *						Fraction of aberrant Protein	Error Frequency (fraction of substituted sites) ≠
			γ	β	S_1	S_2	S_3	S_4	S_5	
WI38	Unstarved	1.0	.106	.886	.0085					
	Starved	.059	.078	.807	.095	.012	.0005		.108	0.0084
WI38-SV40	Unstarved	1.0	.153	.805	.030	.010				
	Starved	.051	.079	.547	.192	.104	.053	.023	.002	.374	0.0683

* Data taken from figure 3-7.

≠ The error frequency (fraction of substituted sites) was calculated as

$$P' = \Sigma i S_i / 9.$$

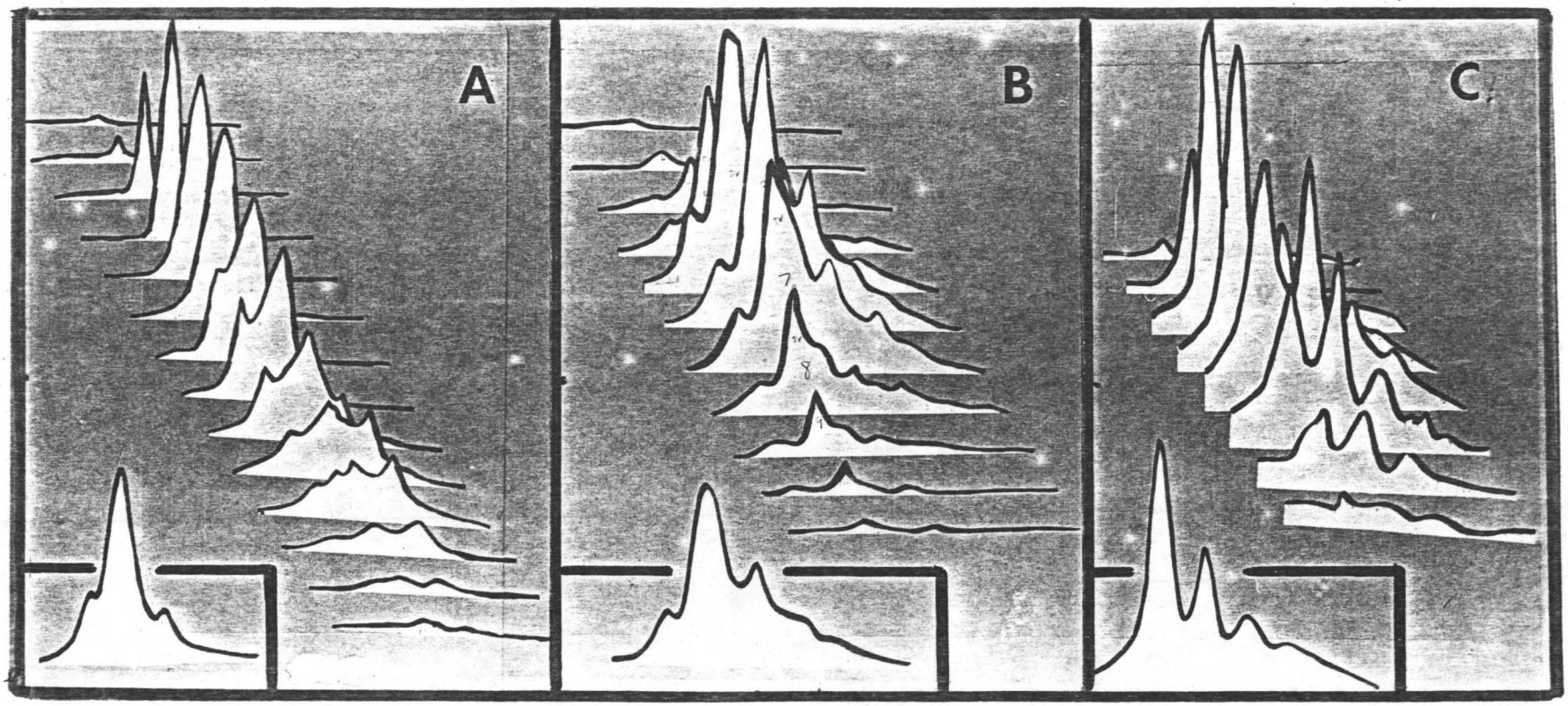

Figure 3-8

Roster scanning of autoradiograms. For roster scanning, the microdensitometer had a slit height of 0.5mm and serial scans were adjacent. Scans of autoradiograms of the actin region from WI38 (A); WI38-SV40 (B); and CHO (C) cells during histidine starvation are shown. The inset in each figure shows the scan obtained when the slit height was equal to the diameter of the largest spot. The error frequencies determined from these scans are shown in Table 3-4.

Table 3-4

Quantitation of Error Frequencies by Roster Scanning

Autoradiogram	Fraction of Substituted Sites (P')	
	Roster Scan	Total Scan
A	0.0178	0.0223
B	0.0677	0.0794
C	0.0893	0.110

Areas corresponding to native actins and each stutter spot were determined for roster and total scans shown in Figure 3-8 and the fraction of substituted sites calculated as described in section 3.1.3.4.

A theoretical model of mistranslation during amino acid starvation suggests that a linear relationship exists between error frequency and the inverse of the relative rate of protein synthesis (section 3.2). Therefore, the error frequencies calculated from autoradiograms were plotted against the reciprocal protein synthetic rates (figure 3-9). In WI38, WI38-SV40 (figure 3-9), and all other cell strains tested, the error frequency increased as the protein synthetic rate decreased. Late-passage WI38 cells did not ave elevated error frequencies compared to early-passage cells. But in contrast, WI38-SV40 cells had dramatically elevated error frequencies compared to their untransformed counterparts.

Table 3-5 shows the mean error frequencies of the cells after normalizing high level mistranslation to the protein synthetic rate. Late-passage cells from fetal, young, or old normal donors did not have elevated error frequencies compared to early-passage cells. In fact, two of the cell strains (WI38 and A2) at late passage had a reduced error frequency compared to their early-passage counterparts ($p < 0.05$). Furthermore, cells from old donors or subjects with progeria or Werner syndrome did not have elevated error frequencies compared to young normal donors. In contrast, the elevated error frequency of WI38-SV40 cells was highly significant when compared to either untransformed counterparts or all diploid fibroblast cells combined ($p < 0.0001$).

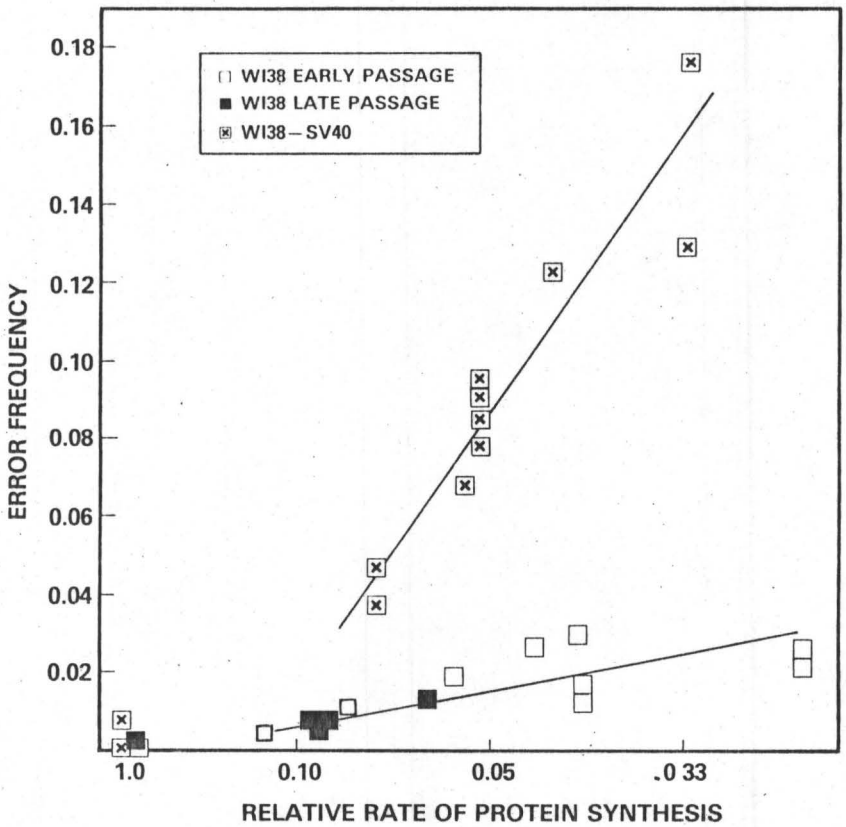

Figure 3-9

Error frequencies plotted against the reciprocal protein synthetic rate for early and late passage WI38 and WI38-SV40. Error frequencies represent the fraction of substituted histidine sites P' as defined in section 3.1.3.4. Each point represents the error frequency determined by quantifying the scan of the autoradiogram from a single gel.

Table 3-5

Error Frequencies of Human Cells
from Young, Old, Progeric, and Werner Syndrome Donors
at Early and Late Passage
and from SV40-Transformed Human Cells

Cell Type	Replicative Lifespan[a]	Error Frequency (P) ± S.E. ($\times 10^4$) (n)[b]	
		Early Passage	Late Passage
Young Donors			
WI38	55	0.6 ± 0.1 (7)	0.4 ± 0.1 (4)[c]
MRC5	65	1.5 ± 0.2 (2)	
A2	65	1.2 ± 0.2 (10)	0.9 ± 0.2 (8)[c]
GM37	50	1.6 ± 0.1 (3)	
Mean of Young Donors		1.0 ± 0.1 (22)	0.7 ± 0.1 (12)
Old Donors			
JO69	50	0.8 ± 0.2 (3)	0.8 ± 0.1 (3)
JO88	48	1.0 ± 0.3 (4)	
Progeria P5	42	1.2 ± 0.2 (6)	
P18	53	1.3 ± 0.3 (4)	
Werner Syndrome WS2	37	1.3 ± 0.3 (2)	
WS3		0.7 ± 0.2 (2)	
WS4		0.5 ± 0.1 (3)	
Mean of Old, Progeric and WS Donors		1.1 ± 0.1 (24)[d]	0.8 ± 0.1 (3)
Mean of All Diploid Cells		1.1 ± 0.1 (45)	0.8 ± 0.1 (15)
Immortal Cells			
WI38-SV40			2.8 ± 0.2 (10)[e]
MRC5-SV40			2.3 ± 0.2 (3)
GM37-SV40			3.1 ± 0.4 (2)

Footnotes to Table 3-5

[a]Maximum number of population doublings (Hayflick, 1965)

[b]Error frequency P is derived by normalizing the fraction of substituted sites P' to the relative protein synthetic rate (r) as described in section 3.2 using the following equation

$$P = P'/12.53(r - 0.92).$$

n is the number of separately analyzed extracts of proteins labeled during histidine starvation.

[c]The hypothesis that late-passage cells from young donors have an error frequency greater than that of the corresponding early-passage cells is rejected ($p < 0.05$).

[d]The hypothesis that early-passage cells from old donors have an error frequency greater by 33% than that of early-passage cells from young donors is rejected ($p < 0.05$).

[e]SV40-transformed WI38 cells have an elevated error frequency compared to WI38 ($p < 0.0001$) or all diploid cells combined at early or late passage ($p < 0.0001$).

Table 3-5 also lists the lifespans of the cell strains in maximum population doublings until senescence. If the *in vitro* lifespan were influenced by the inherent error frequency, one might expect to find an inverse relationship between the total number of population doublings of a cell strain and the calculated level of mistranslation. However, by linear regression analysis and analysis of variance, no such correlation was found ($p > 0.4$), despite the four-fold range in error frequency observed among normal cell strains.

Table 3-6 lists some error frequencies obtained from other human and non-human cell lines. It can be seen that there is a wide variation in the calculated error frequencies from different cell types. Both transformed human lines, HeLa and 293, have error frequencies greater than the mean observed for normal diploid fibroblasts. However, appropriate control cells for comparison are not available. Neither CHO nor NIL-HSV had error frequencies significantly greater than their "normal" counterparts, CHF and NIL, respectively. The observed error rates of Nil hamster cells are about an order of magnitude less than those of the CHO and CHF hamster lines.

Chick embryo fibroblasts had the highest error frequency observed of any cell tested (Figures 3-10, 3-11, and Table 3-6). These cells were the only non-mammalian cells examined. Although the chick cells infected with the temperature sensitive mutant of RSV showed elevated error

Table 3-6

Error Frequencies of Other Human and Non-Human Cells

Cell		Error Frequency P $\times 10^4 \pm$ S.E.	(n)
HeLa		3.7 ± 0.5	(3)
293		1.9 ± 0.1	(6)
CHF		3.4 ± 0.9	(2)
CHO		4.3 ± 0.6	(3)
NIL		0.5 ± 0.1	(3)
NIL-HSV		0.4	(1)
CEF	36°	18 ± 1	(2)
	41°	23	(1)
CEF-RSV	36°	26 ± 2	(2)
	41°	8 ± 1	(2)
CEF-RSVts	36°	42 ± 2	(2)
	41°	14 ± 3	(2)

Cells were treated as described in section 3.1.3.2 except for CEF, CEF-RSV and CEF-RSVts cells. These cells were grown for four days at the indicated temperatures prior to time zero and then assayed as described in section 3.1.3.2 at the indicated temperatures.

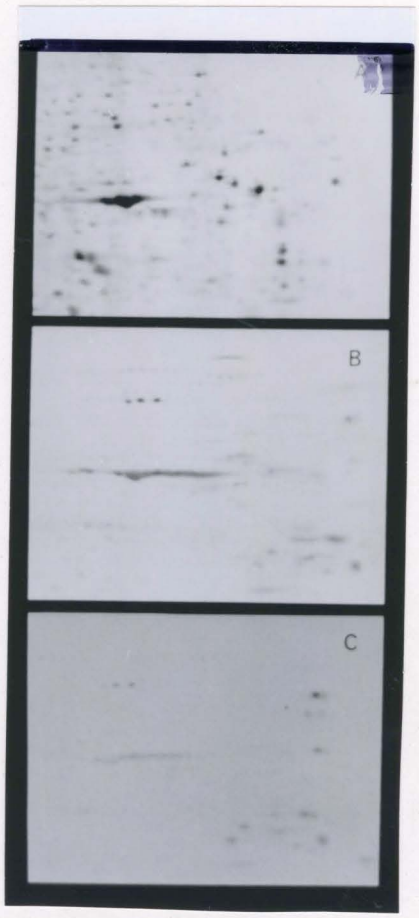

Figure 3-10

Autoradiograms showing proteins synthesized by chick and RSV-infected chick fibroblasts. Cultures were treated as described in section 3.1.3.2 except the temperature was 41 C: (A) normal chick cells labeled in control medium (100% protein synthetic rate); (B) chick cells infected with wild type RSV labeled in the presence of 10mM histidinol (5.5% protein synthetic rate); (C) normal chick cells labeled in the presence of 10 mM histidinol (8.4% protein synthetic rate).

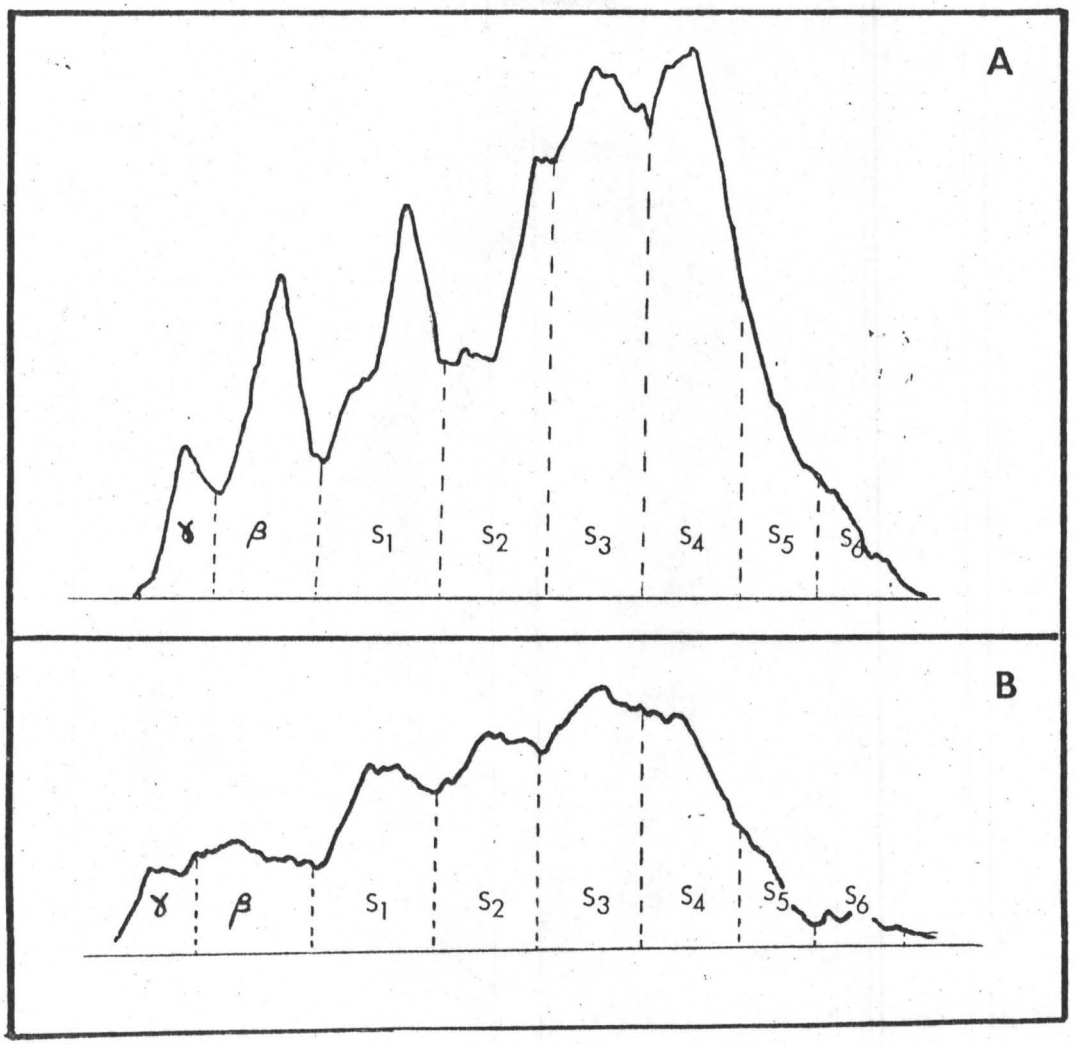

Figure 3-11

Scans of actin regions from autoradiograms of proteins synthesized by RSVts-infected chick cells during histidine starvation at the permissive and nonpermissive temperature. RSVts-infected chick cells were treated as described in section 3.1.3.2 with histidine starvation (5mM histidinol) escept the termperature was 36° (A) or 41° (B). The protein synthetic rate of control RSVts-infected cells (0mM histidinol) was 57% greater at 41° than at 36°. The protein synthetic rate compared to the relevant control during histidine starvation was 15.5% (A) and 5.6% (B).

frequencies at the permissive temperature (36°C) compared to the nonpermissive temperature (41°C), the wild type virus also showed an increased error frequency at the reduced temperature. Unlike the RSV-infected cells, uninfected chick cells did not have a reduced error frequency at the higher temperature. The error frequency of the cells infected with wild type RSV was not increased compared to uninfected cells. These results are discussed in greater detail in the context of a larger collection of normal/transformed pairs (Pollard et al., in preparation).

3.1.5 Discussion

Our direct measurements of mistranslation in human cells do not support the error catastrophe theory of aging in four respects: First, under normal, unstarved conditions "old" (late- passage cells from young donors and cells from old, progeric, or Werner syndrome donors) have proteins that are essentially indistinguishable from "young" (early-passage) cells of normal donors. Second, under conditions of histidine starvation, "old" cells have similar or reduced levels of mistranslation compared to "young" cells. Third, no correlation exists between error frequency and replicative lifespan of cultured diploid cells. Fourth, SV40-transformed ("immortal") cells have elevated error frequencies during histidine starvation compared to early- or late-passage mortal cells.

It is important to ask whether comparisons of error frequencies at drastically reduced rates of protein synthesis are relevant to error frequencies under normal conditions. Three points suggest that such comparisons are valid: (1) conditions which augment mistranslation such as antibiotics, high magnesium concentrations, low temperature, high pH and organic solvents, appear simply to amplify the ambiguity inherent in the protein synthetic apparatus (Woese, 1967, Gorini, 1974). (2) Our values for mistranslation during various degrees of amino acid starvation give estimates of error frequencies at the histidine codon during normal (unstarved) conditions that are consistent over a five-fold range of protein synthetic rates (see section 3.2). (3) The derived error frequencies (Table 3-5) are similar to previously reported data at other codons measured by independent means (Loftfield, 1963; Loftfield and Vanderjadt, 1972; Edelmann and Gallant, 1977a). Thus, we believe that the error frequencies measured here during amino acid starvation provide an accurate estimate of mistranslation under normal conditions.

Although a small increase (for example less than 30%) in the error frequency of old cells may have gone undetected, it is unlikely this would be biologically significant for the following reasons: First, in bacteria, error frequencies 20-fold greater than normal can be induced without loss of viability (Gallant and Palmer, 1979). Second, cultured human cells (Ryan et al., 1974) and Drosophila (Shmookler Reis,

1976) can tolerate substantial incorporation of amino acid analogs into protein without reduction of their lifespan. Third, our studies show that large differences among the normal cell strains do not correlate with lifespan. For example, A2 had a calculated error frequency about twice as large as WI38, but the in vitro lifespan of A2 is in fact about 20% longer than that of WI38. Indeed, SV40-transformed cells, which are immortal, have the greatest error frequencies of any of the human cells analyzed. Therefore, it seems that an elevated level of mistranslation is not involved in generating the "aging" phenotype.

The error catastrophe theory of aging has received some support, but the evidence has so far been indirect (section 1.2.2.2(b)). As we were preparing this work, two reports appeared on comparisons of proteins from "young" and "old" cells by 2-D gel electrophoresis. Wilson et al. (1978) analyzed tissue extracts from young and old rats and Engelhardt et al. (1979) analyzed early and late passage WI38. Both of these reports showed that nearly identical patterns of proteins are found in young and old cells. My results on cells under unstarved conditions confirm and extend these observations. In cell-free extracts from human fibroblasts, the error rate of protein synthesis directed by polyuridylic acid does not increase in late-passage cells or in cells from old, progeric, and Werner syndrome donors (Wojtyk and Goldstein, 1979).

Our observations with SV40-transformed cells suggest that the synthesis of aberrant proteins may be involved in cell transformation, and hence may play a role in carcinogenesis and/or tumor progression. For example, error-containing proteins could lead to an elevated mutation rate or abnormal regulation of gene expression with ultimate loss of of growth control. It is noteworthy that HeLa and 293 cells (both transformed human lines) had error frequencies greater than normal human cells. However, comparisons of some other transformed/untransformed pairs have not supported a general correlation between transformation and error frequency (Table 3-6; Pollard et al., in preparation). It has also been suggested that transformation might affect parameters leading to stabilization of error rates, thus preventing the putative catastrophe and establishing immortality at an elevated error frequency (Holliday, 1975). Our observations on SV40-transformed cells are in accord with this idea, but the relatively low error frequencies of old cells are not.

The results presented in this paper represent the first direct measurements of mistranslation in human cells. We have compared the error frequencies of cell strains from fetal, young, and old normal cells at early and late passage, from subjects with progeria and Werner syndrome and from SV40-transformed cells. While our results indicate that SV40-transformed cells have an elevated error frequency, they do not support the error catastrophe theory of aging.

3.2 Model for mRNA Translation during amino acid starvation applied to the calculation of protein synthetic error rates.

3.2.1 Introduction

Starvation of cells for a single amino acid can induce errors in protein synthesis which are detectable by 2-D gel electrophoresis (section 1.5.3). of "stutter spots" trailing the native (unsubstituted) species towards the basic or acidic end of the gel depending on whether the substitution increases or decreases the isoelectric Although the degree of substitution can be used directly to assess high-level mistranslation in a variety of cells (section 3.1), the utility of this technique would be greatly extended if it provided a measure of the error rate during normal protein synthesis.

O'Farrell (1978) proposed that the increased error frequency observed during amino acid starvation is directly related to the increased step time of the ribosome at the relevant codon, and has presented a method for estimating this increase based on the inhibition of protein synthesis. I have developed this model further using computer simulations of protein synthesis to include other effects of amino acid starvation which influence the synthetic rate. This extension of O'Farrell's model provides a means of extrapolating error frequencies at certain codons determined during amino acid

starvation to the error frequencies occuring in protein synthesis under normal conditions.

3.2.2 Materials and Methods

3.2.2.1 Cell Culture

Human fibroblasts were grown on plastic surfaces at 37°C in Eagles' minimum essential medium supplemented with 15% fetal calf serum (Gibco, U.S.A.), nonessential amino acids, glucose and pyruvate (Goldstein and Littlefield, 1969). A temperature sensitive mutant of Chinese hamster ovary cells involving asparaginyl-tRNA synthetase (asn-7) (Thompson et al., 1975) was grown at 34°C in suspension in α-minimal essential medium (Stanners et al., 1971) containing asparagine-H_2O at 50 μg/ml and 10% fetal calf serum (Reheis) using magnetically stirred spinner flasks in temperature controlled water baths.

3.2.2.2 Measurements of Mistranslation During Amino Acid Starvation

Conditions for amino acid starvation, measurements of protein synthetic rate, and preparation of cell lysates for 2-D gel electrophoreses were as described previously (Parker et al., 1978; section 3.1). Human cells were starved for histidine in the presence of histidinol (section 3.1) and the mutant CHO cells were starved for asparagine at the nonpermissive temperature (Parker et al., 1978). Analysis of autoradiograms of the 2-D gels for the calculation of error

frequencies during histidine starvation was carried out as described in section 3.1. Actin was chosen as a reference protein for reasons given in section 3.1.3.4.

3.2.2.3 Determination of the Weight-Average Molecular Weight (MWw) of Proteins

Lysates from cells labeled for 40 minutes with ^{35}S-methionine during unstarved (normal) and histidine-starvation conditions were prepared as described previously (section 3.1.3.2). The lysates were made 5% in sodium dodecyl sulfate (SDS), brought to 90°C for one minute, and then electrophoresed on 20% SDS slab gels (O'Farrell, 1975). Gels were fixed in methanol/acetic acid/water (1:0.4:2), dried, and exposed to X-ray film (Kodak XR-1). Films were scanned with a Joyce-Loebl microdensitometer. Tracings of the scans were cut out and the R_f corresponding to the position of the weight-average molecular weight of labeled proteins was determined by cutting the tracings vertically into equal-weight halves (Singer et al., 1979). This R_f was related to MWw from a semilog plot of the molecular weight of standards vs their R_f. The loss of very low molecular weight proteins during fixing and drying will cause a slight overestimation of MWw.

3.2.2.4 Measurement of the Fraction of Ribosomes on mRNA

Ribosomes and polysomes were prepared from cytoplasmic extracts and separated from lighter material on linear

sucrose gradients essentially as described earlier (Stanners and Becker, 1971). In brief, approximately 1×10^7 cells, labeled for 2 or 3 generations with ^{14}C-uridine (0.025 μCi/ml, 680 mCi/mmol, Amersham Searle) were harvested, washed and suspended in hypotonic buffer containing Tween 40 and sodium deoxycholate (2:1 v/w, 1.3% final concentration). After passing the suspension through a 26 gauge needle six times, the tonicity was restored to normal and nuclei removed by centrifugation (800g, 3.5 min). The cytoplasmic extract was layered over linear sucrose gradients (10-40%, human cells; 5-50%, CHO cells; 5-40%, HA and T cells, w/w) and centrifuged for 100 minutes at 32000 rpm, 4°C, in an SW 41 rotor. Gradients were pumped through a recording spectrophotometer and 0.27 ml fractions collected. Acid-precipitable material from each fraction was collected on Millipore filters and counted in a low background gas flow counter. The portions of gradients corresponding to polysomes and ribosomes were identified by plots of the optical density and radioactivity vs fraction number (see Stanners and Thompson, 1974). Since the monosome peak has previously been shown not to contain ribosomes engaged in protein synthesis (Stanners and Becker, 1971; Stanners and Thompson, 1974), the fraction of ribosomes on mRNA was calculated as the number of counts in the polysome portion of the curves divided by the number of counts in the combined monosome and polysome areas.

3.2.2.5 Computer Simulation of Protein Synthesis

Simulations of protein synthesis were performed with a CDC 6400 computer. The program is described in detail in section 6.4 but its operation can be understood by examining the flow diagram shown in figure 3-12. Input parameters are (i) mRNA length, (ii) position of modulator codons (histidine or asparagine codons), (iii) minimum interribosome distance, (iv) initiation frequency, (v) step time of the ribosome at each codon. Initiation frequency is the probability of ribosome initiation given that the initiator codon is exposed. The termination frequency is the reciprocal of the step time of the ribosome on the last sense codon in the message. In some simulations, the step times at the modulator codons were random variables uniformly distributed over a specified range (figures 3-20b and 6-3). The actual initiation frequency and step times at certain codons differed from the input specifications during the simulations whenever ribosome initiation or translocation was hindered by "queueing" of previous ribosomes. The program is initiated with one ribosome at the initiator codon and at each iteration, the first ribosome (the one closest to the 3' end of the message) is advanced one codon if the time spent at the current codon was at least as great as the defined step time at that codon. If subsequent ribosomes were to advance, an additional criterion had to be met: the next codon could not be blocked by the previous ribosome. In each simulation the times of initiation, termination and each translocation

Figure 3-12

Flow diagram of computer program simulating protein synthesis. The upper panel depicts the process being simulated. Shown are three ribosomes on the message and another about to initiate. Ribosome R_n is translating a modulator codon j=88(his) on actin mRNA and has caused ribosome R_{n-1} to pause at nonmodulator codon j=75(gly). The minimum interribosome distance in this case is 13 codons. Ribosomes initiate at exposed initiation sites with probability k_i. The lower panel presents a simplified view of the logic flow for the actual program (figure 6-3). Each ribosome is given a number R_n. Associated with R_n at any given time, are two other numbers: the ribosome's current position; and how long it has been there. If ribosome R_n has spent at least the defined step time at a particular codon, and ribosome R_{n+1} is more than D codons further along the message, then ribosome R_n can advance. "FIRST" is the value of R_n for the ribosome closest to the 3'-end of the message. "LAST" is the value of R_n for the ribosome closest to the 5'-end of the message. At each initiation or termination event, FIRST and LAST are modified accordingly. Most input values are defined in sections 3.2.2.5 and 3.2.4.2(b). SDIST is a matrix which keeps track of the occupancy time of each codon by each ribosome, and NR is the number of ribosomes to be monitored.

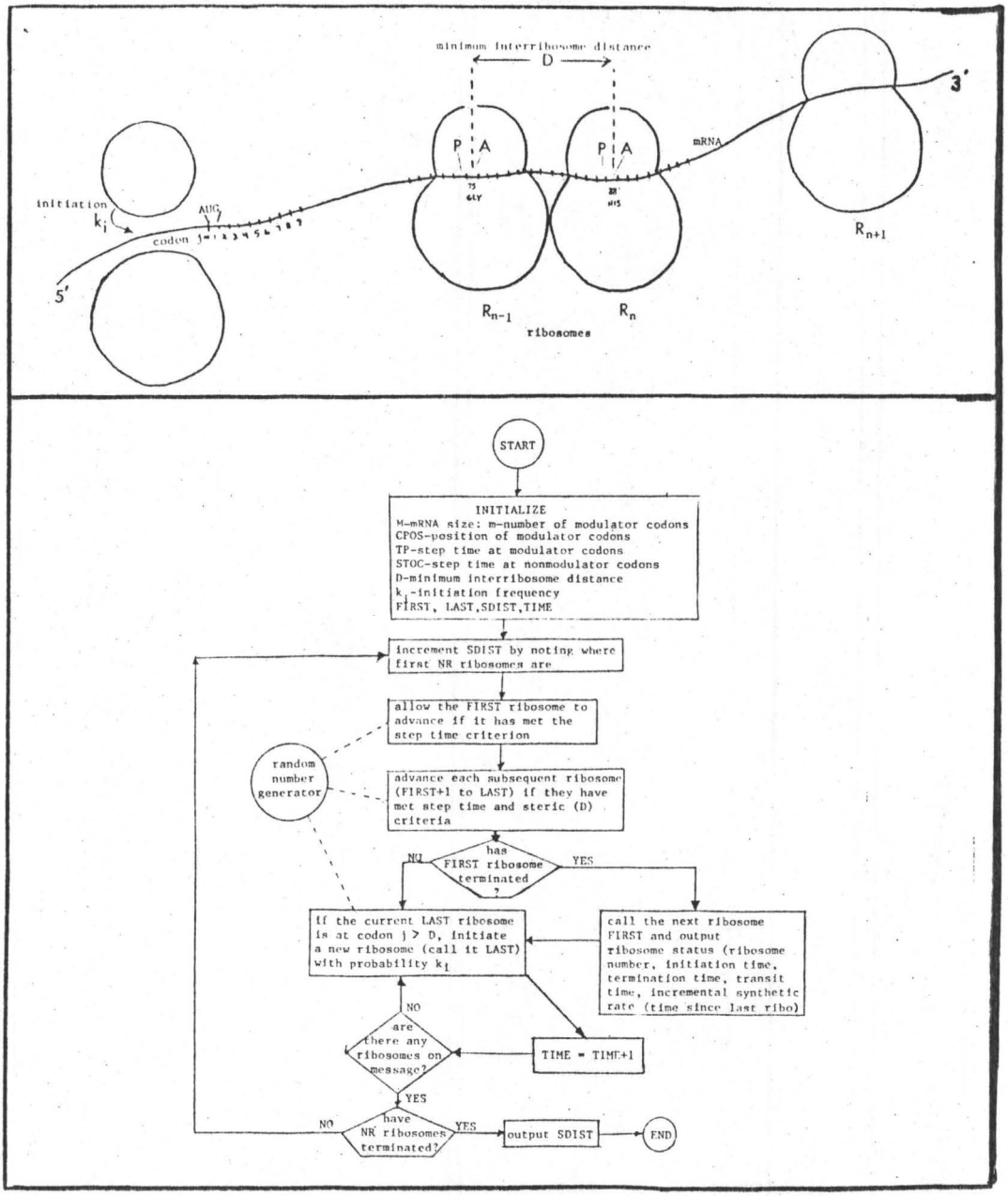
minimum interribosome distance
D
3'
mRNA
P
A
P
A
initiation
k_i
AUG
codon j=1 2 3 4 5 6 7 8 9
5'
R_{n-1}
R_n
R_{n+1}
ribosomes
START
INITIALIZE
M-mRNA size: m-number of modulator codons
CPOS-position of modulator codons
TP-step time at modulator codons
STOC-step time at nonmodulator codons
D-minimum interribosome distance
k_i-initiation frequency
FIRST, LAST,SDIST,TIME
increment SDIST by noting where first NR ribosomes are
allow the FIRST ribosome to advance if it has met the step time criterion
random number generator
advance each subsequent ribosome (FIRST+1 to LAST) if they have met step time and steric (D) criteria
has FIRST ribosome terminated ?
NO
YES
if the current LAST ribosome is at codon j > D, initiate a new ribosome (call it LAST) with probability k_i
call the next ribosome FIRST and output ribosome status (ribosome number, initiation time, termination time, transit time, incremental synthetic rate (time since last ribo)
NO
are there any ribosomes on message?
TIME = TIME+1
YES
NO
have NR ribosomes terminated?
YES
output SDIST
END

3-12

event of every ribosome were available for analysis. Reiterations were continued until a steady state was achieved.

3.2.3 Symbols and Notation

Unprimed symbols denote the normal (unstarved) state. A prime (') denotes starvation for amino acid X. Symbols which are not primed represent parameters which are assumed to be independent of amino acid starvation.

X	the amino acid for which cells are starved
Y	the amino acid which can substitute for X by codon-anticodon mispairing between Y-tRNA and X codons
M	length of the specified mRNA (codons)
m	number of X codons in the mRNA
n, n'	number of ribosomes engaged in translation
$t_{s,x}$, $t'_{s,x}$	mean step time of the ribosome at X codons
t_s^j, $t_s^{j'}$	mean step time of the ribosome at codon position j (j=1,2,3,...,M)
$t_{s,\bar{x}}$, $t'_{s,\bar{x}}$	mean step of the ribosome at non-X (irrelevant) codons
k_i, k'_i	initiation frequency (time units)
D	minimum permissible interribosome distance (codons)
R, R'	protein synthetic rate
λ	mean frequency of Y-tRNA interactions with a ribosome leading to incorporation of amino acid Y at sites corresponding to amino acid X
P, P'	error frequency at codon X (frequency of amino acid Y substitutions at X sites)

3.2.4 Results

3.2.4.1 Mistranslation during Amino Acid Starvation

Analysis of gel autoradiograms of proteins synthesized during histidine starvation has been used to determine the error frequency P' of actin synthesis during histidine starvation (section 3.1). In general, the series of spots seen on 2-D gel autoradiograms are scanned with a densitometer. For a protein with m substitutable sites (m X codons), the fraction of the total area under the scan of this protein is calculated for native (S_o) and substituted proteins (S_i, i=1,2,3,...m; i denotes the number of substitutions in S_i). Allowing S_i to represent these fractional areas, the error frequency P' is therefore obtained by weighting the area under the scan of each stutter spot by the number of substitutions in the protein(s) giving rise to that spot and dividing the total sum of these products by the number of sites available for substitution:

$$P' = \sum_{i=1}^{m} iS_i/m \qquad (1)$$

Both β- and γ-actin contain nine histidine (H) residues and eight asparagine (N) residues (Collins and Ellzinga, 1975; Vandekerckhove and Weber, 1978). Thus

$$P'_H = \sum_{i=1}^{9} iS_i/9 \qquad (2)$$

$$P'_N = \sum_{i=1}^{8} iS_i/8 \qquad (3)$$

Results of analysis of mistranslation during histidine

and asparagine starvation of WI38 and asn-7, respectively, are given in Table 3-7a. The measured error frequency at the his codon during amino acid starvation increases as the overall protein synthetic rate decreases. In the next section we discuss a method of normalizing the error frequency to the overall synthetic rate to yield an estimate of the inherent error rate. However, first it must be shown to what extent premature termination, selective degradation of abnormal proteins, or changes in the number of functioning ribosomes influence the measurements of error frequency or protein synthetic rate.

Since a shift towards a lower mean molecular weight of proteins synthesized during amino acid starvation would indicate either premature termination or preferential translation of small mRNAs, we examined the molecular weight distributions of newly synthesized proteins on SDS gels. Figure 3-13 shows quantitative scans of autoradiograms of proteins synthesized during unstarved and starved conditions. The weight-average molecular weight of proteins synthesized in these experiments decreased from 42000 in complete medium (100% protein synthetic rate) to 38000 in medium lacking histidine and containing histidinol (10.5% protein synthetic rate). These data indicate that in histidine-starved human cells at a relative protein synthetic rate of 10%, there is not a dramatic change in the rate of premature termination or in the size distribution of translated mRNA.

Table 3-7

Error Frequencies at the Histidine Codon in WI38 and the Asparagine Codon in Asn-7

	a		b		
Cell	Relative Protein Synthetic Rate R'/R	Error Frequency P'	Relative Step Time $t'_{s,x}/t_{s,x}$	Error Frequency P x 10^{-4}	
WI38	0.0276	0.019	442	0.44 ± 0.02	(2)
	0.0405	0.016	298	0.55 ± 0.2	(3)
	0.0450	0.022	267	0.81	(1)
	0.0549	0.015	217	0.69	(1)
	0.0592	0.011	200	0.54	(1)
	0.0909	0.005	126	0.40 ± 0.03	(3)
	0.105	0.009	108	0.80 ± 0.2	(2)
	0.126	0.005	88	0.54 ± 0.2	(2)
				mean 0.56 ± 0.1	(15)
Asn-7*	0.047	0.013	192	0.67	(1)

*The experimental work in obtaining autoradiogram of Asn-7 stuttering was done by J.Pollard, J.Chamberlain, and J.Parker. I quantified the scan of the autoradiogram and calculated the error frequency.

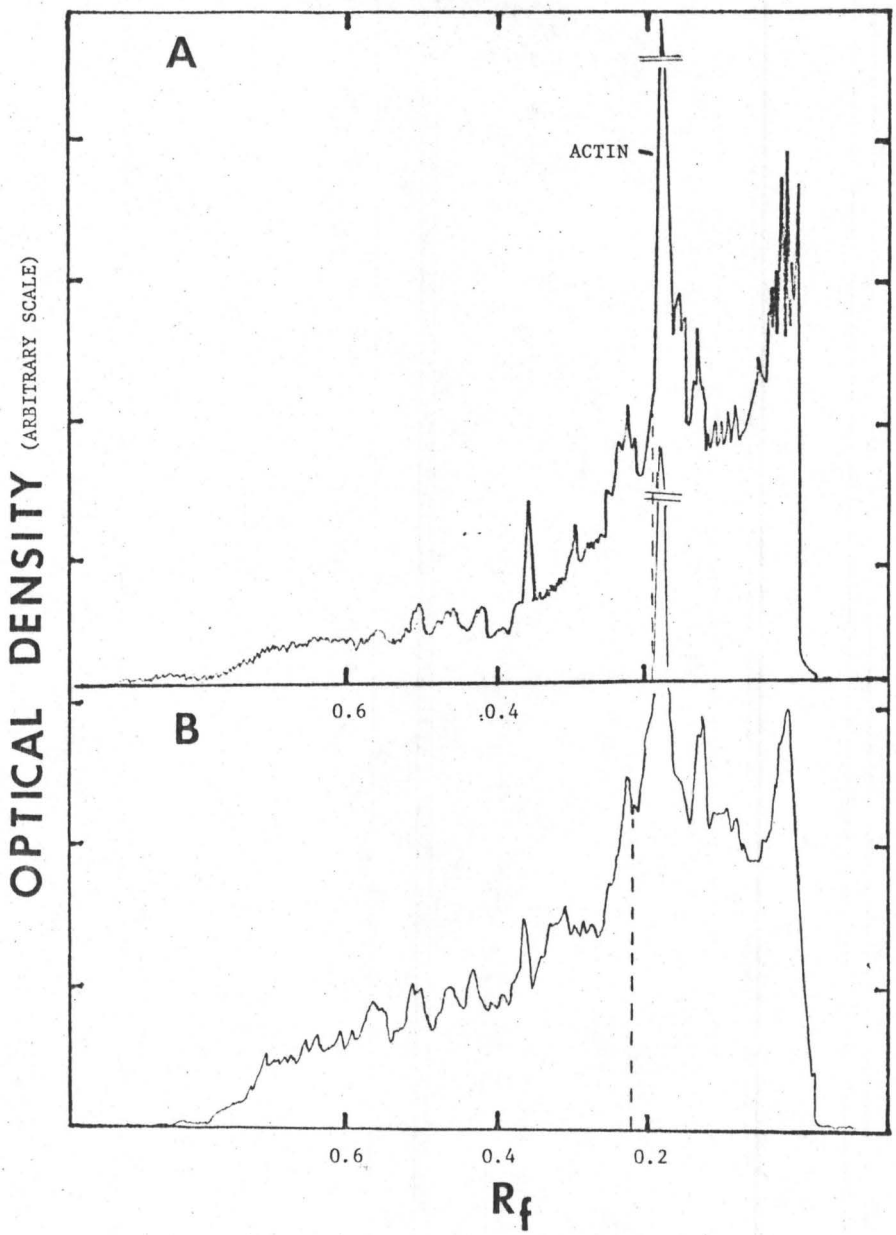

Figure 3-13

Molecular weight distributions of labeled proteins. Cells were labeled for 40 minutes with ^{35}S-methionine as described in section 3.1.3.2 during (A) normal conditions (100% protein synthetic rate) and (B) histidine-starvation conditions (5 mM histidinol, 10.5% protein synthetic rate). Autoradiograms of labeled protein resolved on 20% polyacrylamide SDS gels were scanned and quantified as described in section 3.2.2.3. The dotted lines indicate the position of the weight-average molecular weight proteins. The major peak in the scan is actin.

To determine if error-containing proteins were being degraded significantly during the 40 minute labeling period, we analyzed stutter spots of actin on autoradiograms from cell lysates during pulse-chase experiments (figure 3-14). The data indicate that for at least one hour following the pulse, there is no detectable turnover of either native or substituted actin under conditions of histidine starvation (Table 3-8).

The relative rate of actin synthesis during histidine starvation was determined by rate measurements on actin isolated from one dimensional IEF and SDS gels. In human cells actin synthesis was proportional to the relative rate of overall protein synthesis in (Table 3-9). This may reflect the fact that actin is the major protein synthesized and is typical of overall proteins in molecular weight and frequency of histidine codons (figure 3-13, Table 3-11). But this proportionality is not a prerequisite of the normalization procedure described below. Except for extreme deviations from the mean molecular weight and amino acid composition of total cellular protein, the degree of stuttering can be normalized and used to calculate an inherent error frequency for any protein (see below).

Figure 3-15 shows profiles of ribosomes and polysomes extracted from cells before and after amino acid starvation. The fraction of material in the polysome portions of these curves decreases 10-60% for a variety of cells for either

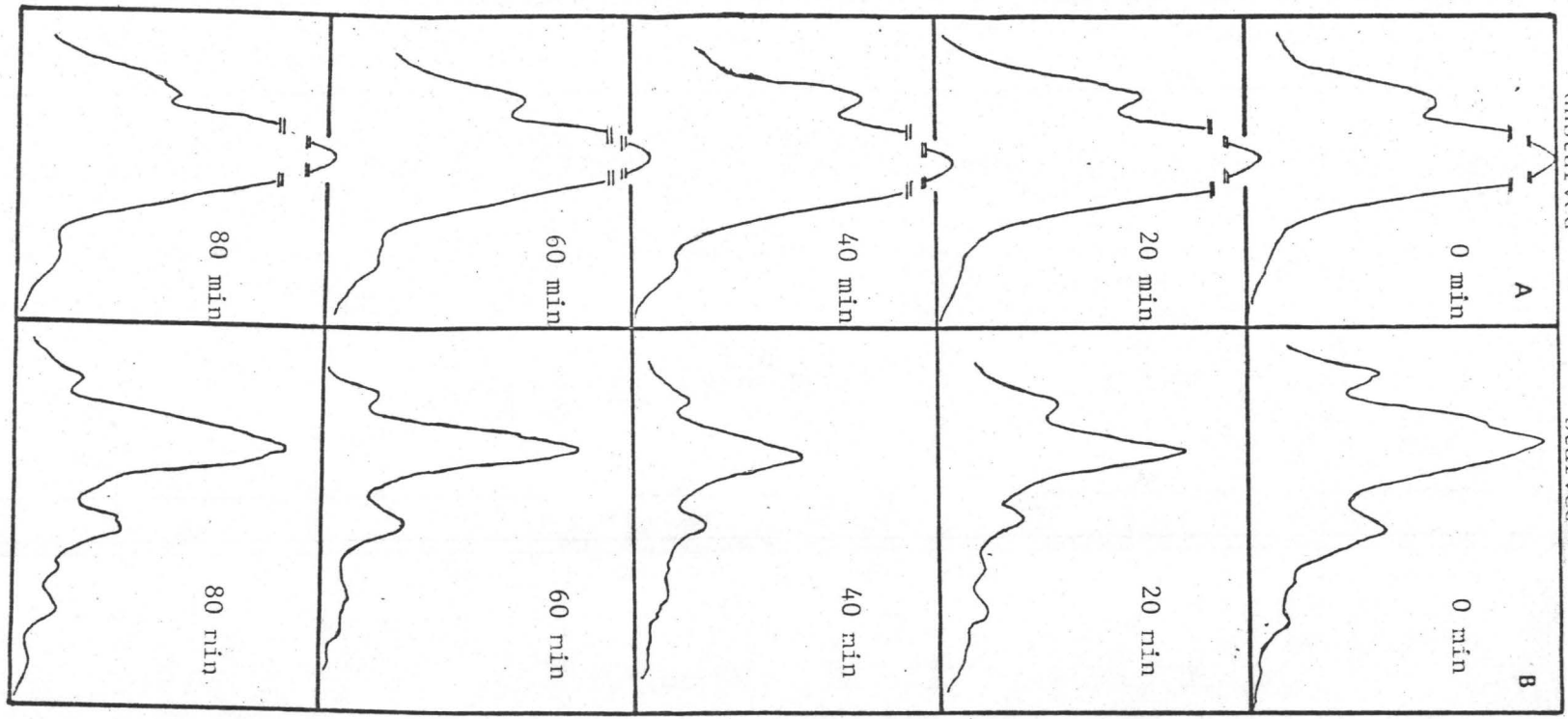

Figure 3-14

Pulse-chase analysis of native and substituted actins. Early-passage WI38 cells were treated as described in section 3.1.3.2. Following the 40 minute labeling period in the presence of histidine (left panels) or 10 mM histidinol (right panels), all dishes were rinsed twice then chased in medium identical to their pulse medium except lacking label and containing excess nonlabeled precursor (phenylalanine or methionine). Shown are scans of the actin region of 2-D gel autoradiograms from lysates prepared at 20, 40, 60, and 80 minutes following the pulse (as indicated). The major peak in each scan is β-actin; γ-actin is the minor peak to the left of β-actin. Scans were integrated and quantified as described in section 3.1.3.4 (see Table 3-8). Analysis of total acid-insoluble material at the end of the chase time indicated degradation of 10.5% of total protein in control cultures (unstarved) and degradation of 47.8% of total protein in starved cultures.

Table 3-8

Stability of Native and Substituted Actins

Histidinol (mM)	Chase Time (min)	Fraction of Total Area Under Scan					
		γ	β	S_1	S_2	S_3	
0	0	0.171	0.771	0.0584			
	20	0.174	0.782	0.0441			
	40	0.205	0.749	0.0457			
	60	0.181	0.771	0.0486			
	80	0.147	0.805	0.0475			
							P'
10	0	0.128	0.601	0.176	0.0608	0.0338	0.0443
	20	0.132	0.583	0.139	0.0930	0.0530	0.0538
	40	0.105	0.593	0.201	0.0765	0.0239	0.0473
	60	0.082	0.658	0.158	0.0616	0.0411	0.0449
	80	0.072	0.652	0.179	0.0676	0.0290	0.0446

Quantitation of data from figure 3-14.

Table 3-9

Relative Rates of Synthesis of Actin and Total Cellular Protein

Histidinol (mM)	Relative Rate of Total Protein Synthesis[a]	Relative Rate of Actin Synthesis[b]	
		IEF Gels	SDS Gels
0	1.00	1.00	1.00
10	0.072 ± 0.005	0.075 ± 0.01	0.066 ± 0.01

Cell strain used for this experiment was normal donor A2 at early passage. Similar results were obtained with late-passage A2.

[a]Relative rate of total protein synthesis was determined as described in section 3.1.3.2.

[b]Actin from one-dimensional gels was analyzed rather than actin from 2-D gels because of difficulties in obtaining quantitative transfer of protein from IEF to SDS gels. Gels were run of protein labeled for 10, 20, 30, and 40 minutes with ^{35}S-methionine. The major actin band was cut from the gels and labeled protein was counted following elution (24 hours with shaking at 37° C in 1N NaOH). Relative rates of actin synthesis were determined from graphs of incorporation versus time during unstarved (0 mM histidinol) and starved (10 mM histidinol) conditions. Labeled actin comprised 3.7% of total labeled protein in this experiment.

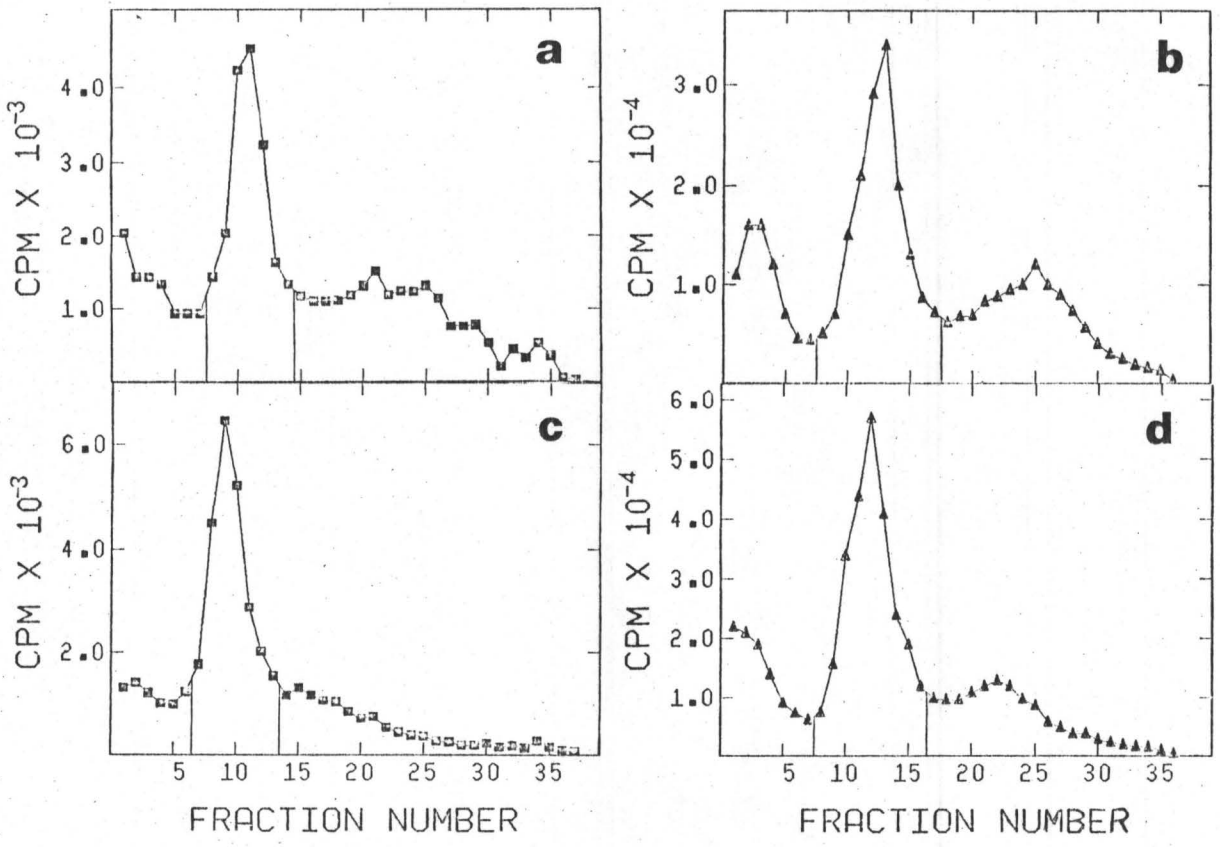

Figure 3-15

Polysome profiles. Ribosomes and polysomes from WI38 (a,c) and asn-7 (b,d) cells labeled for 3 days with ^{14}C-uridine were resolved on linear sucrose gradients as described in section 3.2.2.4. Prior to the preparation of lysates, cultures were divided into two portions and either grown under unstarved conditions (a,b) or under starvation conditions (c,d) (see section 3.1.3.2 for WI38 cells, histidine starvation; and Parker et al., 1978, for asn-7 cells, asparagine starvation. The vertical lines on each profile delineate the monosome peak. The fraction of ribosomes on mRNA was calculated as the number of cpm in material heavier than monosomes (total cpm to the right of the second vertical line) divided by the total cpm in the combined monosome plus polysome fractions (total cpm to the right of the first vertical line). See Table 3-10 for quantitative analysis of these and other polysome profiles.

Table 3-10

Fraction of Ribosomes on mRNA

Cell[‡]	Relative Protein Synthetic Rate	Relative Number of Ribosomes on Message[§]
WI38	0.20	0.64 ± 0.02
	0.13	0.71 ± 0.07
WI38-SV40	0.20	0.82
	0.14	0.92
A2 early passage	0.20	0.69 ± 0.03
	0.18	0.79 ± 0.02
A2 late passage	0.16	0.72 ± 0.02
	0.11	0.73 ± 0.03
Asn-7*	0.10	0.81 ± 0.05
CHO	0.022	0.46 ± 0.05
	0.014	0.63 ± 0.02
HA	0.055	0.36 ± 0.03
	0.024	0.37 ± 0.03
T	0.056	0.48
	0.033	0.57 ± 0.04

[‡]Cell types are described in Table 3-1 except HA and T (Stanners et al., 1963)

[§]The mean fraction of ribosomes on mRNA during normal growth (100% protein synthetic rate) was: 0.53, WI38; 0.56, WI38-SV40; 0.37, A2-early passage; 0.35, A2-late passage; 0.52, asn-7; 0.55 CHO; 0.73, HA; 0.78, T.

*Data collected by J.Pollard and J.Chamberlain.

Results show mean ± one-half range of duplicate gradients.

histdine or asparagine starvation (Table 3-10). It is noteworthy that the fraction of ribosomes on mRNA apparently increases slightly at higher degrees of starvation. This has been observed in other cell strains (Vaughan et al., 1971) and has been interpreted as an increasing effect of starvation on the elongation rate. However, certain qualifications need to be made. First, it is impossible to know whether the extraction procedure has left all polysomes intact in all situations. Second, only for CHO cells were the ribosomes of the monosome peak shown to be not engaged in protein synthesis. And third, in some cells it is technically difficult to resolve monosomes from polysomes and the division between these fractions on the polysome profile is somewhat arbitrary.

3.2.4.2 Mistranslation Under Normal Conditions

(a) The Hypothesis

It is known that amino acid starvation results in low levels of the corresponding aminoacyl-tRNA and that the rate of protein synthesis is somehow coupled to the state of this tRNA (Stanners et al., 1979; Lofgren and Thompson, 1979). If mistranslation occurs at the codon corresponding to the "starved-for" amino acid by mispairing of a charged irrelevant tRNA with the relevant codon (section 1.5.3), then it is logical to construct the folowing hypothesis:

During starvation for amino acid X, low levels of

charged tRNA (X-tRNA-X) reduce the frequency of interactions between X-tRNA-X and X codons. The reduced frequency of these interactions causes ribosomes to pause at X codons, lowering the protein synthetic rate. The increased step time of ribosomes at X codons also increases the probability that a charged irrelevant tRNA (Y-tRNA-Y) will substitute amino acid Y at X-sites through codon-anticodon mispairing.

We assume that:

(1) the normal ribosome step time at codon X ($t_{s,x}$) is representative of the step time for all codons.

(2) Starvation for amino acid X increases the step time at X codons.

(3) The frequency of interactions between Y-tRNA-Y and the X codon which lead to incorporation of Y at X sites does not change with starvation for X.

These assumptions allow us to relate the error frequency during starvation (P_x') to the corresponding error frequency (P_x) through the increased step time of the ribosome at the relevant codon:

$$P_x = \lambda t_{s,x} \qquad (4)$$

$$P_x' = \lambda t'_{s,x} \qquad (5)$$

Therefore $$P_x = P_x'/(t'_{s,x}/t_{s,x}) \qquad (6)$$

We now describe how the ratio $t'_{s,x}/t_{s,x}$ can be obtained from the measured rates of protein synthesis.

(b) A model of mRNA translation during amino acid starvation

Several models of mRNA translation have been developed to analyze the protein synthetic apparatus (Vassart et al.,

1971, Lodish, 1974; Heijne et al., 1979), but so far the direct effect of amino acid starvation on restricting ribosome movement has not been studied theoretically. In the previous section (3.2.4.2.a) I described how an estimate of the increased step time of the ribosome at codons corresponding to the restricted amino acid can be used to relate the inherent error frequency (P) to the observed error frequency (P') measured by 2-D gel analysis of mistranslated proteins. The purpose of this section is to derive the relationship between the step time at the relevant codons and the protein synthetic rate.

The rate of synthesis R for a protein of length M codons depends on the ribosome initiation frequency (k_i), the step time of the ribosome (t_s^j) at each codon, j=1,2,3,...M, and the minimum permissible distance (D) between ribosomes on the mRNA. For simplicity, during normal (unstarved) conditions, we set $t_s^j = 1$, j=1,2,3,...,M-1. Although under normal conditions elongation rates may vary slightly along the message according to the structure of the mRNA or the availability of certain tRNAs, these effects are small (Hunt et al.,1969, Smith, 1975; Heinje et al., 1979) and are assumed to be negligible compared to the effect on $t_{s,x}$ of starvation for amino acid X. However, we have allowed for a possible direct or indirect effect of amino acid starvation on initiation frequency and the elongation rates at irrelevant codons.

Values for k_i, D and t_s^M (termination frequency) were hosen to agree with previously reported values for the average and minimum interribosome distances and the termination frequency (see Vassart et al., 1971; Lodish, 1974; Heijne et al., 1979).

The positions of histidine and asparagine codons in actin mRNA and several hypothetical proteins are shown in Table 3-11. The frequency of histidine in actin is the same as the frequency of histidine in total protein from human fibroblasts; the frequency of asparagine in actin is one half the corresponding frequency in total protein (see Tables 2-1 and 3-12a). The hypothetical proteins have the amino acid composition of total cellular protein from human fibroblasts but a random amino acid sequence of length 373 residues (section 6.3).

In the first analysis, we assume that $t'_{s,\bar{X}} = 1$, that is, the step time at non-X codons is not directly affected by starvation for amino acid X. FIgure 3-16 shows actin synthesis as a function of time for several defined values of $t'_{s,H}$ and $t'_{s,N}$. Although in these simulations the number of ribosomes on the message during steady state declines from $n \simeq 13$ for $t_{s,H} = 1$ to $n' \approx 10$ for $t'_{s,H} \geq 20$, this decrease is not the result of a defined change in the initiation frequency: $k_i = 0.0588$ for all simulations shown in figure 3-16. In fact, for larger values of $t'_{s,H}$, the synthetic rate was found to be surprisingly insensitive to the initiation frequency

Table 3-11

Position of Histidine and Asparagine Codons in mRNAs of Actin and Hypothetical Proteins H1-H5

mRNA	Position of Histidine Codons	Position of Asparagine Codons
actin	40 73 87 88 101 161 173 274 371	79 92 111 115 128 251 279 295
H1	20 39 128 130 156 217 286 289 324	4 57 148 164 186 192 221 250 272 297 301 307 328 332 344 348
H2	56 88 147 162 167 168 197 246 250	39 44 47 54 55 79 106 120 136 158 196 212 225 303 309 313
H3	7 170 229 233 237 274 279 330 338	6 9 32 58 68 82 118 190 197 207 211 224 236 248 270 339
H4	10 23 71 94 103 104 223 241 289	20 34 73 79 81 99 102 129 143 166 242 264 289 301 319 332
H5	69 127 143 150 205 216 270 323 330	40 61 78 91 133 174 188 187 197 200 215 232 248 267 273 308

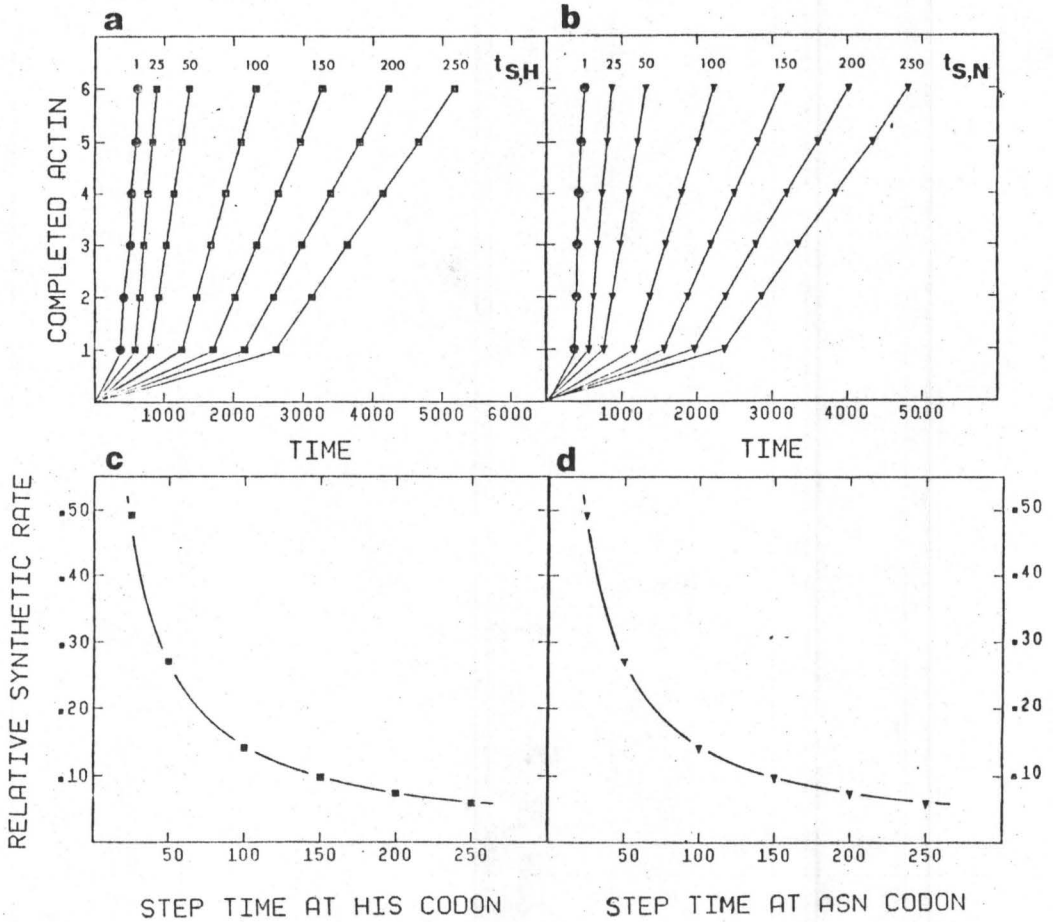

Figure 3-16

Simulations of actin synthesis during histidine and asparagine starvation. Release of the first six actin molecules are shown as a function of time during histidine (a) and asparagine (b) starvation. Translational parameters were set at D=13; k =0.0588; $t'_{S,\bar{x}}$ =1; t_S^{373} =5. Values for the step time at the relevant codons ($t'_{S,H}$, $t'_{S,N}$) are as shown on the figures. The rate of synthesis relative to the unstarved rate ($t'_{S,H}=t'_{S,N}=1$) is shown as a function of $t'_{S,H}$(c) and $t'_{S,N}$ (d).

(Fig.3-17). An eight or sixteen fold decrease in k_i has essentially no effect of the synthetic rate when $t'_{s,H}$ is greater than 50. When $t'_{s,H}$ is relatively small, i.e. during mild amino acid starvation, a lowered initiation frequency has a dramatic effect on the protein synthetic rate, which can be accounted for by the reduced number of ribosomes on the message (Fig. 3-17a&b). The explanation for the anomaly at large values of $t'_{s,H}$ was found by studying the distribution across the mRNA of the actual step times of the ribosomes (Fig. 3-18). Figure 3-18a shows the transit of the first ribosome for $t'_{s,H}$ =100: it pauses for 100 time units at the his codons only. However, the transit of the fifteenth ribosome (figure 3-18b) shows further delays at non-histidine codons at the 5' end of the message. Ribosome queuing extending from a pair of histidine codons at positions 87 and 88 back to the initiator codon inhibits initiation of new ribosomes. In these instances, therefore, variation in the "defined" initiation frequency has no effect on the protein synthetic rate. A similar argument applies to the termination frequency. Ribosomes arrive at the last codon so infrequently that large changes in t^M_s do not affect the synthetic rate (not shown).

An apparent paradox is that ribosome queuing progressively decreases the initiation frequency and increases the transit time of the first 5 or 6 ribosomes, yet the protein synthetic rate is constant after termination of the very first ribosome (figure 3-16a&b). This results from

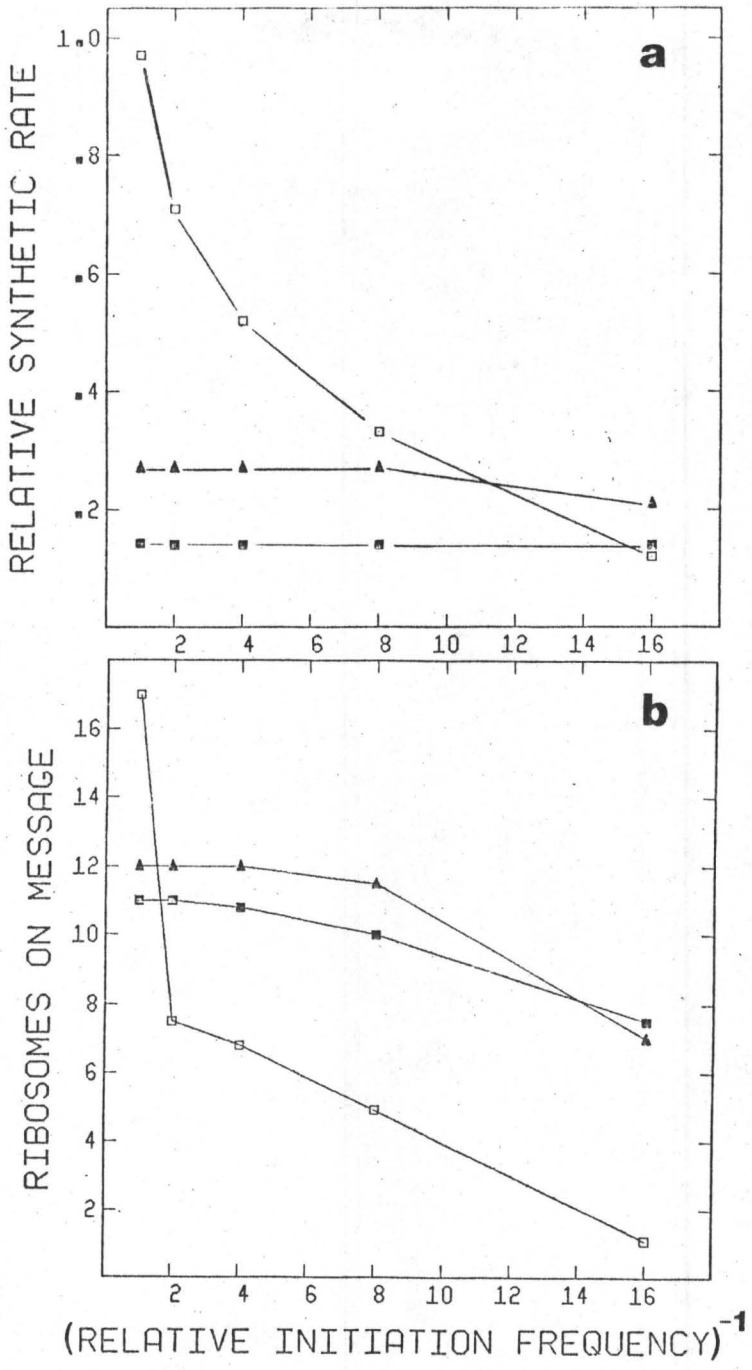

Figure 3-17

Synthetic rates and number of ribosomes on actin mRNA as a function of initiation frequency. The step time at the histidine codon ($t'_{S,H}$) was set at 10 (□), 50 (▲), and 100 (■) and for each the value of k_i was varied from 0.0588 (relative frequency = 1) to 0.0036 (relative frequency = 1/16). Other parameters were as described in figure 3-16. Shown are the relative rates of protein synthesis (a) and the mean number of ribosomes on actin mRNA during the simulations (b).

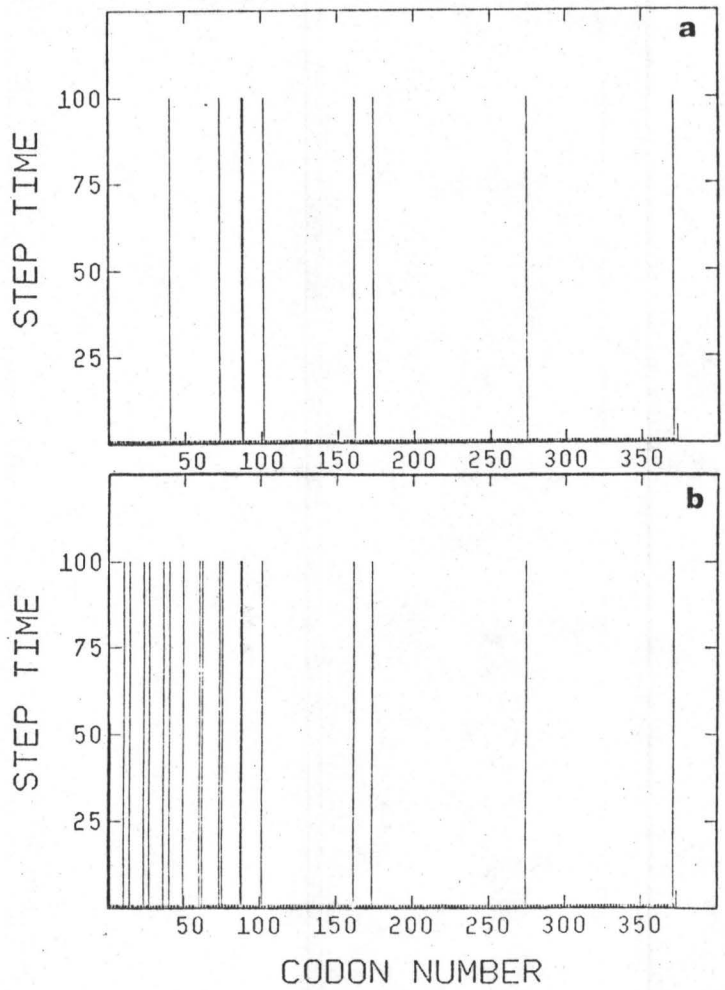

Figure 3-18

Actual step time of the ribosome at each codon in actin mRNA during simulations of histidine starvation. The defined step time of the ribosome at histidine codons was t' =100. Other parameters were as described in figure 3-16. Ribosome number 1 (a) pauses at the nine histidine codons only. Ribosome number 15 (b) pauses at additional codons due to queuing behind histidine codons 87 and 88.

the fact that the rate of ribosome release (i.e. the synthetic rate), is dictated by the rate at which ribosomes negotiate the slowest "cluster" of X codons. This rate is established with the first two ribosomes.

Since clusters of X codons are a property of the mRNA, it is important to determine whether the effects of starvation on the protein synthetic rate of actin are representative of all proteins. Figure 3-19 summarizes the data of figure 3-16a&b and similar data for the hypothetical proteins with a random amino acid sequence and the amino acid composition of total cellular protein (Table 3-11). The relationship between protein synthetic rate and the step time at X codons is in fact relatively insensitive to the actual actual amino acid sequence (given that it is essentially random). The synthetic rate depends more on the frequency of X codons in the message since this determines the probable size of clusters and thus the minimum length of time between ribosomes at termination.

The frequency of histidine codons in actin mRNA is typical of total cellular protein: the relationship between R/R' and $t'_{s,H}/t_{s,H}$ for actin mRNA also applies to hypothetical proteins H1-H5 (figure 3-19) and should apply to total cellular protein. However the frequency of asparagine codons in actin mRNA is roughly one half the frequency observed in total cellular protein. Thus, actin mRNA is translated faster during asparagine starvation than most hypothetical

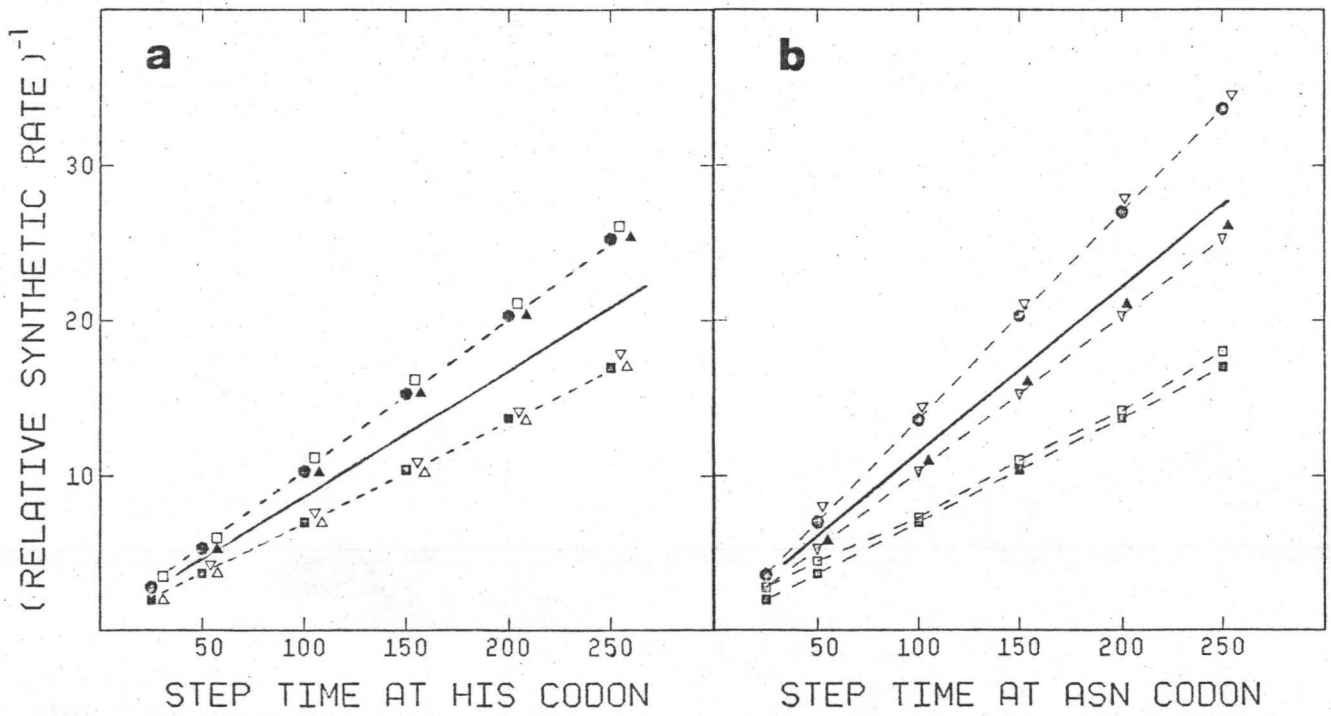

Figure 3-19

The reciprocal of the relative protein synthetic rate as a function of step time at the histidine and asparagine codons for actin and several hypothetical proteins. The standard translational parameters as define in figure 4 were used. Values for the step time at the histidine (a) and asparagine (b) codons varied from 25 to 250. Simulations for actin (■), H1 (▽), H2 (●), H3 (□), H4 (▲), and H5 (△) are shown. The solid lines are drawn through the mean values of R/R' at each $t'_{s,x}$ for actin and H1-H5 (a), and H1-H5 (b).

proteins (and hence average cellular mRNA). The simulated effects of asparagine starvation on actin synthesis are in fact typical of hypothetical proteins that have the asparagine frequency of actin (not shown).

Since synthetic rates are routinely measured for total cellular protein, we require the relationship between R/R' and $t'_{s,x}/t_{s,x}$ for the average cellular protein. The solid lines in Figure 3-19 were drawn to represent average cellular protein. The equations describing these lines are:

$$t'_{s,H}/t_{s,H} = 12.53(R/R'-0.92) \qquad (7)$$

$$t'_{s,N}/t_{s,N} = 9.43(R/R'-0.89) \qquad (8)$$

Derivation of equations 7 and 8 was the purpose of the simulations. These equations allow us to determine the relative step time at the histidine or asparagine codons from the measured inhibition of protein synthesis. However, other simulations described below were required to determine whether these equations were robust, i.e. insensitive to the assumptions of the model.

The value of the minimum interribosome distance, D, used in the simulations above was 13 codons (39 nucleotides). The amount of mRNA protected by a ribosome from nuclease digestion in vitro is about 25 nucleotides (Steitz, 1973; Lehninger, 1976), but the maximum density of ribosomes observed on mRNA is about one per 11-13 codons (Kazanian and Freedman, 1968). Values used for D in other simulations of

protein synthesis have ranged from 10 to 15 (Vassart et al., 1971; Lodish, 1974; Heinje et al., 1979). Since the number of X codons the ribosome covers in a cluster ultimately determines the protein synthetic rate for a given $t'_{s,x}$, we varied D to see if the synthetic rate was sensitive to this parameter (Fig. 3-20a). For actin, the effective size of the cluster of histidine codons at positions 87,88 and 101 changes from 2 to 3 when D changes from 14 to 15. Thus the synthetic rate at D greater than 15 is about 33% slower than the rate at D less than 15. Hypothetical proteins H1-H5 have cluster sizes of 2 or 3 which do not change over the range of D=11-17. The synthetic rate of actin is similar to H1 and H5 at low values of D and H2-4 at high values of D. Similar results were found for asparagine starvation (not shown). It is reasonable to assume, therefore, that the relationship between R/R' and $t_{s,x}/t'_{s,x}$ given in equations 7 and 8 are insensitive to D.

Not all X codons may be translated at the same rate. Different histidine and asparagine codons, (CAU,CAC and AAU,AAC), for example may translate or mistranslate with different efficiencies. Furthermore, the influence of neighboring bases, mRNA secondary structure and the stochastic nature of molecular interactions will contribute to variability in $t'_{s,x}$. Figure 3-20b&c show the results of simulations where all nine histidine codons of actin were allowed to vary about the mean $t'_{s,H}$ (fig. 3-20b) and where the one of the codons was allowed to assume a step time twice

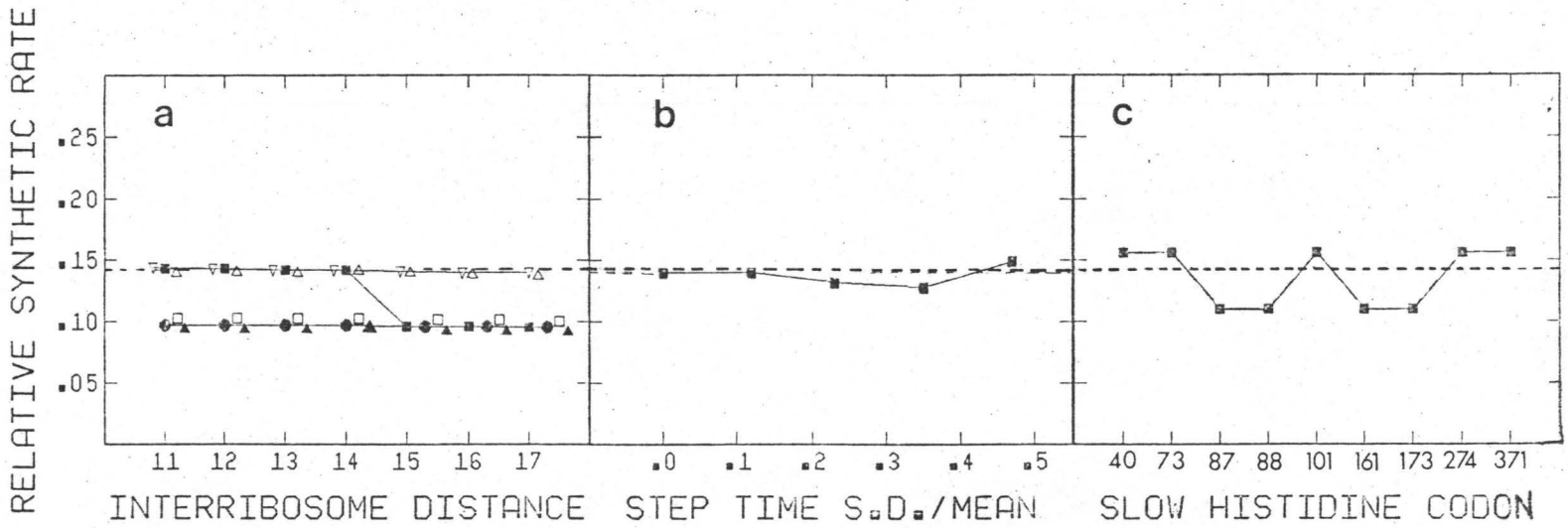

Figure 3-20

Relative synthetic rate during histidine starvation as a function of some translational parameters. The mean step time at the histidine codon was set at 100 in all cases. The synthetic rate to which all values are normalized is the unstarved rate with the standard parameters as defined in figure 3-16. The relative synthetic rate is shown as a function of: (a) D, the minimum permissible interribosome distance, for actin (■), H1 (▽), H2 (●), H3 (□), H4 (▲), H5 (△); (b) the coefficient of variance of the step time at the histidine codon, where a uniform distribution about the mean (100) is assumed; (c) position of a "slow" histidine codon which has a step time twice that of all other histidine codons.

The dotted line in each figure shows the relative synthetic rate of actin at $t'_{s,x}$ =100 with the standard parameters (figure 3-16).

that of all the others (fig. 3-20c). In both cases, the synthetic rate was again found to be relatively insensitive to these variations in the basic model.

Although in size, actin is typical of total cellular protein, it is of interest to note the effect of mRNA size on rate of translation during amino acid starvation. For a given frequency of X codons, the larger the mRNA, the greater the probability of increasing the cluster size of X codons. Therefore, large proteins will tend to be synthesized at a slower rate than small proteins (figure 3-21). This effect is probably sufficient to account for the observed decrease in average molecular weight of proteins synthesized during amino acid starvation (figure 3-13). The step times at relevant codons will be the same in large and small mRNAs, yet their rates of translation will differ. Therefore the relationship between $t'_{s,x}/t_{s,x}$ and R/R' should be determined ideally by weighted averages of relationships from a variety of mRNAs with a size distribution equivalent to that of the cell. However it is unlikely that such an average would differ significantly from the average determined with proteins of average size and amino acid composition.

Although no evidence exists that amino acid starvation has a general effect on elongation rates at all codons, we also examined the relationship between synthetic rate and t' for given values of $t'_{s,H}$ (figure 3-22) When $t'_{s,H} > 50$, doubling or even quadrupling the step time at irrelevant

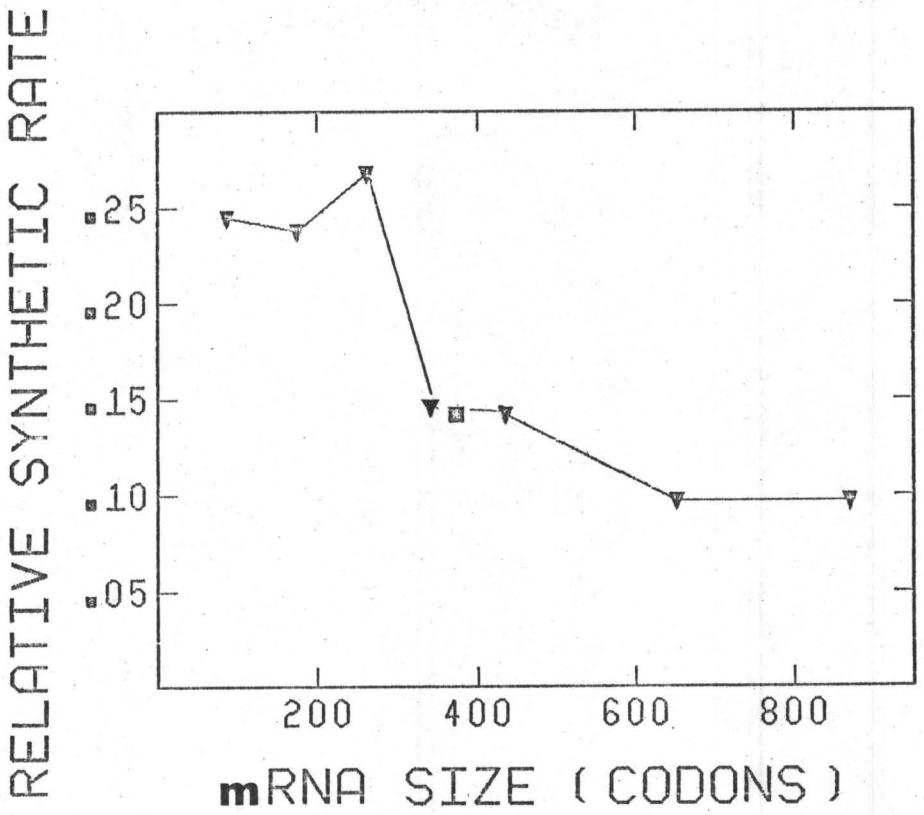

Figure 3-21

Effect of mRNA size on relative protein synthetic rate. Hypothetical proteins (▼) with 2,4,6,8,10,15 and 20 histidine residues in random positions were generated with the restraint that they have the amino acid composition of total cellular protein. The sizes of the respective mRNAs were therefore 87,184 260,347,435,652, and 870 codons in length. The translation rates of these mRNAs with $t'_{S,X}$ =100 and the standard parameters (figure 3-16) were determined in simulations and normalized to the unstarved rate. The relative rate of actin shynthesis (■) during these conditions is also shown.

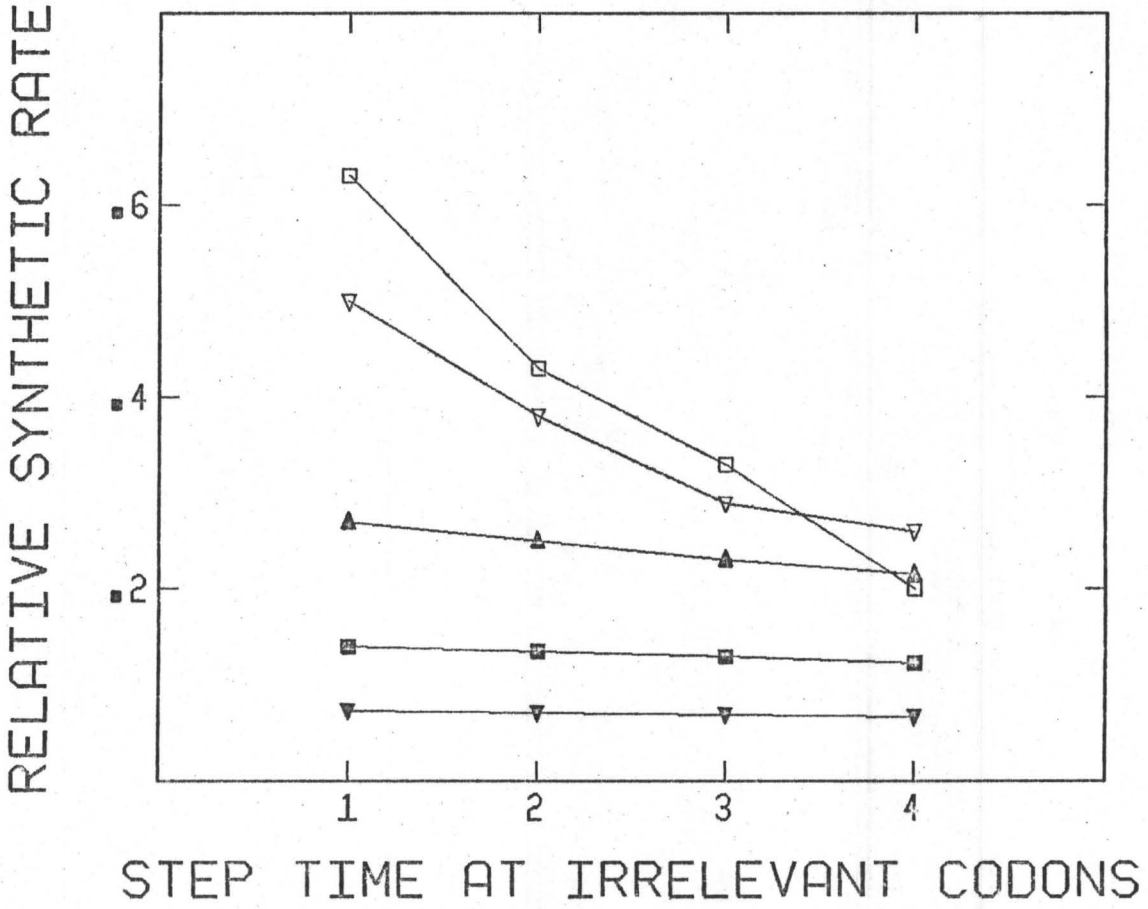

Figure 3-22

Relative rate of actin synthesis during histidine starvation as a function of step time at nonhistidine codons. Step time at the histidine codon was set at 10 (□), 25 (▽), 50 (▲), 100 (■) and 200 (▼) and the step times at other codons allowed to vary from 1 to 4. Other parameters were as defined in figure 3-16.

codons had no significant effect on R'/R. For $t'_{s,H} < 25$, the synthetic rate is sensitive to $t'_{s,H}$. However, even a four fold increase in the step time at non-his codons at small values of $t'_{s,H}$ will not lower the synthetic rate to values observed during extreme amino acid starvation ($R'/R < 0.1$). Since amino acid starvation is known to cause queuing of ribosomes at the relevant codons (see section 1.5.2), one can assume that the inhibition of protein synthesis during extreme amino acid starvation is entirely due to the increased step time at relevant codons: changes in the elongation rates at other codons need not be considered in the derivations of equations 7 and 8.

During mild amino acid starvation, $t'_{s,x}$ has only a small effect on the synthetic rate (figure 3-16c&d) and under these conditions, the effects of uncharged tRNA on the formation of the initiation complex (see Vaughan et al., 1971) or on elongation rates in general may account for most of the observed reduction in the synthetic rate. Indeed, our data on the fraction of functioning ribosomes (Table 3-10) require an effect of amino acid starvation on the initiation frequency; mild starvation, when $t'_{s,x}$ is small, leads to a greater reduction in the number of functioning ribosomes than more severe starvation. If there were no effect on initiation frequency, mild starvation would actually increase the number of ribosomes on the message (figure 3-17b). Therefore, during mild amino acid starvation, analysis of the inhibition of protein synthesis must include determinations

of the initiation frequency. Error frequencies P' are measured at synthetic rates of about 10% or less and it is under these conditions that we find the relationship between R/R' and $t'_{s,x}/t_{s,x}$ given by equations 7 and 8 to be extremely insensitve to the assumptions of the model.

(c) Error Frequency P

Data from the simulations of protein synthesis during extreme amino acid starvation suggest that measurements of the relative protein synthetic rate provide an accurate estimate of the increased step time of the ribosome at the relevant codons. combining equations 2,6,7 and 3,6,8 we have

$$P = P' / \{12.53(R/R'-0.92)\} \quad (9)$$

$$= \sum^{9} iS_i/9\{12.53(R/R'-0.92)\} \quad (10)$$

$$P = P' / \{9.43(R/R'-0.89)\} \quad (11)$$

$$= \sum^{8} iS /8\{9.43(R/R'-0.89)\} \quad (12)$$

The calculated error frequencies at the histidine and asparagine codons during normal growth from observed values of R, R', and P' are shown in Table 3-7b (page 156). At the histidine codon, the error frequency in WI38 cells was $0.56 \pm 0.1 \times 10^{-4}$. Although the error rate varied from 0.40 to 0.81 $\times 10^{-4}$ over a five-fold range in protein synthetic rate, there was no apparent correlation between these parameters: the variation in error frequency reflects experimental error in measuring synthetic rates and in quantifying autoradiograms. In one determination with asn-7 cells, the error frequency at

the asparagine codon was 0.67×10^{-4}.

3.2.5 Discussion

Current methods of determining the error frequency during normal protein synthesis in intact cells suffer major limitations. Direct attempts to measure the substitution frequency of natural amino acids by protein sequencing (Loftfield, 1963; Loftfield and Vanderjadt, 1972) or by incorporation of an amino acid known to be absent from the native protein (Popp et al., 1976; Edelmann and Gallant, 1977a) are restricted to specific proteins in specialized tissues. These methods are usually applied to stable populations of proteins and thus cannot assess the true synthetic error rate: the error rate will be underestimated if selective degradation of error-containing proteins occurs (section 1.3.2). Furthermore, error-containing proteins (or peptides derived from these proteins) may be lost during the isolation procedure. For example, errors which give rise to charge changes in peptides will be overlooked if the peptides are isolated for sequencing on the basis of electrophoretic properties and only the native spot is analyzed. Such approaches are further limited in that they require essentially 100% removal of contaminating proteins. Also, these direct measurements of error frequencies do not discrimate between translational errors and altered mRNA which may arise from transcriptional errors or mutants within the cellular population. Nevertheless, such analyses have

indicated that the error frequency in the final product is less than 10^{-3} and perhaps as low as 10^{-5} per residue.

A third method, which measures a specific type of aminoacyl-tRNA synthetases error, utilizes incorporation of amino acid analogs into protein (Lewis and Tarrant, 1972; Ogrodnik et al., 1975; Hirsch et al., 1978). This method is a sensitive assay of synthetase-charging errors (Hirsch et al.,1978) but only if the ability of the synthetase to discriminate between the analog and natural amino acids is similar to its ability to distinguish one natural amino acid from another. Incorporation of ∝-aminoisobutyric acid into mouse hemoglobin was found to occur about once per 1.4×10^4 amino acids (Hirsch et al., 1978), but insufficient analog was incorporated to determine by sequence analysis which synthetases misacylated their tRNAs.

If specific translational errors could be induced to a readily measured frequency, most of the limitations inherent in direct analysis would be overcome. Although many agents were previously known to induce protein synthetic errors (see Davies, 1969; Gorini, 1974; Hirsch et al., 1978), they were not useful in determining the normal error frequency since there was no means of extrapolating from the high-level error frequencies to the normal rate. This report is the first describing such an extrapolation. There are three steps in the procedure. First, starvation of animal cells for a single amino acid is used to reduce the protein synthetic

rate to low levels ($< 10\%$) and allow quantitation of error frequencies on 2-D gels. Second, the inhibition of protein synthesis is related to the increased step time of the ribosome at the relevant codon by a computer simulation of mRNA translation. And third, measured error rates are then normalized to the increased step times to determine the error frequency at the relevant codon under normal conditions.

Our data from analysis of actin synthesis have allowed determination of the error frequency at the histidine and asparagine codons. In WI38 the frequency of errors in misreading histidine codons was 0.56×10^{-4}. In other human strains, the error frequency varied from 0.4 to 1.6×10^{-4} (section 3.1). In CHO cells with a temperature sensitive defect in asparaginyl-tRNA synthetase the error rate at asparagine codons was 0.7×10^{-4}. Interference of proteins on the basic side of β-actin with stutter spots make the measurements of errors at asparagine codons less reliable (section 3.4). However, the correspondence of error frequencies in these cells from two different animal species suggest that the error rate for codon-anticodon mispairing in the third position may uniformly be about 10^{-4} in mammalian cells. This is slightly higher than the error frequency measured by Edelmann and Gallant (1977a) for cysteine incorporation into flagellin in bacteria. At first, this might seem surprising since animal ribosomes are expected to have a greater fidelity than bacterial ribosomes (see Burrans and Kurtz, 1977). However, misincorporation of cysteine by

codon-anticodon mispairing cannot occur by pyrimidine-pyrimidine mispairing in the wobble position (figure 1-6). Edelmann and Gallant (1977) in fact provided indirect evidence that one or more of the arginine codons were being misread for the cysteine codon by first postion error. Therefore, these data may indicate that first position errors are much less frequent than third position errors.

Lagerkvist (1978) has proposed "2 out of 3" translation for certain families of codons where interaction between the first two bases may be sufficiently strong to direct incorporation. Thus, constraints on specificity of binding in the third position may be somewhat relaxed in all cases and the greatest frequency of errors may result from misreading at this position (see also section 1.4.2.1).

Consistent with this hypothesis is the degree to which asparagine and lysine codons are misread. In both bacterial and animal cells, asparagine starvation readily induced misreading of the asparagine codons producing stutter spots with an increased pI: presumably the asparagine codons are misread for lysine codons by third position pyrimidine-pyrimidine mispairing. Initially, extreme starvation for lysine did not reveal amino acid substitutions at the lysine codon, where either first or third position errors would have been detected on 2-D gel electrophoresis (Parker et al., 1978). However, low levels of errors (stutter spots on the acid side of native species) have now been

detected in bacterial cells with very extreme lysine starvation (Parker and Friesen, 1979). It will be interesting to determine whether the substituted amino acid is asparagine, implying third position purine-purine mispairing, or glutamic acid, implying first position purine-purine mispairing. Since substitution of glutamic acid for a lysine residue is a double charge change, whereas asparagine for lysine is a single charge change, these possibilities could be resolved quickly by analyzing isoelectric points of stuttered proteins where the amino acid composition of the native species is known, as described in section 3.3.

In strains of E.coli with the "stringent response", (rel+ strains), the effects of amino acid starvation on protein synthesis are confounded by the synthesis of guanosine tetraphosphate (ppGpp) which has a pleiotypic effect on metabolism (Gallant and Lazzarini, 1976; O'Farrell, 1978; section 1.5). The independent suppression of protein synthesis by ppGpp can explain the lack of correspondence between amino acid starvation and mistranslation in these strains (O'Farrell, 1978). Rel- bacteria, which lack the stringent response, are affected by amino acid starvation in a manner similar to animal cells (Parker et al., 1978; O'Farrell, 1978) and in accord with the model described here. Consistent with this are the results suggesting that animal cells do not possess a "stringent response" (Stanners and Thompson, 1974; Pollard and Parker, 1977; Pollard et al.,

submitted).

O'Farrell (1978) has suggested that ribosomes forced to pause at codons that are difficult to misread are more likely to terminate prematurely than ribosomes that pause at easily misread codons. Histidine codons are easily misread as asparagine codons by third position pyrimidine-pyrimdine mispairing but leucine and most arginine codons cannot be misread in this manner. Thus, O'Farrell found that histidine starvation apparently did not increase premature termination while arginine and leucine starvation, which induced very low levels of stuttering, led to large increases in the presence of low molecular weight proteins. Whether these low molecular weight proteins reflect premature termination or preferential synthesis of small mRNAs (for example ribosomal protein mRNA) has not been established. However, as yet there is no adequate analysis of error frequencies allowing extrapolation to normal rates when premature termination is a significant factor.

Our data on the size distribution of total protein synthesized in human fibroblasts during histidine starvation (figure 3-13) suggest that any shift towards smaller molecular weight proteins is negligible and in fact may be explained by the relatively greater rate of translation of smaller mRNAs during amino acid starvation (figure 3-21).

Induction of protein synthetic errors by amino acid starvation and detection of these errors by 2-D gel

electrophoresis also provides a unique opportunity to study degradation of abnormal proteins. Overall protein degradation in human cells increased on acute amino acid starvation (figure 3-14), as it does in several other cell types (for review, see Ballard, 1977), but neither native nor error-containing actin were degraded to a measurable extent during the course of the experiments (1-2 hours). It is noteworthy that Baxter and Stanners (1978) did not find increased degradation of total cellular protein on amino acid starvation of HA and T cells, and other workers have failed to see increased degradation of actin species in CHO cells (Pollard and Chamberlain, personal communication) or in E.Coli (Parker, personal communication). Since these observations are in contrast to others showing increased degradation of abnormal proteins (section 1.3.2), a more thorough, quantitative analysis on many proteins is required. Native and substituted actins may be unique in their resistance to cellular proteases.

I have restricted my analysis of error frequency to conditions of histidine starvation where premature termination, changes in the population of translated mRNAs, and degradation of error-containing proteins are not significant. Therefore, I have not incorporated these possible features of mRNA translation into the model. As I have argued, the omission of these variables should not affect the conclusions on the error frequency at the histidine and asparagine codons in cultured human and CHO

cells. However, if this method is to be extended to other systems and other codons further refinements of the theory may be required.

The fidelity of translation was previously shown to correlate inversely with the speed of ribosome movement during mRNA translation (see Kurland, 1977). This is not at odds with the observation of increased mistranslation during amino acid starvation where elongation rates are reduced for the following reason. During evolution, selection for changes in translational factors which increase the specificity of codon-anticodon interactions (and hence fidelity of synthesis) are expected to compromise the speed of peptide bond formation. And on the other hand, mutations which relax the constraints on codon-anticodon interactions and lead to increased rates of elongation will tend to increase the probability of error. However, the reduction in the availability of charged tRNA during amino acid starvation will increase the probability of amino acid substitution through its direct effect on increasing the step time of the ribosome at the relevant codons. It is unnecessary to assume a change in the frequency of codon-anticodon mispairing, i.e. the inherent fidelity of the ribosome. Under these conditions, errors will increase as the synthetic rate decreases.

However, the assumption that the fidelity of the ribosome has not been altered by amino acid starvation is

critical to the analysis. I suspect that ribosomal fidelity may decrease with prolonged and extreme amino acid starvation (see section 3.5), and thus have analyzed error frequencies during acute starvation when the relative rate of protein synthesis is usually between 3 and 12%. The finding that calculated error rates are consistent over this range suggest that under these conditions, the inherent ribosomal fidelity is unchanged.

Levels of uncharged tRNA measured during amino acid starvation in both animal cells and rel- E.coli are not reduced as much as the calculated step time at the relevant codon is increased (section 1.5.2). In its simplest form, the proposal of O'Farrell (1978) that certain isoaccepting species may become completely deacylated while others have high levels of charging cannot be applied to histidine starvation. The histidine codons CAU,CAC are both translated by tRNAs carrying anticodon GUG or QUG (Q is a derivative of G) (see Harada and Nishimura, 1972; Smith, 1975). Anticodon AUG does not exist since its presence would be lethal: anticodon deaminase converts 5'-A to 5'-I and hence, according to the wobble rules (Crick, 1966), would allow misreading of histidine codons for asparagine codons (Topal and Fresco, 1976a&b). However, the relative abundance and translation efficiences of these tRNAs (Smith, 1975) rule out the possibility that the disparity between charging levels and step times can be accounted for on the basis of a differential effect of starvation on charging of these

isoaccepting species. If in fact step times are increased to the levels predicted by the model, then either a nonlinear relationship exists between levels of charged tRNA and ribosome step time, or techniques for measuring charged tRNA concentrations do not accurately reflect the concentration of charged tRNA at the site of protein synthesis *in vivo* (section 1.5.2).

It has recently been shown that there may be specificity for the anticodon in the P site (section 1.4.2.3). Noncognate interactions of peptidyl-tRNA analogs at the P site influence the binding of cognate tRNA at the A site *in vitro* . If this observation applies to translation *in vivo* , it suggests that elongation rates at codons immediately following mistranslated codons may be somewhat reduced. This would have a very minor effect on the overall protein synthetic rate since nearly all codons are translated properly, even at very low synthetic rates. However, we must question whether the perturbation in binding at the A site could alter the error frequency. This would affect the analysis presented here only if the error frequency increased at these irrelevant codons and these errors contributed to the error rates measured by 2-D gel electrophoresis. Data from dipeptide analysis of the products of poly(U) mRNA translation *in vitro* (Bodley and Davie, 1966) suggest that misincorporation errors are in fact independent. Since the phenylalanine codon UUU can be misread as a leucine codon by either first or third position pyrimidine- pyrimidine

mispairing, it is unlikely that noncognate-peptidyl tRNA in the P site affects our analysis of error frequencies at most histidine codons. However, we have no information on what might happen when a pair of adjacent histidine codons present themselves to the ribosome during histidine starvation. There is such a pair in actin at positions corresponding to amino acid residues 87 and 88 and the increased time of noncognate interaction at P site 87 could adversely affect translation of histidine codon 88 (see also section 3.5).

In conclusion, I have developed a method of calculating the normal error frequency at certain codons during mRNA translation which combines experimental and theoretical analysis of error-containing proteins and the kinetics of protein synthesis during amino acid starvation. The error frequency at histidine and asparagine codons in cultured human WI38 and hamster asn-7 cells is 0.6 and 0.7×10^{-4}, respectively.

3.3 Calculation of Protein Isoelectric Points: Application to Analysis of Amino Acid Substitutions

The isoelectric point (pI) of a protein, the pH at which its net charge is zero, is a property of the protein's primary structure and its environment (see Tanford, 1962). Although only five of the natural amino acids carry a charge at physiological pH within the peptide linkage (arginine, lysine, histidine, glutamic acid, and aspartic acid), all amino acids can influence the pI of a protein. The sequence of residues, by defining the primary and secondary structure of the protein, plays an important role in determining the ionic environment and hence the pK_as of the charged residues. Sophisticated attempts to predict the electrical properties of proteins in their native state on the basis of amino acid composition and molecular shape have met with limited success (see Tanford, 1962).

Here I report that the pIs of α-, β-, and γ-actin calculated from a simple analysis of their amino acid composition are close to the observed pIs for these proteins under denaturing conditions. Moreover, the changes in pI of β- and γ-actin produced during amino acid starvation consequent to multiple substitutions of glutamine for histidine or lysine for asparagine are predicted by the compositional analysis. This analysis assumes that the pK_as of the charged residues in denatured proteins are similar to

their pK_as in free amino acid form and that the overall charge in a protein can be obtained by summing the independent contributions of each residue.

The equilibria applying to acidic (A_i^-) and basic (HB_j^+) residues are

$$HA_i \rightleftharpoons H^+ + A_i^- \qquad (1)$$

$$HB_j^+ \quad H^+ + B_j \qquad (2)$$

Applying the Henderson-Hasselbach equation (see Lehninger, 1976) to these equilibria and rearranging to obtain the fraction of charged species:

$$A_i^- / (HA_i + A_i^-) = \{1+10^{(pK_a(A_i) - pH)}\}^{-1} \qquad (3)$$

$$HB_j^+ / (HB_j^+ + B_j) = \{1+10^{(pH - pK_a(B_j))}\}^{-1} \qquad (4)$$

where $pK_a(A_i)$ and $pK_a(B_j)$ are derived from the acid dissociation constants of HA_i and HB_j, respectively.

To obtain the net charge as a function of pH, let $n(A_i)$ and $n(B_j)$ be the number of A_i and B_j residues in the protein, respectively, and sum over all of these residues:

$$\text{Net Charge} = -\sum^{i} n(A_i)/\{1+10^{(pK_a(A_i)-pH)} + \sum^{j} n(B_j)/\{1+10^{(pH-pK_a(B_j))} \qquad (5)$$

The amino acid composition of α-, β-, and γ-actin is shown in Table 3-12a. The number of arg, his, lys, asp, and glu residues in these proteins and the pK_as of the side groups of the residues are shown in Table 3-12b. The pK_as for side groups in free amino acid form and the average pK_as

Table 3-12a

Amino Acid Composition of α-, β-, and γ-Actin and Divergence of β- and γ-Actin Relative to α-Actin

Amino Acid	Number of Residues			Changes Relative to α-Actin*	
	α	β	γ	β	γ
ala	29	29	29	-2+2	-2+2
arg	18	18	18	0	0
asn	11	8	8	-3	-3
asp	23	24	21	-1+2	-2
cys	5	6	6	-1+2	-1+2
gln	11	12	12	+1	+1
glu	28	26	29	-2	+1
gly	28	28	28	0	0
his	9	9	9	0	0
ile	29	27	28	-3+1	-3+1
leu	26	27	27	-2+3	-2+3
lys	19	19	19	0	0
met	16	16	16	-2+2	-2+2
phe	12	13	13	+1	+1
pro	19	19	19	0	0
ser	22	24	24	+2	+2
thr	28	27	27	-5+4	-5+4
trp	4	4	4	0	0
tyr	16	15	15	-1	-1
val	21	22	21	-3+4	-3+3
Total	374	373	373		

Summarized from Collins and Elzinga (1975) and Vandekerckhove and Weber (1978).

*The divergence of β- and γ-actins from muscle α-actin is actually greater than appears from the amino acid composition of these proteins. Therefore the number of changes for each residue is shown. For example, although all three species have 29 alanine resiudes, four changes involving alanine have occurred during the divergence of β- and γ-actins from α-actin. There have been no changes in the number or position of arg, his or lys residues. The differences in the number of asp and glu residues represent changes in the first three or four residues of these proteins.

Table 3-12b

Charged-Residue Composition of α-, β-, and γ-Actin and pKa of Charged-Residue Side Groups

	Number of Residues in Actin			pK_a			
Basic Residues	α	β	γ	(a)	(b)	(c)	(d)
arg	18	18	18	12.5	12.43		12.5
his	9	9	9	6.0	6.67	6.5	6.5
lys	19	19	19	10.5	10.64		10.5
Acidic Residues							
asp	23	24	21	3.9	3.89		3.9
glu	28	26	29	4.3	4.43		4.3

*The pK_a of the side groups for these redidues were determined by titration of (a) the free amino acids (see Lehninger, 1976); (b) small oligopeptides containing histidine (Sober, 1972); (c) metmyoglobin from horse and sperm whale (Cohen et al., 1972). The average pK_a s of the resiudes measured in (b) and (c) are shown. Column (d) shows the values used in the calculations reported here.

of these groups in small peptides or proteins are similar. Although microenvironmental effects can influence the pK s of certain residues within proteins, the overall average is close to the pK_a of the free amino acid form. For example, the pK_as of histidine residues in myoglobin ranged from 5.37 to 8.05, but the average pK_a was 6.5 (Cohen et al., 1972). The pK_as used in the calculations reported here are shown in column (d) of Table 3-12b. The N-terminal amino group and the C-terminal carboxyl group were assigned pK_as of 8.7 and 3, respectively. Solutions to equation (5) were determined at several pH values and plots of net charge versus pH were used to obtain the predicted pI of each protein (figure 3-23 and Table 3-13).

The theoretical pIs are surprisingly close to the pIs of α-, β-, and γ-actin from rat cells measured in isoelectric focusing gels under denaturing conditions (Table 3-13). I measured similar isoelectric points for β- and γ-actin in cultured human fibroblasts (see figure 3-2) and Chinese hamster ovary cells. The observed ΔpI of 0.02 pH units between β- and γ-actin (Garrels and Gibson, 1976) is fully accounted for by the substitution of three glutamic acid residues (pK_a =4.3) in γ-actin for three aspartic acid residues (pK_a =3.9) in β-actin. The theoretical ΔpI for α- and β-actin is greater than the observed ΔpI. However, there are 49 differences in their amino acid sequence (Table 3-12a) and the lack of exact correspondence between observed and predicted pIs may reflect different secondary structures

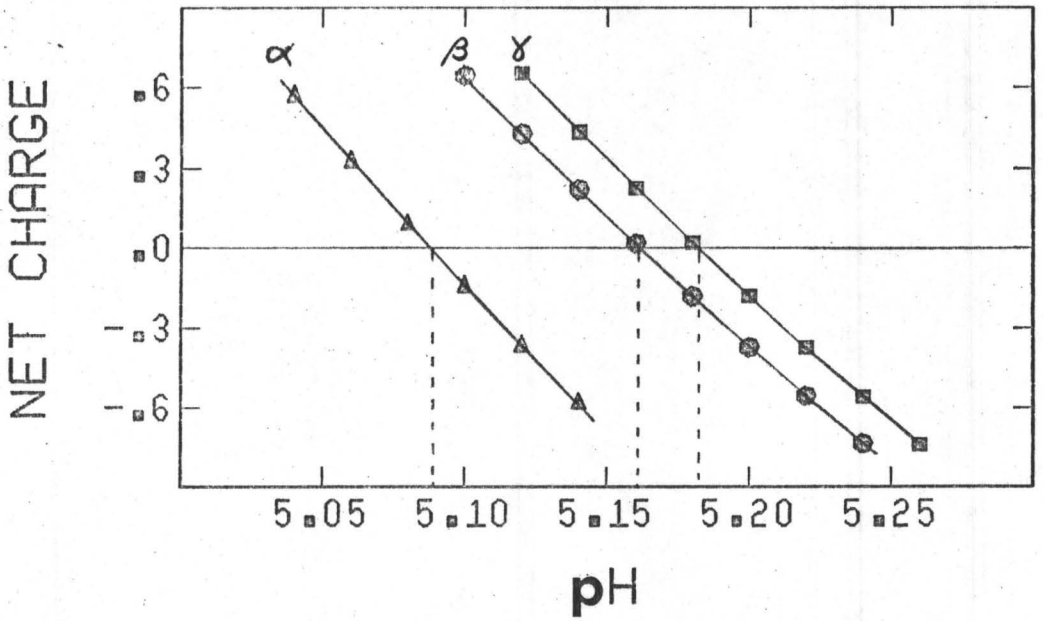

Figure 3-23

Calculated net charge of actin species as a function of pH. The net The net charge on α-, β-, and γ-actins were determined at several pH values using the equation given in section 3.3. The pH values at which the net charge is zero (dotted lines) indicate the pI of the proteins.

Table 3-13

Predicted and Observed pIs of Native Actin Species

Actin	Observed pI*	Predicted pI
α	5.40	5.08
β	5.42	5.16
γ	5.44	5.18

*From Garrels and Gibson (1976)

of these actin species.

To see whether changes in the pI of proteins can be predicted from theoretical calculations, I determined numerically the pIs of native and substituted β-actin (the major form of actin in cultured fibroblasts and CHO cells) and compared the ΔpI/substitution with the observed changes seen on 2-D gel electrophoresis (sections 3.1, 3.2).

Figure 3-24 shows the calculated pIs of native and substituted β-actin. Similar curves, displaced 0.02 pH units downward, were obtained for γ-actin (not shown). Four predictions can be made from these analyses: (i) Substitution of glutamine (or any neutral amino acid) for histidine will initially produce a change in the pI of actin of -0.09 pH units; (ii) The magnitude of this change decreases slightly on each subsequent substitution; (iii) Substitution of lysine for asparagine (or any other neutral amino acid) will initially produce a change in the pI of actin of +0.11 pH units; (iv) The magnitude of this change increases slightly for each subsequent substituion.

Quantitative analysis of autoradiograms from two-dimensional gel elctrophoresis of β- and γ-actin synthesized during amino acid starvation are consistent with these predictions (Table 3-14). The initial ΔpI/substitution during histidine starvation was -0.08 pH units and this value decreased with increasing degrees of substitution. Distortion of the pH gradient near native actin due to large

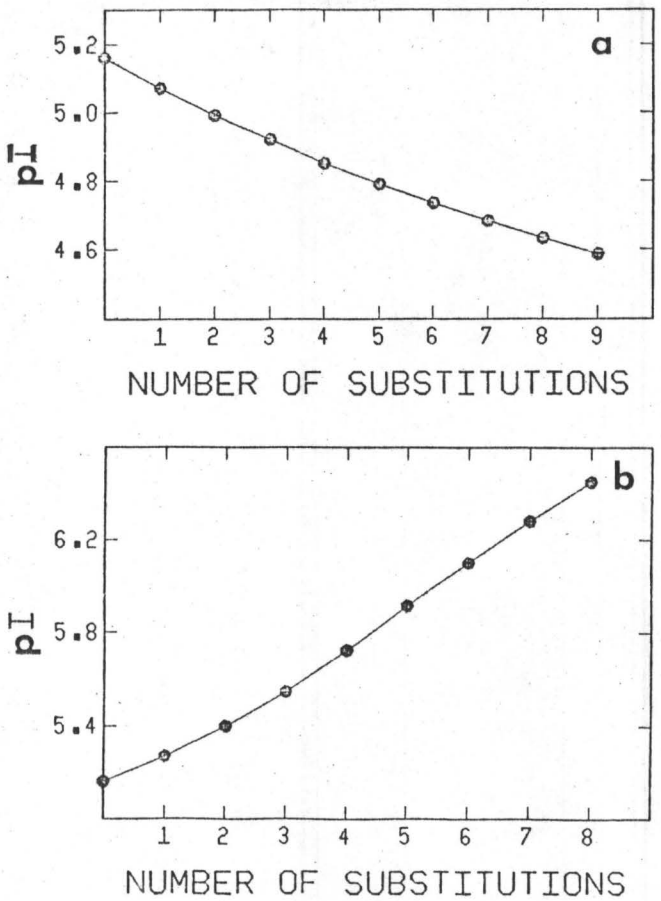

Figure 3-24

Calculated isoelectric points of substituted β-actin. Isoelectric points were determined as described in figure 3-23 for β-actin with 0-9 substitutions of glutamine for histidine (a) and 0-8 substitutions of lysine for asparagine (b).

Table 3-14

Predicted and Observed pI Differences
in Substituted Actins

Actin Species	Predicted versus Observed pI Difference			
	Histidine Starvation		Asparagine Starvation	
	Predicted	Observed	Predicted	Observed
$\beta - S_1$	0.09	0.080 ± 0.01	0.11	0.13*
$S_1 - S_2$	0.08	0.071 ± 0.01	0.13	
$S_2 - S_3$	0.07	0.069 ± 0.01	0.15	

*Single gel obtained by J. Pollard and J. Chamberlain, which I analyzed.

amounts of protein make calculations of pI on the basic side of β-actin less accurate. However, analysis of one autoradiogram of proteins synthesized during asparagine starvation in CHO cells indicates that the pI between β-actin and S1 actin was +0.13 pH units, close to the predicted value of +0.11 pH units. Refinements in isoelectric focusing techniques that allow resolution of changes on the order of 0.005 pH units would be needed to test our analysis more rigorously.

The equation given for the calculation of the isoelectric point of a protein from its amino acid composition should be useful in predicting changes in the pI of other proteins arising from mistranslated or altered mRNAs (for example from mutations) or in proteins which are post-translationally modified.

3.4 Overlapping Pattern of β- and γ-Actin Stuttering

The theoretical difference in pI of β- and γ-actin is 0.02 pH units and this ΔpI is maintained throughout substitution (section 3.3). Since the difference in pI of consecutive, substituted species is about 0.07 pH units/substitution for histidine starvation and 0.12 pH units/substitution for asparagine starvation, it is expected that the series of stutter spots for β- and γ-actin should be only slightly out of phase. With minimal loads of native protein, the ΔpI between β- and γ-actin is observed to be the predicted 0.02 pH units (see section 3.3). However, small protein loads cannot be used in studies of mistranslation since detection of stuttered protein is made difficult. Therefore, local distortion of the pH gradient in the vicinity of β-actin due to a high concentration of protein displaces γ-actin slightly. But since there are few if any native proteins with molecular weight 45000 within 0.5 pH units of the acid side of β-actin, species S_1-S_9 for both β- and γ-actin should be separated by the predicted ΔpH. It is assumed that for a given number of substitutions, both β- and γ-actin fall within the same area of the scan. Here it is shown that for stuttering to the acid side of β-actin, the error in making this assupmption, should it be false, is small.

Assume that there are two native species N_o and n_o, each with m substitutable sites with equal probabilities of substitution. Let the minor species n_o comprise a fraction f of the total (N_o+n_o). If n_o is on the basic side of N_o and stuttering of these species is out of phase by one substitution, then the following patterns develop:

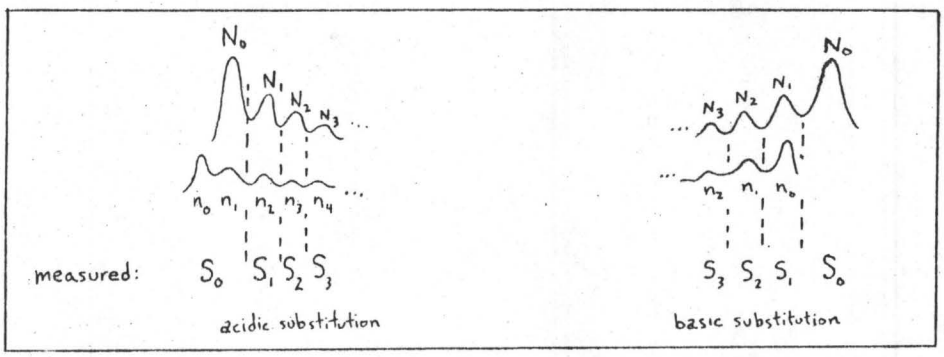

Figure 3-25

Interference of Stuttering of Two Native Species Out of Phase by One Substitution

For acidic substitutions, the calculated error frequency P'(calc) is

$$P'(calc) = \sum iS_i/m$$
$$= \sum iN_i + \sum in_i - \sum n_i)/m$$
$$= P' - f(1-(1-P')^m)/m$$

where P' is the actual error frequency. There is no analytical solution to this equation for P', but for small f and P', one can make the following approximation:

$$P' \doteq P'(calc) + f(1-(1-P'(calc))^m)/m$$

A similar derivation for stuttering to the basic side yields:

$$P' = P'(calc) - f/m$$

The maximum error in assuming no overlap is at small values of P'. For stuttering to the acidic side (away from n_o), the error is not larger than f; for stuttering to the basic side, the error is closer to 1-f. The minor actin species (γ) is on the basic side of the major species (β) and comprises about 20% of total actin. Thus, greater confidence is placed in error frequency calculations at the histidine codon in actin mRNA (stuttering to the acidic side) than at the asparagine codon (stuttering to the basic side). Application of the correction factor to error frequency calculations at the histidine codon determined in different cell strains (section 3.1) increased the error frequency estimates about 20%, but made no qualitative differences to the comparisons reported there.

3.5 Distribution of Stuttered Protein is not Binomial

Parker et al. (1978) and O'Farrell (1978) indicated that differences in the degree to which different proteins stuttered could not be accounted for entirely by their different number of substitutible sites. Furthermore, the intensity of stutter spots for a single protein did not apparently follow the binomial distribution which is expected if all sites have equal probability of substitution. Since neighboring bases are known to influence a variety of nucleic acid interactions (Uhlenbeck et al., 1970; Salser et al., 1969; Romaniuk et al., 1978), such "context effects" could be invoked to explain the deviation from the theoretical distribution of stutter spots. Another possibility is that degenerate codons and isoaccepting species of tRNA mistranslate with different efficiencies. In this section I reexamine the question quantitatively and show that these explanations are not adequate.

For a protein species S with m substitutible sites, each with equal probability of substitution P', the fraction of aberrant protein in species S_0, S_1, S_2,...,S_m follows the binomial distribution:

$$S_i = \binom{m}{i}(P')^i (1-P')^{m-i}.$$

Theoretical values of S_i were determined from this equation for certain measured values of P' and the fraction

of the total area under the scan corresponding to each stutter spot was compared to the predicted values. Figure 3-26 shows scans of actin from two cell strains at protein synthetic rates where significant degrees of stuttering were observed. The hatched bars have areas proportional to the predicted areas for γ-, β-, S_1, S_2, S_3,.... It is seen that although a qualitative agreement exists between the observed and binomial distributions, the quantitative correspondence is poor (Table 3-15). For low error frequencies, S_1 is essentially the only aberrant protein observed and agreement with the binomial distribution is expected. But at high error frequencies, more of the highly substituted species are observed than would be predicted by the model which assumes all sites have equal probability of substitution. This is just the opposite to what is expected if "context effects" or different degenerate codons and isoaccepting species lead to sites with varying degrees of mistranslation. If certain codons were mistranslated more frequently than the mean, while others less frequently, then the distribution of stutter spots would be shifted towards a greater proportion of protein with few substitutions: those "high probability" errors would over populate S_1 and to a lesser extent S_2, while the "low probability" errors would make the higher degrees of substitution less likely to be observed.

Therefore, "context" and codon- or tRNA-specific effects cannot account for the deviation of intensities of stutter spots from the binomial distribution. Alternative

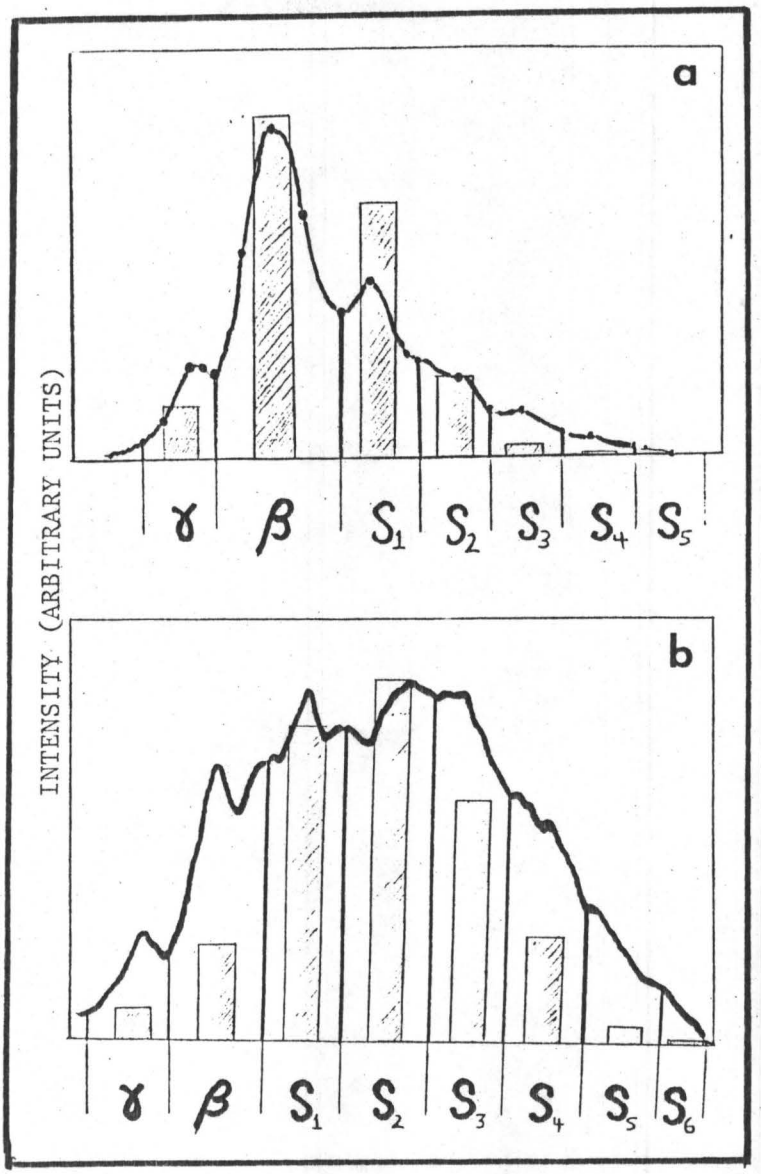

Figure 3-26

Predicted and observed intensities of stutter spots. Scans of autoradiograms of proteins synthesized during histidine starvation and the fraction of substituted sites (P') were obtained as described in section 3.1. In (a), P' = 0.0687; in (b), P' = 0.2224. The relative intensities of native and stuttered protein predicted on the basis of random substitution are shown by the bars. The predicted intensity of native actin was divided between β and γ in proportion to their observed intensities. The absolute values for the observed and predicted intensities for these scans are shown in Table 3-15.

Table 3-15

Predicted and Observed Intensity of Stutter Spots

Error Frequency P'	Species	Fraction of Total Area	
		Predicted	Observed
0.0151	γ	0.077	0.078
	β	0.80	0.80
	S_1	0.12	0.095
	S_2	0.0074	0.020
	S_3	0.0003	0.0005
0.0687	γ	0.07	0.079
	β	0.46	0.66
	S_1	0.35	0.19
	S_2	0.10	0.10
	S_3	0.017	0.05
	S_4	0.0018	0.023
	S_5	0.0001	0.002
0.2224	γ	0.023	0.045
	β	0.081	0.16
	S_1	0.27	0.19
	S_2	0.31	0.23
	S_3	0.20	0.18
	S_4	0.087	0.13
	S_5	0.013	0.06
	S_6	0.005	0.01

explanations are: (1) greater specific activity of ^{35}S-methionine in highly substituted species; (2) scanning artifact; (3) preferential degradation of species with smaller numbers of subsitutions; (4) cooperative effects such that the probability of substitution increases with the number of errors made in a single protein; (5) the error frequency increases during the course of the labeling period; (6) all ribosomes do not have the same fidelilty.

Explanation (1) is unlikely since it requires different pools of met-tRNA-met and segregation of polysomes with lower fidelity into the area of greater specific activity. Explanation (2) can account for part of the effect but not all of it. In section 3.1.4 it was found that the "total scan" method of integrating 2-D gel autoradiograms caused a small over-estimation of the error frequency due to an over-estimation of the intensity of the weaker (highly substituted) spots. There are now sophisticated scanning devices interfaced with computers (for example see Bossinger et al., 1979; Garrels, 1979) and these should be used for rigorous quantitation of 2-D gel autoradiograms. However, the scanning artifact is not as serious as the deviation from the binomial distribution at high degrees of stuttering.

The observed distribution of stutter spots is consistent with the hypothesis of random substitutions if species with only one or two errors are recognized as aberrant actin and are degraded by scavenger proteases (section 1.3.2) while

highly substituted species escape detection. However, pulse-chase experiments (section 3.2.4.1) gave no indication of turnover of stuttered protein.

Possibility (4), that cooperative effects within one growing chain lead to an increased probability of error with increased degrees of substitution requires consideration in view of the observations of Wurmbach and Nierhaus (1979) and Luhrmann et al. (1979). They found that noncognate P-site interactions influence binding of aminoacyl-tRNA to the A-site (section 1.4.2.3). This raises the possibility that an error at one codon could influence the error rate at the next. For most codons, such an effect would not alter the observed patterns of mistranslation (see section 1.4.2.3 and 3.2.5). But the presence of a pair of histidine codons (in actin at positions 87 and 88), could provide a special circumstance: a ribosome that made an error at position 87 must maintain an interaction at the P site between the noncognate peptidyl-tRNA and his-87 codon for an appreciable time while arrested at codon 88. This could conceivable increase the probability of an error at position 88. This conjecture should be tested by amino acid sequencing of a peptide containing positions 87 and 88. One would compare the conditional probability of an error at position 88, given an error at position 87, to the probability of error at position 87 or 88. An observed conditional probability greater than the latter probabilities would provide evidence for cooperativity.

Due to the gradual depletion of histidyl-tRNA-his, the protein synthetic rate decreases slightly during the course of labeling proteins in the presence of histidinol. Therefore, it is expected that the error rate at the end of the incubation will be slightly higher than at the beginning (explanation 5). The sum of binomial distributions is not itself binomial; it is shifted in the direction of the observed distribution of stutter spots. I will not give the mathematical proof of this statement, but one can confirm it by the examples given in Table 3-15. This effect is minimized by keeping the labeling period short (less than one hour). It is also possible that even without continual reduction in the synthetic rate due to depletion of histidyl-tRNA-his ribosomal fidelity decreases during the labeling period as a result of error feedback (Orgel, 1963). This requires turnover of ribosomes or some components of the translational machinery during the labeling period. If newly synthesized ribosomes contain aberrant protein, for example, one might observe an error catastrophe during prolonged amino acid starvation.

Finally, if some ribosomes under normal conditions have a lower fidelity than others, the distribution of stutter spots would be shifted from the binomial distribution as observed (explanation 6). Variations in ribosomal fidelity in diploid cells is expected if genes for ribosomal proteins and RNA are polymorphic. Furthermore, non-uniform post-transcriptional and post-translational modications of

ribosomal components will produce heterogeneity in the population of ribosomes. In this case, the distribution of errors in proteins synthesized by a given ribosome might be binomial, but the sum of distributions from all ribosomes would be non-binomial. This effect is similar to the one described above where ribosomes with low fidelity are produced from abberant protein synthesized during amino acid starvation.

Since the distribution of stutter spots is not strictly binomial, the derivation of P' from the fraction of substituted sites can only be considered as an "average" error frequency. Alterations in the inherent fidelity of the ribosome are expected to be most pronounced at very low protein synthetic rates or during prolonged amino acid starvation. Under such circumstances, the measured fraction of substituted sites may not provide an accurate estimate from which to calculate the error frequency during normal protein synthesis (section 3.2). For this reason, I attempted to measure error frequencies during acute amino acid starvation where the protein synthetic rate was linear and was not reduced to such an extent that large deviations from the binomial distribution of stutter spots were observed.

3.6 Are Translational Errors a Reasonable Explanation of Heat Labile Enzymes in Cultured Human Fibroblasts?

For lack of a convenient, direct assay of protein synthetic error rates, indirect assays of protein structure had previously been used to compare translational fidelity in different biological systems. For example, heat lability of glucose-6-phosphate dehydrogenase (G6PD) and 6-phosophogluconate dehydrogenase (6PGD) in extracts of cultured human fibroblasts were observed to increase with culture age (Holliday and Tarrant, 1972) and in certain pathological states associated with premature aging (see Goldstein, 1978). Similar findings were found with some enzymes in aging nematodes, rats and mice (see Rothstein, 1979). These observations were interpreted as evidence for the error catastrophe theory of aging, which predicts an age dependent increase in the protein synthetic error rate (Orgel, 1963). Although data such as these may reflect significant biological differences between the protein populations of young and old cells, it now seems unlikely that old cells in culture have an increased error frequency (section 3.1).

It is nevertheless useful to determine if translational errors could reasonably account for the observed populations of "altered" protein. For this purpose, we require an estimate of the error frequency from measurements of the

proportion of abnormal protein.

Suppose protein synthetic errors are random and occur at each codon with equal probability p. Then the probability P(x) that a protein of length n residues contains x errors is

$$P(x) = \binom{n}{x} p^x (1-p)^{n-x} \approx (np)^x e^{np}/x! \qquad (p \ll 1)$$

If on the average a critical number of errors x_c must accumulate before a change in the protein is evident (for example, increased heat lability), then the probability of "normal expression" P(norm.exp.) is approximated by

$$P(\text{norm.exp.}) \doteq P(x < x_c) = \sum_{z=0}^{z=x_c-1} P(z).$$

This probability is shown in figure 3-27 for various values of np.

For proteins such as G6PD and 6PGD with an average length ($n \approx 300$-500 residues), it seems unlikely that all substitutions, of any sort, anywhere in the peptide chain, would render it "abnormal", even by very sensitive assays. If all proteins with at least two errors per 300 residues were aberrant ($x_c=2$), then to explain an observation of 20% heat labile enzyme in old cells (see Holliday and Tarrant, 1972; Goldstein, 1978) np must be at least 0.8: i.e. $p \gtrsim 2 \times 10^{-3}$ (figure 3-27). If x_c is 3-5, then error frequencies approaching 0.01 must be invoked. By the same analysis, error frequencies in young cells which have less than 5% heat labile protein must be at least two fold less than error frequencies in old cells. Increased degradation of abnormal proteins (see Ballard, 1977) lowers their frequency in steady

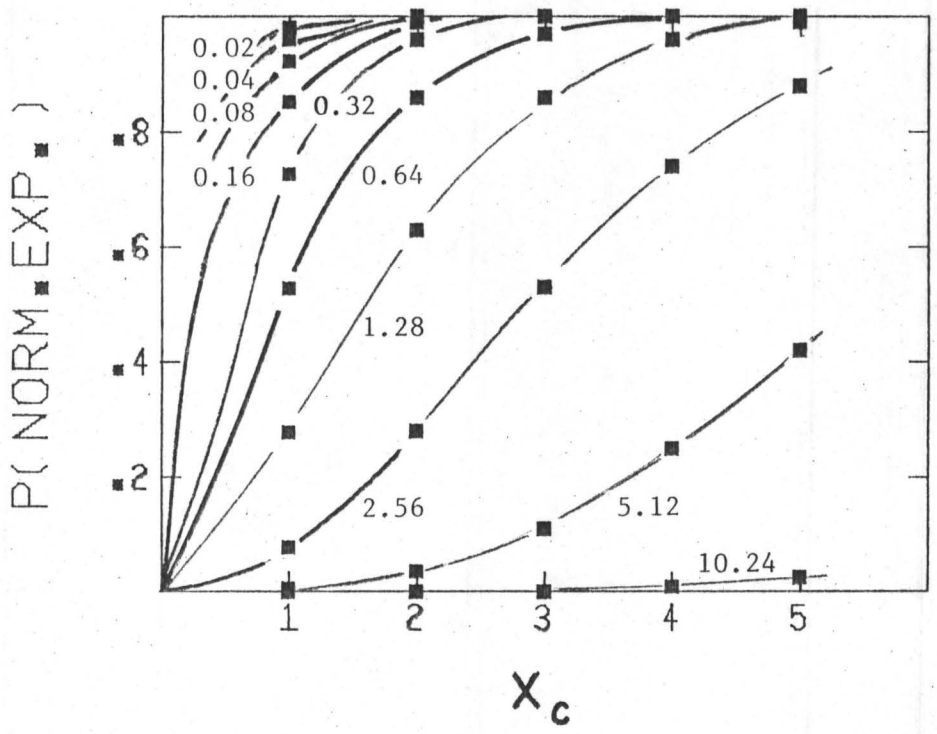

Figure 3-27

Fraction of normal protein as a function of critical number of substitutions for various error frequencies and protein sizes. The probability of normal expression P(norm.exp) is shown as a function of the critical number of substitutions (x_c) for various values of np (protein size x probability of error) from 0.02 to 10.24. The equation describing these lines is given in section 3.6.

State populations relative to native protein. Since the proteins assayed for heat lability were from steady state populations, the derived estimates of error frequencies must be considered as lower bounds. However, our direct comparisons of error rates during histidine starvation in early- and late-passage cells from young and old normal donors and from subjects with features of accelerated aging failed to indicate age-related differences (section 3.1). Extrapolation to error rates during normal protein synthesis provides an estimate of $\approx 10^{-4}$ for both "young" and "old" cultured human fibroblasts (section 3.1, 3.2).

These data suggest that the 10-20% aberrant protein detected in indirect assays of protein structure do not reflect primary sequence changes. Other direct alterations to protein, such as post-translational modifications might be involved in the age-related increase in abnormal protein (Gershon, 1979; Rothstein, 1979). However, another possibility is offered by Duncan et al. (1977). They found that the increased heat lability of G6PD in late passage fibroblasts could be accounted for by the increasing fraction of G6PD tetramer (heat labile form) compared to G6PD dimer (heat stable form). Since the conversion between dimer and tetramer is sensitive to the concentrations of reducing agents and cofactors, differences in "young" and "old" G6PD and other macromolecules detected by indirect assays such as heat lability, may simply relect changes in their tertiary structure which are secondary to more subtle changes in the

intracellular environment (Duncan et al., 1977).

4 SUMMARY AND CONCLUSIONS

This work has answered some specific questions about protein metabolism in aging cells. In addition, it has led to the development of new methods for analyzing protein degradation and mistranslation of mRNA which are of general interest in biology. Since the experimental results have been discussed in chapters 2 and 3, I will restrict this section to a brief summary and statement of the major conclusions. For simplicity of discussion, I define "old" cells as late-passage cells or cells from old, progeric, or Werner syndrome donors and "young" cells as early-passage cells from young, normal donors.

First I have shown that prior to termination of growth, the protein synthetic rate of old cells, on a per mass basis, is not significantly reduced compared to that of young cells. This is despite the fact that old cultures in exponential growth have a reduced rate of cellular replication and protein accumulation.

The second conclusion, directly related to the first, is that the net growth deficit of old cultures results from an increased rate of protein degradation and is not due to protein export or attrition of cells.

Third, proteins synthesized by old cells during

exponential growth are essentially identical to proteins synthesized by young cells when assayed by 2-D gel electrophoresis. This technique is capable of detecting single charge changes in proteins.

Fourth, induction of mistranslation by histidine starvation and analysis of proteins on 2-D gels does not uncover differences in the protein synthetic error rate between young and old cells, nor does it reveal an inverse correlation between error rate and *in vitro* lifespan. It is noteworthy that the longest lived cells, the immortal SV40-transformed lines, had error frequencies greater than their untransformed counterparts.

Thus, the increased degradation of proteins, slow net growth, and reduced lifespan of old cells are not due to increased rates of errors in protein synthesis, but rather to an apparent defect in the regulation of protein synthesis.

A major portion of this thesis has dealt with derivation of equations and construction of theories. Eddington, a famous physicist, was noted for saying "Never fully trust an observational result unless there exists at least one theory to explain it" (Penzias, 1979). This is just the converse of the way most people might phrase the relationship between data and theory. Indeed, it could be argued that data are more trustworthy without the theory, for then there is no chance of experimental bias. However, I think Eddington

meant that all data must be explicable in terms of cause-effect relationships and if some data are contrary to all existing theories, it is as reasonable to doubt the data as it is to doubt the theories. It is true that physicists tend to have more confidence in their theories than biologists: physicists propose "laws" while biologists propose "mechanisms". But I think the importance of theories in biology should not be overlooked. Although biological systems are exceedingly complex and create overwhelming latitude for exceptions, theories become extremely useful when we reduce reactions to the molecular level: one equation can summarize pages of phenomenology.

In the studies of protein turnover, I have derived equations which can be used to obtain estimates of the average rates of synthesis, degradation, and export from the approach to equilibrium method of labeling protein. Similar methods have been used previously for analysis of protein degradation during confluence (Bradley et al., 1976), but this is the first report of their application to cells in exponential growth.

In the studies of mistranslation during amino acid starvation, I have developed a theory relating protein synthesis and ribosome step time into a method of obtaining the error rate during normal protein synthesis. I have also proposed that alterations in the electrical charge of denatured actin (due to mistranslation) can be predicted from

analysis of the amino acid composition and average pK values of the charged residues.

All of these theories are consistent with the presented data. In some cases the theories are an integral part of the conclusions. However, perhaps as important, the theories must make predictions which are testable and which can be used to refute the model. In the next section, I have outlined some predictions and experiments which should be done. Results from these experiments will either strengthen, refute, or call for modifications in the theories, but in any case, they should extend our knowledge of aging and protein metabolism.

5 PROSPECTIVE

Since the riddle of aging has not been solved, there is still the prospect of making major advances in gerontology. In view of the mounting evidence against the involvement of protein synthetic errors in the aging process, other aspects of cellular metabolism should now receive greater attention. For example, new techniques for detecting changes in DNA structure, content, and expression are suited to gerontological research and may provide new insights into the mechanisms of aging. Within the field of protein metabolism, an area which suggests itself from the studies reported here is the regulation of protein turnover. Young fibroblasts regulate the number of lysosomes and the rate of protein degradation during the normal transitions from the proliferative (low cell density) to the nonproliferative (high cell density) state. Since old fibroblasts have reduced growth rates, elevated degradation rates, and increased numbers of lysosomes (section 2), it is possible that old cells have abnormal regulation of the growth transition and are "fixed" in the nonproliferative state. The defect cannot be quite that simple since it is known that young cells kept quiescent for extended periods do not undergo the same decline that continuously dividing cells experience; mitotically young but chronologically old cells maintain their proliferative potential (Dell'Orco et al.,

1973; Goldstein and Singal, 1974; Harley and Goldstein, 1978). It is possible that a primary defect in regulation of protein turnover in old cells causes the aging phenotype, but until further information is available on the normal control of protein degradation, no direct test for this hypothesis can be made. If the regulatory mechanism were known, it could be assayed during aging in vitro and in vivo, but even then, it would be difficult to distinguish a secondary from a primary defect. Only if correction of the defect increased lifespan could a strong case be made for the primary role of the control of protein turnover in senescence.

Induction of synthesis of aberrant proteins by amino acid starvation in cultured cells and the detection of these proteins by 2-D gel electrophoresis is a powerful technique with great potential in biological studies. Although all available data are consistent with the hypothesis that aberrant proteins are products of ribosomal errors in translating mRNA, more direct proof by amino acid sequencing is still required. If the proposed substitutions from several different starvation conditions are confirmed by sequencing, there could be little doubt that these errors occur as proposed. This work is being conducted by J.W.Chamberlain in Dr. C.P.Stanners laboratory. On the strength of the indirect evidence for this theory (section 1.5.3), I have assumed that stuttering reflects mistranslation.

The comparisons reported here indicate that old cells, as defined by the *in vitro* model of cellular senescence, do not have increased rates of mistranslation. However, other "old" cells might also be assayed. For example, post-replicative cells, such as neurones, from young and old donors could be examined. In addition, cells from different tissues in different mammalian and nonmammalian species could be assayed and compared to determine if correlations exist with respect to origin of the cell. Our data indicate some species variability, but no generalization, such as a correlation of error frequency with the lifespan of the species, could be found. It would be of interest to test a larger collection of normal cell types from various species of diverse lifespans to explore this notion further.

The finding that SV40-transformed human cells have increased degrees of stuttering suggests that mistranslation may be associated with transformation in general. Our analysis of other cell types found some support for the relationship between mistranslation and SV40-transformation, but other types of transformation have not shown this trend. Part of the difficulty in this study is the unavailability of appropriately matched transformed/untransformed pairs. Since normal cells display a wide range of stuttering frequencies, it is not possible to relate differences in error frequencies to transformation unless the control cells are essentially identical in all other respects. Where differences in error frequency do appear, it will nevertheless be interesting to

determine (1) the cause of the difference and (2) its physiological significance, if any.

Is increased mistranslation related to expression of certain viral genes? Studies with a temperature sensitive mutant of SV40-transformed human cells, analogous to the studies reported here with RSVts-infected chick cells, would be helpful in answering this question.

Direct assays of mutation rates could be conducted in cultured cells under normal and starved conditions to determine if translational errors affect the fidelity of DNA replication. Leaky expression of repressed genes could also be examined.

Nonphysiological conditions such as altered pH, temperature, ionic strength, or the presence of various toxic agents could be rapidly tested in intact cells for their effect on the fidelity of protein synthesis by the stuttering assay. It is possible that part of the deleterious effects of some of these conditions results from the induction of synthesis of abnormal protein.

Effective amino acid starvation should be readily accomplished in cell free extracts in vitro . If the fidelity and duration of protein synthesis are adequate, analysis of stuttered protein in vitro may provide a better system for testing some of the predictions of the stuttering model. For example, there is no means of achieving extreme

serine starvation in intact mammalian cells. Serine starvation should lead to arginine substitution at certain codons with stuttering to the basic end of 2-D gels. It may be possible to test this prediction *in vitro*. Furthermore, effects of starvation for more than one amino acid may be easier to interpret *in vitro* than *invivo*. What happens, for example, when the amino acid which is most likely to be substituted is also removed during amino acid starvation? If third position errors are most likely, can first position errors be induced by such techniques? Asparagine starvation produces basic stutter spots, supposedly due to lysine substitution. If lysine is limiting, does the ribosome then accept aspartyl-tRNA-asp at asparagine codons by first position error (see figure 1-6), thus producing stuttering towards the acidic end of the gel?

The *in vitro* system also provides a method for studying the causes, at the molecular level, for differences in stuttering between cell lines or differences produced by nonphysiological conditions. Does the increased stuttering of SV40-transformed human cells reside in their tRNA, ribosomes, or soluble factors? This question might be answered in reconstruction experiments *in vitro* where components from different systems are mixed.

Stuttering on 2-D gels can be used to study degradation of abnormal proteins. Pulse-chase analyses reported here have indicated that native and substituted actin species are

stable during the course of the experiments (1-2 hours). However, overall degradation was accelerated during amino acid starvation and other proteins should be analyzed quantitatively in human fibroblasts and other cell types. Proteolytic degradation of aberrant protein may be specific for certain types of alterations or certain classes of proteins.

The relationship betwen step time of the ribosome at relevant codons and protein synthetic rate during amino acid starvation needs experimental verification. This may not be possible with present techniques and even indirect evidence may be difficult to obtain in intact cells where a heterogeneous population of mRNAs are translated. Specialized cells which translate predominantly one mRNA (for example reticulocytes) might be used to study the effects of amino acid starvation on the kinetics of translation, but caution must be exercised since these types of cells might possess unique controls of protein synthesis. Cell-free extracts from an "average" cell programmed with a single natural message of known sequence may be more useful. The distribution of nascent chains during amino acid starvation could be analyzed by chromatographic or electron microscopic studies and used to determine whether ribosomes pause and queue behind the relevant codons (or clusters of relevant codons) as predicted by the computer simulations of protein synthesis (section 3.2).

Transit time measurements and assays of the number of ribosomes on mRNA could be used to test the predictions of the model. In preliminary experiments, I encountered difficulties in measuring transit times during amino acid starvation (unpublished data). Conditions for isolating nascent peptides may not be the same under starvation conditions as they are during normal protein synthesis and premature termination and increased degradation of proteins may interfere with transit time measurements in some cell strains.

Analysis of nascent chains on 2-D gel electrophoresis may prove to be a powerful technique for testing the computer model of protein synthesis during amino acid starvation. I know of no attempts other than preliminary experiments of my own (unpublished) to resolve nascent chains by 2-D gel electrophoresis. A short pulse period could be used to label predominantly nascent peptides. Hydrolysis of the peptidyl-tRNA bond and 2-D gel electrophoresis should reveal a trail of peptides from the native spot which traverses a non-linear path towards lower molecular weight as predicted by the amino acid composition of each peptide of a given size. Under normal conditions, a uniform distribution of ribosomes on the mRNA will give a trail of peptides whose intensity on autoradiograms will be proportional to their specific activity. During amino acid starvation, the trail of peptides is expected to reveal a series of "spots" corresponding to sites where ribosomes pause on the mRNA. It

is possible that analysis at various time intervals under these conditions or in pulse-chase experiments could give extimates for the variable elongation rates of ribosomes along the message. Such experiments may have to be resticted to specialized systems which synthesize only a few proteins.

These prospects for further work on aging, protein synthesis, and mistranslation in cultured human cells are exciting areas of research for gerontologists and molecular biologists. Hopefully, continued application of new techniques and ideas will lead to the solution of one of our oldest questions: why do we age?

6 APPENDICES

6.1 A Note on Computer Programming: IFTRAN-2, FORTRAN EXTENSION FOR STRUCTURED PROGRAMMING

The principle programming language used in these studies was IFTRAN-2 (Fleming, 1977). IFTRAN is a preprocessor of FORTRAN statements (Cress, Dirksen & Graham, 1970) containing certain extended control types. The preprocessor generates a standard FORTRAN program for input to the FORTRAN compiler. The advantage of IFTRAN programming is the structuring of the code into readily recognized blocks. This aids the development of programs in which the logic flow is apparant and reduces the time required to "de-bug" and test new programs. The finished programs are more reliable and are more readily modified. All programs illustrated in these appendices were written with the IFTRAN-2 extensions to standard FORTRAN and were executed on a CDC-6400 computer.

6.2 Computer Program for Analysis of Scans of Autoradiograms

Coordinates assigned to scans of the actin region of autoradiograms were analysed by the program shown in figure 6-1a. The abbreviated documentation in this figure describes the function of the program. Areas were calculated by the trapezoidal rule:

$$\int_a^b f(x)dx \doteq (b-a) \times (f(a) + f(b))/2$$

Simpsons's rule (see Shampine & Allen, 1973) gives a better approximation but was not appropriate for this analysis for two reasons. First, points on the scans were positioned roughly at points of inflection and points of local minima and maxima. Thus, the cumulative error of consecutive line segments was nearly zero. Simpson's rule, on the other hand, is most accurate when at least one additional point lies between each point of inflection and a local minimum or maximum. Second, fractional areas were often adequately described by two points only. The trapezoidal rule needs only the two boundry points whereas Simpson's rule requires a third intermediate point.

The output data from a typical set of input cards are shown in figure 6-1b.

a

```
NO. (..)=NESTING DEPTH                    GENERAL RESEARCH CORPORATION----IFTRAN-2    79/10/

          PROGRAM CBH (INPUT=7001B,OUTPUT=7001B,TAPE5=INPUT,TAPE6=OUTPUT)
      C
      C   DOCUMENTATION...C.B.HARLEY, JAN.4 1979
      C
      C   THIS IS A SPECIALIZED PROGRAM FOR ANALYSIS OF DATA TAKEN FROM QUANTITATIVE
      C   SCANS OF AUTORADIOGRAMS IN STUDIES OF HIGH LEVEL MISTRANSLATION (PNAS 75 1095
      C   (1978)). INPUT DATA ARE...
      C
      C      N        NUMBER OF (X,Y) DATA POINTS (N LESS THAN 40).
      C      YSCALE   O.D. UNITS/UNIT OF Y AXIS
      C      XSCALE   PH UNITS/UNIT OF X AXIS.  NOTE, SCANS OF AUTORADIOGRAMS WERE DONE
      C               AT A 5 TO 1 RATIO, I.E. XRAW=1 UNIT=1CM ON SCAN = 0.2 CM ON AUTO-
      C               RADIOGRAM.
      C      XBETA    X-COORDINATE OF BETA-ACTIN
      C      HEADER   CHARACTER STRING DESCRIBING INPUT DATA (CODED)
      C      XRAW(40)  X COORDINATES OF RAW DATA
      C      YRAW(40)  Y COORDINATES OF RAW DATA
      C      C(11)    THE INDICES FOR VECTOR X BETWEEN WHICH VALUES PARTIAL AREAS ARE
      C               TO BE CALCULATED (SEE BELOW).
      C
      C   WEDGE NUMBER (WEDGE = 1 2 OR 3) SETS YSCALE
      C   YSCALE, XSCALE AND XBETA ARE USED TO CONVERT INPUT (XRAW,YRAW) INTO ABSOLUTE
      C   VALUES (X,Y) SUCH THAT AREAS HAVE UNITS (O.D. X PH). PH IS RELATIVE TO THE PI
      C   OF BETA-ACTIN (NEGATIVE VALUES DENOTE MORE ACID PH, POSITIVE VALUES, MORE
      C   BASIC PH).
      C   N=0 IS THE FLAG TO STOP COMPUTATION.
      C   THE ORIGIN FOR XRAW IS ARBITRARY, BUT THE YRAW ORIGIN MUST BE THE BASELINE
      C   OF THE SCAN.  POINTS START AT THE BASIC END OF GAMMA-ACTIN AND PROCEED
      C   THROUGH TO THE ACID END OF THE STUTTERED ACTINS S1, S2,...  CUT POINTS C(11)
      C   INDICATE THE INDEX OF THE X COORDINATE BETWEEN GAMMA- AND BETA-ACTIN, BETA-
      C   ACTIN AND S1, S1 AND S2, ETC.  THE AREAS UNDER THE CURVE REPRESENTING EACH
      C   OF THESE PROTEINS IS CALCULATED AS DESCRIBED...
      C
      C   VARIABLE CA IS THE CUMULATIVE AREA. CAL= LAST CUMULATIVE AREA AT A CUT POINT.
      C   PARTIAL AREAS AREA(AI) DELINEATED BY THE CUT POINTS C(I) ARE CALCULATED
      C   BETWEEN X(0) AND X(C(1)), X(C(1)) AND X(C(2)), ETC.  AI IS THE AREA INDEX
      C   INDICATING HOW MANY PARTIAL AREAS HAVE BEEN CALCULATED. THUS AREA(1) IS
      C   GAMMA-ACTIN, AREA(2) IS BETA-ACTIN, AREA(3) IS S1 ETC.  WHEN ALL AREAS HAVE
      C   BEEN CALCULATED, AI FRACTIONAL AREAS FAREA(K) ARE COMPUTED.
      C   NEXT, A VARIABLE GLNS, PROPORTIONAL TO THE NUMBER OF GLN SUBSTITUTIONS PER
      C   ACTIN IS CALCULATED WHERE S1 IS ASSUMED TO HAVE ONE SUBSTITUTION, S2 TWO ETC.
      C   FGLNS=GLNS/9 IS THE OVERALL FRACTION OF SUBSTITUTED SITES (SINCE ACTIN
      C   CONTAINS 9 HIS SITES).  FABER IS THE FRACTION OF ABERRANT PROTEIN SYNTHESIZED
      C   I.E. 1-FAREA(1)-FAREA(2)-0.045 (BKG OF 0.045 SUBSTRACTED)
      C
      C   PROBABILITY OF SUBSTITUTION IS CORRECTED FOR BACKGROUND OF 0.005
      C
      C
      C   FOR FURTHER DETAIL CONCERNING THE PROGRAM OR INPUT SPECIFICATIONS, CONSULT
      C   C.B.HARLEY.
      C
      C
          DIMENSION X(40),Y(40),AREA(11),FAREA(11),XRAW(40),YRAW(40)
          INTEGER AI,C(11),HEADER(8),ACTINS(10),WEDGE
          KPAGE=0
      C
      C   OBTAIN DATA AND SCALE TO ABSOLUTE UNITS
      C
          READ9,ACTINS
        9 FORMAT(8A10/2A10)
          READ1,HEADER
        1 FORMAT(8A10)
          READ*,N, WEDGE,XSCALE,XBETA
          WHILE(N.NE.0)
      ( 1)     IF(WEDGE.EQ.1)YSCALE=0.01916
      ( 1)     IF(WEDGE.EQ.2)YSCALE=0.0333
      ( 1)     IF(WEDGE.EQ.3)YSCALE=0.1924
      ( 1)     READ*,(XRAW(I),I=1,N),(YRAW(I),I=1,N),C
      ( 1)     DO(I=1,N)
      ( 2)        X(I)=XSCALE*(XRAW(I)-XBETA)
      ( 2)        Y(I)=2.666*ALOG(2.666/(2.666-YRAW(I)*YSCALE))
      ( 1)     ENDDO
      ( 1) C
      ( 1) C   INITIALIZE
      ( 1) C
      ( 1)     GLNS=0.
      ( 1)     CA=0.
      ( 1)     CAL=0.
      ( 1)     AI=0
      ( 1)     DO(I=2,N)
      ( 2)        CA=CA+(X(I)-X(I-1))*(Y(I)+Y(I-1))/2.
      ( 2)        IF(I.EQ.C(AI+1))
      ( 3)           AI=AI+1
      ( 3)           AREA(AI)=CA-CAL
      ( 3)           CAL=CA
      ( 2)        ENDIF
      ( 1)     ENDDO
      ( 1)     DO(K=1,AI)
      ( 2)        FAREA(K)=AREA(K)/CA
      ( 1)     ENDDO
      ( 1)     DO(K=3,AI)
      ( 2)        GLNS=GLNS+FLOAT(K-2)*FAREA(K)
      ( 1)     ENDDO
      ( 1)     FABER=1-FAREA(1)-FAREA(2)-.045
      ( 1)     FGLNS=GLNS/9.
      ( 1) C
      ( 1) C   SUBTRACT A BKG OF 0.005 FROM FGLNS
      ( 1) C
      ( 1)     PMBC=FGLNS-0.005
```

Figure 6-1 Computer program for analysis of scans of autoradiograms.

Figure 6-1 continued

```
          ( 1)     C
          ( 1)     C   OUTPUT FORMAT
          ( 1)     C
 54    40 ( 1)           IF(MOD(KPAGE,2).EQ.0)PRINT 111
 55    41 ( 1)       111 FORMAT(1H1)
 56    42 ( 1)           KPAGE=KPAGE+1
 57    43 ( 1)           PRINT2,HEADER
 58    44 ( 1)         2 FORMAT(    /    ,10X,'HIGH LEVEL MISTRANSLATION.....',5X,8A10/10X,25
                         1('*')//)
          ( 1)           PRINT3,XSCALE,YSCALE
 60    45 ( 1)         3 FORMAT(     5X,'XSCALE=',F6.4,' PH UNITS/UNIT XR'//5X,'YSCALE=',F6.4,'
                         1OD UNITS/UNIT YR'//)
          ( 1)           IF(N.LE.14)
 63    47 ( 1)
 65    48 ( 2)              PRINT4,N,(XRAW(I),I=1,N),N,(YRAW(I),I=1,N)
 66    49 ( 2)         4    FORMAT(5X,'XR=',=F7.2/5X,'YR=',=F7.2/)
 67    50 ( 2)              PRINT5,N,(X(I),I=1,N),N,(Y(I),I=1,N),AI,(C(I),I=1,AI)
 68    51 ( 2)         5    FORMAT(5X,' X=',=F7.4/5X,' Y=',=F7.4/ 5X,' C=',=I3)
 69    52 ( 2)           ELSE
 71    53 ( 2)              N14=N-14
 72    54 ( 2)              PRINT7,(XRAW(I),I=1,14),N14,(XRAW(I),I=15,N),(YRAW(I),I=1,14
          ( 2)             1),N14,(YRAW(I),I=15,N)
 74    55 ( 2)         7    FORMAT(5X,'XR=',14F7.2/8X,F7.2/5X,'YR=',14F7.2/8X,F7.2/)
 75    56 ( 2)              PRINT8,(X(I),I=1,14),N14,(X(I),I=15,N),(Y(I),I=1,14),N14,(Y
          ( 2)             1(I),I=15,N),AI,(C(I),I=1,AI)
 77    57 ( 2)         8    FORMAT(5X,' X=',14F7.4/8X,F7.4/5X,' Y=',14F7.4/8X,F7.2 /5X,' C=',=
          ( 2)             1I3/)
 78    58 ( 1)           ENDIF
 79    59 ( 1)           PRINT6,AI,(ACTINS(I),I=1,AI),AI,(AREA(I),I=1,AI),AI,(FAREA(I),I
          ( 1)             1=1,AI),FABER,FGLNS,PMBC
 81    60 ( 1)         6    FORMAT(    / 11X,=A10//5X,' AREA ',=(2X,F6.4,2X)/5X,'FAREA ',=(2X,F6
          ( 1)             1.4,2X) ///5X,'FRACTION OF ABERRANT PROTEINS = ',F6.4/ 5X,'FRACTION OF
          ( 1)             1 SUBSTITUTED SITES = ',F6.4 /5X,'FSS CORRECTED FOR BKG          = ',F6
          ( 1)             1.4////)
          ( 1)     C
          ( 1)     C   OBTAIN A NEW SET OF INPUT DATA
          ( 1)     C
 85    61 ( 1)           READ1,HEADER
 86    62 ( 1)           READ*,N,WEDGE, XSCALE,XBETA
 87    63              ENDWHILE
 90    64              STOP
 91    65              END
```

b

```
     HIGH LEVEL MISTRANSLATION.....      H16-2  H16 WI38SV40 GEL 15 0 MM
     ****************************

XSCALE= .0404 PH UNITS/UNIT XR
YSCALE= .0833 OD UNITS/UNIT YR

XR=    2.00    2.80    3.40    3.70    4.20    5.00    5.80    7.20    9.20   11.00   13.00
YR=    1.40    4.00    7.00    6.80   11.00   17.20    9.00    1.25     .30     .20    0.00

 X= -.1212 -.0889 -.0646 -.0525 -.0323 0.0000  .0323  .0889  .1637  .2424  .3232
 Y=  .1192  .3559  .5580  .6368 1.1227 2.0553  .8803  .1062  .0251  .0167 0.0000
 C=  4  8  9 10 11

      GAM-ACTIN BETA-ACTIN  S1-ACTIN  S2-ACTIN  S3-ACTIN

 AREA   .0278     .1445     .0053     .0015     .0007
FAREA   .1547     .3036     .0295     .0085     .0038

FRACTION OF ABERRANT PROTEINS = -.0033
FRACTION OF SUBSTITUTED SITES =  .0064
FSS CORRECTED FOR BKG, GAMMA  =  .0019



     HIGH LEVEL MISTRANSLATION.....      H16-1-2                    WI38SV40 GEL 19
     ****************************

XSCALE= .0303 PH UNITS/UNIT XR
YSCALE= .0833 OD UNITS/UNIT YR

XR=    1.00    2.10    2.90    3.30    3.50    4.20    5.00    6.00    7.00    7.80    8.80    9.00   10.20   11.00
      12.00   13.00   15.00   15.90
YR=    0.00    1.10    2.60    2.70    2.40    6.00    9.70    7.00    4.20    3.10    3.00    2.40    1.50
       1.30     .90     .20    0.00

 X= -.1212 -.0879 -.0636 -.0515 -.0455 -.0242 0.0000  .0303  .0606  .0848  .1151  .1212  .1576  .1818
      .2121  .2424  .3030  .3272
 Y= 0.0000  .0932  .2259  .2350  .2078  .5535  .9626  .6580  .3750  .4827  .2716  .2624  .2078  .1280
       .11     .08     .02    0.00
 C=  5  9 12 14 16 17 18

      GAM-ACTIN BETA-ACTIN  S1-ACTIN  S2-ACTIN  S3-ACTIN  S4-ACTIN  S5-ACTIN

 AREA    .0096     .0667     .0234     .0126     .0064     .0028     .0002
FAREA    .0785     .5476     .1926     .1037     .0529     .0231     .0017

FRACTION OF ABERRANT PROTEINS =  .3289
FRACTION OF SUBSTITUTED SITES =  .0733
FSS CORRECTED FOR BKG, GAMMA  =  .0833
```

6.3 Generation of a Random Amino Acid Sequence with a Specified Amino Acid Composition

To relate high level mistranslation during amino acid starvation to the error frequency during normal protein synthesis, it was necessary to determine the relationship between step time at the relevant codon and the protein synthetic rate (Section 3.2). This relationship varies from one protein to another depending on its amino acid sequence and therefore to determine if actin was representative of overall protein, I analyzed several hypothetical sequences in addition to the actin mRNA sequence.

The position of histidine or asparagine residues were of most interest. In some cases, a table of random numbers (Selby, 1967) was used to determine these positions. However, for general analysis of protein synthesis under various conditions, it is useful to have a complete, random amino acid sequence for a protein of length M residues with a specified amino acid composition. The program shown in figure 6-2a was written for this purpose. M integers are sequentially selected at random on the interval $[1,M]$. If the integer has been previously chosen, the closest unchosen integer, alternately above or below the selected integer, is found. The interval $[1,M]$ is subdivided according to the frequencies F(i), i= 1,2,3,...,20, and the amino acid to which the integer corresponds is appended to the sequence.

```
      PROGRAM TST (INPUT,OUTPUT,TAPE5=INPUT,TAPE6=OUTPUT)
C     PROGRAM TO GENERATE A   M-RESIDUE PROTEIN WITH A RANDOM SEQUENCE AND THE
C     SPECIFIED AMINO ACID COMPOSITION.
C
C     VARIABLES...
C
C     AAMN(20)      20 CHARACTER VECTOR OF THE AMINO ACIDS USING 1-LETTER ABBREV.
C     F(20)         THE MOLAR FREQUENCIES OF THE 20 AMINO ACIDS.
C     RP1(  M)      RANDOM PROTEIN 1.  THE PROTEIN REQUIRED.
C     S(  M)        THE SEQUENCE 1,2,3,...,M
C     FLAG          LOGICAL VARIABLE--SEE BELOW
C
C     METHOD        SELECT A RANDOM NUMBER N BETWEEN 1 AND M.    IF THE NUMBER HAS
C     BEEN PICKED BEFORE, FIND THE CLOSEST AVAILABLE NUMBER BELOW (ABOVE) THE
C     SELECTED NUMBER IF FLAG=.TRUE.(.FALSE.).
C     DIVIDE THE SEQUENCE S INTO 20 PARTS...
C     1...M  F(1),  M  F(1)+1...M  (F(1)+F(2)), ETC...    IF N FALLS IN THE ITH
C     BLOCK, INSERT AAMN(I) ONTO THE RP1 SEQUENCE
C
      INTEGER RP1(500),AAI,AAMN(20)
      DIMENSION F(20)
      READ1,AAMN
    1 FORMAT(20A1)
      READ2,F
    2 FORMAT(16F5.3/4F5.3)
      M=374
      DO(K=1,3)
         CALL RANPRO(  M,F,AAMN,RP1,S)
C
C     OUTPUT
C
         PRINT12,M
   12    FORMAT(1H1////10X≠RANDOM PROTEIN OF LENGTH≠I4//////)
         PRINT11,(AAMN(I),F(I),I=1,20)
   11    FORMAT(5X≠COMPOSITION≠//20(10XA1,3X,F5.3/))
         PRINT10
   10    FORMAT(///5X≠SEQUENCE:≠//)
         PRINT3,(RP1(I),I=1,M)
    3    FORMAT(5X,5(10A1,2X)/)
      ENDDO
      STOP
      END


      SUBROUTINE RANPRO(M,F,AAMN,RP1,S)
      INTEGER RP1(M),S(M),AAI,AAMN(20)
      DIMENSION F(20)
      LOGICAL FLAG
      FLAG=.FALSE.
      DO(J=1,M)
         S(J)=J
      ENDDO
C
C     SELECT A NUMBER, WITHOUT REPLACEMENT BETWEEN 1 AND M
C
      DO(J=1,M)
         N=IRG(1,M)
         IF(FLAG)
            WHILE(S(N).EQ.0)
               N=N-1
               IF(N.EQ.0)N=M
            ENDWHILE
         ELSE
            WHILE(S(N).EQ.0)
               N=N+1
               IF(N.EQ.M+1)N=1
            ENDWHILE
         ENDIF
         FLAG=.NOT.FLAG
         S(N)=0
C
C     N HAS BEEN DETERMINED.  NOW DETERMINE WHICH AA THIS CORRESPONDS TO.
C
         AAI=0
         SFI=0.
         UNTIL(FLOAT (M) *SFI.GE.FLOAT(N)-.001)
            AAI=AAI+1
            SFI=SFI+F(AAI)
         ENDUNTIL
         RP1(J)=AAMN(AAI)
      ENDDO
      RETURN
      END


      FUNCTION IRG(M,N)
C     RANDOM NUMBER GENERATOR TO PROVIDE AN INTEGER  BETWEEN M AND N.
C     LINEAR CONGRUENTIAL METHOD OF GENERATING PSEUDO-RANDOM NUMBERS.
C
      DATA ID,IY/2147483548,568731/
      IY=MOD(15625*IY+22221,ID)
      IRG=M+(N-M+1)*IY/ID
      RETURN
      END
```

Figure 6-2 Computer program for generating a random amino acid sequence with a specified composition.

6.4 Computer Simulation of Protein Synthesis During Amino Acid Starvation

The program shown in figure 6-3a was written to theoretically analyze the kinetics of ribosome movement on mRNA during amino acid starvation. The prime purpose of the simulations was to relate protein synthetic rate to the increased step time of ribosomes at codons corresponding to the starved amino acid. The logic flow of the program is described in section 3.2 and further illustrated by the documentation associated with the program (comment (C) statements).

The UNTIL construct "UNTIL(NM.EQ.0)...END UNTIL" reads data cards specifying the mRNA length and position of the modulator codons. Any number of the translational parameters can be varied as desired with appropriate "DO" constructs. For each input mRNA, the simulations are generated for all specified variations in the translational parameters. For example, in the program illustrated (figure 6-3a), all parameters are held constant except TP, the mean "defined" step time of the ribosome at modulator codons (i.e. $t'_{s,x}/t_{s,x}$).

The DO construct "DO(TP=50,150,50)...ENDDO" generates three simulations of protein synthesis as the mean value of TP takes on values 50,100,150. In each case TP is a random variable uniformly distributed about the mean value plus or minus 20%. At the beginning of each simulation, one ribosome is initiated at the first codon and iteration continues until

NR=4 ribosomes have completed synthesis of the mRNA. The input mRNA for the simulation shown was actin. The results of the simulation are shown in figure 6-3b.

Figure 6-3. Program to simulate protein synthesis.

a

```
FTN CD.
NUMBER  NO.  (..)=NESTING DEPTH
     1    1              PROGRAM CPH(INPUT=7018,OUTPUT=7018,TAPE5=INPUT,TAPE6=OUTPUT)
C
C    PROGRAM TO COMPUTE PROTEIN SYNTHETIC RATE ON AN    MRNA AS A FUNCTION OF STEP
C    TIMES AT CODONS. PROGRAM ALLOWS FOR FLEXIBLE MODELING OF TRANSLATION
C    PARAMETERS AND IS PARTICULARLY SUITABLE FOR ANALYSIS OF PROTEIN SYNTHETIC
C    RATE, RIBOSOME QUEUING AND POLYSOME DISTRIBUTIONS DURING A.A. STARVATION.
C
C    R(90 ,2) IS A MATRIX REPRESENTING 90  RIBOSOMES.
C
C    R(K,1)  GIVES THE POSITION OF RIBOSOME K ON THE MRNA FOR (1.LE.R(K,1).LE.NM)
C    R(K,1)=0 DENOTES RIBOSOME K HASN"T INITIATED YET
C    R(K,1)= NM+1 DENOTES RIBOSOME HAS COMPLETED MRNA TRANSLATION
C    R(K,2) = THE LENGTH OF TIME (TIME UNITS) RIBOSOME K MUST WAIT ON CODON R(K,1)
C    R(K,2) = 1 IF R(K,1) IS NOT A MODULATOR CODON (SEE CDOS BELOW)
C    R(K,2) AT MODULATOR CODONS (SEE CDOS) IS A RANDOM VARIABLE WITH MEAN TP AND
C    UNIFORM DISTRIBUTION OVER THE RANGE (MMD,MPD)
C
C    RIBOSOME K ON CODON R(K,1) CAN MOVE TO THE NEXT CODON IF IT MEETS 2 CRITERIA.
C    1.  IT HAS BEEN ON CODON R(K,1) FOR A TIME AT LEAST EQUAL TO R(K,2)
C    2.  RIBOSOME K-1 IS    .GT.    D CODONS FURTHER DOWN THE MESSAGE.
C
C    VARIABLES
C
C    NM...THE NUMBER OF CODONS IN THE MRNA
C    NC...THE NUMBER OF CODONS FOR THE STARVED A.A. IN THE MRNA
C    CDOS...THE POSITION OF THE CODONS FOR THE STARVED A.A.
C    RESID...HEADER (NAME OF PROTEIN OR IDENTIFYING LABEL)
C    IV(IVC)...THE TIME RIBOSOME IVC INITIATED TRANSLATION
C    TP...MEAN R(K,2) AT MODULATOR CODONS
C    STOC...R(K,2) AT NON-MODULATOR CODONS (STEP TIME AT OTHER CODONS)
C    MMD,MPD...DEFINE RANGE OF R(K,2) AT MODULATOR CODONS
C    D...MINIMUM DISTANCE (IN CODONS) ALLOWED BETWEEN RIBOSOMES
C    FIRST...ROW INDEX OF THE RIBOSOME CLOSEST TO THE 3" END OF THE MRNA
C    LAST...  ROW INDEX OF THE RIBOSOME CLOSEST TO THE 5" END OF THE MRNA
C    KREVIS...IF KREVIS IS 1 KI=4 IS REVISED  WHEN NO. OF RIBOSOMES ON MESSAGE
C             IS TOO LOW OR TOO HIGH
C    KI=4...10000    * THE PROBABILITY OF INITIATING (PER UNIT TIME)
C    TERM...TIME REQUIRED TO TERMINATE FROM THE LAST CODON (RELEASE TIME)
C    I...  THE I.E. THE ITERATION INDEX
C    ILP...TIME OF TERMINATION OF THE PREVIOUS RIBOSOME
C    TT...TRANSIT TIME OF THE RIBOSOME
C    RN...NORMAL PROTEIN SYNTHETIC RATE, I.E.  1/(D+1/KI)
C    RP...THE INSTANTANEOUS SYNTHETIC RATE IN CHAINS COMPLETED PER TIME UNIT
C
     2    2              INTEGER D,FIRST,R( 90,2),FIRSTF,STOC,  SDIST(15,870),SDIST2(90,2)
                        1,TP,CDOS(20),RESID(30),IV(90)
C
C    INITIALIZE
C
                        KREVIS=0
                        NP=4
                        TP=100
                        STOC=1
                        D=13
                        KI=.5E-6
                        ENE.07333333
                        READ 200, NM,NC,RESID
   200 FORMAT(2I5,7A1)
                        READ 201,(CDOS(K),K=1,NC)
   201 FORMAT(20I4)
                        UNTIL(NM.EQ.0)
                            NP1=NP+1
                            DO(TP=50,150,50)
                                EM=.5
                                MMD=IFIX(EM*TP)
                                MPD=IFIX((2.0-EM)*TP)
                                ILP=0
                                PRINT200,RESID,NM,NC,NC,(CDOS(K),K=1,NC)
   200                          FORMAT(1H1///5X30A1,5X,I3" CODONS IN TOTAL,"I2" MODULATOR CO
     1DONS AT POSITIONS"// 3X(I4,/))
                                PRINT2, D,FLOAT(KI=-)/10000.,STOC,TP,(1.-EM)*TP
                    2           FORMAT(/5X"D    "I3/5X"KI  "F9.6/5X"STOC" I3/5X"TP  "I3"("F4.
                     11")"/)
                                PRINT4
                    4           FORMAT(" RIBOSOME INIT  TERM   TT   N     RP    RP/RN  RN/R
                     10"/)
C   INITIALIZE
                                R1S=0.
                                R2S=0.
                                R3S=0.
                                R4S=0.
                                R5S=0.
                                R6S=0.
                                IVC=1
                                IV(1)=1
                                DO(KKK=1,NP)
                                    DO(KL=1,NM)
                                        SDIST(KKK,KL)=0
                                    ENDDO
                                ENDDO
                                I=0
                                FIRST=1
                                LAST=1
                                R(1,1)=1
                                R(1,2)=STOC
                                R(NP,1)=0
C
C   REITERATE UNTIL  NP RIBOSOMES HAVE TRANSLATED THE MESSAGE.
C
                                UNTIL (R( NP,1).EQ.NM+1)
C
C   LET SDIST(KKK,KL) GIVE A MEASURE OF THE AMOUNT OF TIME CODON KL IS
C   OCCUPIED BY RIBOSOME KKK.  AT THE END OF EACH TIME INTERVAL, SDIST(KKK,KL)
C   INCREMENTED BY ONE IF A RIBOSOME IS AT CODON KK.
C
                                    FIRSTF=MINI(NP,LAST)
                                    IF(FIRST.LE.FIRSTF)
                                        DO(KKK=FIRST,FIRSTF)
                                            SDIST(KKK,R(KKK,1))=SDIST(KKK,R(KKK,1))+1
                                        ENDDO
                                    ENDIF
```

Figure 6-3a, continued

```
C
C  ALLOW THE FIRST RIBOSOME TO ADVANCE IF IT HAS MET THE STEP TIME LIMIT
C
                    R(FIRST,2)=R(FIRST,2)-1
                    IF(R(FIRST,2).LE.0)
                       R(FIRST,1)=R(FIRST,1)+1
                       R(FIRST,2)=STOC
                       DO(INC=1,NC)
                          IF(R(FIRST,1).EQ.CPOS(INC))
                             R(FIRST,2)=IRG(MMD,MPD)
                             ESCAPEDO
                          ENDIF
                       ENDDO
                       IF(R(FIRST,1).EQ.NM)R(FIRST,2)=5
                    ENDIF
C
C  NOW ADVANCE EACH SUBSEQUENT RIBOSOME (WORKING BACK ALONG THE MRNA FROM
C  K=FIRST+1 TO LAST) IF THEY MEET THE TWO CRITERIA LISTED ABOVE
C
                    IF((FIRST+1).LE.LAST)
                       DO(K=FIRST+1,LAST)
                          R(K,2)=R(K,2)-1
                          IF((R(K,2).LE.0).AND.((R(K-1,1)-R(K,1)).GT.D))
                             R(K,1)=R(K,1)+1
                             R(K,2)=STOC
                             DO(INC=1,NC)
                                IF(R(K,1).EQ.CPOS(INC))
                                   R(K,2)=IRG(MMD,MPD)
                                   ESCAPE DO
                                ENDIF
                             ENDDO
                          ENDIF
                       ENDDO
                    ENDIF
C
C  IF THE FIRST RIBOSOME HAS TERMINATED, INCREMENT FIRST
C  OUTPUT POLYSOME STATUS
C  IF KREVIS IS 1,
C  ADJUST KIE4 IF TOO MANY OR TOO FEW RIBOSOMES ARE ON MESSAGE
C
                    IF(R(FIRST,1).EQ.NMP1)
                       PP=1./FLOAT(I-ILR)
                       PP=PP/EN
                       PRI=EN/PP
                       PRINT9,FIRST,IV (FIRST),I,I-IV (FIRST),LAST-FIRST,PP,R
     1F,PRI
  9                    FORMAT(4X,I2,4X,I5,I6,I6,I3,2F8.4)
                       IF(FIRST.GT.1)
                          R1S=R1S+PP
                          R2S=R2S+PP
                          R3S=R3S+PRI
                          R1SS=R1SS+PP**2
                          R2SS=R2SS+PP**2
                          R3SS=R3SS+PRI**2
                       ENDIF
                       IF(KREVIS.EQ.1)
                          IF(LAST-FIRST.LT.8.OR.LAST-FIRST.GT.11)
                             IF(LAST-FIRST.LT.8)
                                KIE4=IFIX(1.4*FLOAT(KIE4))

                                IF(LAST-FIRST.LT.4)KIE4=1.4*FLOAT(KIE4)
                                PRINT15,FLOAT(KIE4)/10000.
                             ELSE
                                KIE4=IFIX(.7*FLOAT(KIE4))
                                PRINT15,FLOAT(KIE4)/10000.
 15                             FORMAT(1H+,T60,"KI REVISED TO"F6.4)
                             ENDIF
                          ENDIF
                       ENDIF
                       FIRST=FIRST+1
                       ILR=I
                    ENDIF
C
C  INITIATE A NEW RIBOSOME AT CODON 1 WITH PROBABILITY KI (USE RANDOM NUMBER GEN
C  ERATOR) IF THE CURRENT LAST RIBOSOME IS AT LEAST D CODONS DOWN THE MESSAGE.
C  IF INITIATION IS SUCCESSFUL, INCREMENT LAST.
C  IF NO RIBOSOMES ARE ON MESSAGE REPEAT INITIATION ATTEMPT.
C
 25                 IF(R(LAST,1).GT.D)
                       IF(IRG(1,10000).LE.KIE4)
                          IVC=IVC+1
                          IV(IVC)=I
                          LAST=LAST+1
                          R(LAST,1)=1
                          R(LAST,2)=STOC
                       ENDIF
                    ENDIF
                    IF(LAST.LT.FIRST)I=I+1
                    IF(LAST.LT.FIRST)GOTO25
C
C  INCREMENT TIME
C
                    I=I+1
                 ENDUNTIL
```

Figure 6-3a, continued

```
C   OUTPUT MEANS AND S.D."S
              XN=FLOAT(NR-1)
              R1M=R1S/XN
              R2M=R2S/XN
              R3M=R3S/XN
              R1SD=SQRT((R1SS-R1S**2/XN )/(XN-1))
              R2SD=SQRT((R2SS-R2S**2/XN )/(XN-1))
              R3SD=SQRT((R3SS-R3S**2/XN)/(XN-1))
              PRINT16,R1M,R2M,R3M,R1SD,R2SD,R3SD
    16        FORMAT(/5X"MEAN VALUES AFTER R1"T31,3F8.4/5X."S.D."T31,3F8.4
     1)
C   OUTPUT DATA FROM SDIST IN SDIST2 ON  CODONS ON WHICH RIBO. PAUSES
C   OUTPUT IS IN PAIRS FOR EACH RIBOSOME.  THE FIRST NUMBER OF EACH PAIR IS THE
C   POSITION OF THE CODON AT WHICH THE RIBOSOME PAUSES.  THE SECOND NUMBER OF
C   EACH PAIR IS THE LENGTH OF THE PAUSE.
              DO(KKK=1,NR)
                 IL=0
                 DO(K=1,NM)
                    IF(SDIST(KKK,K).GT.STOC)
                       IL=IL+1
                       SDIST2(IL,1)=K
                       SDIST2(IL,2)=SDIST(KKK,K)
                    ENDIF
                 ENDDO
                 PRINT6,KKK,     (SDIST2(J,1),SDIST2(J,2),J=1,IL)
     6           FORMAT(/3X"R"I1,3X10(I3",",I3,2X)/5(8X10(I3,",",I3,2X)/))
              ENDDO
C   OUTPUT INITIATION DATA
              PRINT10,      (IV(KK),KK=1,IVC)
    10        FORMAT(1H0"     INITIATION TIMES..."4(/5X,15I6))
           ENDDO
C
C   READ DATA FOR ANOTHER MESSAGE.
C
              READ 200, NM,NC,RESID
              READ 201,(CPOS(K),K=1,NC)
         ENDUNTIL
         STOP
         END


         FUNCTION IRG(M,N)
C
C   RANDOM NUMBER GENERATOR BASED ON LINEAR CONGRUENTIAL METHOD FOR INTEGERS WITH
C   EVEN DISTRIBUTION BETWEEN M AND N INCLUSIVE
C
         DATA ID,IY/2147483648,568731/
         IY=MOD(15625*IY+22221,ID)
         IRG=M+(N-M+1)*IY/ID
         RETURN
         END
```

```
        ADEIBLL.   79/09/24.MCMASTER - SYSTEM B
15.29.06.MRNA4.JC2.
15.29.06.                                          C.B.HARLEY
15.29.11.USER,7426021,.
15.29.11.CHARGE,PSGOLD.
15.29.17.IPFL, MAX FL AVAILABLE  114000B WORDS.
15.29.20.ATTACH,IFTRAN/UN=FLEMING.
15.29.23.IFTRAN.
15.29.25. STOP IFTRAN2
15.29.27.ROUTE(OUTPUT,DC=PR,DEF,FC=AA)
15.29.28. ROUTE COMPLETE.
15.29.28.SETTL,100.
15.29.28.REWIND,IFTN.
15.29.28.MAP,OFF.
15.29.31.FTN,I=IFTN,GO.L=0,PL=6000,OPT=2.
15.30.05./O    2.699 CP SECONDS COMPILATION TIME
15.30.05.LGO
15.33.06.   CM LWA+1 = 513418, LOADER USED  655003
15.33.14.      STOP
15.33.14.        13562 WORDS NEVER USED
15.33.14.        2.287 CP SECONDS EXECUTION TIME
15.33.14.****************************************
15.33.14.                                       *
15.33.14.JOBCOST. APPROXIMATE COST= $   1.56  ***
15.33.14.IPFL. MAX FL USED   70000B WORDS.
15.33.14.UREAD,          0.002KUNS.
15.33.14.URFF,           0.015KUNS.
15.33.14.USMS,           5.174KUNS.
15.33.14.UECP,           7.573SECS.
15.33.14.AESR,           9.335SRUS.
```

Figure 6-3b

b

```
    ACTIN, HISTIDINE                         373 CODONS IN TOTAL, 9 MODULATOR CODONS AT POSITIONS
  40  73  87  88 101 161 173 274 371

  D    13
  KI     .058800
  STOC  1
  TP    50(10.0)
RIBOSOME INIT  TERM   TT   N      RP      RP/RN   RN/RP

   1         1   838   837 11   .0012    .0358 27.9333
   2        16   953   937 11   .0035    .2609  3.8333
   3        35  1059  1024 11   .0004    .2470  3.5333
   4        62  1161  1099 11   .0004    .2941  3.4000

  MEAN VALUES AFTER R1              .0007    .2793  3.5889
  S.D.                              .0006    .0169   .2219

 R1     40, 41    73, 59    87, 56    88, 47   101, 59   161, 60   173, 59   274, 57   371, 44   373,  5

 R2     27, 39    40, 56    73, 44    74,  3    75, 47    87, 52    88, 57   101, 59   160, 11   161, 43
       173, 42   274, 57   371, 59   373,  5

 R3     14, 33    27, 55    40, 59    62, 38    73, 59    75, 50    87, 59    88, 46   101, 51   161, 40
       173, 60   274, 56   371, 51   373,  5

 R4      1, 19    14, 56    27, 59    40, 56    60, 41    62, 50    73, 56    74,  4    75, 46    87, 45
        88, 58   101, 42   160,  7   161, 59   173, 49   274, 48   371, 44   373,  5

  INITIATION TIMES...
      1    16    35    62   108   175   233   300   456   530   634   747   887   957  1065
```

```
    ACTIN, HISTIDINE                         373 CODONS IN TOTAL, 9 MODULATOR CODONS AT POSITIONS
  40  73  87  88 101 161 173 274 371

  D    13
  KI     .058800
  STOC  1
  TP   100(20.0)
RIBOSOME INIT  TERM   TT   N      RP      RP/RN   RN/RP

   1         1  1250  1249 12   .0008    .0240 41.6667
   2        23  1545  1522 13   .0036    .1074  9.3333
   3        72  1711  1639 13   .0060    .1407  7.5333
   4        91  1993  1902 10   .0037    .1115  8.9667

  MEAN VALUES AFTER R1              .0044    .1317  8.1111
  S.D.                              .0014    .0411  2.2741

 P1     40,111    73, 84    87,116    88, 93   101, 90   161, 80   173, 94   274, 94   371,119   373,  5

 P2     27,102    40,118    73,101    75, 74    87,112    88,119   101,120   161, 86   173,118   274,110
       371, 97   373,  5

 P3     14, 66    27,118    40, 99    60, 14    62, 74    73,117    75,113    87, 97    88,100   101, 90
       160, 48   161, 92   173, 98   274, 94   371, 88   373,  5

 P4      1, 60    14,118    27, 88    40, 98    60,116    62,113    73, 94    74,  4    75,100    87, 95
        88,114   101,100   160,  9   161,118   173,114   274,104   371, 94   373,  5

  INITIATION TIMES...
      1    23    72    91   212   322   403   521   761   951  1163  1399  1582  1824
```

```
    ACTIN, HISTIDINE                         373 CODONS IN TOTAL, 9 MODULATOR CODONS AT POSITIONS
  40  73  87  88 101 161 173 274 371

  D    13
  KI     .058800
  STOC  1
  TP   150(30.0)
RIBOSOME INIT  TERM   TT   N      RP      RP/RN   RN/RP

   1         1  1739  1738 10   .0006    .0173 57.9667
   2        15  2076  2041 11   .0032    .0946 10.5667
   3        40  2317  2277 13   .0048    .1149  9.7000
   4        60  2661  2601 10   .0029    .0872 11.4667

  MEAN VALUES AFTER R1              .0033    .0989 10.2444
  S.D.                              .0005    .0144  1.4112

 R1     40,127    73,135    87,150    88,162   101,129   161,173   173,150   274,174   371,170   373,  5

 R2     27,126    40,146    73,127    74, 20    75,162    87,132    88,149   101,170   160,  2   161,165
       173,159   274,175   371,152   373,  5

 R3     14,114    27,146    40,157    62,144    73,163    75,118    87,136    88,171   101,147   160, 41
       161,147   173,166   274,126   371,138   373,  5

 R4      1,107    14,146    27,157    40,124    49, 21    60,163    62,118    73,149    75,158    87,178
        88,138   101,170   160, 15   161,169   173,133   274,151   371,144   373,  5

  INITIATION TIMES...
      1    15    40    60   203   369   556   666   983  1331  1623  1921  2196  2487
```

7 REFERENCES

Allen, R.E., Raines, P.L. and Regen, D.M. (1969) Biochim. Biophys. Acta., 190, 323-336.

Arca, M., Frontal, L., Sopara, O., and Tecce, G. (1967) Biochim. Biophys. Acta. 145, 284.

Ames, B.N. and Hartman, P.E. (1963) Cold Spring Harbor Symp. Quant. Biol. 28, 349.

Anderson, W.F. (1969) Proc. Natl. Acad. Sci. U.S.A. 62, 566-573.

Baird, M.B., Samis, H.V., Massie, H.R. & Zimmerman, J.A. (1975) Gerontol. 21, 57-63.

Balazs, E.A. (1977) in "Handbook of the Biology of Aging", eds. C.E. Finch & L.Hayflick (van Nostrand Reihnold Co., N.Y.)

Ballard, F.J. (1977) Essays in Biochem. 13, 1-37.

Baserga, R.L. (1977) in "Handbook of the Biology of Aging", eds. C.E. Finch & L.Hayflick (Van Nostrand Reinhold Co., N.Y.) pp. 101-121.

Baxter, G. & Stanners, C.P. (1978) J. Cell Physiol. 96, 139-145.

Becker, W.M. (1979) Nature 280, 719-720.

Block, R. and Haseltine, W.A. (1974) in "Ribosomes" eds. M.Nomura, A.Tissieres and P.Lengyel (Cold Spring Harbor Laboratory) pp. 747-761.

Bodley, J.W. and Davie, E.W. (1966) J. Mol. Biol. 18, 344-355.

Bonner, W.M. & Laskey, R.A. (1974) Eur. J. Biochem. 46, 83-86.

Bonnet, J. (1974) Biochemie 56, 541.

Bossinger, J., Miller, M.J., Vo, K-P., Geiduschek, E.P., and Xuong, N-H. (1979) J. Biol. Chem. 254, 7986-7998.

Bradley, M.O. (1977) J. Biol. Chem. 252, 5310-5315.

Bradley, M.O., Dice, J.F., Hayflick, L., and Schimke, R.T. (1975) Exp. Cell Res. 96, 103-112.

Bradley, M.O., Hayflick, L., and Schimke, R.T. (1976) J. Biol. Chem. 251, 3521-3529.

Britten, R.J. and Kohne, D.E. (1968) Science 161, 529-540.

Brunschede, H. and Bremer, H. (1971) J. Mol. Biol. 57, 35-57.

Burrans, L. and Kurtz, D. (1977) J. Mol. Biol. 112, 349-352.

Cashel, M. and Gallant, J. (1974) in "Ribosomes" eds. M.Nomura, A.Tissieres and P.Lengyel (Cold Spring Harbor Laboratory) pp. 733-745.

Castor, L.N. (1977) J. Cell. Physiol. 92, 457-468.

Chambers, R.W. (1971) Prog. Nucl. Acid Res. Mol. Biol. 11, 489-525.

Chapeville, F., Lipmann, F., von Ehenstein, G., Weisblum, B., Ray, W., and Benzer, S. (1962) Proc. Natl. Acad. Sci. U.S.A. 48, 1086.

Choe, B-K. and Rose, N.R. (1976) Geront. 22, 89-108.

Collins, J.H. & Elzinga,M. (1975) J. Biol. Chem. 250, 5915-5920.

Cohen, J.S., Hagenmaier, H., Pollard, H. and Schechter, A.N. (1972) J. Mol. Biol. 71, 513-519.

Comfort, A. (1969) "The Biology of Senescence", (Elsevier, N.Y.).

Coons, S.F., Smith, L.F. and Loftfield, R.B. (1979) Fed. Proc. 38, 328. (abstract).

Cress, P., Dirksen, P., and Graham, J.W. (1970) "Fortran IV with Watfor and Watfiv", Prentice-Hall Inc., N.J.

Crick, F.H.C. (1966) J. Mol. Biol. 19, 548.

Cristofalo, V.J. (1976) Gerontol. 22, 9-27.

Cristofalo, V.J. (1970) in "Aging in Cell and Tissue Culture" ed. Holeckova and Cristofalo (Plenum Press, N.Y.).

Csullog, G.W. (1976) M.Sc. Thesis, McMaster University, Hamilton, Ontario.

Daniel, C.W. (1977) in "Handbook of The Biology of Aging", ed. C.E. Finch & L.Hayflick (Van Nostrand Reinhold Co., N.Y.) pp 122-158.

Davies, J. (1969) Prog. Mol. & Subcell. Biol. 1, 47-81.

Davies, J., Gilbert, W., and Gorini, L. (1964) Proc. Natl. Acad. Sci. U.S.A. 51, 883.

Dayhoff, M.O. (1972) "Atlas of Protein Sequence and Structure" Vol. 5 (National Biomedical Research Foundation, Washington, D.C.)

Dawkins, R. (1978) "The Selfish Gene" (Paladin, N.Y.).

Dean, R.T. and Riley, P.A. (1978) Biochim. Biophys. Acta 539, 230-237.

Dell'Orco, R.T., Mertens, J.G., and Kreuse, P.F., Jr. (1973) Exptl. Cell Res. 77, 356-360.

Dell'Orco, R.T. and Guthrie, P.L. (1976) Mech. Age. Devel. 5, 399-407.

DeWolfe, M.S., Baskurt, S., and Cochrane, W.A. (1967) Clin. Biochem. 1, 75-81.

Dice, J.F., Hess, E.J., and Goldberg, A.L. (1979) Biochem. J. 178, 305-312.

Duncan, M.R., Dell'Orco, R.T., and Guthrie, P.L. (1977) J. Cell. Comp. Physiol. 93, 49-56.

Ebel, J.P., Giege, R., Bonnet, J., Kern, D., Befort, N., Fasiolo, F., Gangloff, J., and Dirheimer, G. (1973) Biochimie 55, 547-557.

Edelmann, P. & Gallant, J. (1977a) Cell 10, 131-137.

Edelmann, P. and Gallant, J. (1977b) Proc. Natl. Acad. Sci. U.S.A. 74, 3396-3398.

Engelhardt, D.L., Lee, G.T.Y. & Moley, J. (1979) J. Cell. Physiol. 98, 193-198.

Ezekiel, D.H. (1964) Biochem. Biophys. Res. Comm. 14, 64.

Feinstein, S.E. and Altman, S. (1978) Genetics 88, 201-219.

Fersht, A.R. and Dingwall, C. (1979a) Biochem. 18, 1238-1244.

Fersht, A.R. and Dingwall, C. (1979b) Biochem. 18, 1245-1249.

Fersht, A.R. and Kaethner, M.M. (1976) Biochem. 15, 3342-3346.

Finch, C.E. (1977) in "Handbook of the Biology of Aging", eds. C.E. Finch & L.Hayflick (Van Nostrand Reinhold Co., N.Y.) pp. 262-317.

Fleming, W.H. (1977) "IFTRAN-2...FORTRAN Extension for Structured Programming" (McMaster University Department of Applied Mathematics, McMaster University, Hamilton, Ontario).

Fox, J.E.B. (1976) PhD thesis, McMaster University, Hamilton, Ont.

Friedman, S.M., Berezney, R., and Weinstein, I.B. (1968) J. Biol. Chem. 243, 5044-5048.

Gallant, J. & Palmer, L. (1979) Mech. Ageing & Develop. 10, 27-38.

Garrels, J. (1979) J. Biol. Chem. 254, 7961-7977.

Garrels, J.I. and Gibson, W. (1976) Cell 9, 793-805.

Gershon, D. (1979) Mech. Ageing & Develop. 9, 189-196.

Gey, G.O., Coffman, W.O., and Kubicek, M.T. (1952) Can. Res. 12, 264-265.

Girardi, A.J., Jensen, F.C. & Koprowski (1965) J. Cell. Comp. Physiol. 65, 69-83.

Goldberg, A.L. and dice, J.F. (1974) Ann. Rev. Biochem. 43, 835-969.

Goldberg, A.L. and St. John, A.C. (1976) Ann. Rev. Biochem. 45, 747-803.

Goldstein, S. (1974) Exp. Cell Res. 83, 297-302.

Goldstein, S. (1978) in "The Genetics of Aging" ed. E.L.Schneider (Plenum Press, N.Y.) pp. 171-224.

Goldstein, S. & Harley, C.B. (1879) Fed. Proc. 38, 1862-1867.

Goldstein, S. & Littlefield, J.W. (1969) Diabetes 18, 545-549.

Goldstein, S. & Moerman, E.J. (1975) New Engl. J. Med. 292, 1306-1309.

Goldstein, S., Moerman, E.J., Seoldner, J.S., Gleason, R.E. & Barnett, D.M. (1979) J. Clin. Invest. 63, 358-370.

Goldstein, S. and Singal, D.P. (1972) Exptl. Cell Res. 75, 278-282.

Goldstein, S. and Varmuza, S.L. (1978) Can. J. Biochem. 56, 73-79.

Gordon, J. (1967) Proc. Natl. Acad. Sci. U.S.A. 58, 1574-1578.

Gorini, L. (1969) Cold Spring Harb. Symp. Quant. Biol. 34, 101-109.

Gorini, L. (1974) in "Ribosomes", eds. Nomura, M., Tissieres, A., & Lengyle, P. (Cold Spring Harbor Laboratory, Cold Spring Harbor, N.Y.), pp. 791-803.

Graham, F.L., Smiley, J., Russell, W.C., Nairn, R. (1977) J. Cell. Virol. 36, 59-72.

Green, H. (1977) Cell 11, 405-416.

Grosjean, H.J., de Henau, S., and Crothers, D.M. (1978) Proc. Natl. Acad. Sci. U.S.A. 75, 610-614.

Gurskaya, G.V. (1968) "The Molecular Structure of Amino Acids", Consultants Bureau, New York.

Hansen, B.S., Vaughan, M.H. & Wang, L.J. (1972) J. Biol. Chem. 247, 3854-3857.

Harada, F. and Nishimura, S. (1972) Biochem. 11, 301-308.

Harley, C.B. & Goldstein, S. (1978) J. Cell. Physiol. 97, 509-517.

Harley, C.B. and Goldstein, S. (1980) Science (in press).

Harley, C.B., Goldstein, S., Pollard, J.W. & Stanners, C.P. (1979a) Fed. Proc. 38, 328 (abstract).

Harley, C.B., Shmookler Reis, R.J. and Goldstein, S. (1979b) Canadian Association on Gerontology, Abstracts of Meetings, 3.

Harley, C.B., Pollard, J.W., Chamberlain, J.W., Stanners, C.P., and Goldstein, S. (1980) Proc. Natl. Acad. Sci. U.S.A. (in press).

Harrison, B.J. and Holliday, R. (1967) Nature 213, 990-992.

Haseltine, W.A. and Block, R. (1973) Proc. Natl. Acad. Sci. U.S.A. 70, 1564-1568.

Haurowitz, F. (1963) "The Chemistry and Function of Proteins" (Academic Press, N.Y.)

Hayflick, L. (1965) Exptl. Cell Res. 614-636.

Hayflick, L. (1973) Am. J. Med. Sci. 265, 432-445.

Hayflick, L. (1977) in "Handbook of The Biology of Aging", ed. C.E. Finch & L.Hayflick (Van Nostrand Reinhold Co., N.Y.) pp. 159-188.

Hayflick, L. and Moorhead, P.S. (1961) Exptl. Cell Res. 25, 585-621.

Heijne, G.von, Nilsson, L., and Blomberg, C. (1978) Eur. J. Biochem. 92, 397-402.

Hendil, K.B. (1977) J. Cell. Physiol. 92, 353-364.

Hirsch, G., Grunder, P., and Popp, R. (1976) Interdiscipl. Topics Geront. 10, 1-10.

Hirsch, G.P. (1978) in "The Genetics of Aging" ed. E.L.Schneider, (Plenum Press, N.Y.) pp. 91-134.

Hirsch, H.R. (1978) Mech. Ageing and Develop. 8, 51-62.

Hirsch, G.P., Holland, J.M., and Popp, R.A. (1978) Birth Defects, Orig. Art. Ser. 14, 431-448.

Hoffmann, G.W. (1974) J. Mol. Biol. 86, 349-362.

Holland, J.J., Kohne, D., and Doyle, M.W. (1973) Nature 235, 316-319.

Holliday, R. (1975) Fed. Proc. 34, 51-55.

Holliday, R. and Tarrant, G.M. (1972) Nature 238, 26-30.

Holliday, R. and Pugh, J.E. (1975) Science 187, 226-232.

Holliday, R., Huschtscha, L.I., Tarrant, G.M. and Kirkwood, T.B.L. (1977) Science 198, 366-372.

Holliday, R. and Stevens, A. (1978) Geront. 24, 417-425.

Holmes, W.M., Hatfield, G.W. and Goldman, E. (1978) J. Biol. Chem. 253, 3482-3486.

Hopfield, J.J. (1974) Proc. Natl. Acad. Sci. U.S.A. 71, 4135-4139.

Hosbach, H.A. and Kubli, E. (1979a) Mech. Ageing Develop. 10, 131-140.

Hosbach, H.A. and Kubli, E. (1979b) Mech. Ageing Develop. 10, 141-149.

Hunt, T., Hunter, T., and Munro, A. (1968) J. Mol. Biol. 36, 31.

Hunt, T., Hunter, T., and Munro, A. (1969) J. Mol. Biol. 43, 123.

Jacobson, K.B. (1966) Cold Spring Harbor Symp. Quant. Biol. 31, 719.

Jakubowski, H., Pastuszyn, A. and Loftfield, R.B. (1978) Biochim. Biophys. Acta 520, 568-576.

Jelenc, P.C. and Kurland, C.G. (1979) Proc. Natl. Acad. Sci. U.S.A. 76, 3174-3178.

Kaftory, A., Hershko, A., and Fry, M. (1978) J. Cell. Physiol. 94, 147-160.

Kawai, S. and Hanafusa, H. (1971) Virol. 46, 470-479.

Kazazian, H. and Freedman, M. (1968) J. Biol. Chem. 243, 6446-6450.

Kirkwood, T.B.L. and Holliday, R. (1975a) J. Theor. Biol. 53, 481-496.

Kirkwood, T.B.L. and Holliday, R. (1975b) J. Mol. Biol. 97, 257-265.

Kohn, R.R. (1971) "Principles of Mammalian Aging", Prentice-Hall Inc., N.J.

Kontermann, K. and Bayreuther, K. (1979) Gerontol. 25, 261-274.

Kozak, M. (1978) Cell 15, 1109-1123.

Kurland, C.G. (1977) Ann. Rev.Biochem. 46, 173-200.

Kurtz, D.I. (1979) Geront. 25, 228-230.

Lagerkvist, U. (1978) Proc. Natl. Acad. Sci. U.S.A. 75, 1759-1762.

Lee, G.T-Y. and Engelhardt, D.L. (1977) J. Cell. Physiol. 92, 293-302.

Lehninger, A. (1975) "Biochemistry" (Worth Publishers, Inc., N.Y.).

Lewis, C.M. and Holliday, R. (1970) Nature 228, 877.

Lima, L. and Macieira-Coelho, A. (1972) Exp. Cell Res. 70, 279-284.

Lither, F. and Ponten, J. (1966) Intern. J. Cancer 1, 579-588.

Litt, M. (1976) Science 193, 428-429.

Littlefield, J.W. (1976) "Variation, Senescence, and Neoplasia" (Harvard University Press, London).

Lodish, H.F. (1974) Nature 251, 385-388.

Lofgren, D.J. and Thompson, L.H. (1979) J. Cell. Physiol. 99, 303-312.

Loftfield, R.B. (1963) Biochem. J. 89, 82-92.

Loftfield, R.B. (1972) Prog. Nuc. Acid Res. 12, 87-128.

Loftfield, R.B. & Vanderjadt, D. (1972) Biochem. J. 128, 1353-1356.

Lovgren, T.N.E., Petersson, A., and R.B.Loftfield (1978) J. Biol. Chem. 253, 6702-6710.

Lowry, O.H., Rosebrough, N.J., Farr, A.L. & Randall, R.J. (1951) J. Biol. Chem. 193, 265-275.

Luhrmann, R., Eckhardt, H. and Stoffler, G. (1979) Nature 280, 423-425.

Luppis, B., Bargellesi, A., and Conconi, F. (1972) Biochem. 9, 4175.

MacDonald, C. and Gibbs, J. (1969) Biopolymers, 7, 707-725.

Makinodan, T. (1977) in "Handbook of the Biology of Aging", eds. C.E. Finch & L.Hayflick (Van Nostrand Reinhold Co., N.Y.) pp. 379-408.

Martin, E.M., Yegian, C.D. and Stent, G.S. (1963) Biochem. J. 88, 46P.

Martin, G., Sprague, C.A., Norwood, T.H., and Pendergrass, W.R. (1974) Amer. J. Pathol. 74, 137-154.

McKee, E.E., Cheung, J.Y., Rannels, D.E. & Morgan, H.E. (1978) J. Biol. Chem. 253, 1030-1040.

Mitra, S.K. (1978) FEBS Letters 91, 78.

Mitra, S. and Smith, C. (1969) Biochim. Biophys. Acta 190, 222-224.

Morrow, J. & Garner, O. (1979) Gerontol. 25, 136-144.

Naughton, M.A. and Dintzis, H.M. (1962) Proc. Natl. Acad. Sci. U.S.A. 48, 1822.

Nirenberg, M.W. and Leder, P. (1964) Science 145, 1399-1407.

Nishimura, S. (1972) Prog. Nucl. Acid Res. Mol. Biol. 12, 49-85.

Norris, A.T., and Berg, P. (1964) Proc. Natl. Acad. Sci. U.S.A. 52, 330.

O'Farrell, P.H. (1975) J. Biol. Chem. 250, 4007-4021.

O'Farrell, P.H. (1978) Cell 14, 545-557.

Ogrodnik, J.P., Wulf, J.H., and Cutler, R.G. (1975) Exp. Geront. 10, 119-136.

Olovnikov, A.M. (1971) Doklady Biochem. 201, 394-397.

Olovnikov, A.M. (1973) J. Theor. Biol. 41, 181-190.

Orgel, L.E. (1963) Proc. Natl. Acad. Sci. U.S.A. 49, 517-521.

Orgel, L.E. (1970) Proc. Natl. Acad. Sci. U.S.A. 67, 1476.

Parker, J., Pollard, J.W., Friesen, J.D. & Stanners, C.P. (1978) Proc. Natl. Acad. Sci. U.S.A. 75, 1091-1095.

Parker, J. and Friesen, J. (1979) Mol. Gen. Genetics. (in press).

Pedersen, F.S., Lund, E. and Kjeldgaard, N.D. (1973) Nature New Biol. 243, 13-15.

Penzias, A.A. (1979) Science 205, 549-554.

Pollard, J.W., Lam, T., and Stanners, C.P., submitted, J. Cell. Physiol.

Pollard, J.W. and Parker, J. (1977) Nature 267, 371-373.

Pollard, J.W. and Stanners, C.P. (1979) J. Cell. Physiol. 98,571-586.

Popp, R.A., Bailiff, E.G., Hirsch, G.P., and Conrad, R.A. (1976) Interdiscipl. Topics Geront. 9, 209-218.

Popper, K.R. (1965) "Conjectures and Refutations" (Harper and Row, N.Y.).

Prasad, K.N. (1974) "Human Radiation Biology" (Harper and Row, Md).

Prasanna, H.R. and Lane, R.S. (1979) Biochem. Biophys. Res. Comm. 86, 552-559.

Protzel, A. and Morris, A.J. (1973) J. Biol. Chem. 248, 7438-7444.

Robbins, E., Levine, E.M., and Eagle, H. (1970) J. Exp. Med. 131, 1211-1222.

Romaniuk, P. (1979) Ph.D. Thesis, McMaster University, Ontario.

Romaniuk, P.J., Hughes, D.W., Gregoire, R.J., Neilson, T., and Bell, R.A. (1978) J. Amer. Chem. Soc. 100, 3971-3972.

Rothstein, M. (1979) Mech. Ageing & Develop. 9, 197-202.

Ryan, J.M., Duda, G. & Cristofalo, V.J. (1974) J. Gerontol. 29, 616-662.

Sacher, G.A. (1978) in "The Genetics of Aging" ed. E.L.Schneider, (Plenum Press, N.Y.) pp. 151-168.

Safer, B. and Anderson, W.F. (1978) in "CRC Critical Reviews in Biochemistry", pp 261-290.

Salser, W., Fluck, M. and Epstein, R. (1969) Cold Spring Harb. Symp. Quant. Biol. 34, 513-520.

Samis, H.V. (1978) in "The Genetics of Aging", ed. E.L. Schneider Plenum Press, N.Y., pp 7-26.

Savageau, M.A. and Freter, R.R. (1979a) Proc. Natl. Acad. Sci. U.S.A. 76, 4507-4510.

Savageau, M.A. and Freter, R.R. (1979b) Biochem. 18, in press.

Schneider, E.L. (1978) in "Genetic Effects on Aging" ed. D.Bergsma D.E.Harrison (Allan Liss, Inc., N.Y.) pp. 159-170.

Schneider, F.H. and Nandy, K. (1977) J. Gerontol. 32, 132.

Schwartz, A.G. and Moore, C.J. (1977) Exp. Cell Res. 109, 449-450.

Selby, S.M. (1967) "Standard Mathematical Tables" (Chemical Rubber Co., Cleveland).

Shakespeare, V. and Buchanan, J.H. (1976) Exp. Cell Res. 100, 1-8.

Shampine, L.F. and Allen, R.C., Jr. (1973) "Numerical Computing" (W.B. Saunders Co., Toronto).

Shall, S. and Stein, W.D. (1979) J. Theor. Biol. 76, 219-231.

Shmookler Reis, R.J. (1976) Interdiscipl. Topics Gerontol. 10, 11-23.

Shmookler Reis, R.J. and Goldstein, S. (1979) Canadian Association on Gerontology, Abstracts of Meetings, 2.

Simons, J.W.I.M. (1970) in "Aging in Cell and Tissue Culture", ed. E.Holeckova & V.J.Cristofalo (Plenum Press, N.Y.) pp. 25-39.

Singer, J., Roberts-Ems, J., Riggs, A.D. (1979) Science 203, 1019-1021.

Skoultchi, A., Ono, Y., Moon, H.M. and Lengyel, P. (1968) Proc. Natl. Acad. Sci. U.S.A. 60, 675-682.

Smith, D.W.E. (1975) Science 190, 529-535.

Sober, H.A. (1979) "Handbook of Biochemistry, Selected Data for Molecular Biology" (Chemical Rubber Co., Cleveland), p. J201.

Sprinzl, M. and Cramer, F. (1978) Prog. Nucl. Acid Res. and Mol. Biol. 22, 1-69.

Stanners, C.P. (1968) Biophysical J. 8, 231-251.

Stanners, C.P., Adams, M.E., Harkins, J.L. & Pollard, J.W. (1979) J. Cell. Physiol. 100, 127-138.

Stanners, C.P. and Becker, H. (1971) J. Cell. Physiol. 77, 31-42.

Stanners, C.P., Eliceiri, G.L. & Green, H. (1972) Nature New Biol. 230, 52-54.

Stanners, C.P. and Thompson, L.H. (1974) in "Control of Proliferation in Animal Cells" eds. B.Clarkson & R.Baserga (Cold Spring Harbor Laboratory) pp. 191-203.

Stanners, C.P., Till, J.E. and Siminovitch, L. (1963) Virol. 21, 448-463.

Stanners, C.P., Wightman, T.M., and Harkins, J.L. (1978) J. Cell. Physiol. 95, 125-137.

Steitz, J.A. (1973) Proc. Natl. Acad. Sci. U.S.A. 70, 2605-2609.

Strehler, B.L., Hirsch, G.P., Gusseck, B., Johnson, R., and Bick, M. (1971) J. Theor. Biol. 33, 429-474.

Strehler, B.L. (1962) Time, Cells and Aging , Academic Press, N.Y.

Swim, H.E. and Parker, R.F. (1957) Am. J. Hyg. 66, 235-243.

Tai, P-C., Wallace, B.J. and Davis, B.D. (1978) Proc. Natl. Acad. Sci. U.S.A. 75, 275-279.

Tanford, C. (1962) Adv. Prot. Chem. 17, 69.

Thompson, L.H., Harkins, J.L. and Stanners, C.P. (1973) Proc. Natl. Acad. Sci. U.S.A. 70, 3094-3098.

Thompson, L.H., Stanners, C.P., and Siminovitch, L. (1975) Som. Cell Genetics 1, 187-208.

Thompson, R.C. and Stone, P.J. (1977) Proc. Natl. Acad. Sci. U.S.A. 74, 198-202.

Todd, H.J. (1978) Mech. Ageing and Develop. 7, 33-52.

Topal, M. and Fresco, J. (1976a) Nature 263, 285-288.

Topal, M. and Fresco, J. (1976b) Nature 263, 289-292.

Uhlenbeck, O.C., Baller, J. and Doty, P. (1970) Nature 225, 508-510.

Upton, A.C. (1977) in "Handbook of the Biology of Aging", eds. C.E. Finch & L.Hayflick (Van Nostrand Reinhold Co., N.Y.) pp. 513-535.

Vandekerckhov, J. & Wever, K. (1978) Eur. J. Biochem. 90, 451-462.

Vassart, G., Dumont, J.E., and Cantraine, F.R.L. (1971) Biochim. Biophys. Acta 247, 471-485.

Vaughan, M.H., Jr., Pawlowski, P.J., and Forchhammer, J. (1971) Proc. Natl. Acad. Sci. U.S.A. 68, 2057-2061.

Vaughan, M.H. and Hansen, B.S. (1973) J. Biol. Chem. 248, 7087-7096.

Von der Haar, F. and Cramer, F. (1976) Biochem. 15, 4131.

Walton, K.E., Styer, D., and Gruenstein, E.I. (1979) J. Biol. Chem. 254, 7951-7960.

Warburton, M.J. and Poole, B. (1977) Proc. Natl. Acad. Sci. (U.S.A.) 74, 2427-2431.

Watson, J.D. (1972) Nature New Biol. 239, 197-201.

Watson, J. (1976) "Molecular Biology of the Gene" (W.A. Benjamin, Inc., Menlo Park).

Weber, M.J. (1972) Nature New Biol. 235, 58-61.

Weinstein, I.B., Ochoa, M., and Friedman, S.M. (1966) Biochemistry 5, 3332-3339.

Wilson, D.L., Hall, M.E. & Stone, G.C. (1978) Gerontol. 24, 426-433.

Winslow, R.M. and Ingram, V.M. (1966) J. Biol. Chem. 241, 1144.

Woese, C.R. (1967) Prog. Nuc. Acid Res. Mol. Biol. 7, 107-172.

Woolhouse, H.W. (1974) Sci. Prog. Oxf. 61, 123-147.

Wojtyk, R.I. and Goldstein, S. (1979) J. Cell Biol. 83, 428A (abstract).

Wurnbach. P. and Nierhaus, K. (1979) Proc. Natl. Acad. Sci. U.S.A. 76, 2143-2147.

Yarus, M. (1972) Proc. Natl. Acad. Sci. U.S.A. 69, 1915-1919.

Yarus, M. and Berg, P. (1970) Anal. Biochem. 35, 450.

Yatscoff, R.W., Goldstein, S., and Freeman, K.B. (1978) Som. Cell Gen. 4, 633-645.

Yegian, C.D., Stent, G.S. and Martin, E.M. (1966) Proc. Natl. Acad. Sci. U.S.A. 55, 839.

Yegian, C.D. and Stent, G.S. (1969) J. Mol. Biol. 39, 45-58.

Zavada, J. and NacPherson, I. (1970) Nature 225, 24-26.

Zs.-Nagy, I. (1978) J. Theor. Biol. 75, 189-195.